AN INTEGRATED APPROACH TO UNRAVELLING MALARIA CELL SIGNALLING PATHWAYS

Thesis submitted for the degree of

Doctor of Philosophy

at the University of Leicester

by

Michele Graciotti

Department of Cell Physiology and Pharmacology

University of Leicester

2012

"In God we trust, all the others must bring data."

W. Edwards Deming

"This was the first demonstration of a protein kinase. [...]

I dropped the study of protein kinases, and like the base Indian, cast a pearl

away, else richer than all his tribe."[1]

Eugene P. Kennedy

Abstract

AN INTEGRATED APPROACH TO UNRAVELLING MALARIA CELL SIGNALLING PATHWAYS

Michele Graciotti

In the current thesis we analyse protein phosphorylation pathways in *P. falciparum,* the protozoa responsible for the most virulent form of malaria in order to both understand the role and scope of this protein modification in the parasite, and to explore its feasibility as a new drug target.

With the aim to map phosphorylation pathways controlled by *P. falciparum* Casein Kinase 2 (PfCK2), we developed a new chemical-biological approach based on γ-modified ATP analogues bearing reporting groups on the transferred phosphate in order to selectively tag CK2 substrates. Despite being able to efficiently synthesise a small set of analogues, the data presented here shows that the P-N linkage bond between the nucleotide and the tag is stable during the assay conditions but not during the product analysis due to its acidic liability (e.g. with HPLC, MALDI); suggesting that a different type of linkage should be chosen in the future.

Detailed characterisation studies of the parasite PfCK2 presented here showed a number of important features differing from human CK2. Docking analyses with a CK2 inhibitor showed that the PfCK2 ATP binding pocket is smaller than human CK2 due to the presence of Val116 and Leu45 which in the human kinase are replaced by more bulky isoleucine residues: Ile120 and Ile49. The difference between the human and parasite CK2 orthologues extends further to mechanisms of activation and regulation. Shown here is the autophosphorylation of PfCK2 that, unlike the human orthologue, occurs within subdomain I at Thr63. This autophosphorylation is essential for full catalytic activity. In addition we also showed that Thr63 phosphorylation regulates the interaction between the calalytic α-subunit and the regulatory β_2-subunit.

Here, we also presented evidence for tyrosine phosphorylated proteins in parasite infected red blood cells. PfCK2 can act as a dual specificity kinase phosphorylating *P. falciparum* Minichromosome Maintenance protein 2 (PfMCM2) on Tyr16 *in vitro*. It is therefore possible that PfCK2 may contribute to tyrosine phosphorylation within the parasite.

Finally, we also reported a study regarding MCM2-Ser13 phosphorylation which successfully identified PfCK1 as the kinase responsible for this event.

Publications

Solyakov L, Halbert J, Alam MM, Semblat JP, Dorin-Semblat D, Reininger L, Bottrill AR, Mistry S, Abdi A, Fennell C, Holland Z, Demarta C, Bouza Y, Sicard A, Nivez MP, Eschenlauer S, Lama T, Thomas DC, Sharma P, Agarwal S, Kern S, Pradel G, Graciotti M, Tobin AB, Doerig C. Global kinomic and phospho-proteomic analyses of the human malaria parasite Plasmodium falciparum. *Nat. Commun.* **2**, 565 (2011).

Acknowledgements

First of all, I would like to thank and express all my gratitude to my three supervisors: Andrew, Glenn and Paul (in alphabetical order) for taking me on to do my PhD within your group and for the support, advice, knowledge and encouragement you have given me. You have all in different ways guided me and transmitted your love for science especially when things were not going as they were supposed to be and I needed a boost.

I wish to thank as well all the members, past and present, of the organic chemistry lab and Andrew's lab. They have been both two really nice environments to work in and I truly enjoyed my time with all of you guys. A special thank to Debbie, Mahmood, Lev and Adrian whose constant advise and help has been particularly precious and to Kat who happily shared with me data, thoughts, worries and laughs throughout our PhD adventure.

Another thanks goes as well to all my friends I made here and especially to the little Italian community of Leicester PhD students, for all the fun and memorable times we had together. I will miss immensely our Sundays lunches and the Wednesdays cinema club.

To my mum, my sister and my dad, thanks for having given me all the support encouragement and sympathy I needed during these years.

A final special thank you to my partner Sam for his proof-reading and because he has always been there to listen and help me in whichever way he could.

Abbreviations

AA – Amino acid

ACN - Acetonitrile

ADP - Adenosine-5'-diphosphate

ATP - Adenosine-5'-triphosphate

BOC - Tert-Butyloxycarbonyl

CIP – Calf intestinal alkaline phosphatase

CK2 – Casein kinase II

DHB - 2,5-dihydroxy benzoic acid

DIPEA - N,N-Diisopropylethylamine

DMF – Dimethylformamide

DMSO - Dimethylsulfoxide

DCC - N,N'-dicyclohexylcarbodiimide

ECL – Enhanced chemiluminescence

EDAC - 1-ethyl-3-(3-dimethylaminopropyl)carbodiimide

EDC - 1-ethyl-3-(3-dimethylaminopropyl)carbodiimide

EDTA - Ethylenediaminetetraacetic acid

ePK - Eukaryotic protein kinase

Fmoc - 9-fluorenylmethyloxycarbonyl

FRET - Fluorescence resonance energy transfer

HBTU - O-Benzotriazole-N,N,N',N'-tetramethyl-uronium-hexafluoro-phosphate

HPLC – High performance liquid chromatography

Hrs - Hours

IPTG – Isopropyl β-D-thiogalactopyranoside

iRBC – Infected red blood cells

MALDI-TOF - Matrix-assisted laser desorption/ionization time-of-flight mass

spectrometry

MCM2 - Minichromosome maintenance complex component 2

MeOH - Methanol

PfCK2 – *Plasmodium falciparum* casein kinase II

PPh$_3$ - Triphenylphosphine

RT – Room temperature

SPPS – Solid phase peptide synthesis

TEAA - Triethylammonium acetate

TEAB - Triethylammonium bicarbonate

TEMED - Tetramethylethylenediamine

TFA – Trifluoroacetic acid

THF – Tetrahydrofuran

Wt – wild type

Contents

Chapter 1 Introduction

1.1   Malaria: history of the disease and current facts

Malaria is one of the most widespread diseases of our time causing both 247 million cases and more than 1.2 million deaths every year, mostly among under-5-years old children.[2] The disease is endemic in sub-Saharan Africa, South Asia and parts of South America since the infection is dependent upon mosquitoes of the *Anopheles* genus that live only in tropical areas. In addition to the human cost, malaria also imposes a massive economic burden, contributing substantially to poverty in the developing world. It is estimated to reduce economic growth by ~1.3%",[3] creating a vicious disease/poverty cycle that thwarts malaria control.[4] Eradication of malaria is therefore one of the major goals of modern Science, and is supported by the international community, with both public agencies (e.g. WHO) and private foundations like the Bill and Melinda Gates Foundation, who together set a global Malaria Eradication Research Agenda (MalERA) in 2007.[5]

The disease is caused by protozoan parasites of the genus *Plasmodium* which infect and destroy blood cells leading to fever, severe anaemia, cerebral malaria and, if untreated, death. From an evolutionary point of view, malaria predates humanity. While the *homo sapiens* species is only 200,000 years old, malaria parasites have been found in mosquitoes preserved in amber from the Palaeogene period; approximately 30 million years old.[6] To explain this gap, it has been proposed that humans may have originally caught *Plasmodium falciparum* from gorillas.[7]

Figure 1.1: Since its outset, malaria has always caused vast human losses and great economic impacts. Here the self-portrait of Albrecht Dürer one of the most famous victims of this disease (A. Dürer, *Self-portrait*, 1498).

Since then, malaria has had a major impact on human survival and historical reports can be found across every civilized society from China in 2700 BC (the oldest written account) through Greek, Roman, Indian, Arabic and European physician records up to the modern times.[8] Even Herodotus, Dante, and Shakespeare mention the characteristic periodic fevers in their works[9] underlining once more the massive medical, social and economical impact malaria has always represented for humans. Ancient Romans believed it came from the horrible fumes of the swamps, hence the term *mal'aria* which means "bad air". This idea persisted until the 19th century when the malaria parasite was discovered and the modes of transmission became clear.

From the outset, malaria has been a life threatening disease, causing the premature loss of great geniuses like the renaissance painter Albrecht Dürer among others (**Figure 1.1**) but, despite the achievements of modern medicine, today more people are at risk of suffering from malaria than at any other time in history. In fact, it has been calculated that presently, no less than 40% of the world's population live in countries where the disease is endemic[10] (**Figure 1.2**).
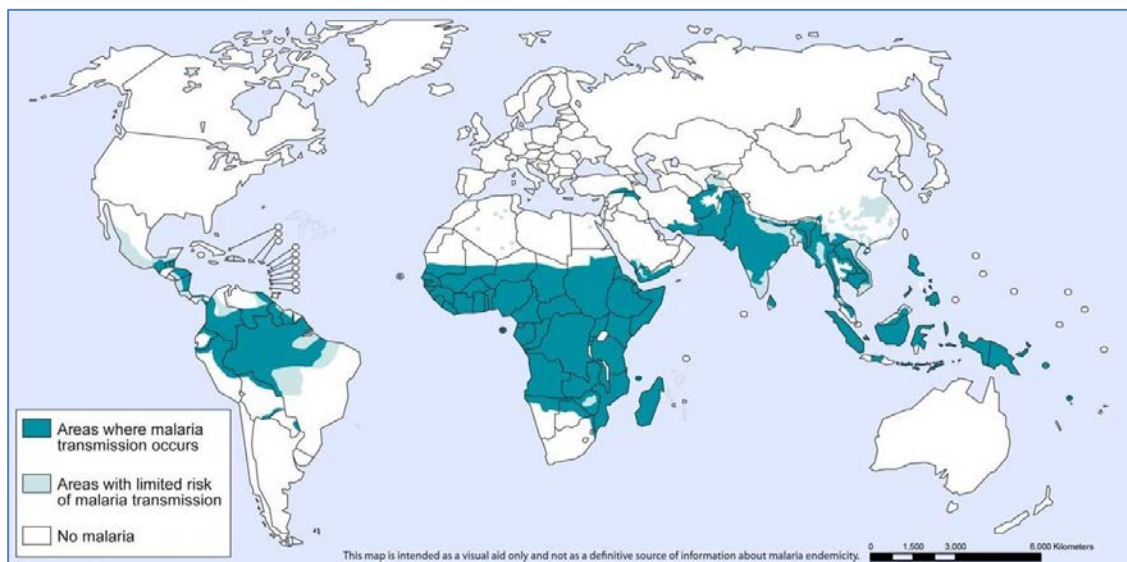
Figure 1.2: World map showing malaria endemic countries (source: WHO website)

For these reasons, interest from the scientific community has increased in the last decade in the global fight to control malaria through the development of a suitable vaccine in the long term as well as new drug treatments in the short term.

1.2 Biology of the malaria parasite

Malaria is caused by eukaryotic, unicellular, protozoan parasites of the genus *Plasmodium*, belonging to the Apicomplexa phylum. This is a broad category of protists containing an apical complex (after which the group is named) that helps the parasite to penetrate the host cell as exemplified by the invasion of *P. falciparum* into host erythrocytes during the blood stage infection. The apical complex consists of anteriorly located structures called micronemes, rhoptries and dense granules secreting enzymes that altogether assist the entry to the host cell (**Figure 1.3**).
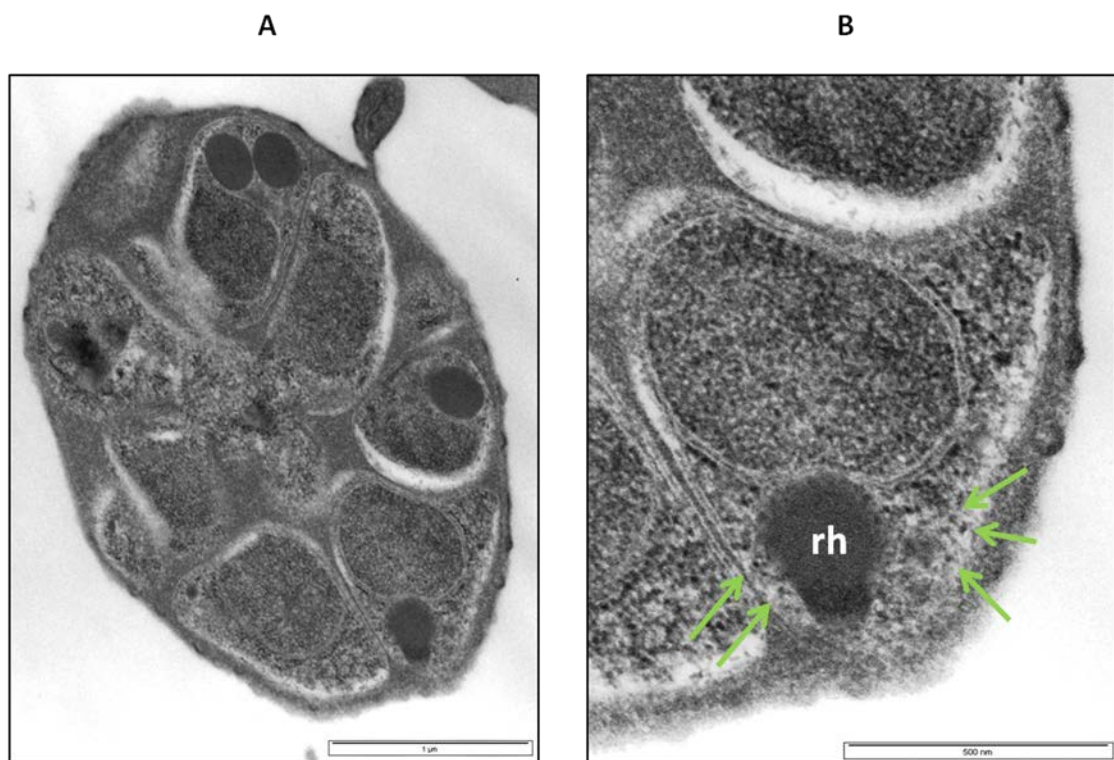
Figure 1.3: (A) Transmission electron micrograph (TEM) of developing merozoites in a late stage schizont of *Plasmodium falciparum*. (**B**) Detailed view of a longitudinally sectioned merozoite within a red blood cell showing a rhoptry (rh) at the apical end and micronemes (green arrows) that have not yet reached the apical position.

In order to gain access into the host cell, the parasite first attaches itself to the erythrocytic membrane and then undergoes apical reorientation to finally invade the cell[11] (**Figure 1.4**).
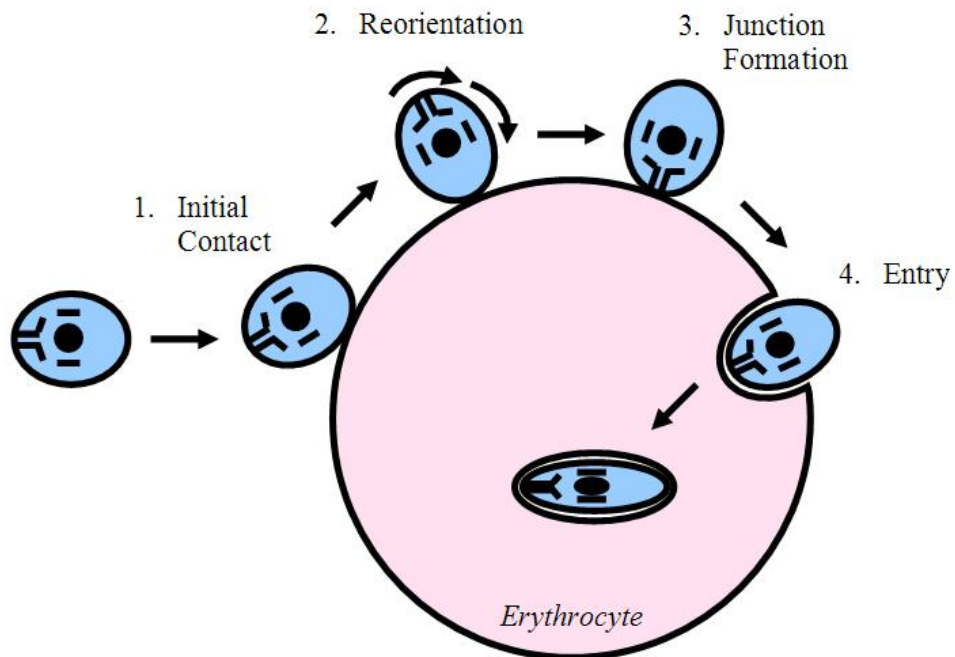
Figure 1.4: Merozoite Invasion of Erythrocytes. Invasion involves an initial "long-distance" recognition of surface receptors (1) followed by a reorientation process (2), a tight junction is formed involving high-affinity ligand receptor interactions (3). This tight junction then moves from the apical to posterior pole powered by the parasite's actin-myosin motor. By this process, the parasite does not actually penetrate the membrane but invades in a manner that creates a parasitophorous vacuole.

Another cell biological peculiarity shared by apicomplexans is a rudimental plastid called apicoplast that was acquired by secondary endosymbiosis between a free-living ancestor of these parasites and a red alga.[12] Although the apicoplast has lost its

photosynthetic properties, it is essential for parasite survival and it is here that anabolic pathways take place in a fashion akin to plants[4] (e.g. the isopentenyl diphosphate synthesis not found in any other metazoan).

It is rather fascinating that during its evolution *Plasmodium* parasites have chosen a metabolically highly reduced cell lacking compartments, genetic programmes and protein synthesis pathways as a host.[13] However, it is worth noting that erythrocytes, in the absence of a nucleus, are the only type of human cells lacking MHC class I molecules providing therefore a first mean of immune system evasion for the intracellular pathogen.

The main source of nutrition for *Plasmodium* species comes from the digestion of haemoglobin, releasing free heme[14] as a byproduct. This iron-containing prosthetic group is toxic to cells causing formation of reactive oxygen species and therefore oxidative stress. Parasites avoid this by converting it into insoluble and chemically inert crystals called hemozoin. In particular, detoxification through biocrystallization is distinct from the detoxification process in mammals which involves enzymatic degradation,[15] and is considered therefore a potential "Achilles' heel" to exploit in malaria treatment.

1.3 Life cycle

The five main species of malaria parasites known to infect humans include: *P. falciparum*, *P. vivax*, *P. ovale, P. malariae* and *P. knowlesi*. Their life cycle is particularly

complex, featuring a succession of proliferation and differentiation events involving both sexual and asexual (**Figure 1.5**).
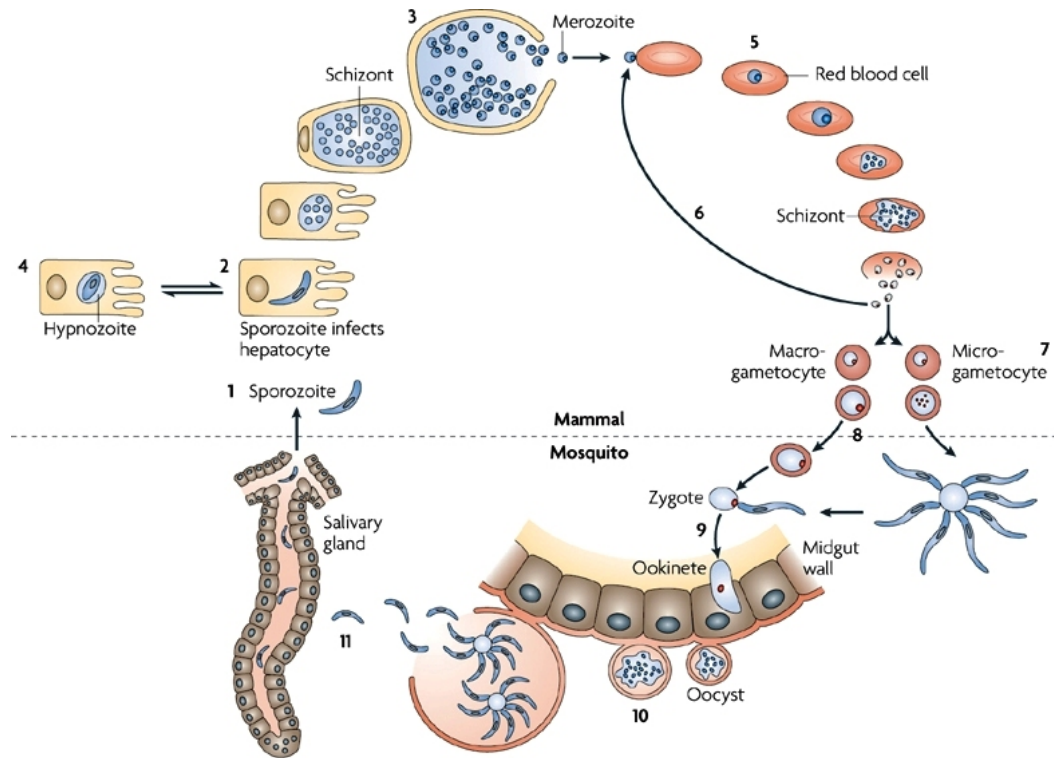
Figure 1.5: Life cycle of a malaria parasite, see text for further explanation (adapted from[16]).

The infection starts via the bite of an infected mosquito of the genus *Anopheles*, which releases sporozoites into the bloodstream (**1**). These are then rapidly taken up into the liver where they invade hepatocytes (**2**) and undergo a first round of cell growth and division called exo-erythrocytic shizogony, producing several thousands merozoites (**3**). When liver cells eventually rupture, merozoites are released into the bloodstream where they are now able to invade red blood cells (**4**). The invasion occurs as shown in **Figure 1.4** through first contact with the host cell, followed by reorientation that

juxtaposes the required molecular machinery (apical complex) with the host membrane, followed by entry. Upon invasion, merozoites differentiate into young trophozoites, often called "ring" stage due to their peculiar morphology, which feed on the erythrocyte by taking in small amounts of its cytoplasm largely constituted by haemoglobin (**Figure 1.6**). In the next schizont stage, the parasite undergoes another cycle of cellular division called intra-erythrocytic shizogony producing new merozoites that after rupture of the iRBC are released into the blood stream, ready to trigger a new reproductive cycle (**6**). Interestingly, this intra-erythrocytic cycle occupies a time frame characteristic of each species lasting 24 hours for *P. knowlesi*,[17] 48 hours for *P. falciparum* and *vivax*, and 72 hours for *P. malariae*[18] which also correspond to the classical peaks of fever observed clinically. After the invasion though, some merozoites arrest their cell cycle and differentiate into male and female gametocytes (**7**). These sexual cells do not contribute to pathology, but nonetheless are required to conclude the parasite's life cycle. The sexual stage is then completed inside the mosquito. After the blood meal, male and female gametocytes fuse together in the gut producing a zygote which further evolves to form an ookinete (**9**). The last stage of this cycle is the maturation of this ookinete into an oocyst which divides to form multiple haploid sporozoites (**10**). The latter finally migrate to the insect's salivary glands where they are primed to infect a new human host during a subsequent blood meal (**11**).

The life cycle described so far is common to all *Plasmodium* protozoans, however there are few key differences between species, important from a treatment and eradication perspective. *P. falciparum* is the most lethal form and is therefore currently the most important target.
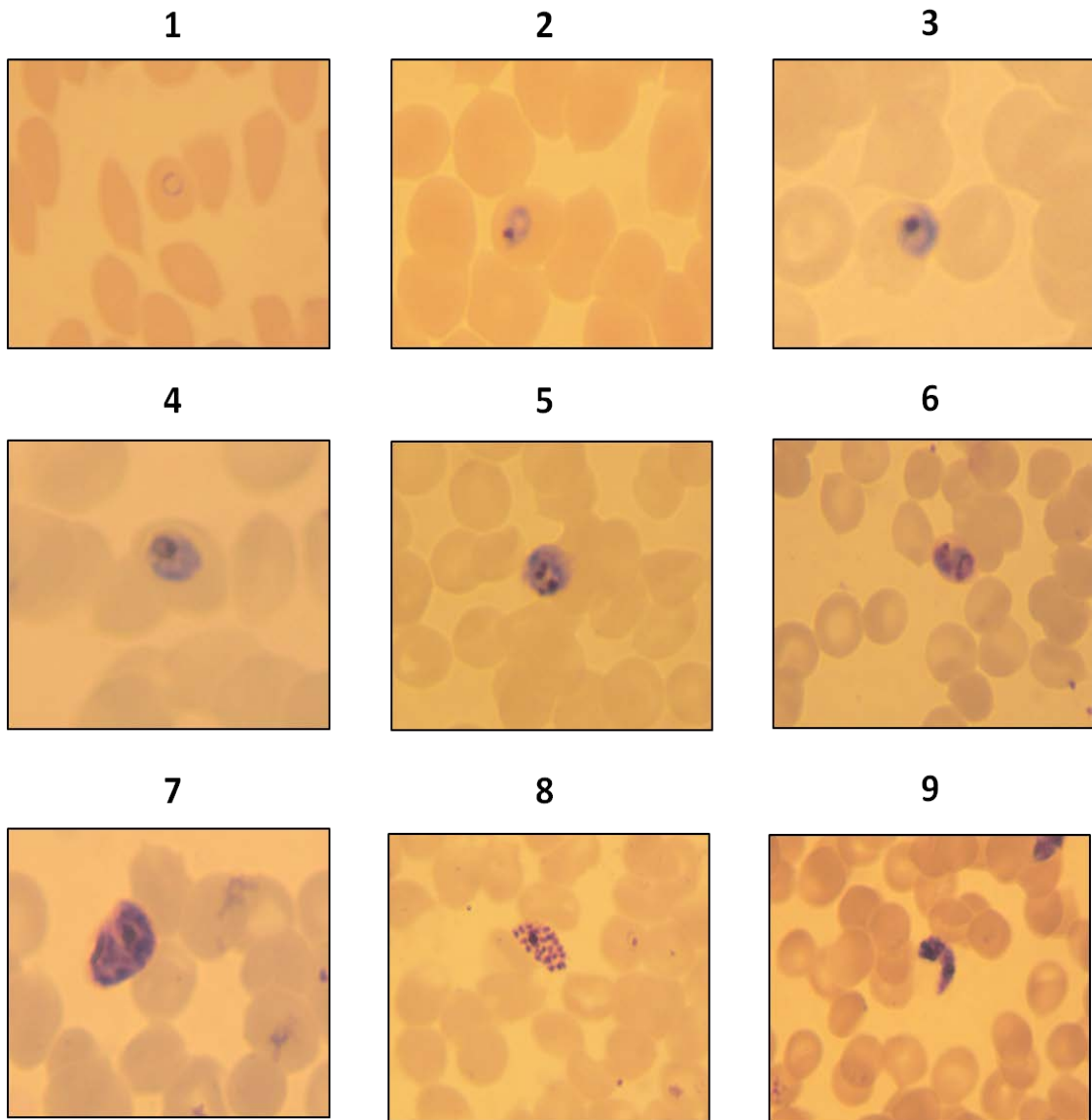
Figure 1.6: Pictures of giemsa stained thin blood smears showing intra-erythrocytic stages of the human malaria parasite *P. falciparum*. 1-2: young and old rings; 3-5: young and old trophozoites; 6-7: young and old schizonts; 8: fragmented schizont containing merozoites, 9: gametocyte (pictures obtained in the lab, see section **2.7.1**).

This is mainly due to a higher burden of merozoites[18] compared to other species and to its unique ability of modifying the surface of RBCs so that they can adhere to the endothelium preventing the clearing of the infection in the spleen.[19] This property,

not shared by any other protozoan parasite, results in the cytoadherence and accumulation of iRBCs in essential organs, such as heart or brain, leading to dysfunctions or even organ failure. Such medical complications are known as *severe malaria*[20] or *cerebral* malaria if it particularly affects the brain.

P.vivax is the second major cause of malaria accounting for ~40% of global cases; it is rarely fatal but still causes substantial morbidity in the world.[21] This species preferentially invades immature red blood cells[11] thanks to the recognition of a specific membrane protein called Duffy antigen, which is expressed in greater quantities on reticulocytes than on mature erythrocytes.[22] After infection, while in the case of *P. falciparum* all sporozoites develop directly to merozoites released into the bloodstream, for *P. vivax* some of them become dormant at the liver stage. These forms known as hypnozoites are able to trigger another cycle of infection months or years later after the initial exposure. Such ability to relapse is also shared by *P. ovale* and is a major issue for clinical treatment. In fact, an ultimate cure must have the ability to clear not only the current infection but also the dormant liver stage in order to avoid a recurrence of the disease. *P. malariae* is also able to cause chronic disease but in this case the relapse is due to persistence of parasites in the blood at very low densities.[23] Despite that, both *P. ovale* and *P. malariae* cause milder infections and remain highly sensitive to common antimalarials; therefore they do not constitute a major concern at the current stage.

1.4 Current strategies of control

Although a vaccine is not available yet, there are several classes of drugs currently used to treat malaria. In particular, all of these treatments target the intra-erythrocytic stage of the parasite life cycle, when symptoms are first detectable. The oldest class is the quinoline family which is based on quinine: a natural alkaloid extracted from the bark of cinchona trees. Bark extracts from this South America native plant were extensively used by Indians of Peru as antipyretic and have been eventually brought to Europe by Jesuits in the XVII century (**Figure 1.7**).
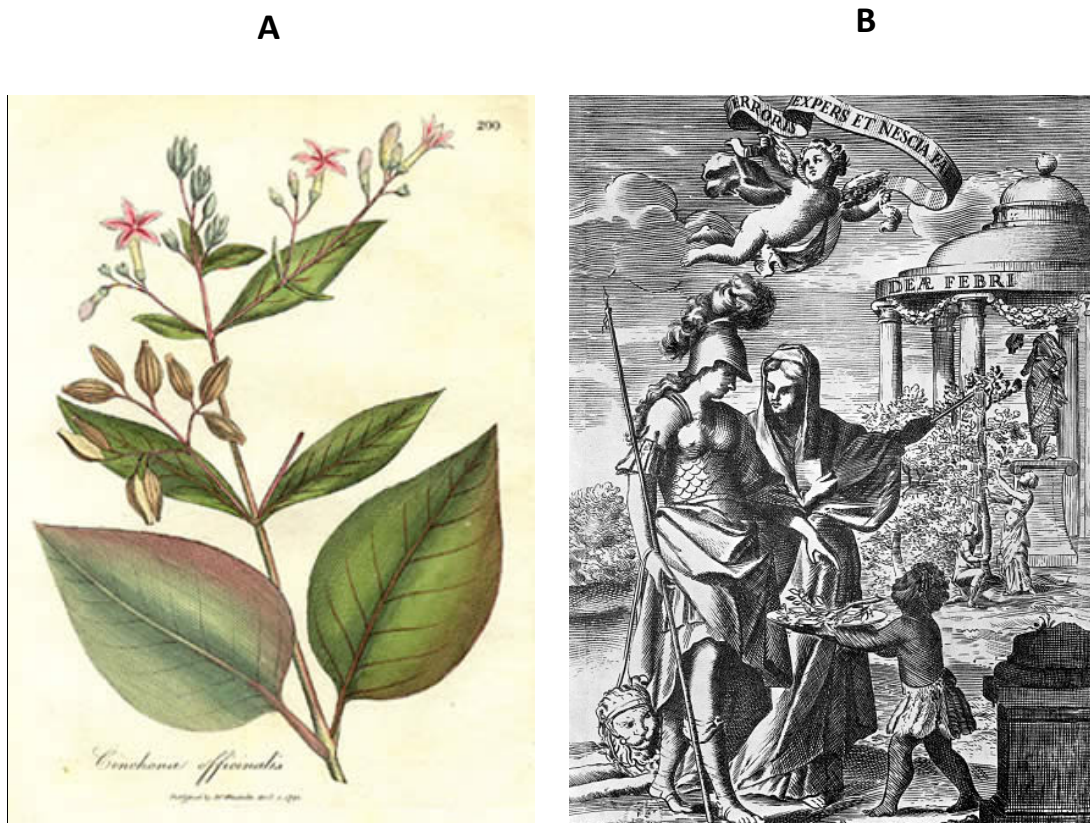
Figure 1.7: A: *Cinchona officinalis*. **B:** a 17th century engraving: Peru offers a branch of Cinchona to Science.

Jesuits started to use natural extracts also in the treatment of malaria gaining them the name of Jesuit's bark; while their potent efficacy established them as the first line treatment against the disease until modern times. Synthetic derivatives of quinine such as chloroquine and mefloquine have been also developed due to spread of resistance, during the 19th and 20th centuries. They all share the same mode of action causing parasite death by blocking the biocrystallization process of cytotoxic heme into hemozoin.[24]

Antifolates including sulfadoxine and proguanil constitute a different class of drugs against *Plasmodium* infections. These drugs are enzyme competitive inhibitors able to block the folic acid synthesis pathway, which is essential to parasite growth. The parasite in fact is unable to use host-synthesised pyrimidines and must therefore make its own.[25]

The last class of drugs currently in use is derived from the extracts of *Artemisia annua.*[26] Although their use as antimalarials in Chinese culture is well documented since the fourth century, they became effectively known to the Western world only in the late 70s due to the long historical and political isolation of the country. Despite that, nowadays, artemisinin and its analogues constitute the treatment of choice according to the WHO guidelines in the so-called ACT (Artemisinin Combination Therapy). In combination therapies two or more drugs, preferably with different modes of actions, are administered at the same time in order to reduce risks of drug resistance. In the particular case of *P. falciparum*, considering that the frequency of resistance is estimated at 1 in 10^{10} parasites and the parasite burden is usually around 10^{12} parasites, combining two medicines greatly lowers the possibility that a resistant

parasite will emerge.[27] However, despites ACTs, resistance against these drugs has been reported[16, 28] making the quest for a new generation of treatment an urgent task.

1.5 Evaluation of kinases as drug targets

In the search for new drugs in malaria therapy there are currently two major approaches. In the traditional "whole parasite" screening approach chemical libraries are screened in *in vivo* tests with infected erythrocytes cultures looking for potential parasite-killing agents.[29] Despite being "traditional", this approach is still largely used and has very recently turned successful with the identification of spiroindolones as a new class of antimalarial drug candidates.[30] One particular advantage of the parasite-based screening lies in the selection of compounds that may act against multiple targets, lowering therefore the chances of developing new drug-resistant strains.

However, the publication of the *Plasmodium falciparum* genome sequence[31] in 2002 has boosted the so-called "rational design" screening approach in the last years. Here, molecular targets (e.g. enzymes or important receptors) are identified, validated, expressed and finally screened in *in vitro* tests against a library of potential interacting compounds. The advantage of this latter approach is in the easier identification of the mechanisms of action of the drug and, therefore of the possible mechanisms of resistance.[32] Furthermore, in this way, the identification of the molecular targets upstream, during the drug development process, can be driven by the choice of brand-new targets to use in combination therapies.

Among different possible scenarios for the new generation of antimalarials, protein kinases (PKs) constitute an appealing opportunity for several reasons, although still rather unexploited. PKs are protein enzymes able to catalyse the transfer of a phosphate group from ATP to a protein substrate on a serine, threonine or tyrosine residue. The resulting phosphorylated state of a protein is usually physiologically transient and the reverse process is catalysed by enzymes called phosphatases.[33] Such a seemingly simple mechanism plays in reality a crucial role in the regulation of many cellular processes in eukaryotes such as: signal transduction pathways, cell cycle progression, and enzymatic activity among the others. The importance of this protein family is in particular underscored by the large number of genes encoding for PKs which e.g. comprises 1.5-2% of the total human genome.[34] Secondly, the catalytic mechanism and overall structure of PKs are conserved and it is well established that small molecules can bind to their catalytic site.[35] Hence, it is of no surprise that PKs have been extensively studied as targets for therapeutic intervention for important diseases such as cancer, diabetes, inflammation and neurodegenerative disorders;[36] leading for example to the successful design of the commercially available PK inhibitor imatinib for the medical treatment of chronic myelogenous leukemia.[37]

The vast distance that separates malaria parasites (Alveolates) from the animal hosts (**Figure 1.8**) is reflected by many profound peculiarities in their basic biology, leading to the suggestions that divergences are likely to be found also at the kinase level in order to achieve selective inhibition. Therefore, in the last decade, growing interest has been showed for this particular class of drug targets also in the malaria context, while many studies have flourished describing the feasibility of such approach.[38,39] Importantly, it is interesting to observe that kinases constitute also a nice example of

how the two above-mentioned approaches can work in tandem. A recent parasite-based screening from GSK[40] has in fact identified 13,533 hits able to inhibit parasite growth at 2μM concentration among the 2 million compounds present in the screening collection.
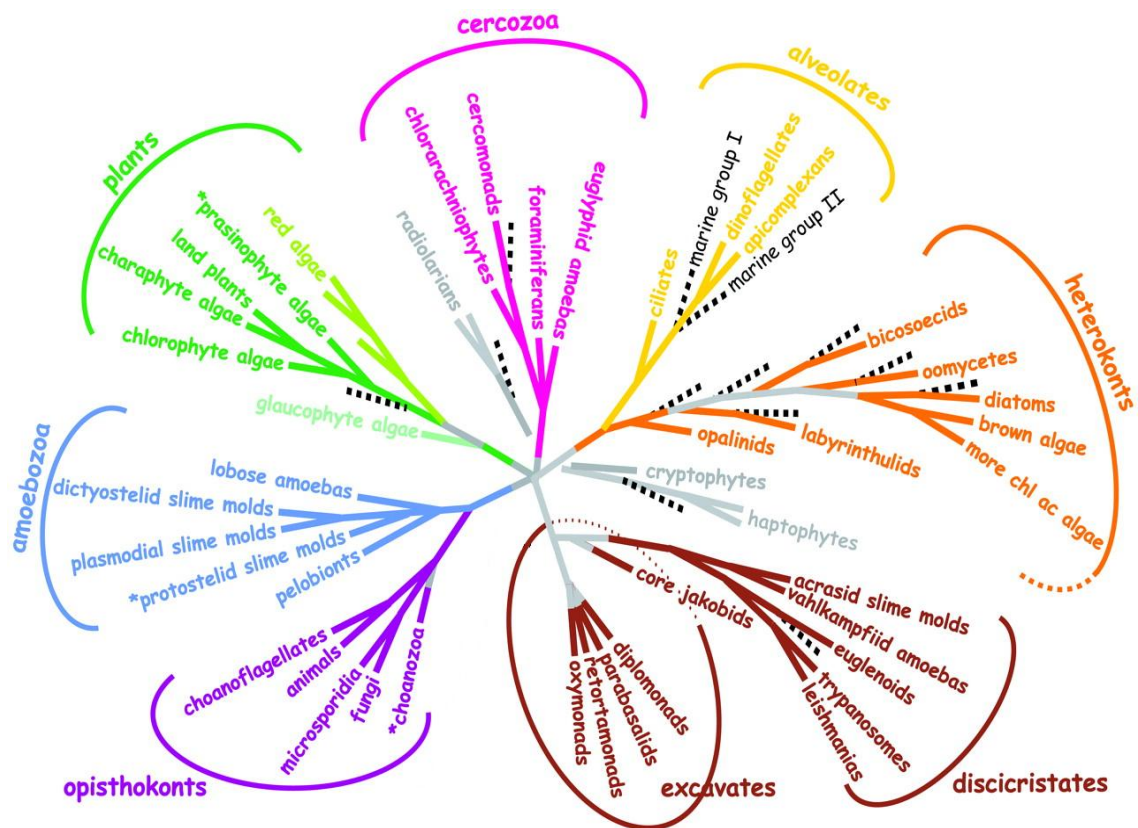
Figure 1.8: Phylogenetic tree showing the putative relationships between the major types of eukaryotic organisms (adapted from[41]).

Surprisingly, hypotheses regarding their modes of action generated by searching archived target activity data of hits in the internal GSK databases, strongly identified parasite kinases are their most important target, by far (**Figure 1.9**). This study

therefore, not only validates kinases as feasible novel targets, but also represents a starting point for exploring this possibility in future molecular-based screenings.
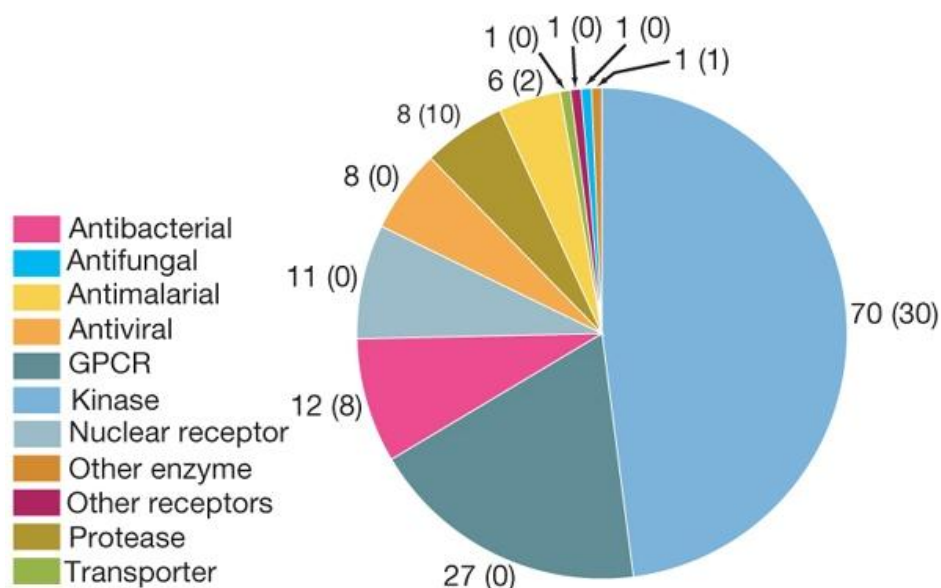
Figure 1.9: Distribution of target classes affected by the compounds in the GSK screening based on hypothetical modes of action. Number of targets in each class is indicated, with the number of identified malarial orthologues (BLASTP E-value ≤ 1.0-20) in parentheses (adapted from[40]).

1.6 Protein kinases: structure, function and evolution

The first report for protein kinase activity dates back to 1954 when Gene Kennedy described a liver enzyme able to catalyse the phosphorylation of casein.[42, 43] Soon afterwards, Krebs and Fischer determined that the same process was involved in the regulatory mechanism of glycogen phosphorylase activity with the discovery of phosphorylase kinase.[44, 45] These two major discoveries have opened up a brand-new scenario for modern science to explore, and 50 years later we are now able to describe

the overall structure, function and evolution of one of the largest protein families in eukaryotes genomes.

1.6.1 Structure

In the "pregenomic era", a comparative analysis of all the available sequences of eukaryotic protein kinases (ePKs) done by Hunter and Hunks successfully determined conserved residues and motifs shared by enzymes belonging to different organisms, underlining therefore a common origin.[46] Twenty years later, their classification of the protein kinase catalytic core in 11 subdomains is still valid and helpful in defining the structural basis for protein kinase activity (**Figure 1.10**). Moreover, the first solving of a protein kinase crystal structure (PKA)[47] has helped in the assignment of a function to these conserved motifs.

The structure of an ePK is essentially constituted by two lobes: the N-terminal lobe rich in β-sheets and involved in ATP binding; and the C-terminal one rich in α-helixes, responsible for protein substrate recognition and binding.
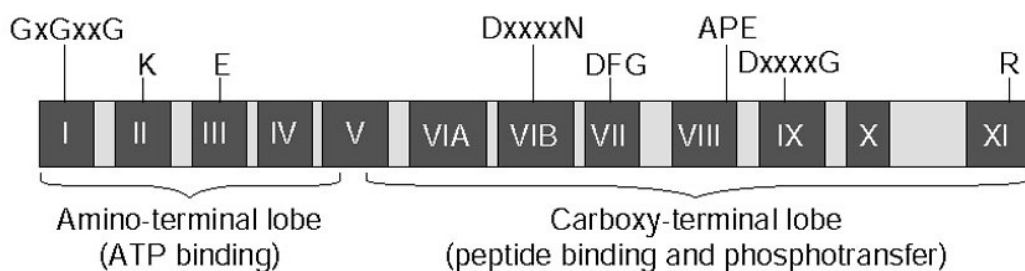
Figure 1.10: The ePK catalytic domain: the 12 conserved subdomains are indicated by roman numerals. The positions of amino-acid residues and motifs highly conserved are indicated above the subdomains (adapted from[48]).

Also, the two lobes are linked by a flexible hinge segment, while the catalysis occur at the interface of the two lobes often referred to as the catalytic cleft. Subdomains I to V comprise the N terminal lobe while subdomains V to XI constitute the C terminal end. In particular, the glycine rich loop GxGxxG in subdomain I forms a hairpin enclosing part of the ATP molecule while the right orientation of the ATP substrate is further ensured by electrostatic contacts between a conserved lysine in subdomain II and an aspartate in subdomain III with the α- and β- phosphates. The C terminal contains instead the conserved motif HRDxxxxN in which the aspartate is thought to act as a base acceptor; another conserved aspartate appears in the DFG motif in subdomain VII which binds the Mg^{2+} ion usually associated with ATP. Finally, the other residues indicated are involved in hydrogen bonding providing structural stability.

1.6.2 Classification and function

The completion of the human genome sequence has enabled a deeper study and classification of the full complement of human protein kinases. In particular, in our case this analysis is of crucial importance for a comparative study with the *Plasmodium falciparum* kinome in a drug-target perspective. So far, the most complete genomic study carried out in 2002[34] has identified 518 kinases which altogether account for 1.7% of the total human genome making the protein kinase family one of the largest gene families in eukaryotes. In the same study, human kinases were also classified in 8 major subfamilies, primarily by sequence comparison of their catalytic domains (**Figure 1.11**). This classification is not just merely dictated by a rational approach, but constitutes instead a first basis for inferring protein kinase functions.
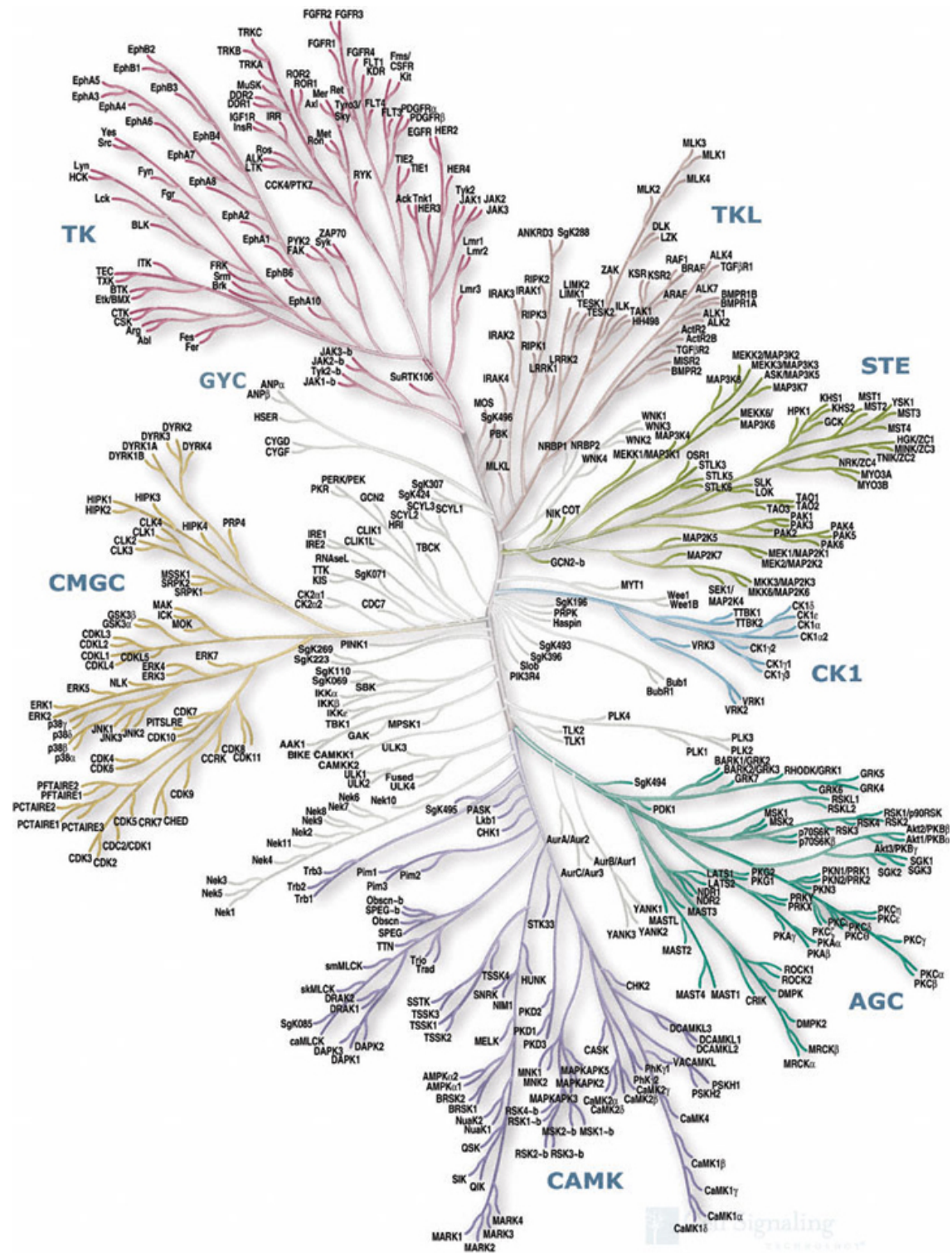
Figure 1.11: Phylogenetic tree depicting the relationships between members of the complete superfamily of human protein kinase. Each kinase is at the tip of a branch; the similarity between various kinases is inversely related to the distance between their positions on the tree diagram (adapted from www.kinase.com).

In fact, kinases having closely-related catalytic domains tend also to be similar in overall structural topology, have similar modes of regulation, and similar substrate specificities. These properties of human kinases can be therefore often inferred from other family members in human or in model organisms.[49]

The 8 conventional ePKs groups are:

- AGC

- CAMK

- CK1

- CMGC

- RGC

- STE

- TK

- TKL

The AGC group is named after the protein kinase A, G, and C families (PKA, PKC, PKG) which have a long history as cytoplasmic serine/threonine kinases regulated by secondary messengers such as cyclic AMP (PKA), cyclic GMP (PKG) or lipids (PKC).[50]

The CAMK group is primarily characterised by calcium/calmodulin modulation of enzyme activity. Most of the members of this group exhibit activation by the binding of Ca^{2+} or calmodulin to a small C-terminal domain. As with the closely related AGC group, the CAMK group, in general, appear to prefer substrates containing basic residues. There are two types of CAMK: the specialized CAMKs as for example MLCK (myosin light chain kinase) that phosphorylates myosin determining muscle

contraction, and the multifunctional CAMKII subfamily, involved in many signalling cascades and thought to be important mediators of learning and memory.[51]

CK1 is a small group of kinases with a high sequence homology (53%–98% identical), but very distinct from other kinase groups for example by the presence of the sequence SIN instead of APE in kinase domain VIII.[52] The general consensus phosphorylation site is S/TpXXS/T requiring therefore a prior phosphorylation event.[53] Members of this family have a myriad of substrates and function as regulators of signal transduction, circadian rhythms, chromosome segregation and DNA repair.[54]

The CMGC group is named after some of its members including: cyclin-dependent kinases (CDKs), mitogen-activated protein kinases (MAP kinases), glycogen synthase kinases (GSK) and CDK-like kinases and it is an essential and typically large group of kinases found in all eukaryotes. CDKs regulate the progression through the different phases of the cell cycle in association with their activating partners cyclins. Tumour progression is frequently associated with genetic or epigenetic alterations in CDKs (or cyclins), which help sustain proliferation with independence from external mitogenic or anti-mitogenic signals. MAP kinases were discovered in the late 1980s and, together with their immediate upstream phosphorylating kinases, are among the most highly studied signal transduction molecules. They play a key role in the regulation of many cellular processes and MAPK cascades participate extensively in the control of cell fate decisions such as proliferation, differentiation and death across all eukaryotic phyla and in all tissues of metazoans. GSK3, initially described as a key enzyme involved in glycogen metabolism, is now known to regulate a diverse array of functions. GSK3 is a well-established component of the Wnt pathway, which is essential for establishing

the entire body pattern during embryonic development. Notably, also CK2, a crucial kinase with a very large number of substrates[55] belongs to the CMGC group.

The STE group consists of homologues of yeast sterile 7, 11 and 20 kinases. These sequentially phosphorylate each other and then activate the downstream MAP kinases belonging to the CMGC group. In particular, Ste20 members phosphorylate Ste11 kinases and are therefore called MAP3Ks. Once activated Ste11 kinases phosphorylate Ste7 kinases which then act on MAPK kinases. For this reason, Ste11 and Ste7 members are also referred to as MAP3K and MAP2K respectively. These molecules are components of signalling pathways that relay, amplify, and integrate signals from a variety of extracellular stimuli, thereby controlling the genomic and physiological response of a cell to its environment.

Kinases belonging to the tyrosine Kinase group (TK) phosphorylate almost exclusively tyrosine residues, as opposed to most other kinases that are selective for serine or threonine or from dual specificity kinases which phosphorylate serine/threonine in addition to tyrosine. The group appears to be the youngest of kinase groups, as it is absent from plants and unicellular organisms like *Dictyostelium* and yeast. They are further divided into two classes: receptor and non-receptor PTKs. The first class typically contains an extracellular domain which upon binding to effector molecules (e.g. growth factors) induces structural changes in the intracellular domain and activates the tyrosine kinase function. The second class is made up of cytoplasmatic proteins that usually function close to the surface of the cell and are involved in signal transduction as the former group.

Tyrosine kinase-like kinases (TKL) are serine-threonine protein kinases named so because of their close sequence similarity to tyrosine kinases. TKLs are by far the largest group of kinases in land plants, where they often constitute ca. 80% of the plant kinome. This group is also well represented in metazoans where it's linked with the activation of apoptotic pathways. Some TKL families, such as RAFs and MLKs, are involved in the MAPK cascade and act as MAP3K. Others like IRAK and RIPK members are involved in immune response signalling, while others, as for example LIM kinases, are regulators of the cytoskeleton.[56]

The receptor guanylate cyclases are a small ePK group similar in sequence to the TK group found in metazoa but absent from fungi, plants and protists. RGC members are single-pass transmembrane receptors with an active guanylate cyclase domain and a kinase domain on the intracellular side.[57] This kinase domain binds ATP but is usually inactive. However, a study on the photoreceptor guanylate cyclise showed that this specific member of RGC family presents Mg^{2+}-dependent serine auto-phosphorylating kinase activity.[58] In particular, this kinase activity is unaffected by Ca^{2+}, cyclic nucleotides and phorbols, but is inhibited by high concentrations of staurosporine.

1.6.3   Evolution

As stated earlier, ePKs are one of the most expanded gene families in eukaryotes and their deregulation or mutation is often associated with important diseases (e.g. cancer, leukemia, neurodegenerative disorders).[36] These main observations underscore the crucial role they play in eukaryotic systems, a role that is further confirmed by analysing their evolution. ePKs evolved in a divergent manner from much simpler eukaryotic-like kinases (ELKs), an enzyme class abundant but poorly

understood in prokaryotes.[59] The overall structural organisation consisting of two lobes and a hinge region with the ATP moiety buried in the catalytic cleft is conserved between the two groups. However, what is strikingly different is that ePKs are tightly regulated. In fact, unlike metabolic enzymes their function is not to simply turnover product in the most efficient manner, but rather to act as molecular switches. They help maintain the cellular homeostasis by initiating a cascade of events in response to extracellular stimuli such as hormones, neurotransmitters or stress. This means that ePKs activity is only transient and therefore needs to be regulated. There are a number of ways in which kinases can be regulated, from effector binding (cyclins, calmodulin), to phosphorylation (MAPK2, MAPK for example); a feature that has a particular importance also in the kinase classification, but which is totally lacking in prokaryotes. In other words, it is the complex network of kinase activity and regulation often cross-talking (e.g. the MAPK cascade) that has enabled the complexity of eukaryotic organisms. To further stress the point of the close link between ePKs and eukaryote evolution another important study by G. Manning *et al*[60] has analysed existing differences between different eukaryote kinomes (in particular: budding yeast, worm, fly and human). The general conclusion has been that all major kinase groups and most kinase families are conserved throughout metazoans, many of which are also found in yeast. However, specific family expansions or losses are observed in different types of organisms, and several families are species-specific (**Figure 1.12**). These remarks suggest how some pathways can vary or be specifically regulated in different organisms; an observation which is of particular importance if we aim to selectively target the parasite kinome in the presence of host kinases.
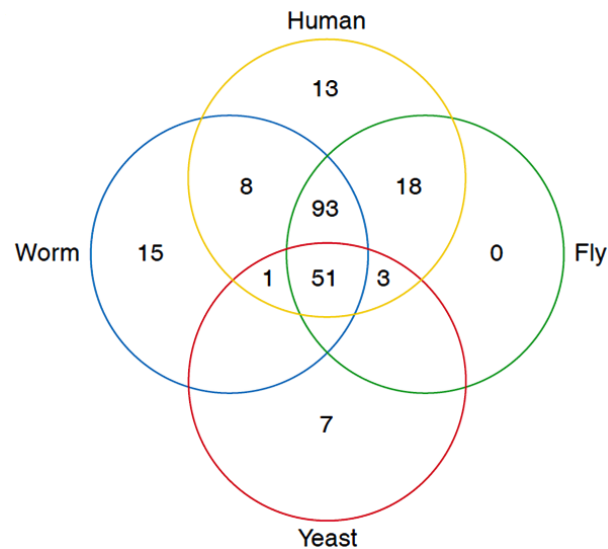
Figure 1.12: Distribution of the 209 kinase subfamilies among genomes of the model organisms: *H. sapiens*, *C. elegans*, *S. cerevisiae*, *D. melanogaster* (adapted from[60]).

1.6.4   Regulation

Since protein kinases act as molecular switches in eukaryotes, understanding their mechanisms of regulation is of crucial importance to analyse the role they play within the cell. As has already been described, there are a number of ways in which these enzymes are controlled: from the binding of messengers (e.g. cyclic AMP in PKA) or additional subunits (as cyclins in the case of CDKs) to autoregulatory processes like autophosphorylation or interaction with upstream kinases (e.g. MAPK cascade). However, a key aspect of regulation that is shared by most kinases (that are then often further controlled by the mechanisms enlisted above) is the phosphorylation of a specific residue in subdomain VII[61] (**Figure 1.13**). This phosphorylation site is located in the activation segment which spans from the DFG to the APE motif in the C terminal lobe.
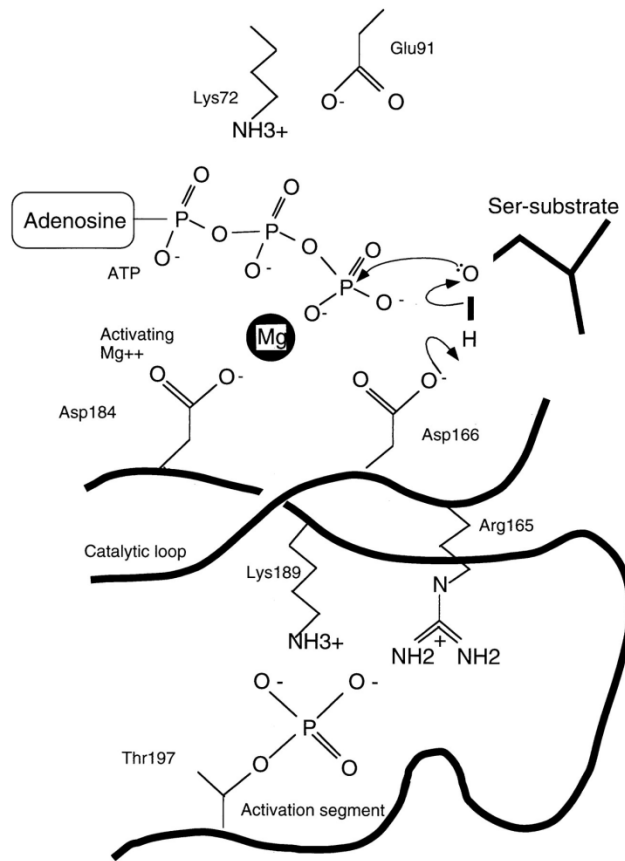
Figure 1.13: A schematic representation of ATP binding site and activation segment of RD ePKs showing conserved residues involved in phospho-transfer and enzyme folding (numbers are based on PKA; adapted from[61]).

It has been shown[62,63] that phosphorylation of this conserved site caused by either an autophosphorylation event or by an upstream kinase is crucial to induce rearrangements to an active conformation, at least for RD kinases. RD kinases constitute the vast majority of ePKs and are characterized by a conserved Arg residue preceding the catalytic Asp in subdomain VI. In this case, the phosphate group introduced is crucial as it acts as an organising centre to correctly orient the catalytic aspartate and the rest of the molecule for efficient substrate binding and transfer reaction. The role of the phosphate group is essentially to neutralise the charges

around the Arg and help the correct orientation of the catalytic Asp by forming a salt bridge with the conserved Arg. In the absence of the phospho-group such a configuration is disfavoured and the kinase is inactive. Non-RD kinases lack this conserved Arg and are often controlled by associated receptors (e.g. Toll-like receptors[64]). However, since most ePKs are RD kinases,[61] understanding the molecular basis of such processes also in *Plasmodium* could provide a good opportunity to interfere with kinase regulation and therefore cellular homeostasis.

1.7 The *Plasmodium falciparum* kinome

In the post-genomic era, the complete sequencing of the *Plasmodium falciparum* genome[31] has enabled not only the identification and classification of the parasite kinases, but also several detailed comparison studies with kinomes of other organisms.[34,65,66] These studies have underlined important evolutionary divergences from other metazoans and especially from the host human species, further stressing the feasibility of a kinase-based approach to cure malaria (**Figure 1.14**).

According to genomic analysis, the protein kinase complement of *Plasmodium falciparum* is constituted by ~85 members accounting for ~2% of the total genome, a percentage comparable to the one observed in yeast and human.[34] The primary sequence of these proteins conforms to the model described by Hanks[46] with the catalytic domain divided into XI subdomains. However, either adjacent or within the conserved subdomains there are often large insertions of charged or polar residues whose function is yet to be understood.
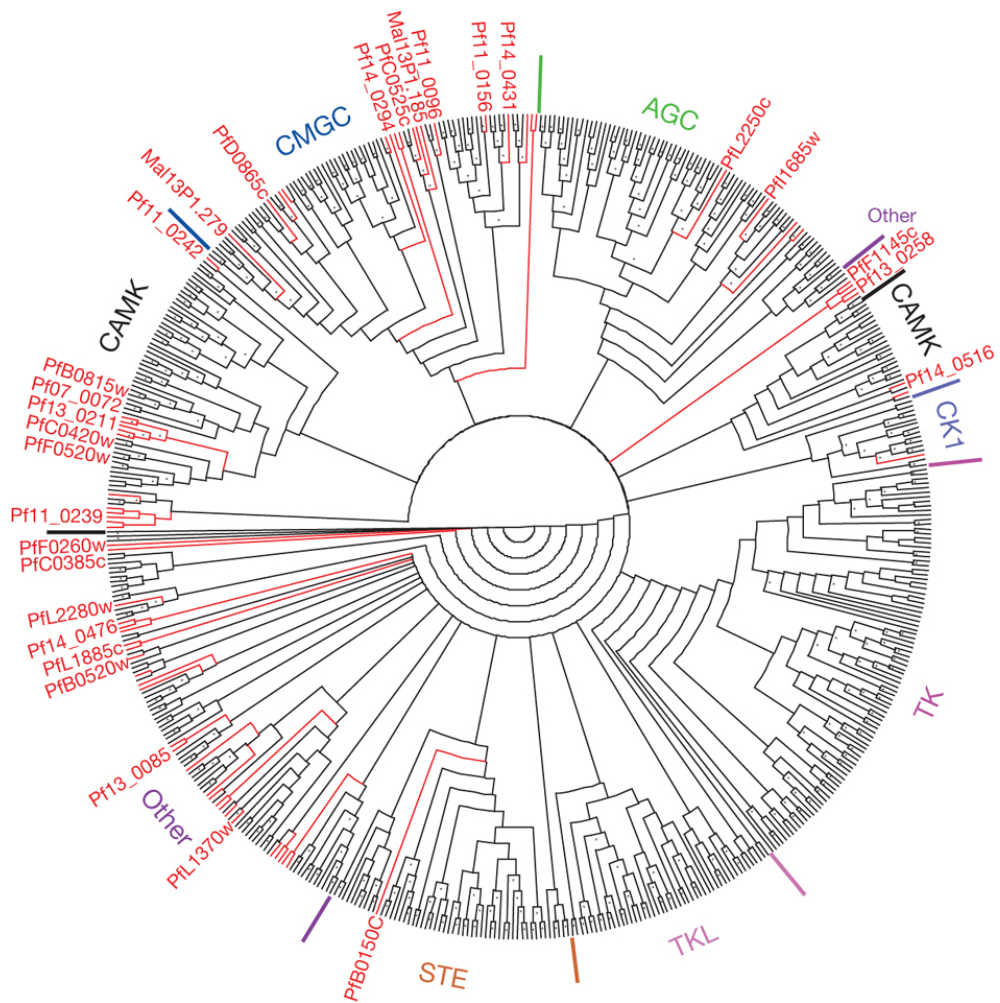
Figure 1.14: Neighbour-joining tree based on pairwise amino acid sequence similarity for all known human and *P. falciparum* kinases. Parasite and human lineages are coloured red and black, respectively (adapted from[40]).

From their position and hydrophilicity it has been speculated that they may form surface loops that can interact with effector molecules, other proteins or even substrates, without interfering with kinase folding and activity.[67] Moreover, from the classification of the kinases into the commonly accepted family scheme[34] other surprising and important peculiarities appear suggesting that selective inhibition is an achievable goal.

1.7.1 The CMGC group

Bioinformatic analyses identified eighteen kinases belonging to this family, making it the most prominent group in the *Plasmodium* kinome.[68] It is interesting to note that usually CMGC kinases are involved in the control of cell proliferation and development in eukaryotic systems; therefore their relative abundance may link to the complex life cycle of the parasite and to the presence of several stages of proliferation. In particular, six CDKs were identified and at least two of these are regulated by cyclin binding like their human homologues. The threonine phosphorylation site present in the activation loop which is essential for kinase activity of human CDKs is overall conserved but its phosphorylation has not been observed in malaria parasites.[69] This suggests therefore different modes of regulation. Also in the CMGC group two enzymes Pfmap-1 and Pfmap-2 were classified as atypical MAPKs. Interestingly, classical MAPKK analogues usually controlling the activity of MAPK through phosphorylation in the MAP cascade are absent in *Plasmodium*, a unique feature of this species in the eukaryote kingdom. Three members were identified in the GSK-3 subfamily. The most closely related to human has been recently characterized as showing similar modes of regulation (especially autophosphorylation on a tyrosine residue) and exportation to red blood cell cytoplasm.[70] Finally, a single orthologue of casein kinase 2 has been identified, together with two regulatory subunits.[71]

1.7.2 The AGC group

Five *Plasmodium* kinases cluster within the AGC group[68] and three of them have been characterized so far. The PKA homologue has been shown to respond to cAMP levels and pharmacological experiments suggest that this cAMP-PKA pathway regulates

cytosolic calcium levels.[72] The PfPKG homologue has also been studied[73] and it constitutes one of the few examples were selective inhibition has been achieved *in vivo,* showing in particular the crucial role played by this enzyme in the differentiation from gametocytes to gametes.[74] Analyses of PfPKB demonstrated the lack of a PH domain that in human PKB interacts with phosphoinositide, regulating the enzyme activity.[75] This domain is replaced by a calmodulin-binding domain involving therefore a different type of modulation for PfPKB activity.[76]

1.7.3 The CAMK group

The CAMK group contains thirteen kinases in *Plasmodium* and five of these possess a calcium binding domain found only in plants and ciliates but not in Metazoans.[68] This observation, together with the fact that Ca^{2+} signalling regulates motility and host invasion in *Plasmodium*[77] has recently attracted large attention to this subgroup of kinases.

1.7.4 The CK1 group

Although this family is vastly expanded in various organisms (e.g. ~80 members in nematodes), the parasite possesses a single member of this group named PfCK1. PfCK1 has been isolated and characterized[78] showing a high similarity with human CK1 α isoform and sensitivity to the CK1 inhibitor CK1-7 at analogue concentrations similar to the bovine enzyme.[67]

1.7.5 The TKL group

Five malaria enzymes were initially classified into this group,[68] however more recent analyses reduced the group down to four members.[56] In the same study, PfTKL3 was

further characterized, showing the presence of a putative SAM motif and two MORN (Membrane Occupation and Membrane Nexus) motifs at the N-terminus. MORN motifs are involved in membrane interactions, while SAM domains are protein-protein interaction mediators. The domain organisation of PfTKL3 is not seen in any mammalian TKLs making this enzyme a semi-orphan kinase lacking a clear human orthologue.

1.7.6 The RGC, TK and STE groups

No members of these groups have been identified with bioinformatic analyses. Interestingly, the simultaneous absence of STE family members which usually act as MAP2K and MAP3K kinases, with the presence of MAP enzymes points to a divergent organisation of the MAPK pathways in *Plasmodium*. In particular, it has been demonstrated that the MAP kinase Pfmap-2 is phosphorylated and activated by PfNEK-1 which therefore act as a MAPK kinase but does not belong to any of the classical families.[79] The fact that TyrKs are usually involved in hormone-response receptor-linked pathways suggests that this family arose as an adaptation to intracellular communication in multicellular organisms. Therefore, their absence in *Plasmodium* is of no surprise. However putative members have been found in a few unicellular eukaryotes.[80]

1.7.7 The "other" group

This group collects all the parasite kinases that share common folding and subdomain architecture of ePKs but cannot be linked to any of the major groups describe by Hunter on the basis of the human kinome.[34] Many apicomplexan kinases fall into this group reflecting their deep evolutionary divergence from humans.[66] In *Plasmodium*

falciparum four of these enzymes display features from more than one family of ePKs and are therefore classified as "composite" enzymes.

1.7.8   The FIKK group

In the genomic study of Ward *et al.* a distinct cluster of 21 orphan protein kinases was identified and named after a shared Phe-Ile-Lys-Lys motif in the N-terminal region.[68] Further analyses[81] revealed that this family is specific to apicomplexas, while the presence of a single copy in most of *Plasmodium* genomes indicates a rapid and presumably recent expansion in the *P. falciparum* species. Interestingly, these enzymes feature an export element motif and have also been experimentally observed in the host cell membrane.[82]

1.7.9   Kinome-wide reverse genetics analysis

To further prove the hypothesis that parasite kinases represent potential and attractive targets to cure malaria a knock-out strategy has been recently developed and applied during the blood stage asexual cycle in *P. falciparum.*[83] In this study, attempts to inactivate each single kinase of the entire complement of 65 ePK genes that constitute the *P. falciparum* kinome (excluding the 21 FIKKs which are likely redundant) was achieved following a homologous recombination, single crossover gene disruption strategy. The results showed that out of the 65 enzymes, 36 were required to complete the intra-erythrocytic asexual cycle since their genomic exclusion resulted in a lethal phenotype (**Table 1.1**). The so-demonstrated essential role played by most of *Plasmodium* PKs together with the deep divergence between the host and the parasite kinomes described above strongly supports a brand-new approach based on targeting this class of enzymes to tackle malaria.[84]

PlasmoDB identifier	Name	Protein kinase group/family
PF11_0377	PfCK1	Casein Kinase 1
PF13_0258	PfTKL3	Tyrosine kinase-like
PFB0520w	PfTKL1	Tyrosine kinase-like
PFF1370w	PfPK4	eIF2α kinase
PFL1370w	Pfnek-1	NimA
PFC0755c	Pfcrk-4	CMGC/CDK
PF13_0206	PfPK6	CMGC/CDK
PFD0740w	Pfcrk-3	CMGC/CDK
MAL13P1.279	PfPK5	CMGC/CDK
PF10_0141	Pfmrk	CMGC/CDK
PFD0865c	Pfcrk-1	CMGC/CDK
PF11_0147	Pfmap-2	CMGC/MAPK
PF11_0096	PfCK2	CMGC/CK2
MAL13P1.84	—	CMGC/GSK3
PFC0525c	PfGSK3	CMGC/GSK3
PF11_0156	PfCLK3	CMGC/CDK-like
PF14_0431	PfCLK1/Pflammer	CMGC/CDK-like
PFC0105w	PfCLK4	CMGC/CDK-like
PF14_0408	PfCLK2	CMGC/CDK-like
PFL1885c	PfPK2	CamK
PFB0815w	PfCDPK1	CDPK
PF13_0211	PfCDPK5	CDPK
PFF0520w	PfCDPK2	CDPK
PFC0420w	PfCDPK3	CDPK
PFF0260w	PfARK1	Aurora
PFC0385c	PfARK2	Aurora
MAL13P1.278	PfARK3	Aurora
PF11_0464	—	AGC-related
PF11_0227	—	AGC-related
PF14_0346	PfPKG	AGC
PFL2250c	PfPKB	AGC
PFI1685w	PfPKA	AGC
MAL7P1.91	PfEST	Orphan
PF11_0488	—	Orphan
PF14_0516	PfKIN	Orphan
PF13_0085	PfPK9	Orphan

Table 1.1: *Plasmodium falciparum* PKs considered as likely dispensable for the erythrocytic asexual cycle (adapted from[83]).

1.8 CK2: a peculiar and rather fascinating protein kinase

Protein kinase CK2 (CK2), formerly known as casein kinase II is a serine/threonine protein kinase ubiquitously expressed and highly conserved throughout the eukaryote kingdom. This particular enzyme, was the first PK to be ever described and isolated back in 1954.[42] Ironically, although both their names derive from the very early report of kinase activity against casein, neither of these enzymes is responsible for casein phosphorylation *in vivo*.[85] Being studied for more than 50 years, CK2 is now a very well

characterised enzyme, with more than 300 substrates in mammalian cells reported so far.[55] In particular, the human genome encodes for two α catalytic isoforms (α and α')[86] and a single regulatory (β) subunit.[87] The α and α' subunits are structurally analogous but are products of two different genes and they possesses a catalytic domain homologous to other protein kinases. When expressed in the absence of the β subunit they are both enzymatically active; however, the presence of β subunits enhances the basal activity and modulates the specificity of protein interactions. The different subunits are present in human cells in tetrameric complex comprising two identical β subunits and two catalytic ones assembled in α/α, α/α', or α'/α' configuration (**Figure 1.15**).
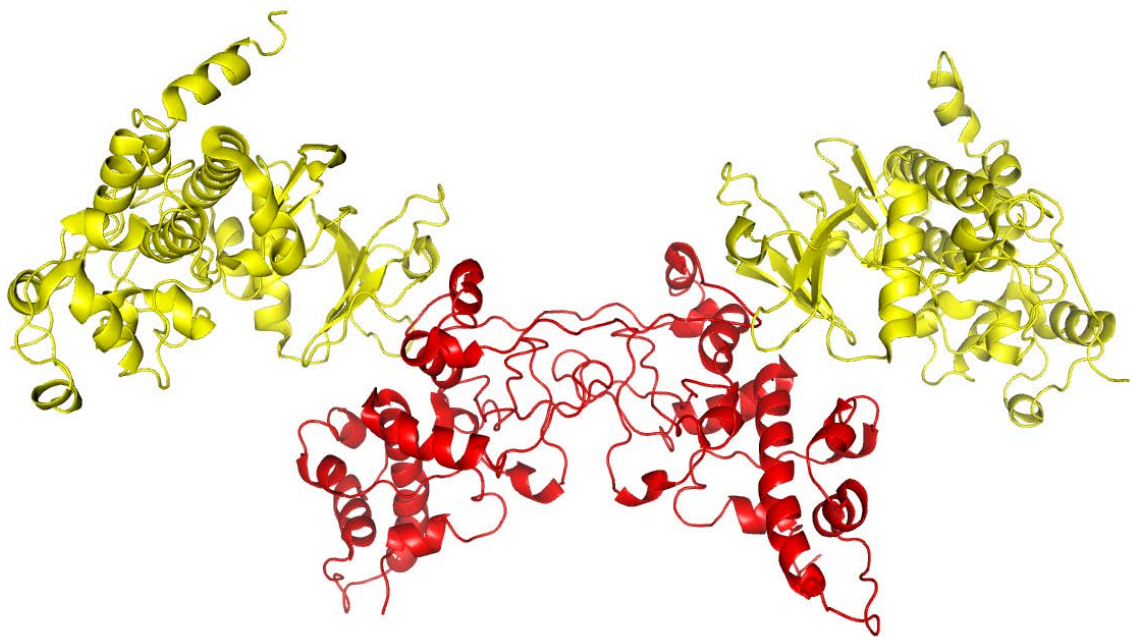
Figure 1.15: Crystal structure of CK2 human holoenzyme showing the two β subunits in red and two α subunits in yellow (PDB file: 1JWH, resolution: 3.10Å).[88]

Biochemical studies focusing on yeast and human CK2 have underlined rather peculiar and fascinating features for this enzyme with increasing evidence for its feasibility as a drug target in cancer and viral infections among the others.[89] For example, while other kinases are usually regulated in a very tight fashion, CK2 spontaneous basal activity is insensitive to any known second messenger or phosphorylation process. CK2 is therefore referred to as a constitutively active kinase whose physiological regulation still remains elusive nowadays.[90] Furthermore, despite being traditionally classified as a serine/threonine kinase there is now ample evidence for having *in vivo* tyrosine phosphorylation activity both in yeast which lacks *bona fide* protein tyrosine kinases[91] and in mammalian cells.[92] Finally, the insensitivity to staurosporine, the most potent and universal PK inhibitor together with its use of GTP as phosphate donor makes CK2 an unorthodox member of the kinase family.

1.8.1 *Plasmodium falciparum* CK2α

The *Plasmodium falciparum* genome encodes for a single putative CK2α orthologue (gene PF11_0096) named *Pf*CK2 that presents an overall 65% sequence identity with *Homo sapiens* CK2. A biochemical characterization of this protein has been recently published,[71] showing peculiar features shared by CK2 enzymes. The study demonstrated that bacterial expressed recombinant *Pf*CK2 is able to phosphorylate casein and also to autophosphorylate, although a role for this latter event has not been established yet. *In vitro* tests also showed that *Pf*CK2 has similar affinities for ATP and GTP as phosphate donors with respectively a K_m value of 16.7μM for ATP and 34.9μM for GTP. The Pf enzyme is also able to phosphorylate the CK2 peptide RRRADDSDDDDD with a K_m of 137.5 μM and it is inhibited by the CK2-specific inhibitor

TBB (3,4,5,6-tetrabromobenzotiazole) with an IC_{50} curve comparable to that of human CK2 (*Pf*CK2 IC_{50}: 2μM, *Hs*CK2 IC_{50}: 1.5μM). Together, this data confirms that *Pf*CK2 is a true member of the CK2 family. In the same study, the application of the aforementioned reverse genetic approach to *Pf*CK2 has demonstrated that blood-stage parasites lacking the enzyme are unable to survive. The evidence that *Pf*CK2 is essential for parasite viability validates it as a potential drug target. Despite this fact, no other studies regarding the role of *Pf*CK2 in the parasite biology with potential substrates or mechanisms of regulation have been reported in the literature so far.

1.8.2 **Plasmodium falciparum CK2β_1 and CK2β_2**

While humans possess only a single CK2 regulatory subunit, the *Plasmodium falciparum* genome analysis revealed the presence of two putative regulatory subunits named *Pf*CK2β_1 (PF11_0048) and *Pf*CK2β_2 (PF13_0232), bearing respectively 33% and 39% of identity with their human counterpart. Pull-down assays performed with bacterial expressed recombinant proteins showed that *Pf*CK2α is able to interact with both regulatory subunits *in vitro.*[71] Furthermore, reverse genetics analyses showed that both *Pf*CK2β_1 (PF11_0048) and *Pf*CK2β_2 subunits are essential for parasite viability during the intra-erythrocytic stage.[93] Although the stoichiometry of the *Pf*CK2 holoenzyme is not known, co-immunoprecipitation analyses of *Pf*CK2β_1 or *Pf*CK2β_2 from transgenic parasite lines expressing tagged subunits revealed that the two regulatory subunits were presents in similar amounts, together with PfCK2α. This evidence suggests that hetero-complexes containing both β_1 and β_2 may be equally abundant.[93] Moreover, the same study showed that the two immunoprecipitates obtained with PfCK2β_1 and *Pf*CK2β_2, despite displaying significant overlap in the

identity of recovered proteins, also contains specific hits suggesting functional non-redundancy.

1.9   Tyrosine phosphorylation

In comparison to threonine and serine, tyrosine phosphorylation (pTyr) was discovered much later, in 1980, in fortuitous circumstances during the study of kinase activity associated with the polyomavirus. As elegantly described by Tony Hunter in two seminal papers,[94,95] the breakthrough discovery was made during a routine phospho-amino analysis by using an "old" buffer whose pH had accidentally dropped from the stated 1.9 to 1.7. This casual change had permitted the resolution of phospho-tyrosine from phospho-threonine that co-eluted in the previous conditions. In the 30 years since its discovery, tyrosine phosphorylation has emerged as a fundamentally important mechanism of signal transduction and regulation in all eukaryotic cells, governing many processes, including cell proliferation, cell cycle progression, signalling and transcriptional activation.[96] After the description of several signalling cascades (e.g. Ras-MAPK, STAT pathways) it became clear how pTyr signalling is usually mediated by a toolkit of three distinct functional modules: a tyrosine kinase (TyrK), and a phosphotyrosine phosphatase (PTP) controlling the tyrosine phosphorylation state and a Src Homology 2 domain (SH2) that recognise and binds to the pTyr residue triggering the downstream cascade[97] (**Figure 1.16**). More recently, a new domain termed Phospho Tyrosine Binding domain (PTB) has been identified and associated with a function analogous to the SH2 domains.[98]
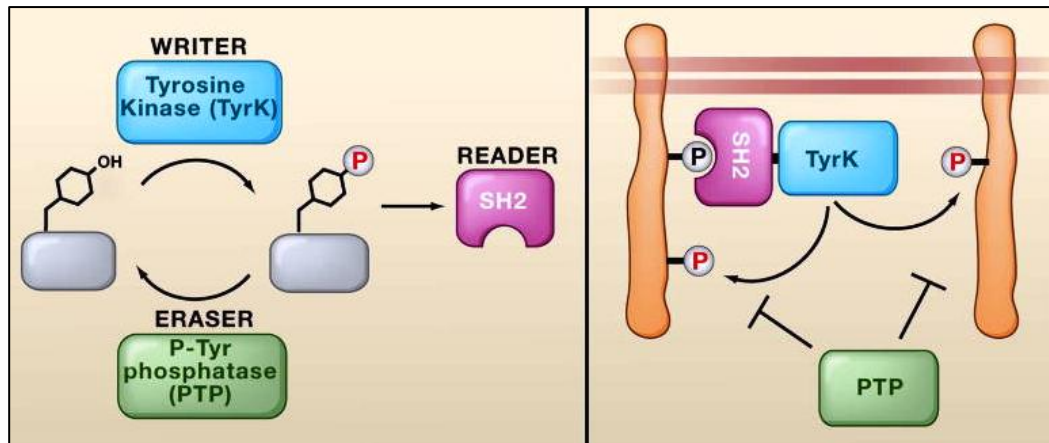
Figure 1.16: Left panel: diagram representing the three components of a pTyr signalling platform. Right panel: example of a typical pTyr signal cascade showing the recruitment of an SH2-TyrK protein to an initiating pTyr site that leads to Tyr phosphorylation amplification through a positive feedback loop (adapted from[99]).

The main difference between these two domains is that while SH2-type domains recognize phosphotyrosine residues and adjacent carboxy-terminal residues, it is residues that are amino-terminal to the phosphorylated tyrosine residue that confer PTB-domain binding specificity.[100] The modular classification described above has turned out to be particularly useful not only for the direct description of pTyr signalling pathways, but also for the comparison of this molecular system among different species from an evolutionary point of view. Since tyrosine phosphorylation plays a central role in growth factor cell response, and in the control of cell differentiation and development, it has been thought for a long time that pTyr events were an exclusive prerogative of higher eukaryotes. However, recent reports (reviewed in[101]) of the presence of pTyr signalling cascade components in model lower eukaryotes have changed this earlier assumption (**Figure 1.17**).
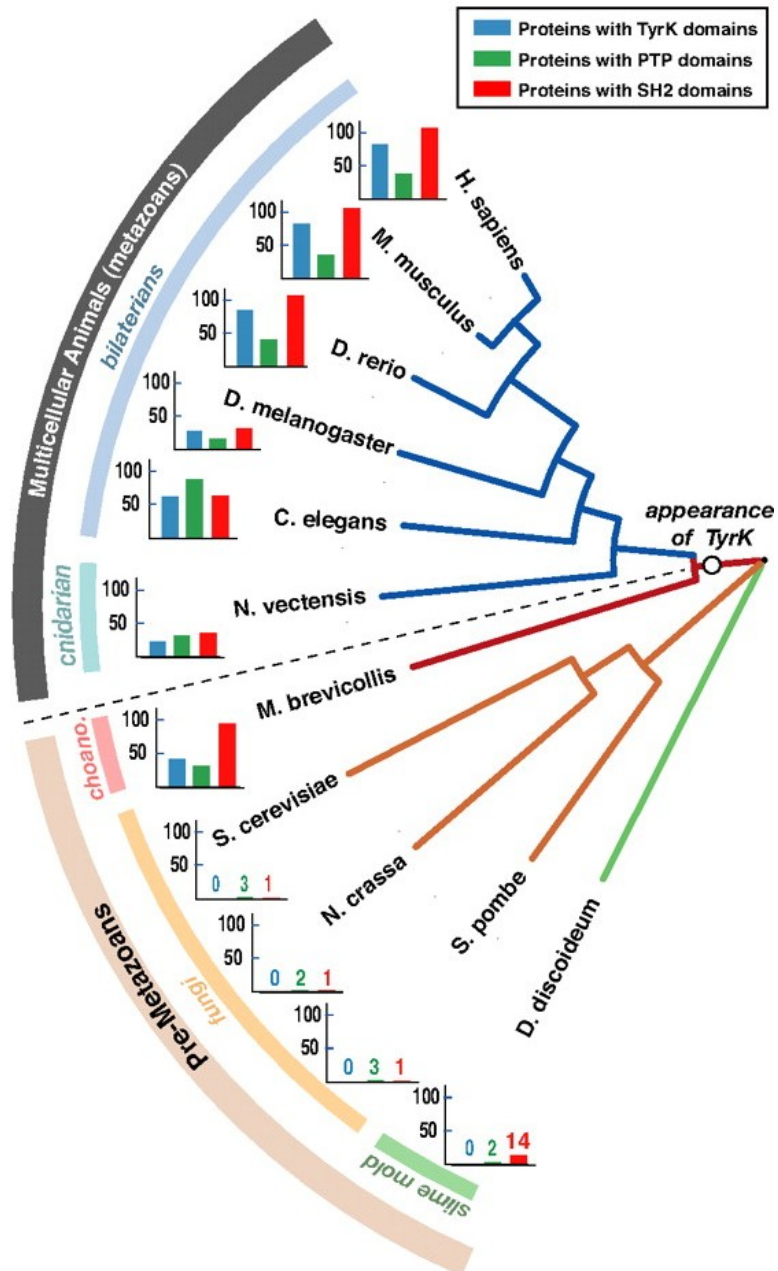
Figure 1.17: Number of proteins containing TyrK, PTP, or SH2 domains by species. Only choanoflagellates and metazoans have high numbers of all three domains. All other pre-metazoans only have small numbers of PTP and SH2 domain proteins (no TyrK). These data imply an early evolution of PTP and SH2 domains, followed by an expansion in all domains only after invention of the TyrK domain (adapted from[102]).

The most ancient organism to possess a full pTyr signalling kit is the chronoflagellate *Monosiga brevicollis* which is the closest single cell eukaryote to animals. Furthermore, genetic analyses have showed the presence of PTP and SH2 domains also in the amoeba *Dictyostelium discoideum* which however lacks *bona fide* tyrosine kinases. Interestingly, this organism is characterised by a unicellular lifestyle in the presence of bacterial food which starts to aggregate and to form multicellular structures when food is depleted. It has been showed that the elements of *Dictyostelium* pTyr machinery are involved in such differentiation process, underlying the role that pTyr signalling has played in cellular response to external stimuli since its origin and in the advent of metazoan multicellularity.[99]

The simplest pTyr machinery so far described in the eukaryote kingdom belongs to the fungus *Saccharomyces cerevisiae*. In fact, sequence analyses of the budding yeast have showed the presence of a single SH2 domain prototype and three PTPs.[102] Although the single SH2 domain does not show pTyr binding, its sequence and structure are closely related to functional SH2 proteins and can be therefore considered as their evolutionary ancestor. Interestingly, phospho-amino analysis of yeast has also revealed a small but significant population of pTyr.[103]

1.9.1 Tyrosine phosphorylation in *Plasmodium falciparum*

As previously described, the *Plasmodium falciparum* kinome lacks any *bona fide* tyrosine kinase, and the recognised tyrosine kinase-like kinases have only been associated with Ser/Thr phosphorylation activity, so far. Moreover, no reports for the presence of putative SH2 domains in *Plasmodium falciparum* genome can be found in literature. Instead, several PTPs have been recognised[104] and in one case linked with *in*

vitro pTyr phosphatase activity.[105] Regarding pTyr occurrence, early accounts have demonstrated the presence of tyrosine phosphorylation activity associated with the parasite membrane, during the intra-erythrocytic stage;[106] while, more recently, a phospho-aminoacid analysis carried out in our lab by Dr. Lev Solyakov has showed that pTyr accounts for ~1% of the total phospho-proteome during the schizont stage (**Figure 1.18**).
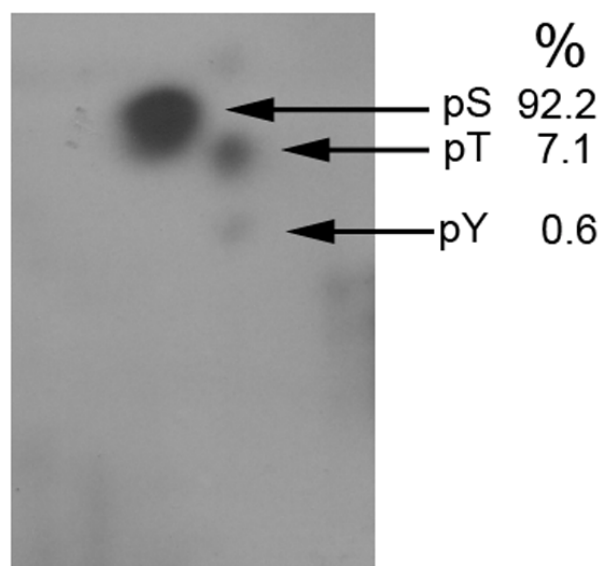
Figure 1.18: Autoradiograph of a phospho-aminoacid analysis of *P. falciparum* lysate from metabolically labelled schizont stage parasites (adapted from[83]).

This presence, as in other eukaryotes lacking conserved tyrosine kinases (e.g. *S. cerevisiae*), can be explained by the activity of dual-specificity kinases. In fact, despite overall belonging to Ser/Thr kinase groups, this type of enzymes can also phosphorylate tyrosine residues. However, apart from this preliminary data, no important study regarding pTyr pathways in *P. falciparum* describing substrates, dual-specificity kinases and potential roles for such events have been carried out so far.

Aim of the project

Malaria is one of the most widespread diseases in the modern World where both 247 million cases and 1.2 million deaths are registered every year. The spread of drug resistance in *Plasmodium falciparum*, the parasitic protozoan responsible for the vast majority of lethal cases of malaria, renders the development of novel chemotherapeutic agents an urgent task. Kinases are important regulatory enzymes in eukaryotes involved in key processes such as homeostasis, metabolism, and cell cycle progression and constitute already successful targets in the treatment of other diseases (e.g. cancer, leukemia). Thus, elucidation of their role also in the context of malaria could potentially reveal important pathways to be targeted by the next generation of antimalarials.

The aim of the present study is to functionally characterise *Plasmodium falciparum* CK2 (PfCK2), one of the most interesting and crucial members of the kinase family in *Plasmodium falciparum*. The pleiotropic nature of CK2 has already been showed in mammalian cells together with its high basal activity and ubiquitous expression, underlining a central role in the cell biology of eukaryotes. According to genome analyses, *Plasmodium falciparum* possesses only one member of the CK2 family which has already been isolated and shown to be essential during the parasite intra-erythrocytic stage. However, potential substrates, mechanisms of *in vitro* inhibition, and interaction with the two regulatory subunits present in *P. falciparum* still remain elusive. The focus of this work is therefore to shed light on such aspects in order to

both improve our understanding over the role played by PfCK2 in the parasite biology, and to potentially lead to the design of parasite specific PfCK2 inhibitors.

The second aim of my PhD thesis is to investigate the scope and importance of tyrosine phosphorylation in *Plasmodium falciparum*. This post-translational modification has been associated for a long time with only higher eukaryotes, in particular due to the lack of putative tyrosine kinases in lower eukaryotes genomes. However, preliminary data obtained in our lab showed that, despite the absence of putative tyrosine kinases in the *P. falciparum* genome, tyrosine phosphorylation accounts for ~1% of the *Plasmodium falciparum* phospho-proteome. Thus, the work here presented focuses on the study of *Plasmodium falciparum* tyrosine phosphorylation pathways, with the attempt to isolate and determine potential substrates as well as the kinases responsible for such events. Such analyses altogether, are aimed at improving our understanding of phosphorylation pathways in *Plasmodium falciparum*, thus verifying their potential as prospective anti-malarial drug targets.

Chapter 2: Material and Methods

2.1 Materials

2.1.1 Reagents

Chemical reagents were purchased from Sigma Aldrich (Dorset, UK) except for: N-hydroxysuccinimide biotin ester from ABCR GmbH (Karlsruhe, Germany), quinalizarin from CHEMOS GmbH (Regenstauf, Germany), and D4476 from Tocris Bioscience (Bristol, UK). Solvents were purchase from Fischer Scientific (Loughborough, UK).

Cell culture reagents were purchased from Invitrogen (Glasgow, UK), BL21-codon plus and XL1-Blue competent cells were purchased from Agilent Technologies (Stockport, UK), α-select chemically competent cells were from Bioline (London, UK). For GST fusion proteins, the pGEX-4T vector was provided by our collaborator Christian Doerig (Monash University, Melbourne Australia); for His$_6$-tagged fusion proteins the vector pQE-30 was also provided by Christian Doerig while pLEICS-05 was provided by Dr. Xiaowen Yang (University of Leicester, Leicester UK). The coding DNA for N-terminal fragment MCM2 expression was purchased from Eurofins MWG Operon (Ebersberg, Germany), inserted in a pCR2.1 vector.

Radioisotope [^{32}P]-ATP (specific activity 3000Ci7mmol) was purchased from Perkin Elmer Life Science. [^{32}P]-orthophosphate (10mCi/ml) was purchased from Amersham Bioscience UK limited (Buckinghamshire, UK). High performance autoradiography film was purchased from GE Healthcare (Buckinghamshire, UK).

For SDS-PAGE gels, Tris-HCl buffer and 30% acrylamide solution and precision plus unstained protein standards were purchased from Bio-Rad (Herefordshire, UK); TEMED, ammonium persulfate, Brillant Blue G-Colloidal solution and Brillant Blue R-250 were purchased from Sigma Aldrich.

For Western Blotting experiments, nitrocellulose transfer membrane was purchased from Whatman (Dassel, Germany) and Western Blot film from Bio-Rad. ECL Western Blot detection system and Tween-20 were purchased from Amersham Biosciences UK limited. High performance chemiluminescence film was purchased from GE Healthcare and Ponceau staining solution from Sigma Aldrich.

His-tag antibody was purchased from Santa Cruz Biotechnology Inc. (Santa Cruz CA, USA). MCM2, and PF11_0156 both phospho-specific and structural antibodies were purchased as a custom synthesis from Eurogentec (Southampton, UK). Polyclonal rabbit and rat secondary antibodies were purchased from Bio-Rad. For pull-down assay anti-phosphotyrosine, recombinant clone 4G10®agarose conjugate was purchased from Millipore (Waltford, UK).

For phosphotyrosine immunoprecipitation Anti-Phosphotyrosine, recombinant clone 4G10 agarose coniugate was purchased from Millipore. For GST fusion protein purification, Amintra glutathione resin was purchased from Expedeon (Haxton, UK), while for His_6 tagged proteins the Ni-NTA superflow nickel-charged resin from Qiagen (Crawley, UK) was used. For elution, protease and phosphatase inhibitor cocktail tablets were purchased from Roche (Mannheim, Germany) and dialysing cassettes from Bio-Rad.

For DNA purification, Nucleospin Extract II kits were purchased from Macherey-Nagel (Düren, Germany) and Plasmid Isolation kits from Roche. Enzymes for molecular biology (BamHI, DpnI, EcoRI) were purchased from Roche except for PfuTurbo DNA Polymerase from Stratagene (La Jolla CA, USA), PfuUltra from Agilent Technologies and Phusion DNA Polymerase and T4 DNA ligase from New England Biolabs (Ipswich, MA, USA). 10x SuRE/Cut buffer H was purchased from Roche and recombinant His6-TEV was provided by Protex (University of Leicester).

For kinase assay, human casein kinase II, 10x CK2 kinase buffer and CK2 peptide substrate RRRADDSDDDDD were purchased from New England Biolabs, RRREEETEEE peptide from Promega (Southampton, UK) and ZipTip from Millipore.

For Immunocytochemistry, VECTASHIELD mounting medium with DAPI was purchased from Vector Laboratories Inc. (Burlingame CA, USA).

Columns for protein separation and desalting: Resource Q (1ml), Resource S (1ml), HiTrap Blue (1ml) and HiTrap heparin HP (1ml), Hi Trap Desalting (5ml) were all purchased from GE Healthcare except from CHT ceramic hydroxyapatite purchased from Bio-Rad.

2.1.2 Apparatus

The following apparatus has been used in the experimental procedures:

for centrifuging eppendorf: Eppendorf centrifuge 5417R;

for Bradford assay: Eppendorf biophotometer;

for radioactive counting: Wallac Winspectral 1414 liquid scintillation counter;

for protein separation: GE Amersham Pharmacia AKTA Purifier

for immunocytochemistry: Zeiss LSM 510 confocal microscope.

2.1.3 General buffers composition

Coomassie stain: 50% MeOH, 10% acetic acid, 40% water, 0.05% Brilliant Blue R-250

Krebs buffer (10x): 1.26M NaCl, 25mM KCl, 250mM $NaHCO_3$, 12mM NaH_2PO_4, 12mM $MgCl_2$, 25mM $CaCl_2$, pH 7.2

Laemmli buffer (2X): 4%SDS, 20% glycerol, 10% 2-mercaptoethanol, 0.004% bromphenol blue and 0.125M Tris, pH 6.8

LB culture medium: 10g/l NaCl, 10g/l tryptone, 5g/l yeast extract, pH 7.5

PBS buffer: 8g/l NaCl, 0.2g/l KCl, 1.44g/l Na_2HPO_4, 0.24g/l KH_2PO_4, pH 7.4

Running SDS-PAGE gel solution: 1g/l Brillant Blue 25mM Tris, 192mM glycine, 0.1%SDS pH 8.3

SOC medium: 2% Tryptone, 0.5% Yeast Extract, 10mM NaCl, 2.5mM KCl, 10mM $MgCl_2$, 10mM $MgSO_4$, 20mM glucose

TAE buffer: 40mM Tris acetate, 1mM EDTA

TBS buffer: 20mM Tris, 150mM NaCl, pH 7.4

TBS-T buffer:20mM Tris, 150mM NaCl, 0.1% tween, pH 7.4

TEG buffer: 50mM Tris, 0.5mM EDTA, 5% β-glycerol phosphate, pH 7.6

2.2 Chemical synthesis

2.2.1 General Experimental information

Solvents were evaporated at reduced pressure using a Buchi Rotavapor rotary evaporator.

Thin layer chromatography of compounds was carried out using Merk silica gel 60 F254 thin layer chromatography plates.

To purify compounds, column chromatography was carried out using Fluka silica gel 60.

Low resolution electrospray mass spectra were recorded using a Micromass Quattro-LC mass spectrometer using electrospray ionisation from solution and a quadrupole analyser.

Nuclear Magnetic Resonance spectra were recorded using Bruker Biospin DPX300 – 5mm QNP probe (1H) with Z axis gradient, XWIN-NMR v 3.5-p10, 1H=299.90 MHz; and Bruker Biospin DPX400 – 5mm QNP probe (1H), XWIN-NMR v 3.5-p16, 1H=400.13 MHz.

MALDI-TOF spectra were recorder using a Voyager-DE STR Biospectrometry Workstation.

2.2.2 Synthesis of 1-azido-2-(2-(2-(2-azidoethoxy)ethoxy)ethoxy)ethane (3)[107]
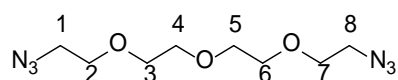
compound (**3**)

To a solution of tetra-ethylene glycol (3.46ml, 20mmol) in THF (22ml) was added methane sulfonyl chloride (4.64 ml, 60mmol). The solution was cooled to 0°C and triethylamine (6.97ml, 50mmol) added dropwise over an hour. The reaction mixture was then allowed to warm up to room temperature and left stirring overnight. After that, the mixture was diluted with water (22ml) and organic solvent was removed by rotary evaporation. To the aqueous mixture $NaHCO_3$ (1.512g, 18mmol) and NaN_3 (5.2 g, 80mmol) were then added and refluxed overnight. The mixture was finally extracted with chloroform (100ml) five times, the organic layer dried with $MgSO_4$, filtered and concentrated *in vacuo*. Flash column chromatography (SiO_2) eluting with $MeOH:CHCl_3$ 1:1 provided (**3**) (3.273 g, 67 %) as a yellow pale oil.

^{1}H NMR (400MHz, $CDCL_3$) δ3.42 (4H; t, ^3J = 5.24Hz; CH_2 1,8), 3.69-3.79 (12H; m, CH_2 2,3,4,5,6,7).

2.2.3 Synthesis of 2,2'-(2,2'-oxybis(ethane-2,1-diyl)bis(oxy))diethanamine (4)[108]
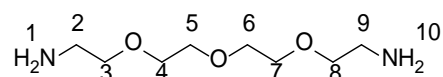
compound (**4**)

To a solution of (**3**) (4.88g, 20mmol) in degassed MeOH (30ml) was added 10% Pd/C (1.25g). The reaction mixture was saturated with H_2 gas and stirred at room temperature overnight. The reaction mixture was filtered and solvent removed by rotary evaporation providing (**4**) (3.538g, 92%) as a yellow pale oil.

ES-MS: [M+1]: 193

^{1}H NMR (400MHz, $CDCL_3$) δ1.89 (4H; s, NH_2 1,10), 2.87 (4H; t, ^3J = 4.6Hz $CH_2$2,9), 3.52 (4H; t, ^3J = 5.2Hz; CH_2 3,8), 3.62-3.68 (8H; m, $CH_2$4,5,6,7).

2.2.4 Synthesis of Tert-butyl (2-(2-(2-(2-aminoethoxy)ethoxy)ethoxy)ethyl) carbamate (5)[109]
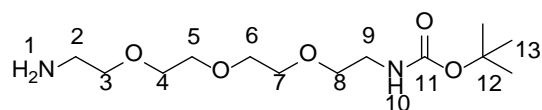
compound (5)

To a solution of (4) (3.85g, 20mmol) in THF (60ml) and MeOH (15ml) a THF solution (20ml) of BOC$_2$O (3.93g, 18mmol) was added dropwise under N$_2$ atmosphere for 3 hours. The reaction mixture was then left stirring overnight. The solution was finally concentrated and the product purified with flash chromatography (SiO$_2$) eluting with a gradient MeOH : CH$_2$Cl$_2$ (1:4) that provided (7) (1.93g, 33%) as a yellow pale oil.

ES-MS: [M+1]: 293

^{1}H NMR (400MHz, CDCL$_3$) δ1.46 (9H; s, CH$_2$ 13), 1.94 (2H; s, NH$_2$ 1), 3.23-3.27 (2H, m, CH$_2$ 2), 3.35 (2H, t, ^3J = 5.08Hz, CH$_2$9), 3.61 (4H, t, ^3J = 5.1Hz CH$_2$ 3,8), 3.62-3.93 (8H, m, CH$_2$4,5,6,7), 5.32 (1H; s, NH$_2$ 10).

2.2.5 Synthesis of Tert-butyl(13-oxo-17-((3aR,4R,6aS)-2-oxohexahydro-1H-thieno[3,4-d]imidazol-4-yl)-3,6,9-trioxa-12-azaheptadecyl)carbamate (19)[110]
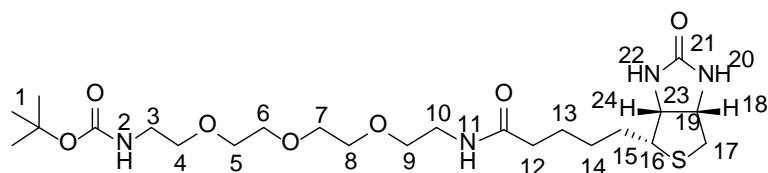
Compound (19)

Compound (5) (1.2g, 4mmol) was mixed together with biotin N-hydroxysuccinimide ester (1.77g, 4mmol), HCl 1M (4ml, 4mmol) and NaHCO$_3$ (0.84g, 10mmol) in DMF

40ml). The reaction was left stirring overnight and concentrated by rotary evaporation. The mixture was purified by flash column chromatography (SiO$_2$) eluting with MeOH:DCM 1:9 that provided (**19**) (0.865g, 42%) as a yellow pale oil.

ES-MS: [M+1]: 520

^{1}H NMR (400MHz, CDCL$_3$) δ 1.23-1.31 (2H, m, CH$_2$ 14), 1.35-1.37 (2H, m, CH$_2$ 13), 1.45-1.50 (2H, m, CH$_2$ 15), 1.57 (9H, s, CH$_3$ 1), 2.23-2.35 (2H, m, CH$_2$ 12), 3.20-3.54 (4H, m, CH$_2$ 3,10), 3.64-3.69 (12H, m, CH$_2$ 4,5,6,7,8,9) 3.78-3.95 (2H, m, CH$_2$17), 4.55-4.67 (2H, m, CH 24,18).

2.2.6 Synthesis of N-(2-(2-(2-(2-aminoethoxy)ethoxy)ethoxy)ethyl)-5-((3aS,4S,6aR)-3a,6a-dimethyl-2-oxohexahydro-1H-thieno[3,4-d]imidazol-4-yl)pentanamide (6)

Compound (**6**)

A solution of Compound (**19**) (0.987g, 2mmol) in TFA:CHCl$_3$ 1:1 (20ml) was stirred for 30min. The mixture was concentrated by rotary evaporation and subsequently dissolved up in THF (30ml) and evaporated to dryness (3x). Same procedure was repeated (3x) with water (30ml) providing (**8**) (0.839g, 47%) as a yellow pale oil.

ES-MS: [M+Na]: 441

^{1}H NMR (400MHz, CDCL$_3$) δ 1.44-1.59 (2H; m, CH$_2$ 14), 1.67-1.90 (4H, m, CH$_2$ 13,15), 2.15-2.38 (2H; m, CH$_2$ 12), 2.71-2.82 (2H; m, CH$_2$ 17), 2.92-3.02 (1H; m, CH16), 3.16-

3.29 (2H; m, CH$_2$ 2), 3.42-3.54 (2H; m, CH$_2$ 9), 3.58-3.76 (12H; m, CH$_2$3,4,5,6,7,8), 4.39-4.47 (1H; m, CH 24), 4.55-4.66 (1H; m, CH 18).

2.2.7 Synthesis of the ATP biotin analogue (7)[111]
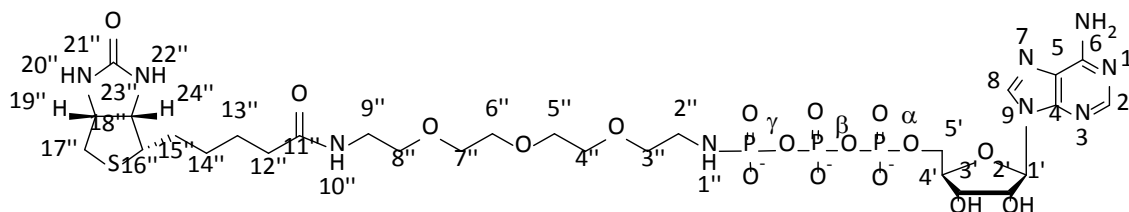
Compound (7)

Adenosine 5'-triphosphate disodium salt hydrate (0.174g, 0.315mmol) was dissolved in water (150ml) mixed with EDAC (0.293g, 1.89mmol), compound **6** (0.263g, 0.63mmol) and left stirring for 2hrs at room temperature. The mixture was then concentrated with a freeze drier and purified by ion exchange chromatography on a Sephadex column running a gradient between 50mM and 600mM of TEAB (pH7.8). To further purify the ATP analogue a reverse phase HPLC was also performed running a gradient from 2% to 30% of solvent B (solvent A: water 0.1% TEAA; solvent B: 80% ACN 20% water 0.1% TEAA) providing (**9**) (61.7mg, 21%) as a white powder. The product was finally dissolved in water to a final 25mM concentration. The concentration was determined by measuring the absorbance at 260nm, using a molar extinction coefficient of 15,000 M^{-1}cm^{-1}.[112]

ES-MS: [M+1]: 908

^{1}H NMR (400MHz, D$_2$O) δ 1.28-1.36 (2H; m, CH$_2$ 14''), 1.45-1.60 (4H; m, CH$_2$ 13'', 15''), 2.19 (2H; t, ^3J =7.16Hz, CH$_2$ 12''), 2.98-3.04 (2H; m, CH$_2$ 2''), 3.19-3.24 (2H; m, CH$_2$ 9''), 3.28-3.35 (2H; m, CH$_2$ 17''), 3.49 (1H; t, ^3J = 5.76Hz, CH 16''), 3.52-3.72 (12H, m, CH$_2$ 3'',4'',5'',6'',7'',8''), 4.3-4.35 (2H; m, CH$_2$ 5'), 4.50-4.53 (2H; m, CH 4',24''), 4.64-4.73

(1H, m, CH 19''), 4.72-4.75 (2H; m, CH 2',3'), 6.07 (1H, d, ^3J = 6.04Hz CH 1'), 8.19 (1H; CH 2), 8.50 (1H; s, CH 8).

^{31}P NMR (400MHz, D$_2$O) δ -23.13-22.33 (1P; m, P β), -11.74-11.06 (1P; m, P α), -1.59-1.12 (1P; m, P γ).

2.2.8 Synthesis of tert-butyl (13-oxo-3,6,9-trioxa-12-azaheptadec-16-yn-1-yl)carbamate (20)[113]
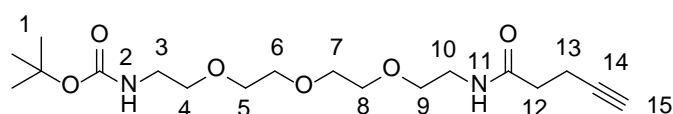
Compound (20)

Pentynoic acid (0.235g, 2.4mmol), DIPEA (1ml, 6mmol), DMAP (40mg, 300μmol) and DCC (0.6g, 3mmol) were dissolved in DMF (8ml) and left stirring for 30min. At the same time, compound (5) (0.7g, 2.4mmol) was dissolved in DMF (4ml), treated with DIPEA (1ml, 6mmol) and left stirring for 30min. The two solutions were then mixed together and left stirring overnight. The mixture was concentrated by rotary evaporation and purified by flash column chromatography (SiO$_2$) eluting with ethyl acetate that provided (20) (0.894g, 47%) as a yellow pale oil.

ES-MS: [M+1]: 373

^{1}H NMR (400MHz, CDCL$_3$) δ (9H, s, CH$_3$ 1), 2.04 (1H, t, ^3J = 2.60Hz, CH 15), 2.41-2.47 (2H, m, CH$_2$ 13), 2.53-2.59 (2H, m, CH$_2$ 12), 3.47-3.53 (2H, m, CH$_2$ 3), 3.28-3.39 (2H, m, CH$_2$ 10), 3.55-3.62 (4H, m, CH$_2$ 4,9), 3.63-3.70 (8H, m, CH$_2$ 5,6,7,8).

2.2.9 Synthesis of N-(2-(2-(2-(2-aminoethoxy)ethoxy)ethoxy)ethyl)pent-4-ynamide (8)
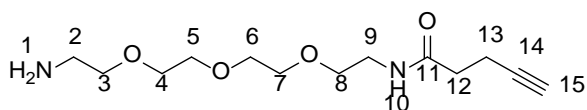
Compound (8)

Compound (20) was dissolved in a 1:1 mixture of TFA:CHCl$_3$ (20ml) and stirred for 30min at RT. The solution was then evaporated to dryness by rotary evaporation, dissolved up in THF (30ml) and evaporated to dryness again (3x). Same procedure was repeated (3x) with water (30ml) affording (8) (0.379g, 58%) as a yellow pale oil.

ES-MS: [M+1]: 273

1H NMR (300MHz, CDCL$_3$) δ 2.02 (1H; t, ^3J = 2.49Hz, CH15), 2.44-2.52 (4H; m, CH$_2$ 12,13), 2.95 (2H; m, CH$_2$ 2), 3.00 (2H; m, CH$_2$ 9), 3.45-3.50 (4H, m, CH$_2$ 3,8), 3.55-3.66 (8H; m, CH$_2$ 4,5,6,7), 6.85 (1H; s, NH 10), 7.8 (2H; s, NH$_2$ 1).

2.2.10 Synthesis of ATP alkyne analogue (9)[111]
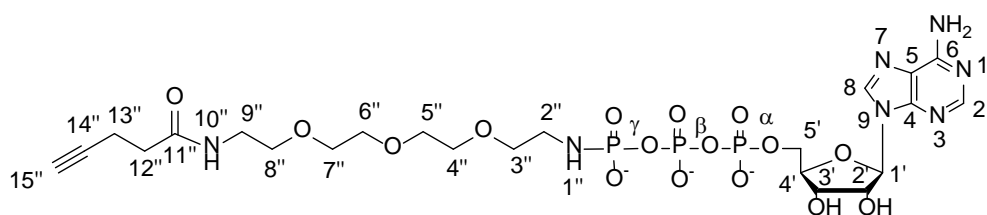
Compound (8)

Adenosine 5'-triphosphate disodium salt hydrate (0.174g, 0.315mmol) was dissolved in a solution of 1:1 water:THF (60ml) mixed with EDC (0.23g, 1.9mmol), compound (5) (0.172g, 0.63mmol) and left stirring for 2hrs at room temperature. The mixture was then concentrated by freeze drying and purified by ion exchange chromatography on a

Sephadex column running a gradient between 50mM and 600mM of TEAB (pH7.8). To further purify the ATP analogue a reverse phase HPLC was also performed running a gradient from 2% to 30% of solvent B (solvent A: water 0.1% TEAA; solvent B: 80% ACN 20% water 0.1% TEAA) providing (**9**) (61.7mg, 21%) as a white powder. The product was finally dissolved in water to a final 25mM concentration. The concentration was determined by measuring the absorbance at 260nm, using a molar extinction coefficient of 15,000 $M^{-1}cm^{-1}$.[112]

ES-MS: [M-1]: 760

1H NMR (300MHz, D_2O) 2.21-2.24 (1H; m, CH 15''), 2.26-2.34 (4H; m, CH_2 12',13'), 2.88-2.96 (2H, m, CH_2 2''), 3.19-3.28 (2H, m, CH_2 9''),3.37-3.54 (12H, m, CH_2 3'',4'',5'',6'',7'',8''), 4.02-4.15 (2H; m, CH_2 5'), 4.19-4.26 (1H; m, CH 4'), 4,37-4.43 (1H, m, CH 3'), 4.58-4.70 (1H, m, CH 2'), 5.94 (1H, d, ^3J = 5.94Hz CH 1'), 8.07 (1H; CH 2), 8.40 (1H; s, CH 8).

^{31}P NMR (400MHz, D_2O) δ -23.29-22.67 (1P; m Pβ), -11.85-11.38 (1P; m, P α), -1.78-1.32 (1P; m, P γ).

2.2.11 Synthesis of 2-(2-(2-(2-azidoethoxy)ethoxy)ethoxy)ethanamine (10)[114]
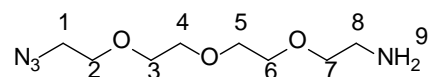
Compound (**10**)

Compound (**3**) (4.4g, 18mmol), was mixed together with H_3PO_4 85% (1.5ml, 20mmol), water (25ml) and cooled to 0°C. A solution of PPh$_3$ (4.4g, 17mmol) in diethylether (20ml) was added drop-wise under nitrogen atmosphere while keeping the temperature below 5°C. After the addition the mixture was allowed to warm up to

room temperature and left stirring overnight. The biphasic solution was separated and the aqueous layer washed with diethylether (100ml) three times. KOH (5.3g, 95mmol) was dissolved in water (10ml) and added drop-wise at 0°C; the mixture was then left stirring at 0°C overnight. The solution was filtered and the filtrate cooled to 0°C and basified with KOH 10M. The mixture was finally extracted with $CHCl_3$ (100ml) four times and the extract dried over $MgSO_4$. Flash column chromatography (SiO_2) eluting with $CHCl_3$:MeOH 5:1 provided (**10**) (2.433g, 62%) as a yellow pale oil.

ES-MS: [M+1]: 219

1H NMR (400MHz, $CDCL_3$) δ1.57 (2H; s, NH_2 9), 2.88 (2H; t, ^3J = 4.6Hz $CH_2$8), 3.38-3.42 (2H; m, $CH_2$1), 3.50-3.54 (2H, m, CH_2 7), 3.62-3.70 (10H; m, $CH_2$2,3,4,5,6).

2.2.12 Synthesis of the ATP azide analogue (11)[111]
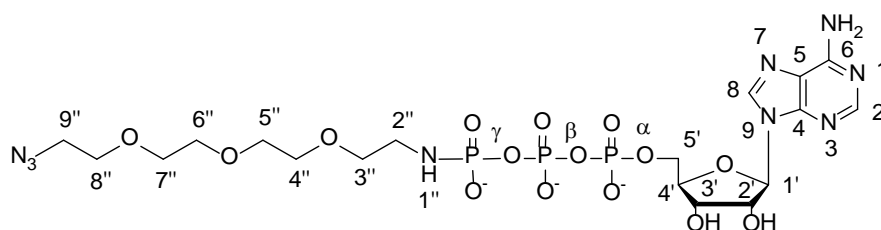
Compound (**11**)

Adenosine 5'-triphosphate disodium salt hydrate (0.174g, 0.315mmol) was dissolved in a solution of 1:1 water:THF (60ml) mixed with EDC (0.283g, 1.89mmol), compound (**10**) (0.137g, 0.63mmol) and left stirring for 2hrs at room temperature. The mixture was then concentrated by freeze drying and purified by ion exchange chromatography on a Sephadex column running a gradient between 50mM and 600mM of TEAB (pH7.8). To further purify the ATP analogue a reverse phase HPLC was also performed running a gradient from 2% to 30% of solvent B (solvent A: water 0.1% TEAA; solvent

B: 80% ACN 20% water 0.1% TEAA) providing (**11**) (39.2mg, 18%) as a white powder. The product was finally dissolved in water to a final 25mM concentration. The concentration was determined by measuring the absorbance at 260nm, using a molar extinction coefficient of 15,000 $M^{-1}cm^{-1}$.[112]

ES-MS: [M+1]: 708

1H NMR (300MHz, D_2O) 2.92-3.03 (2H; m, CH_2 2''), 3.34-3.41 (2H; m, CH_2 9''), 3.54-3.62 (12H, m, CH_2 3'',4'',5'',6'',7'',8''), 4.08-4.18 (2H; m, $CH_2$5'), 4,26-4.32 (1H, m, CH 4'), 4.60-4.75 (2H, m, CH 2',3'), 6.02 (1H, d, ^3J = 5.91Hz CH 1'), 8.16 (1H; CH 2), 8.46 (1H; s, CH 8).

^{31}P NMR (300MHz, D_2O) δ -23.17-22.53 (1P; m P β), -11.62-11.12 (1P; m, P α), -1.35-1.18 (1P; m, P γ).

2.2.13 Attempted synthesis of the ATP-dansyl analogue (13)[111]
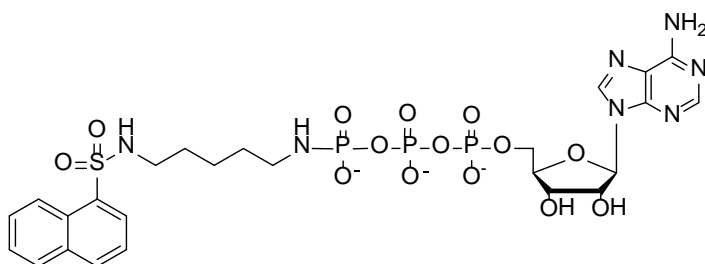
Compound (**13**)

Adenosine 5'-triphosphate disodium salt hydrate (0.138g, 0.25mmol) was dissolved in water (20ml) mixed with EDAC (0.233g, 1.5mmol), dansylcadaverine (0.168g, 0.5mmol) and left stirring for 2hrs at room temperature. The mixture was then concentrated by freeze drying and purified by ion exchange chromatography on a Sephadex column

running a gradient between 50mM and 600mM of TEAB (pH7.8). At this stage no ATP derivative was observed in the chromatogram. The mixture was also analysed by HPLC, but also in this case only the starting material ATP was detected. The same reaction was repeated overnight, and in alternative in a solution of 1:1 water:DMF (30ml) but in both cases, neither the ion exchange chromatography nor the HPLC analysis detected any product.

2.2.14 Synthesis of 3-(4-(3-(2-(2-aminoethoxy)ethylamino)-3-oxopropyl)-1H-1,2,3-triazol-1-yl)-2-oxo-2H-chromen-7-yl acetate (15)[115]
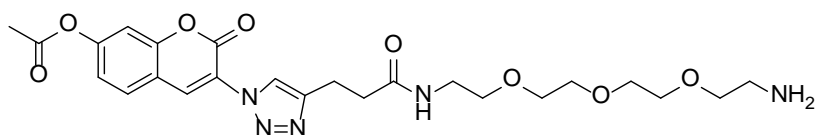
Compound (**15**)

Compound (**8**) (73.5mg, 0.27mmol) was mixed with 3-azido-2-oxo-2H-chromen-7-yl acetate (85.8mg, 0.35mmol), CuSO$_4$ (67mg, 0.27mmol), ascorbic acid (0.19g, 1.08mmol) and left stirring for 1 hour at RT. The solvent was removed on a freeze drier overnight. The sample was then dissolved in ethyl acetate (20ml), washed with a NaCl saturated water solution (20ml) twice and purified by HPLC providing (**15**) (7.5mg, 6.5%) as a yellow powder.

ES-MS: [M+1]: 518

2.2.15 Attempted synthesis of compound (16)[111]
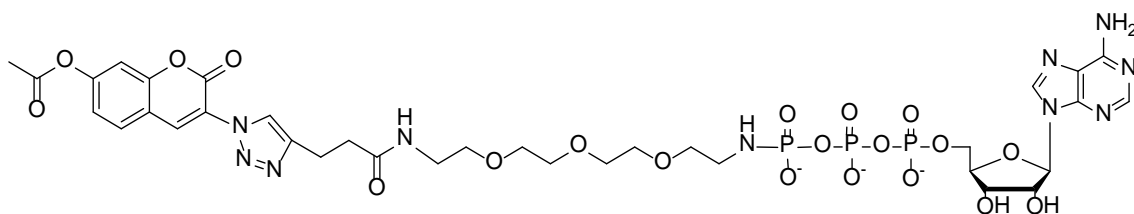
Adenosine 5'-triphosphate disodium salt hydrate (7mg, 12.8μmol) was dissolved in water (4ml) mixed with EDC (11.9mg, 77μmol), compound (15) (7.5mg, 17.5μmol) and left stirring for 2hrs at room temperature. The mixture was then concentrated with a freeze drier and purified by ion exchange chromatography on a Sephadex column running a gradient between 50mM and 600mM of TEAB (pH7.8). At this stage no ATP derivative was observed in the chromatogram.

2.2.16 Synthesis of the ATP coumarin analogue (18)[115]
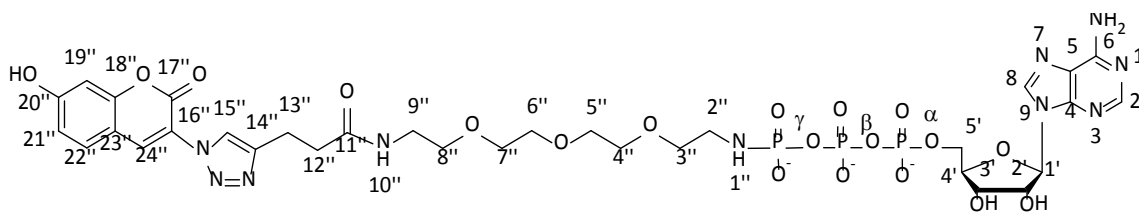
Compound (18)

Compound (9) (18.6mg, 25μmol) was mixed with 3-azido-7-hydroxy-2H-chromen-2-one (10mg, 50μmol), CuSO$_4$ (12.5mg, 50μmol) and ascorbic acid (70mg, 400μmol) in water (4ml) and left stirring for 1 hour at RT. The mixture was then concentrated by freeze drying and purified by ion exchange chromatography on a Sephadex column running a gradient between 50mM and 600mM of TEAB (pH7.8). To further purify the ATP analogue a reverse phase HPLC was also performed running a gradient from 2% to 30% of solvent B (solvent A: water 0.1% TEAA; solvent B: 80% ACN 20% water 0.1%

TEAA), providing (**18**) (3.5mg, 15%) as a yellow powder. The product was finally dissolved in water to a final 25mM concentration. The concentration was determined by measuring the absorbance at 260nm, using a molar extinction coefficient of 15,000 $M^{-1}cm^{-1}$.[112]

ES-MS: [M-1]: 963

^{1}H NMR (400MHz, D_2O) δ 2.09-2.15 (2H, m, CH_2 2''), 2.33-2.37 (4H, m, CH_2 12'',13''), 2.91-3.05 (2H; m, CH_2 9''), 3.38-3.62 (12H, m, CH_2 3'',4'',5'',6'',7'',8''), 4.06-4.32 (3H; m, CH 4', CH_2 5'), 4.38-4.52 (2H, m, CH 2',3'), 5.92 (2H, m, CH 19,21), 6.62 (1H, m, CH 1'), 7.35 (2H, m, CH 22'',24'') 8.11 (1H; CH 2), 8.40 (1H; s, CH 8).

2.2.17 Synthesis of the Fmoc- fluorescent peptide: Fmoc-RRREEETEEE

The peptide Fmoc-RRREEETEEE was synthesised using a standard Fmoc solid phase peptide synthesis procedure[116]. Briefly, 2-chlorotrityl chloride resin (77mg, 100μmol) was mixed with Fmoc-Glu(OtBu)-OH (85mg, 200μmol), DIPEA (100μl, 600μmol) and DCM (1.6ml), and left shaking for 3 hours at RT. The mixture was then washed once with MeOH:DIPEA 2:1 (5ml), three times with DCM:MeOH:DIPEA 17:2:1 (5ml), three times with DCM (5ml), three times with DMF (5ml), and three times with DCM (5ml). Finally, the mixture was dissolved in dioxane (15ml) and dried twice by rotary evaporation to remove any HCl residues. Each amino acid was then coupled with the following procedure: the resin was washed with 20% piperidine in DMF (2ml) for 10min, dried and washed again with 20% piperidine in DMF (2ml) for 10min. After three washes with DMF (3ml), a solution of the amino acid (200μmol) and the HBTU coupling reagent (200μmol) in 1M DIPEA in DMF (2ml) was added to the resin and left shaking for an hour. After three washes with DMF (3ml), the same procedure was then

repeated for the next amino acid. After the coupling of the last amino acid the piperidine treatment was avoided in order to maintain the fluorescent Fmoc group. To recover the peptide, the resin was treated with 95%TFA 2.5% triisopropylsilane 2.5% water (3ml) for 3 hours. The collected solution was mixed with diethyl ether (25ml) and centrifuged at 2,000xg for 15min. The pellet was resuspended in water (3ml) and purified by reverse phase HPLC running a gradient from 10% to 70% of solvent B (solvent A: water 0.1%TFA; solvent B: ACN 0.1% TFA). To verify the purity of the product a MALDI-TOF analysis has been run using a 50% ethanol 50% water saturated solution of α-cyano-4-hydroxycinnamic acid as a matrix.

2.2.18 Synthesis of the fluorescein peptide: 5(6)-carboxyfluorescein-RRREEETEEE

The peptide RRREEETEEE was synthesised using the same standard Fmoc solid phase peptide synthesis procedure reported above. In this case, the Fmoc protecting group from the last AA was also removed and the peptide was kept on the resin for the coupling with the fluorescent probe. 5(6)-Carboxyfluorescein (47mg, 125μmol) was pre-incubated with HBTU (47.4mg, 125μmol) and DIPEA (350μl) in DMF (1.5ml) for 10min, for activation. The solution was then mixed with the resin containing the synthesised peptide and left to react overnight at RT. To recover the final product, the resin was treated with 95% TFA 2.5% triisopropylsilane 2.5% water (3ml) for 3 hours. The collected solution was mixed with diethyl ether (25ml) and centrifuged at 2,000xg for 15min. The pellet was resuspended in water (3ml) and purified by reverse phase HPLC running a gradient from 10% to 70% (solvent A: water 0.1%TFA; solvent B: ACN 0.1% TFA). To verify the purity of the product a MALDI-TOF analysis has been run using

a 50% Ethanol 50% water saturated solution of α-cyano-4-hydroxycinnamic acid as a matrix.

2.2.19 Chemical biotinylation of casein

β-casein (10mg) was mixed with biotin (10μmol) in PBS buffer (50μl) and incubated at RT for 30min. 1.5M TRIS-HCl pH 8.8 (100μl) was added to stop the reaction. The sample was finally dialysed overnight in PBS buffer.

2.3 Protein expression

2.3.1 Preparation of glutathione S-transferase (GST)-fusion protein

BL21-competent cells were incubated with pGEX-2T vector containing the coding sequence for bacterial expression of the protein of interest as translational fusions with GST (~1μg) in ice for 30min. Heat shock was then performed by incubating the cells in a water bath at 42°C for 20s followed by incubation in ice for 2min. Cells were then grown in SOC medium (500μl) for 1hr and then diluted in LB medium (100ml) and grown overnight at 37°C under ampicillin (50mg/l) and chloramphenicol (50mg/l) selection pressure. Cells were then diluted 1:10 in LB and grown for a further 2hr at 37°C. GST-fusion protein expression was induced by addition of isopropyl β-D-thiogalactopyranoside (IPTG, 100μM final concentration) at 37°C for 4 hrs. Bacteria were harvested by centrifugation (10,000xg, 15min, 4°C), re-suspended in ice-cold PBS buffer and subjected to sonication (3x30s with 10s break, 4°C). Disrupted cells were centrifuged (50,000xg, 20min, 4°C) and the GST-fusion protein was purified from supernatant by incubation with glutathione Sepharose beads (500μl, 2hrs, 4°C)

followed by washes in PBS (2x10ml) and final elution in PBS containing glutathione (20mM, 5ml).

2.3.2 Preparation of immobilised glutathione S-transferase (GST)-fusion protein

The same procedure previously reported for the preparation of a water soluble GST-fusion protein was followed (see section **2.3.1**). However in this case, the last elution step with PBS and glutathione (20mM) was avoided. The beads containing the recombinant protein were finally resuspended instead in PBS (0.5ml).

2.3.3 Preparation of His$_6$-tagged fusion protein

BL21-competent cells were incubated with pLEICS-05 vector (or in alternative pQE-30 for shPfCK2β_2) containing the coding sequence for bacterial expression of the protein of interest as translational fusions with His$_6$ (~1µg) in ice for 30min. The same heat shock and cell culturing procedures were followed as previously reported (see section **2.3.1**). However in this case, the harvested cells were resuspended in lysis buffer (20mM Tris, 150mM NaCl, 1mM DTT, 20mM imidazole) and subjected to sonication (3x30s with 10s break, 4°C). Disrupted cells were centrifuged (50,000xg, 20min, 4°C) and the His$_6$-fusion protein was purified from supernatant by incubation with nickel-charged resin (1ml, 2hrs, 4°C) (1ml, 2hrs, 4°C) followed by washes in the same lysis buffer (2x10ml) and final elution with lysis buffer containing 350mM imidazole (5ml).

2.3.4 Preparation of immobilised His$_6$-fusion protein

The same procedure previously reported for the preparation of a water soluble His$_6$-fusion protein was followed (see section **2.3.3**). However in this case, the last elution

step with lysis buffer containing 350mM imidazole was avoided. The beads containing the recombinant protein were finally resuspended instead in lysis buffer (0.5ml).

2.4 Kinase assay

2.4.1 CK2 *in vitro* kinase assay with full length casein

CK2 activity was tested in a final volume of 20µl containing:20mM Tris/HCl (pH 7.5), 50mM KCl, 10mM $MgCl_2$, 5µg β-casein and 1mM ATP or ATP analogue. The solution was incubated for 10 min at 37∘C and after that 5x laemmli buffer (5µl) was added to stop the reaction. Samples were then placed in a water bath at 60°C for 3min, loaded on a 12% SDS-PAGE gel and run for 40min at 200mV. Gel-bound proteins were transferred to a nitrocellulose membrane for Western Blot analysis (see section **2.8.1**).

2.4.2 CK2 *in vitro* kinase assay with a peptide substrate

CK2 enzyme (~1pmol) was incubated in a final volume of 50µl containing: 200µM peptide substrate, 20mM Tris/HCl (pH 7.5), 50mM KCl, 10mM $MgCl_2$, and 1mM ATP (or ATP analogue), for 2hrs at 37∘C. The sample was then placed in ice and kinase reaction stopped by the addition of 0.5M orthophosphoric acid (5 µl). Results were analysed with one of the following techniques: mass spectrometry (see section **2.4.4**), HPLC analysis (see section **2.4.5**) or FRET (see section **2.4.6**).

2.4.3 CK2 inhibition assay

CK2 activity was tested in a final volume of 25 µl containing 20mM Tris/HCl (pH 7.5), 50mM KCl, 10mM $MgCl_2$, 200µM synthetic peptide substrate RRRADDSDDDDD and 0.1mM [γ -^{32}P]-ATP (500–1000 c.p.m./pmol), 0.5µg enzyme, and incubated for 10 min

at 37°C. Assays were stopped by addition of 5 µl of 0.5M orthophosphoric acid before spotting 15µl aliquots on to phospho-cellulose filters. Filters were washed in 0.05% orthophosphoric acid (5–10 ml each) four times then once in methanol and dried before counting.

2.4.4 Mass spectrometry analysis

Samples from an *in vitro* kinase assay with a peptide substrate were first purified with a ZipTip prior to the analysis, in order to remove high salt concentration. Briefly, a ZipTip was first permeabilised in ACN and then washed with 0.1%TFA. After that, 10µl of the reaction mixture were loaded on the ZipTip and discarded. The ZipTip was washed with 30µl of 0.1%TFA. The sample was then eluted from the ZipTip with 10µl of a 50%ACN-0.1%TFA solution. Finally, 1µl from the eluted sample was mixed with 1µl of matrix: 10mg/ml DHB, 50%ACN, 0.1%H_3PO_4 loaded on a MALDI plate and analysed by MALDI-TOF.

2.4.5 HPLC analysis

Samples from an *in vitro* kinase assay with a fluorescent peptide substrate were analysed on an HPLC system using a gradient: from 10% to 70% of solvent B using one of the following solvent systems:

- Solvent A: 0.1%TFA in water pH: 2, solvent B: 0.1%TFA in ACN,

- Solvent A: water, solvent B: ACN,

- Solvent A: water ammonium acetate 20mM pH: 6.5, solvent B: 85%ACN ammonium acetate 20mM pH: 6.5,

- Solvent A: water ammonium bicarbonate 20mM pH: 9, solvent B: 80%ACN ammonium bicarbonate 20mM pH: 6.5,

- Solvent A: PBS buffer 20mM pH: 6.5, solvent B: ACN.

2.4.6 FRET analysis

A sample from an *in vitro* kinase assay carried out using the synthesised 5(6)-carboxyfluorescein-RRREEETEEE peptide as a CK2 substrate was diluted in water to 500µl final volume prior to analysis. The emission spectrum was then recorded after excitation at 441nm (donor excitation peak). As a control, the emission spectrum of the ATP coumarin (FRET donor) was also recorded in the same conditions.

2.4.7 PfCK2 autophosphorylation assay

Bacterial expressed GST-PfCK2 (~2µg) was incubated for 10min at 37°C in a final volume of 20µl containing: 20mM Tris/HCl (pH 7.5), 50mM KCl, 10mM MgCl$_2$, and 50µM [γ-^{32}P]-ATP (500–1000 c.p.m./pmol). The reaction was stopped by adding 5x laemmli buffer (5µl), the sample was then placed in a water bath at 60°C for 3min, loaded on a 12% SDS-PAGE gel and run for 40min at 200mV. The gel was dried for 1hr under *vacuum* at 80°C and exposed to autoradiographic film. For the GST control, GST-containing beads (~5µg) were incubated with GST-PfCK2 (~2µg) in the same conditions. The sample was then spun down (15,000xg, 1min, 4°C), and the supernatant removed. Proteins were finally eluted from the beads with 2x laemmli buffer (10µl), loaded on the same SDS-PAGE gel and analysed as reported above.

2.4.8 CK2 and CK1 *in vitro* kinase assay with radioactive ^{32}P-ATP and casein

CK2 and CK1 activity was tested in a final volume of 20µl containing: the enzyme (1µg) 20mM Tris/HCl (pH 7.5), 50mM KCl, 10mM MgCl$_2$, 5µg β-casein and 50µM [γ-^{32}P]-ATP (500–1000 c.p.m./pmol). The solution was incubated for 10 min at 37∘C and after that 5x laemmli buffer (5µl) was added to stop the reaction. Samples were then placed in a water bath at 60°C for 3min, loaded on a 12% SDS-PAGE gel and run for 40min at 200mV. The gel was dried for 1hr under *vacuum* at 80°C and exposed to autoradiographic film.

2.4.9 *In vitro* kinase assay with a parasite lysate and recombinant GST-PfMCM2

Glutathione beads containing bacterial expressed GST-PfMCM2, or GST as a negative control) (~5µg, 15µl) were incubated for 10min at 37°C in a final volume of 30µl containing: a saponin-treated parasite lysate (50µg, 10µl, see section **2.7.3**) or a ion exchange column fraction see section **2.9.3**) , 20mM Hepes (pH 7.5), 20mM β-glycerol phosphate, 10mM MgCl$_2$, and 50µM [γ-^{32}P]-ATP (500–1000 c.p.m./pmol). The reaction mixture was then centrifuged 15,000xg for 3min, the supernatant removed and 2x laemmli buffer (5µl) were added to the pellet. The sample was then placed in a water bath at 60°C for 3min, loaded on a 12% SDS-PAGE gel and run for 40min at 200mV. The gel was dried for 1hr under *vacuum* at 80°C and exposed to autoradiographic film.

2.4.10 Kinase assay with PfCK2 immobilised on glutathione beads

Bacterial expressed GST tagged PfCK2 immobilised on glutathione beads (~2µg) was incubated for 20min at 37° in a final volume of 100µl containing: 100µg of a previously heat inactivated iRBC lysate sample (see section **2.5.4**), 20mM Tris/HCl (pH 7.5), 50mM KCl, 10mM MgCl$_2$, and 50µM [γ-^{32}P]-ATP (500–1000 c.p.m./pmol). The sample was

then spun down at 15,000xg for 1min and the supernatant separated from the pellet with a pipette. After that, 5x laemmli buffer (25µl) was added to the supernatant and 2x laemmli buffer (10µl) to the pellet. Both samples were then placed in a water bath at 60°C for 3min, loaded on a 12% SDS-PAGE gel and run for 40min at 200mV. The gel was dried for 1hr under *vacuum* at 80°C and exposed to autoradiographic film.

2.5 Molecular Modelling

2.5.1 Building of a homology model of *P. falciparum* CK2

Amino acid sequences of CK2α subunits from *Homo sapiens* (CAB65624), and *Plasmodium falciparum* (AAN35684; PlasmoDB PF11_0096) were aligned using ClustalW2. A homology model for the *P. falciparum* CK2 catalytic subunit was then built using Modeller 9.10,[117] and the human CK2 crystal structure as a template (PDB code: 1JWH). Five different models were calculated and the best one was chosen based on the total number of violated restraints. A second model was also built including the conserved water molecule, following the same procedure.

2.5.2 Docking simulation

A docking simulation with the inhibitor quinalizarin has been performed with the calculated homology model for *P. falciparum* CK2, using the programme GOLD.[118] In particular, GoldScore was used as a scoring function. Hydrogen atoms were introduced in the protein structure with the default GOLD command and in the ligand molecule with the programme HyperChem. To strictly validate the model generated and to calibrate the docking protocol, a docking analysis has been first performed using the

apo structure of the co-crystal model of CK2 (PDB code: 3FL5), with the CK2 inhibitor quinalizarin. The result was then compared with the reported co-crystallization structure (PDB code: 3FL5).

2.6 Pull down assay

2.6.1 Pull-down with shPfCK2β_2 and pre-incubation with ATP

Bacterial expressed His$_6$-PfCK2 (~5μg) was incubated for 10min at 37°C in a final volume of 20μl containing: 20mM Tris/HCl (pH 7.5), 50mM KCl, 10mM MgCl$_2$, and 1mM ATP. A negative control was also run in parallel in the same conditions, in the absence of ATP. Samples were then mixed with glutathione beads containing GST-shPfCK2β_2 (30μl) in a final volume of 30μl containing: 20mM Tris/HCl (pH 7.5), 50mM KCl, 10mM MgCl$_2$ and incubated for 30min at 37°C shaking at 500xg. Samples were then centrifuged at 15,000xg for 2min, and the supernatant removed by aspiration. Beads were then washed with reaction buffer (200μl) and finally eluted with 2x laemmli buffer (10μl). Samples were finally separated by SDS-PAGE on 12% acrylamide gels and transferred to a nitrocellulose membrane for Western Blot analysis using anti-His tag antibody (1:2000 dilution).

2.6.2 Pull-down with shPfCK2β_2 and pre-incubation with calf intestinal phosphatase

Immobilised His$_6$-PfCK2 (500μl) was incubated for 2hrs at RT in a final volume of 1ml containing: 20mM Tris/HCl (pH 7.5), 50mM KCl, 10mM MgCl$_2$, and CIP (20μl, 200U). Samples were then mixed with glutathione beads containing GST-shPfCK2β_2 (30μl) in a final volume of 30μl with: 20mM Tris/HCl (pH 7.5), 50mM KCl, 10mM MgCl$_2$ and incubated for 30min at 37°C shaking at 500xg. Samples were then centrifuged at

15,000xg for 2min, and the supernatant removed by aspiration. Beads were subsequently washed with reaction buffer (200μl) and finally eluted with 2x laemmli buffer (10μl). Samples were then separated by SDS-PAGE on 12% acrylamide gels and transferred to a nitrocellulose membrane for Western Blot analysis using anti-His tag antibody (1:2000 dilution).

2.6.2 Pull-down with anti-phosphotyrosine antibody

A sample from parasite lysate (500μg) was mixed with anti-phosphotyrosine antybody coniugated to agarose beads (30μl) and TEG buffer in a final volume of 250μl, and incubated for 3hrs at 4°C while rotating. The sample was then centrifuged at 15,000xg for 3min and the pellet washed with TEG buffer (500μl) centrifuging and discarding the supernatant each time. Proteins bound to the beads were finally eluted with either laemmli buffer (20μl) for one-step elution, or twice with a solution of 100mM phenyl phosphate (20μl) followed by elution with laemmli buffer (20μl). The samples were loaded on a SDS-PAGE gel run for 40min at 100V and the gel was the dried and exposed to autoradiografic film. In alternative, gel lanes were cut and provided to PNACL facility (University of Leicester) for LC-MS\MS analysis (see section **2.9.2**).

2.7 Parasitology and biochemical techniques

2.7.1 *P. falciparum* cell culturing and lysis

Chloroquine-susceptible strain (3D7) of *P. falciparum* were grown in Petri dishes suspended at 5% hematocrit in RPMI 1640 medium containing: 10% human serum, glucose (40mg/l), hypoxanthine (20mg/l), $NaHCO_3$ (1.8g/l) and gentamycin (0.9g/l).

Cultures were firstly synchronized by sorbitol treatment[119]. Briefly, samples were incubated with 1M sorbitol (5ml) for 20min and centrifuged at 2,000xg for 5min; the pellet was washed twice with RPMI 1640 medium (10ml) and finally resuspended in culture media. Cultures were carried out at 37°C in an atmosphere of 2% oxygen 5% carbon dioxide and 93% nitrogen and kept growing to a final 5% parasitemia level, then harvested on a magnetic column (Miltenyi Biotech) using Krebs buffer for elution.

2.7.2 Lysis of a total iRBC sample

The purified pellet containing *P.falciparum*-infected red blood cells (see section **2.7.1**) was lysed by incubation in 1%NP-TEG buffer in the presence of protease and phosphatase inhibitor cocktail tablets (Roche) for 10min in ice. The sample was then spun down at 15,000xg for 1min and supernantant stored at -20°C.

2.7.3 Lysis of a total iRBC sample into a parasite and a RBC fractions

The purified pellet containing *P.falciparum*-infected red blood cells (see section **2.7.1**) was lysed by incubation in PBS containing 0.1% saponin for 10min in ice. The sample was then centrifuged at 15,000xg for 3min and the supernatant recovered constituting the iRBC sample. The pellet was washed twice in PBS (500μl) and then incubated with 1% NP-TEG buffer (300μl) in the presence of protease and phosphatase inhibitor cocktail tablets (Roche) for 10min in ice. The sample was then spun down at 15,000xg for 1min and supernantant stored at -20°C constituting the parasite fraction.

2.7.4 *In vivo* radioactive labelling of iRBC

Purified iRBC from chloroquine-susceptible strain (3D7) of *P. falciparum* cell culture (see section **2.7.1**) (~50μl pellet volume) were resuspended in 500μl Krebs buffer

(phosphate free) and incubated with 20–25µl fresh ^{32}P-orthophosphate for 30min at 37°C. Following incubation the pellet was washed twice with 1ml PBS containing protease and phosphatase inhibitors (Roche) and lysed with lysis buffer: 50mM Tris, 0.5mM EDTA, 5% β-glycerophosphate, pH 7.6, supplemented with a protease inhibitor tablet and 1% NP-40 (see section **2.5.2**).

2.7.5 Heat inactivation

A *P. falciparum* lysate (see section **2.7.3**) was incubated in a water bath at 55°C for 2min.

2.7.6 CIP treatment

CIP, or alternatively biotinylated CIP (30µg) was incubated for the indicated length of time at 37°C in a final volume of 80µl containing: 100µg of a previously heat inactivated iRBC lysate sample (see section **2.5.5**), 50mM Tris-HCl 100mM NaCl, 10mM MgCl$_2$, 1mM dithiothreitol at pH 7.9. After that, 5x laemmli buffer (20µl) was added to the sample, then placed in a water bath at 60°C for 3min, loaded on a 12% SDS-PAGE gel and run for 40min at 200mV. The gel was dried for 1hr under *vacuum* at 80°C and exposed to autoradiographic film.

2.7.7 Streptavidin pull-down

A CIP treated sample of an iRBC lysate (see section **2.7.6**) was incubated with streptavidin beads (30µl) and left rotating fo 1hr at 4°C. The sample was then centrifuged at 15,000xg for 1min and the supernatant placed in a water bath at 60°C for 3min after the addition of 5x laemmli buffer (25µl). The sample was finally loaded

on a 12% SDS-PAGE gel and run for 40min at 200mV. The gel was dried for 1hr under *vacuum* at 80°C and exposed to autoradiographic film.

2.7.8 *In vivo* inhibition test

A *P. falciparum* cell culture sample (0.5ml) was mixed with the inhibitor compound dissolved in 0.1%DMSO at the indicated concentration and incubated for 30min at 37°C. Cells were then centrifuged at 15,000xg for 3min and lysed as previously described see (section **2.7.3**). The parasite fraction was then run on a SDS-PAGE gel and transfer to nitrocellulose for Western Blot analysis (see section **2.9.1**).

2.8 Molecular biology

2.8.1 DNA miniprep

The DNA template (50ng) was mixed with XL-1 Blue supercompetent cells (100µl) and incubated for 30min in ice. A heat shock was performed by incubating the mixture in a water bath at 42°C for 45s and subsequently placed in ice for 2min. Cells were then grown in SOC medium (500µl) for 1hr, then the mixture (20µl) was plated on agar petri dishes containing ampicillin (50mg/l) and grown overnight at 37°C. Single colonies were then selected from the plates and grown in LB medium (5ml) overnight at 37°C under ampicillin (50mg/l) selection pressure. The plasmid was then extracted, purified with Plasmid Isolation kit (Roche) and submitted to PNACL facility (University of Leicester) for sequencing. A small portion of the purified plasmid (10µl) was also digested with the BamHI and EcoRI restriction enzymes and run on a 1% agarose gel for 1hr at 100V. The gel was finally incubated in an ethidium bromide solution

(0.5µg/ml) for 10min and DNA bands revealed under UV light to check for the presence of the insert into the vector.

2.8.2 DNA digestion with a restriction enzyme

The DNA template (1µg) was mixed with 10x SuRE/Cut buffer H (2µl) and the restriction enzyme (BamHI or EcoRI) (10U, 1µl) in water (20µl final volume). The reaction mixture was incubated at 37°C for 1hr and then purified with Nucleospin Extract II kit. Part of the sample (10µl) was also run on a 1% agarose gel for 1hr at 100V. The gel was finally incubated in an ethidium bromide solution (0.5µg/ml) for 10min and DNA bands revealed under UV light.

2.8.3 pGEx-2T vector construction coding for GST-PfMCM2 protein expression

The provided DNA encoding for the N-terminal fragment of PfMCM2 was digested with BamHI, and EcoRI restriction enzymes (see section **2.8.2**), loaded on a 1% agarose gel and run for 1hr at 100V. The gel was then incubated in an ethidium bromide solution (0.5µg/ml) for 10min and the corresponding band cut from the gel and dissolved in water (1ml). The solution was purified using a Nucleospin Extract II kit. The eluted sample (10µl) was then mixed with T4 DNA ligase (2µl), 10x T4 DNA ligase buffer (2µl) in water (20µl final volume) and incubated at 25°C for 5hrs. The reaction mixture (5µl) was finally transfected in XL-1 Blue supercompetent cells following the protocol previously reported to obtain the purified plasmid (see section **2.3.1**).

2.8.4 Single point mutation

The template vector (30ng) was mixed with: 5' and 3' primers designed for the desired mutation (125ng, see **Appendix**), 10x *PfuUltra* buffer (5µl), dNTP mix (200µM for each

nucleotide), *PfuUltra* HFG DNA polymerase (1µl, 2.5U) in a final volume of 50µl. The mixture was then incubated in a PCR machine with the following temperature programme:

Segment	Cycles	Temperature	Time
1	1	98°C	2min
2	18	98°C	30s
		55°C	1min
		68°C	1 min/Kb
3	1	68°C	5min

Then, *Dpn* I restriction enzyme (1µl, 10U) was added to the reaction mixture and incubated at 37°C for 1hr. The reaction mixture (1µl) was then transfected in XL-1 Blue supercompetent cells following the protocol previously reported to obtain the purified plasmid (see section **2.3.1**).

2.8.5 His$_6$-tag cleavage

A sample of the His$_6$-tagged protein of interest (1mg, 1ml) was mixed with recombinant His$_6$-TEV (10mg) and dialysed overnight in 2L of lysis buffer (20mM Tris, 150mM NaCl, 1mM DTT, 20mM imidazole) using a dialysing cassette (MWCOs 2KDa). The product was then purified and isolated by collecting the flowthrough from a column containing nickel-charged resin (1ml).

2.8.6 Gene amplification and insertion into pGEX and pLEICS05 plasmid vectors

A cDNA library sample (30ng) was mixed with: 5' and 3' primers (125ng, see **Appendix**), 5x HF buffer (10μl), dNTP mix (200μM for each nucleotide), Phusion DNA Polymerase (0.5μl, 2.5U) in a final volume of 50μl. The mixture was then incubated in a PCR machine with the following temperature programme:

Segment	Cycles	Temperature	Time
1	1	98°C	1min
2	18	98°C	45s
		55°C	40s
		72°C	1 min/Kb
3	1	72°C	10min

The solution was then purified using a Nucleospin Extract II kit and the eluted sample (10μl) was digested with BamHI restriction enzyme (see section **2.8.2**). The product was then loaded on a 1% agarose gel and run for 1hr at 100V. The gel was incubated in an ethidium bromide solution (0.5μg/ml) for 10min and the corresponding band cut from the gel and dissolved in water (1ml). The solution was purified again using a Nucleospin Extract II kit. For the GST fusion protein, the eluted sample (10μl) was then mixed with T4 DNA ligase (2μl), 10x T4 DNA ligase buffer (2μl) in water (20μl final volume) and incubated at 25°C for 5hrs. The reaction mixture (5μl) was finally transfected in XL-1 Blue supercompetent cells following the protocol previously reported to obtain the purified plasmid (see section **2.8.1**).

For the His_6-tag fusion protein, the amplified coding DNA was provided instead to the PROTEX facility (University of Leicester) for insertion into the pLEICS05 vector.

2.9 General techniques

2.9.1 Western Blot analysis

Western Blotting was performed according to conventional protocols. Briefly, samples were separated by SDS-PAGE on a 12% acrylamide gel and transferred to a nitrocellulose membrane with a Western Blot apparatus at 25mA for 1hour. The membranes were first blocked in blocking solution (5% milk in TBS-T buffer) and then incubated with the primary antibody diluted in the same buffer. After washing with TBS-T buffer (3x15min) the membrane was incubated with the secondary antibody diluted in the blocking solution for 1hr. The membrane was washed again in TBS-T (3x15min), incubated with a 1:1 solution of luminol and ECL for 5min and finally exposed to autoradiographic film.

When β-casein was used as a substrate the following blocking solution was used for blocking and antibody dilution: 5% bovine serum albumin, 10% goat serum in TBS-T buffer.

2.9.2 LC-MS\MS analysis

The protein sample (~5μg, 10μl) was diluted in 2x laemmli buffer (10μl), then placed in a water bath at 60°C for 3min, and finally loaded on a 12% SDS-PAGE gel. The gel was run for 40min at 200mV and then incubated in the fixing solution: 7% acetic acid in 40% methanol for 1hr, rinsed with water and finally incubated in the staining solution:

Brillant Blue G-Colloidal solution for 1hr. After that, the gel was destained for 1min in the destaining solution: 10% acetic acid in 25% methanol, and then washed and stored in 25% methanol solution. The band relative to the protein of interest was finally cut and submitted to the PNACL facility (University of Leicester) for LC-MS\MS analysis.

2.9.3 Protein fractionation with ion exchange chromatography

A *P. falciparum* lysate obtained as previously reported (see section **2.7.3**) was diluted in binding buffer (3ml): 10mM Tris, 5mM EDTA, 20mM β-glycerol phosphate, pH 7.4, loaded on the ion exchange column, washed with binding buffer (10ml) and finally eluted. For elution a gradient of the following two solvents system was used:

Solvent A: : buffer A: 10mM Tris, 5mM EDTA, 20mM β-glycerol phosphate, pH 7.4;

Solvent B: 10mM Tris, 5mM EDTA, 20mM β-glycerol phosphate, pH 7.4 1M NaCl.

In particular, gradients used with each type of column are indicated in the table below:

column	final salt concentration
RQ batch elution	1M
RQ	0.5M
Heparin	0.75M
hydroxyapatite	1M
Blue	1M
RS	0.5M

For the batch elution with RQ column, a flow rate of 1ml/min over 3min was used, while in all the other fractionations the flow rate was lowered to 0.5ml/min over 10min. Collected fractions were dialysed using a de-salting column and eluting in kinase buffer: 20mM Hepes, 20mM β-glycerol phosphate, 10mM $MgCl_2$. Each fraction (15μl) was finally tested in *in vitro* kinase using GST-PFMCM2 as a substrate (see section **2.4.9**).

2.9.4 Immunocytochemistry

iRBCs from parasite cultures (see section **2.7.1**) were plated on a glass coverslip, dried at RT for 10min and then washed in TBS buffer for 5min. Cells were subsequently fixed by incubation in 4% PFA in TBS for 3min. After washing in TBS for 5min, the sample was permeabilised by incubating in TBS buffer containing 0.1% Triton X-100 for 30min. The coverslip was then washed with TBS for 5min and incubated overnight in blocking solution (10% Goat Serum, 1% BSA in TBS containing 0.1% Triton X-100) at 4°C. The sample was incubated at RT with the primary antibody dissolved in blocking solution for 1hr. After four washes in TBS buffer containing 0.1% Triton X-100 the sample was incubated with the FITC-coupled secondary antibody dissolved in the blocking solution, for 1hr. After four washes in TBS buffer containing 0.1% Triton X-100 and a final wash in TBS, a drop of Vectashield mounting media containing DAPI was added to the coverslip, this was then cover with a glass slide, sealed and analysed with a Confocal microscope.

Chapter 3: A novel chemical-biological approach for the identification of *P. falciparum* CK2 substrates

3.1 Introduction

Protein phosphorylation is one of the most important covalent post-translational modifications regulating the functional status of proteins and peptides in eukaryotic organisms. Hence it has attracted large interest from the scientific community over the years. However, deciphering phosphorylation networks is a challenging task for several reasons. First of all, eukaryotic protein kinases usually share a highly conserved ATP binding site due to their common origin.[48] This hampers the use of small molecule inhibitors because of their lack of absolute specificity. Secondly, the analysis is complicated by the intrinsic complexity of phosphorylation patterns and the very large number of phosphorylation sites. In fact, it has been speculated that over 50% of all proteins are supposedly phosphorylated at some stage and that there are more than 100 000 estimated phosphorylation sites in the human proteome.[120]

The standard procedure for identifying protein phosphorylation in a pathway is to first isolate the candidate substrate through biochemical fractionation and then analyse it by Edman degradation or MS to determine the specific site of phosphorylation.[121] Although usually successful, this procedure is time-consuming and requires

optimisation for every single protein. Alternatively, phospho-proteins can be detected using standard Western Blotting procedures.[122,123] High-quality antibodies to phospho-tyrosine residues are now commercially available however, antibodies that specifically recognize phospho-serine and phospho-threonine residues are typically sensitive to amino acid sequence context and do not provide universal detection. To overcome these limitations, several strategies for phospho-peptide labelling and enrichment have been developed including immobilized metal affinity chromatography,[124] covalent phosphate modification,[125] and bio-orthogonal affinity purification.[126] In spite of these recently developed chemical tools, the labelling and detection of phospho-proteins in complex mixtures (e.g. cell lysates) still remains challenging.

Given the importance of phosphorylation pathways also in the malaria context, we decided to develop and apply a novel enzymatic approach that detects specifically *Plasmodium falciparum* CK2 (PfCK2) substrates in cellular lysates. The first approach is based upon a method recently describe by M. Pflum *et al*,[127] that has already proved successful with the human CK2 homologue (**Figure 3.1**). Several studies[128,129] have shown in fact that human CK2 tolerates γ-modified ATP analogues as phospho-donors in kinase reactions. Such an unusual feature, shared with only two other kinases (PKA and Abl kinase) is due to the specific orientation of the ATP substrate in the CK2 binding pocket that leaves the γ-phosphate exposed to the solvent. This solvent exposed nature allows the binding of γ-phosphate modified ATP analogues.
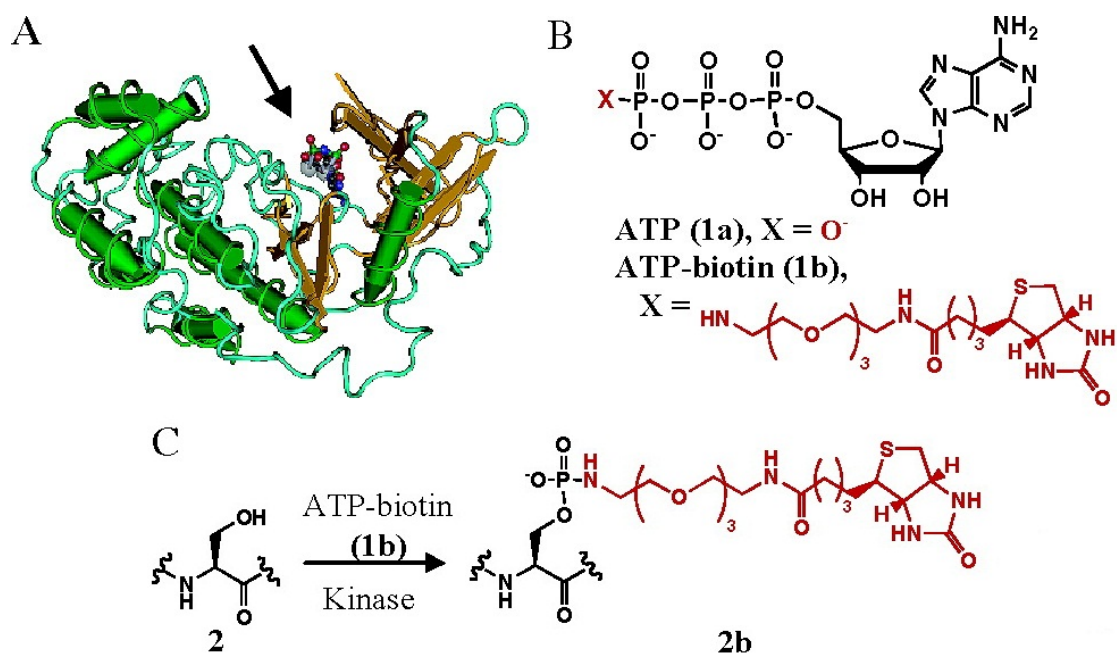
Figure 3.1: Schematic representation of the novel enzymatic approach to detect CK2 substrates. **A:** CK2 in complex with the ATP analogue, AMPPnP (Pubmed pdb: 1DAW). The arrow points to the solvent-exposed γ-phosphate of AMPPnP. **B:** General structure of γ-phosphate modified ATP analogues. **C:** ATP-biotin (**1b**) acts as a kinase co-substrate to promote phosphorylation-dependent biotinylation of peptides and proteins (**2b**).

Particularly, the modified analogues are designed to bear substituent groups such as biotin, fluorophore or azide that enable labelling and identification of phospho-proteins.[129] Despite the fact that a crystal structure for *Pf*CK2 has not been reported yet, the high sequence identity between this and the human enzyme (62%)[71] suggests that this approach could be used also with the *Plasmodium falciparum* homologue. Furthermore, thanks to the already observed *Pf*CK2 tolerance towards GTP,[71] a similar set of γ-modified GTP analogues can be used in principle in order to increase the kinase specificity of such nucleotide probes excluding e.g. the PKA and Abl kinases that

are not able to accept GTP as a phosphate donor. Therefore, the aims of this chapter were to synthesise a focused set of γ-phosphate modified ATP analogues bearing reporting groups of different nature, and to test them with recombinant PfCK2 in order to identify the feasibility and scope of this new chemical-biological approach.

3.2 Probe synthesis

3.2.1 Synthetic route

A focused set of γ-modified purine triphosphate analogues bearing a linker and a range of chemical reporter groups were synthesised. Probes (**7**), (**9**), (**11**), (**13**), (**16**) were prepared by coupling of the probe amine (**6**), (**8**), (**10**), (**12**), (**15**) with the corresponding activated adenosine nucleoside triphosphate (ATP). Syntheses were designed in a combinatorial way, so that the analogues in the set would share the same linker. The synthetic strategy commenced with the preparation of a common linker (**4**) which was further derivatised with the desired reporting group (**6**), (**8**), (**10**), (**12**), (**15**) and finally coupled with ATP to afford derivatives (**7**), (**9**), (**11**), (**13**), (**16**). As showed in **Scheme 3.1**, the covalent linker between the ATP and the chemical tag was prepared by introducing two azide functions to tetraethylene glycol (**1**), followed by reduction to two amine groups. The resulting (bis)amine (**4**) was then mono-protected with BOC in order to introduce only a single reporter group at the other end of the molecule. The probe was finally coupled with ATP using EDC, a water soluble analogue of DCC. The generally low yields were mainly due to product loss during the two step purification process. With this procedure three ATP analogues were synthesised bearing the following reporting groups: biotin, alkyne, and azide (**Table 3.1**).
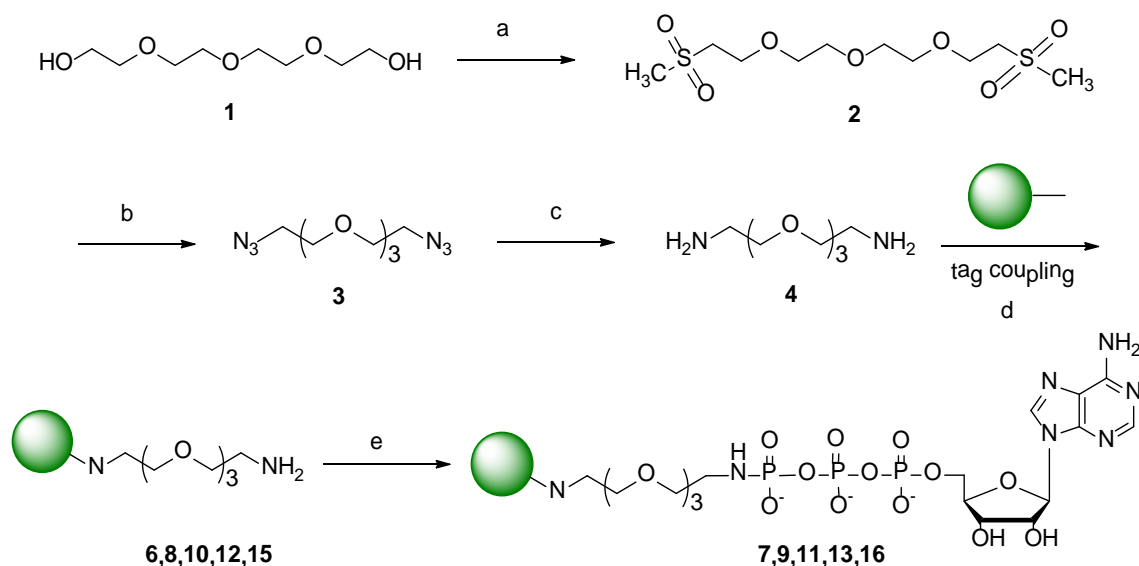
Scheme 3.1:. Preparation of γ-modified ATP analogues (**7**), (**9**), (**11**), (**13**), (**16**). *Reagents and conditions:* (a) CH_3SO_2Cl, triethylamine (b) NaN_3, $NaHCO_3$, 67% (c) Pd/C, H_2, 92% (d) tag coupling with the linker, (the rag is schematically represented by a green sphere, see following schemes for each specific procedure,) (e): ATP, EDC, yields see **Table 3.1**.

In particular, the biotin was chosen due to its strong binding affinity with streptavidin which can be used to pull out the phosphorylated peptide or proteins from the reaction mixture.[130] The alkyne and azide tags were chosen for their ability to react promptly in bio-orthogonal reactions such as Huisgen cycloaddition (also known as click chemistry)[131] enabling further derivatisation and enrichment of phospho-peptides (**Figure 3.2**). Following this route, compound (**9**) was further reacted with coumarin azide in order to produce the fluorescent ATP analogue (**18**).

Entry	Tag	Starting material	Product	Yield (%) [a]
1		**6**	**7**	21
2		**8**	**9**	19
3	N₂—	**10**	**11**	18
4		**12**	**13**	-
5		**15**	**16**	-
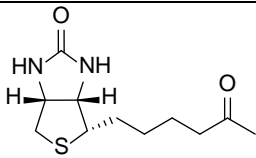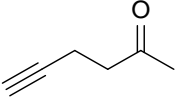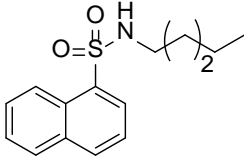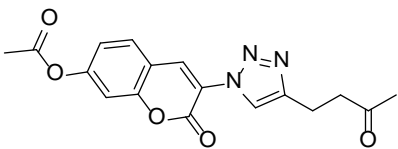
Table 3.1: Probe coupling with ATP. [a]: (1eq) starting material, (0.5eq) ATP, (6eq) EDC,

1hr, RT.
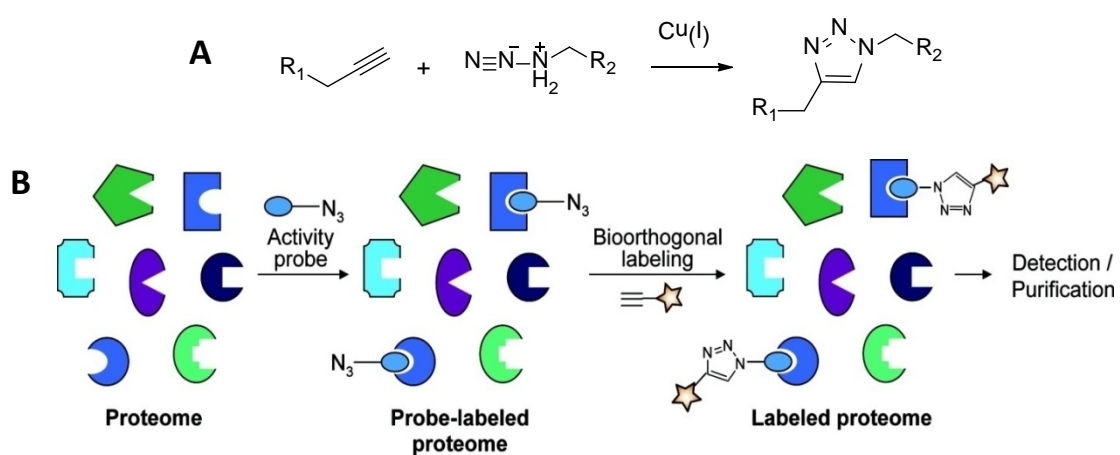
Figure 3.2: A: general reaction scheme for the copper(I)-catalysed azide-alkyne

Huisgen cycloaddition. **B:** schematic representation for click chemistry bioorthogonal

labelling. In this case, CK2 substrates are labelled by activity probes through the kinase

reaction. The products are then selectively tagged and detected via click chemistry.

3.2.2 Synthesis of the ATP biotin analogue (7)

In order to prepare the ATP biotin analogue (**7**), compound (**4**) was first mono-protected with BOC and then coupled with N-hydroxysuccinimide biotin ester, a reactive derivative of biotin. After deprotection, the product was then left to react with ATP in the presence of EDC for 2hrs at RT. In order to remove any un-reacted ATP impurities the reaction mixture was first purified by ion-exchange chromatography, followed by HPLC.
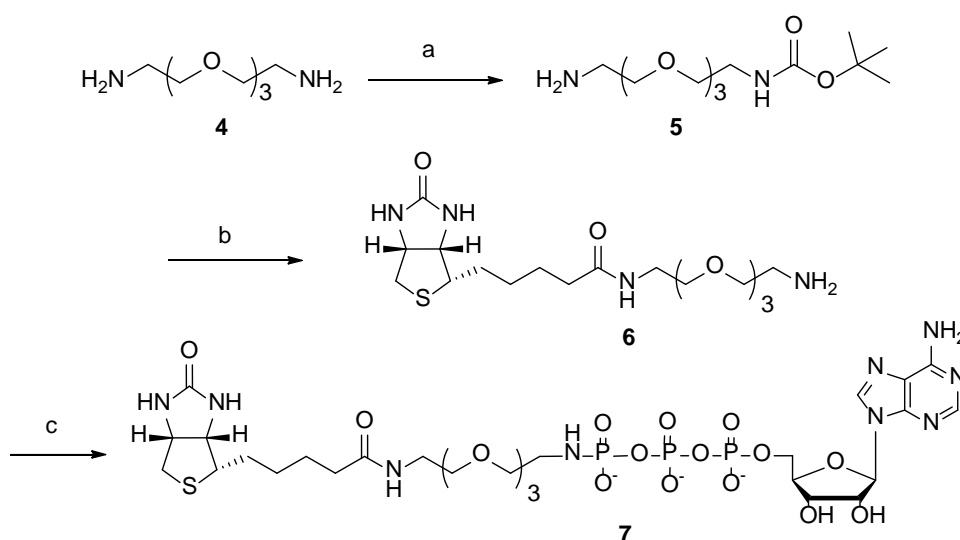
Scheme 3.2: Synthetic route to the ATP biotin analogue (**7**). *Reagents and conditions: (a) BOC$_2$O, (b) i) biotin N-hydroxysuccinimide ester, NaHCO$_3$, ii) TFA, 47% (c) ATP, EDC, 21%.*

The removal of ATP was particularly important in order to ensure that the ATP analogue is the only phosphate donor species present in the sample. As shown in **Figure 3.3**, ion exchange chromatography was not sufficient to achieve this and it is only after HPLC that any detectable traces of ATP are removed.
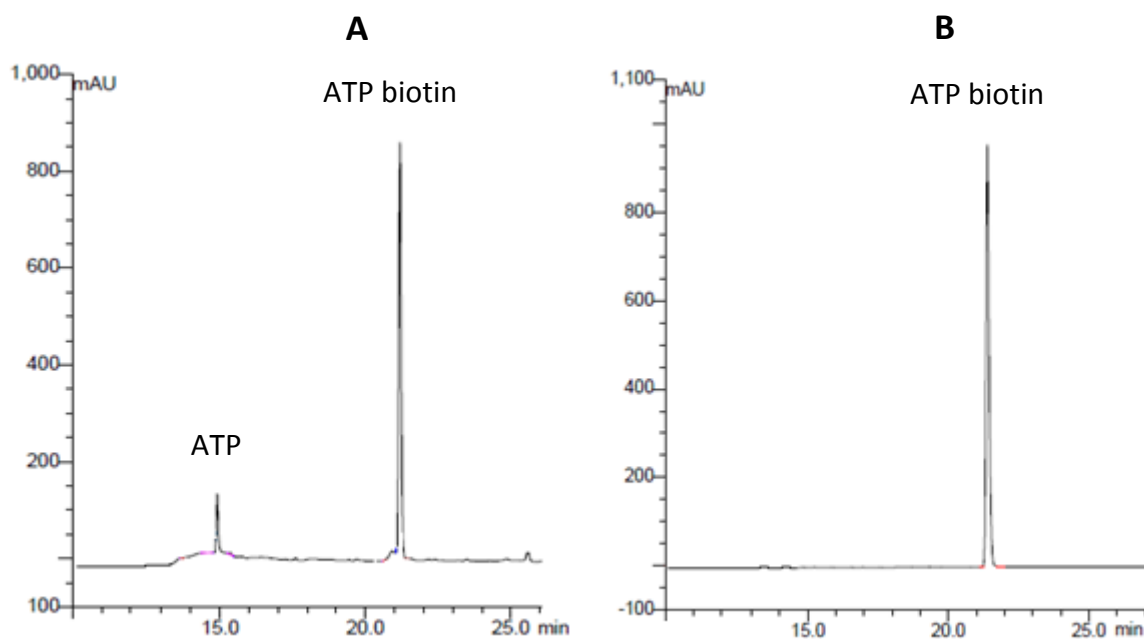
Figure 3.3: Purification of the ATP biotin analogue (**7**): samples before HPLC purification (**A**), and after (**B**) were analysed by analytical HPLC (λ_{abs}: 260nm). ATP impurities eluting at ~15min are still present after ion exchange chromatography, but completely removed by subsequent HPLC purification.

3.2.3 Synthesis of the ATP alkyne analogue (9)

The ATP alkyne (**9**) was prepared following the procedure shown in **Scheme 3.3**. Briefly, the mono-protected amine (**5**) was coupled with 4-pentynoic acid followed by BOC deprotection with TFA. The resulting compound was then coupled with ATP and purified using the same protocol as for ATP biotin (**7**).
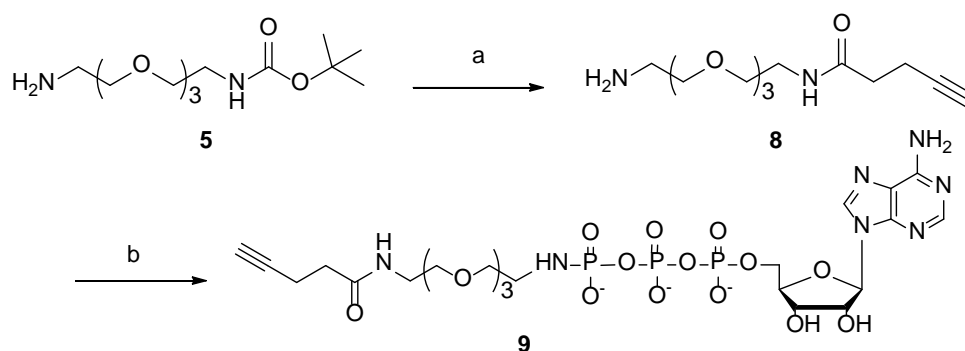
Scheme 3.3: Synthetic route to the ATP alkyne analogue (**9**). *Reagents and conditions:*

(a) i) pentynoic acid, DCC, ii) TFA 58% (b) ATP, EDC, 19%.

3.2.4 Synthesis of the ATP azide (11)

The preparation of ATP azide (**11**) involved selective reduction of a single azide by a

Staudinger reaction (**Scheme 3.4**).[132] This is a mild method of reducing an azide to an

amine under controlled conditions. In this case 0.9 equivalents of PPh_3 were used as

reducing agent. The product was then coupled with ATP and purified as previously

described (see section **3.2.2**).
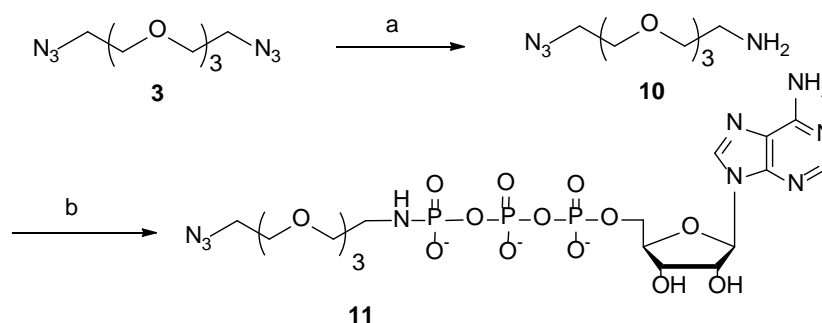
Scheme 3.4: Synthetic route to the ATP azide analogue (**11**). *Reagents and conditions:*

(a) PPh_3, 62% (b) ATP, EDC, 18%.

3.2.5 Synthesis of the ATP dansyl analogue (13)

A coupling reaction with ATP and the commercially available compound dansyl cadaverine was attempted in order to prepare the corresponding fluorescent phosphoramidate (**13**). However, in this case the common route to prepare the ATP analogue (**13**) used for the other ATP derivatives (**7**), (**9**), (**11**) was not successful (**Scheme 3.5**). No product was detected either by ion exchange chromatography or HPLC analysis of the reaction mixture. Slight modifications to the protocol such as increasing the reaction time to overnight or decreasing the polarity of the solvent by using a mixture of 1:1 water:DMF were not successful either. As a consequence of this, the synthesis attempt was abandoned and a different route was followed in order to obtain a fluorescent ATP analogue (see following section **3.2.6**).
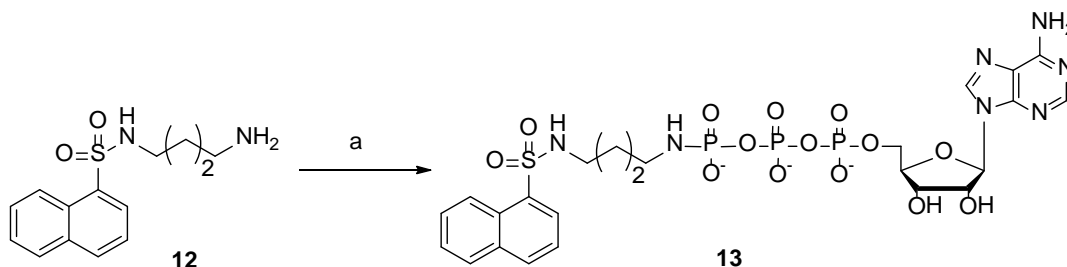
Scheme 3.5: Synthetic route to the ATP dansyl analogue (**13**). *Reagents and conditions:* ATP, EDC.

3.2.6 Synthesis of the ATP coumarin analogue (18)

Following the unsuccessful synthesis of the ATP dansyl cadaverine derivative (**13**), a different strategy was tested in order to obtain a fluorescent ATP analogue. In this

case, a fluorescent probe was obtained by reacting the terminal alkyne present in compound (**8**) with a coumarin azide (**14**) *via* azide-alkyne Huisgen cycloaddition[115] (**Scheme 3.7**). Interestingly, none of the reagents in this reaction are fluorescent while the final product is able to fluoresce because of the formation of a highly conjugated system[115] (**Scheme 3.6**) (λ_{ex}=441nm, λ_{em}=495).
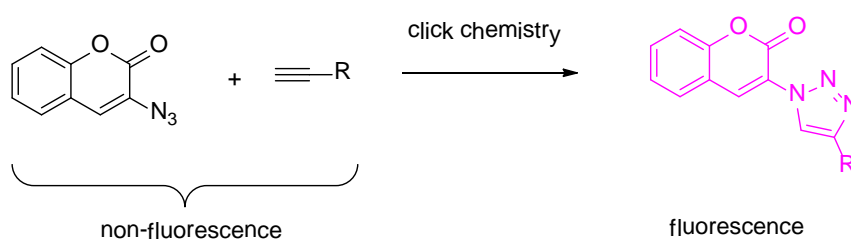
Scheme 3.6: General strategy for Copper(I)-catalyzed 1,3-dipolar cycloaddition reaction of non-fluorescent 3-azidocoumarins and terminal alkynes affording intense fluorescent 1,2,3-triazole products.

The formation of (**16**) was detected by an increase in fluorescence emission at 340nm nm which corresponded to the emission of the coumarin triazole core. After HPLC purification, (**15**) was then coupled with ATP using our standard procedure employed for the other analogues (**7**), (**9**), (**11**). However, as in the previous route no product (**16**) was observed in the reaction mixture after analysis by either ion exchange chromatography or HPLC. It is possible to speculate that the coupling reaction did not work due to low solubility of (**15**) in the aqueous solvent. To overcome this problem, a different route was attempted in order to obtain the ATP coumarin analogue (**18**) (**Scheme 3.8**). In this case, a more polar coumarin azide (**17**) lacking the acetyl

protecting group was coupled to the ATP alkyne analogue (**9**) *via* an azide-alkyne

Huisgen cycloaddition and purified by HPLC. Again, also for this reaction, none of the

reagents were fluorescent while the final product is able to fluoresce thanks to the

formation of a highly conjugated system. The formation of the correct product was

therefore confirmed by analysing the fluorescent trace of the chromatogram at 340nm

and by mass spectrometry analysis.
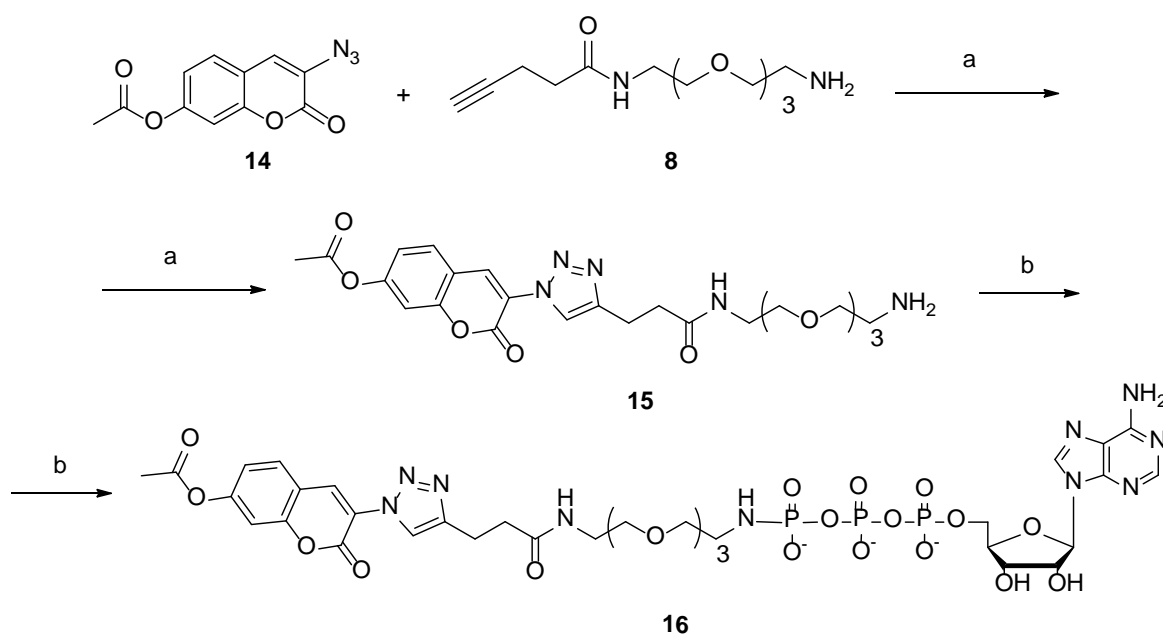
Scheme 3.7: Synthetic route one to the ATP coumarin analogue (**16**). *Reagents and conditions:* (a) CuSO$_4$, ascorbic acid (b) ATP, EDC.
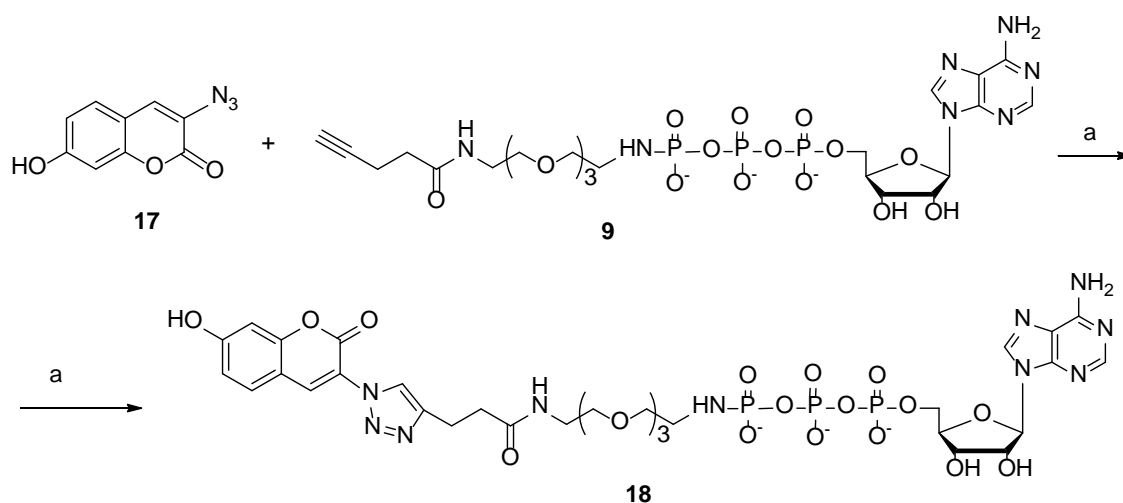
Scheme 3.8: Synthetic route two to the ATP coumarin analogue (**18**). *Reagents and conditions:* (a) CuSO$_4$, ascorbic acid, 15%.

3.3 Enzymatic assays

The four different ATP analogues (**7**), (**9**), (**11**), (**18**) were then tested for their ability to act as phosphate group donors in *in vitro* kinase assays using human CK2. At this stage, the commercially available enzyme was preferred to the bacterial expressed *P. falciparum* homologue for practical reason in order to first establish the technique in the lab and then, in a later stage to subsequently implement it with the target *Plasmodium* homologue. In particular, due to the difficulties encountered in detecting the probe transfer, several analytical techniques were used in this context.

3.3.1 Western Blot analysis

In this case, the ATP biotin analogue (**7**) was tested in an *in vitro* kinase assay with the human CK2 enzyme and β-casein as a substrate. After incubation, the sample was loaded on a 12% SDS-PAGE gel, transferred to nitrocellulose paper and tested with a

streptavidin antibody, in order to detect the enzymatic transfer of the biotin tag to the CK2 substrate. This preliminary test was carried out in the same conditions described by Pflum *et al*[127] in order to reproduce the published data, establishing the same technique in our lab.
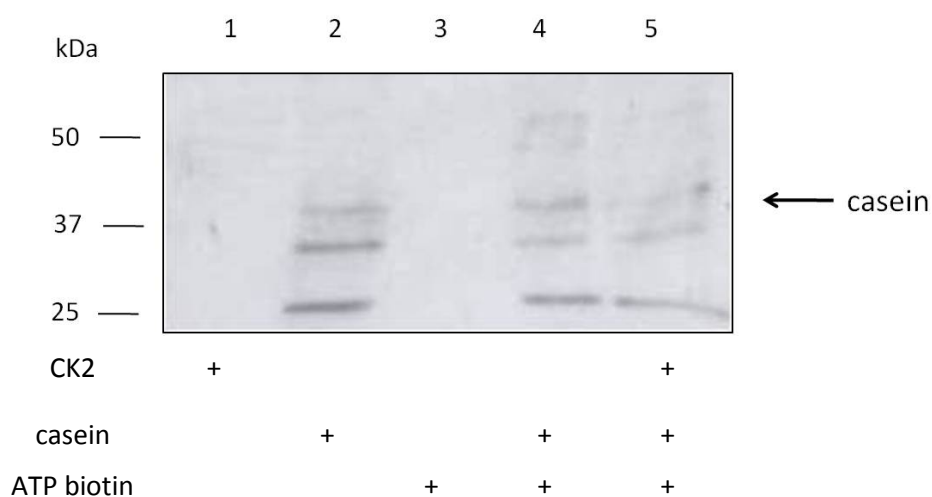
Figure 3.4: Analysis of the biotinylation of casein catalysed by CK2 in the presence of ATP biotin (**7**). CK2 was incubated with casein and ATP biotin (**7**) at 37°C for 10min; proteins were then resolved on SDS-PAGE and analysed by Western Blot using HRP-coniugated streptavidin. Results (lane 5) show that no active transfer occurred in the assay conditions. Results are representative of three independent experiments.

The results (**Figure 3.4**) showed a cross reactivity of the streptavidin antibody with the substrate in the control (lane 2); however no strong recognition was observed in the presence of (**7**) and CK2, suggesting that the transfer of the biotin reporting group did not occur in the assay conditions. Nevertheless, the fact that several bands appear in the Western blot and that streptavidin also recognised the unreacted substrate

undermines the reliability of such result at this stage. In order to test the quality of the streptavidin antibody, as a further control, samples from the *in vitro* kinase assay were analysed by Western Blot together with a chemically biotinylated β-casein. Also in this case (**Figure 3.5**), the same cross reactivity of the streptavidin antibody was observed in the presence of β-casein. However, a much stronger signal was detected for the biotinylated β-casein in the control lane.

At this point, it is worth noting that the chemical biotinylation of β-casein results in the transfer of many biotin functions to a single protein, while the enzymatic process with CK2 and compound (**7**), if occurring, would transfer a single tag per protein at the specific CK2 phosphorylation site. Therefore, it can be hypothesised that the strong signal observed in the control lane for the chemical biotinylated β-casein was due to a large number of biotin functions in the sample, while the biotin transfer mediated by CK2 potentially provided an amount of biotinylated product not sufficient to generate a detectable signal with this particular antibody. In conclusion, these results, taken altogether, demonstrate that transfer of the tag could not be detected in these assay conditions followed by Western Blot analysis. This fact can be due to three main reasons: i) the ATP biotin analogue (**7**) is not accepted by CK2 (however this would contradict previous reports by Pflum *et al.*[127]); ii) the poor specificity of the antibody or iii) the instability of the tag linkage in the assay condition (e.g. boiling the samples in laemmli buffer prior SDS-PAGE loading) causing its loss and subsequent lack of detection.
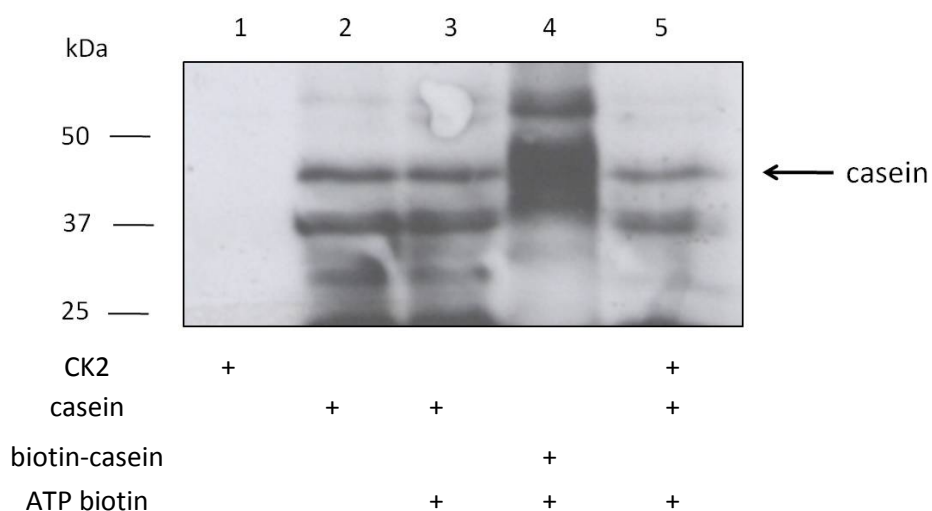
Figure 3.5: Analysis of the biotinylation of casein catalysed by CK2 in the presence of ATP biotin (**7**). CK2 was incubated with casein and ATP biotin (**7**) at 37°C for 10min; proteins were then resolved on SDS-PAGE and analysed by Western Blot using HRP-coniugated streptavidin. Results highlight that the HRP-coniugated streptavidin interacts efficiently with the biotinylated casein control showing increased intensity compared to background (lane 4), while no CK2-driven biotin transfer is observed in the assay conditions (lane 5). Results are representative of three independent experiments.

3.3.2 Mass spectrometry analysis

In order to unambiguously demonstrate that CK2 can accept γ-modified ATP analogues and catalyse the transfer of the phosphate tag to its substrates, a mass spectrometry based analysis was tested. In this case, an *in vitro* kinase assay was carried out by incubating the enzyme with either the ATP analogue or ATP as a positive control, together with a peptide containing a consensus sequence for CK2 phosphorylation.

After the kinase reaction, the sample was then desalted using a ZIP-TIP and subsequently analysed by MALDI-TOF. The mass spectrometry analysis was chosen as it is possible to easily distinguish the three different species of the peptide, the phospho-peptide and the tagged phospho-peptide, by simply looking at their masses. In particular, in this specific analysis the commercially available peptide with the following sequence RRREEETEEE was chosen (see **Table 3.2**). This has already been reported as CK2 kinase substrate[127]. Interestingly, results from this study showed that just a phosphorylated peptide (1442Da) was observed in all cases, with either ATP or the ATP analogues (**7**), (**9**), (**11**), (**18**) despite the presence of the tag on the phosphate donor molecule in the latter cases (**Figure 3.6**).

Phospho-tag	Mass (Da)
-	1362
PO_4	1442
Biotin	1887
Alkyne	1681
Azide	1641
coumarin	1884

Table 3.2: Mass of the CK2 substrate peptide RRREEETEEE and the relative tagged phosphopeptide products after the kinase reaction with ATP and ATP analogues (**7**), (**9**), (**11**), (**18**).
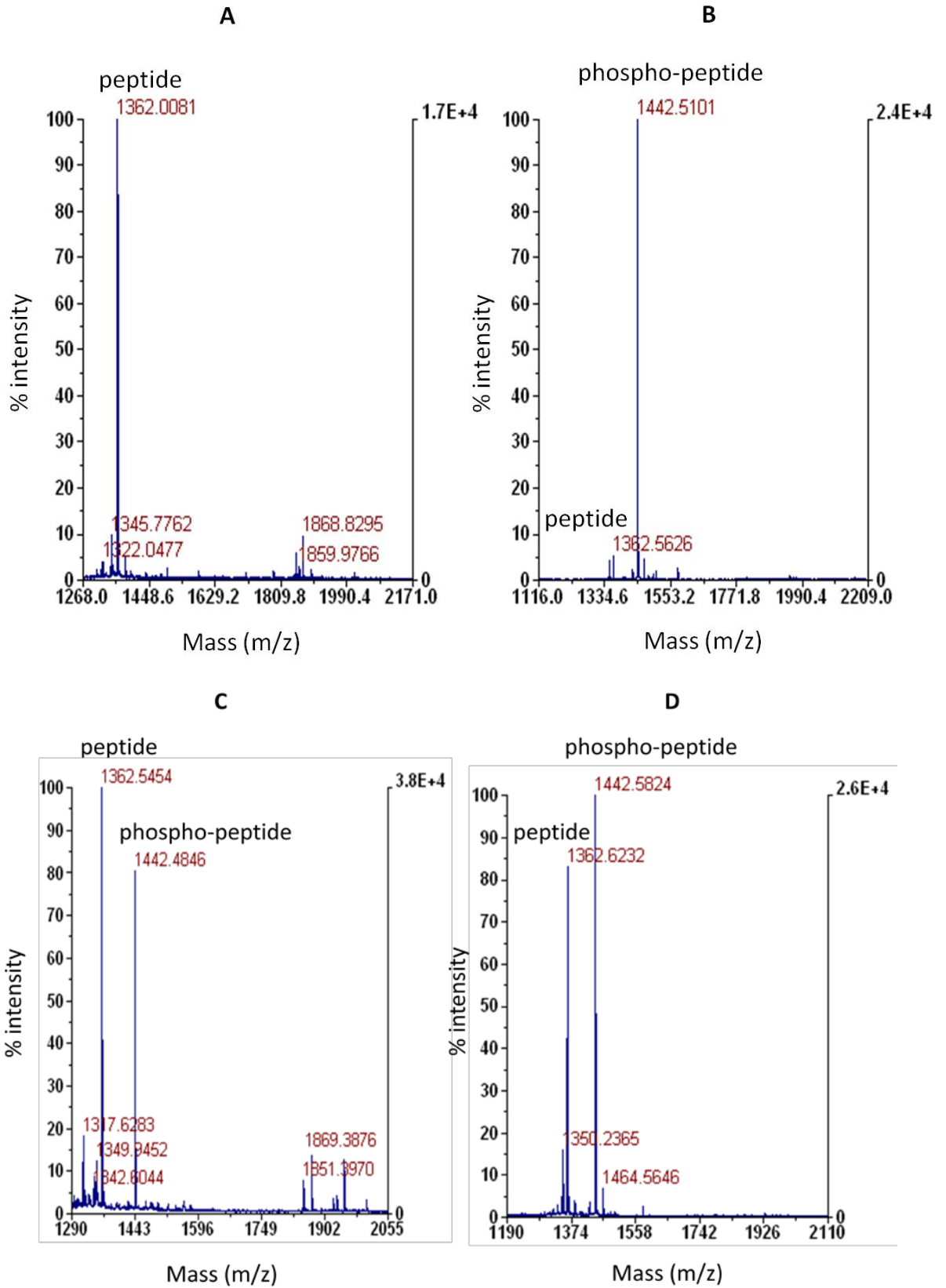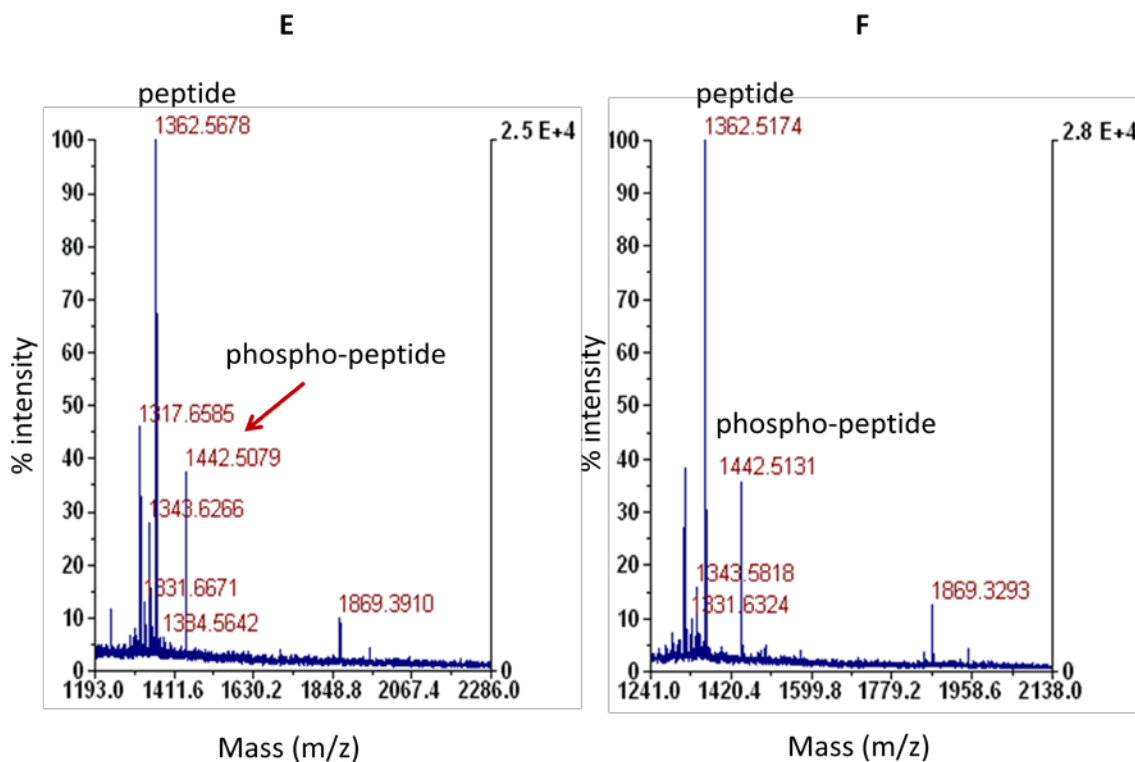
Figure 3.6: MALDI-TOF analysis of *in vitro* kinase assay with the peptide RRREEETEEE, CK2 and ATP/ATP analogues as phosphate donors. (**A**): peptide control; kinase reaction with: (**B**): ATP; (**C**) ATP biotin analogue (**7**); (**D**): ATP alkyne analogue (**9**); (**E**) ATP azide analogue (**11**); (**F**): ATP coumarin analogue (**18**).

Instead, the transfer of the reporting group was never detected in the conditions of the analysis and the peak observed at 1869Da should be considered as an impurity since it is present also in the peptide control. This experimental evidence is particularly surprising given the purity of the ATP analogues (see **Figure 3.3**), which did not contain any detectable traces of ATP that could have explained the occurrence of a simple phosphate transfer. A possible explanation of such discrepancy could be due again to the instability of the tag in the condition of the analysis .

On the basis of this data what can be hypothised is that the ATP analogue is in fact accepted by CK2 in the kinase reaction but the tag then gets cleaved during the condition of the analysis (see section **3.3.4**).

3.3.3 HPLC analysis

An HPLC method was developed in order to detect the transfer of the phosphate-tag to a peptide substrate catalysed by CK2. Given the very low concentrations of the peptide in the kinase assay conditions, to increase the sensitivity of the technique a fluorescence-based HPLC detection system was used together with a fluorescent peptide substrate. To this aim, a peptide with the same sequence as the one previously used in the mass spectrometry analysis (RRREEETEEE) has been synthesised by Fmoc solid phase peptide synthesis (SPPS) following standard procedures.[116] At this stage, the most facile method to introduce a fluorescent probe into the peptide substrate was to exploit the natural fluorescent properties of the Fmoc protecting group. Therefore, cleavage of the Fmoc function from the last coupled amino acid was omitted. After the SPPS, the peptide was cleaved from the resin and purified by HPLC (**Figure 3.7**). The purity of the product was finally confirmed by both HPLC and mass spectrometry analyses.
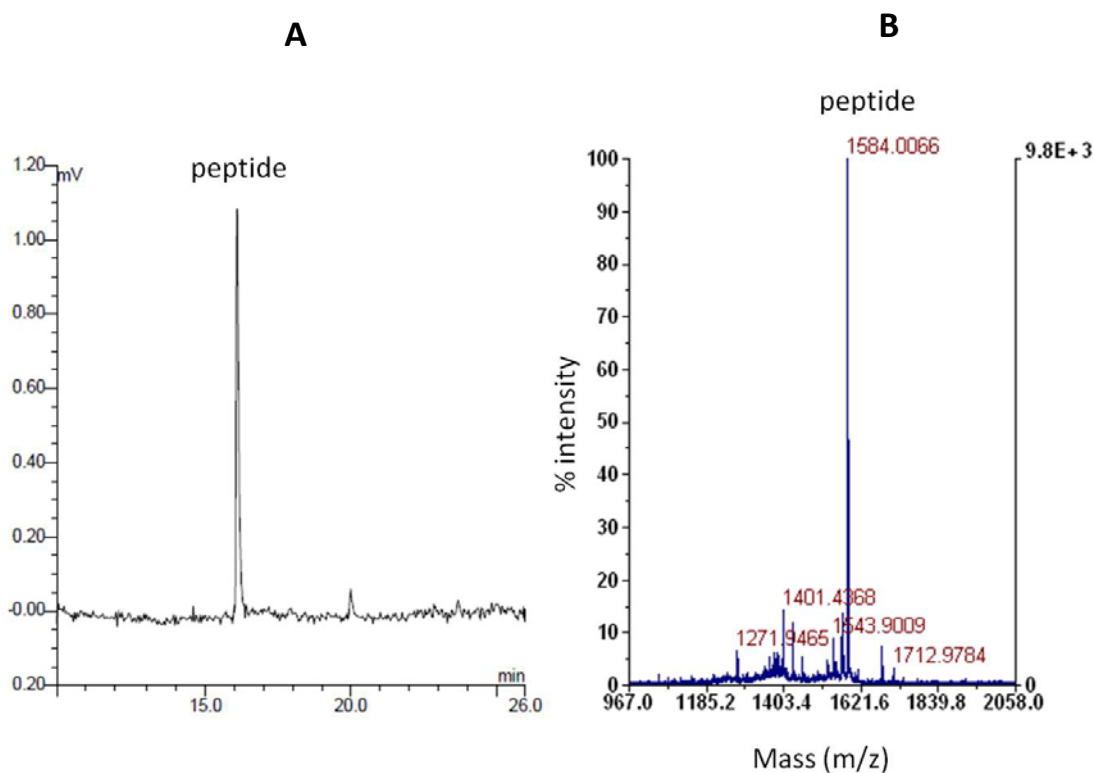
Figure 3.7: Purity of the synthesised fluorescent peptide Fmoc-RRREEETEEE. **A:** HPLC analysis (emission chromatogram registered at: λ_{ex}=280nm λ_{em}=340nm); **B:** MALDI-TOF analysis (peptide MW: 1584Da).

In order to verify that the introduction of the fluorescent tag did not interfere with the substrate recognition by CK2 and with the kinase reaction, an *in vitro* kinase assay was carried out followed by MALDI-TOF analysis. Results showed that the kinase reaction occurred and that a phosphate group was efficiently transferred to the peptide substrate resulting in a mass shift of +80Da (**Figure 3.8**). Having demonstrated that the fluorescent peptide was acting as an actual substrate of CK2, samples from an *in vitro* kinase assay were then analysed by HPLC.
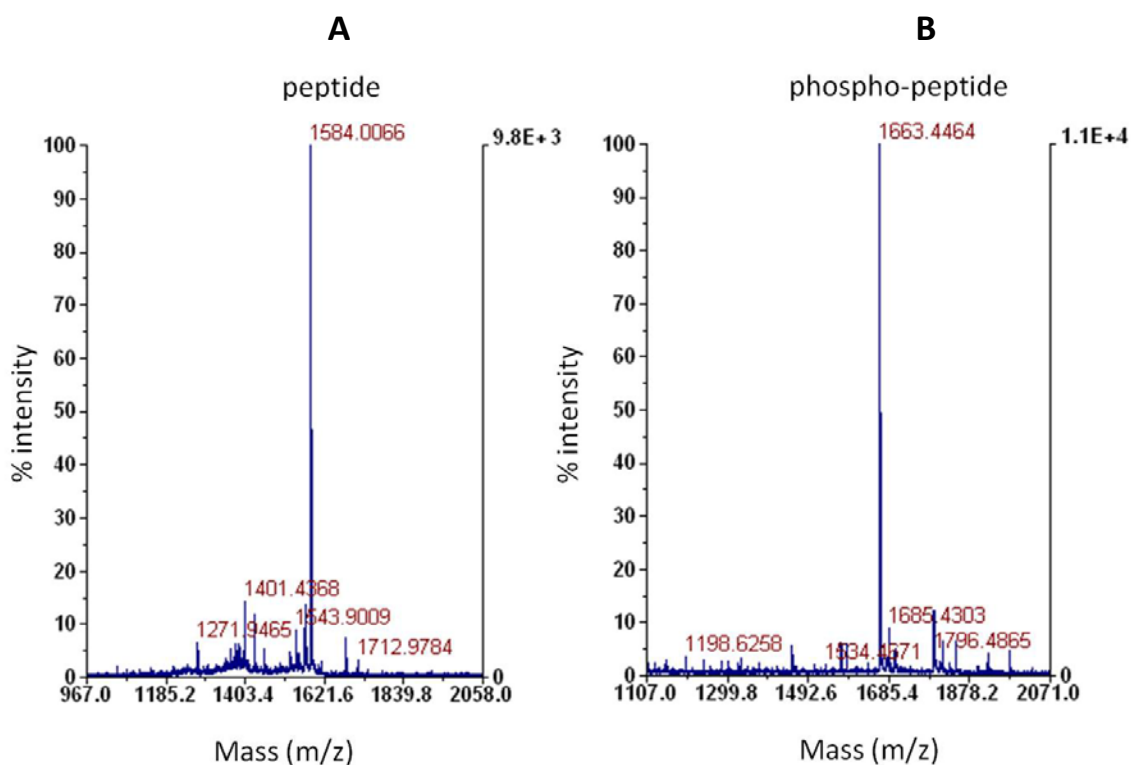
Figure 3.8: MALDI-TOF analysis of *in vitro* kinase assay with the fluorescent peptide Fmoc-RRREEETEEE, CK2 and ATP: **A:** peptide control; **B:** kinase reaction with ATP.

Resulting data showed that a kinase reaction occurred in the presence of both the ATP and the ATP analogue (**11**) corresponding to a slight shift in the retention times for the fluorescent peptide species in the chromatogram., respectively 14.5 and 15.5min for the peptide and the phospho-peptide (**Figure 3.9**). However, transfer of the tag was not detected in the condition of the analysis. Also in this case, such result can be explained by two main reasons: i) ATP analogues (**7**), (**9**), (**11**), (**18**) were not accepted by CK2 and the phosphorylation of the peptide observed was due to the presence of ATP impurities in the sample (although no ATP traces were detected after the purification of ATP analogues by HPLC analysis (see **Figure 3.3**)) or ii) the ATP analogues (**7**), (**9**), (**11**), (**18**) were tolerated by CK2 as phosphate donors but the tag

was cleaved in the condition of the analysis (see section **3.3.4**). At this stage, in order to find conditions that would improve the stability of the tag during the sample analyses allowing its detection, several buffer systems at different pH were tested during the HPLC analysis of *in vitro* kinase assays. Such buffers included: water; ammonium acetate 20mM pH: 6.5, ammonium bicarbonate 20mM pH: 9 and PBS buffer 20mM pH6.5. Unfortunately, in none of the cases it was possible to detect any peak for the fluorescent peptide. This is probably due to the highly acidic nature of the peptide sequence (RRREEETEEE) that requires a strong buffer in order to protonate the acidic functions and maintain the peptide species all in the same charge state.
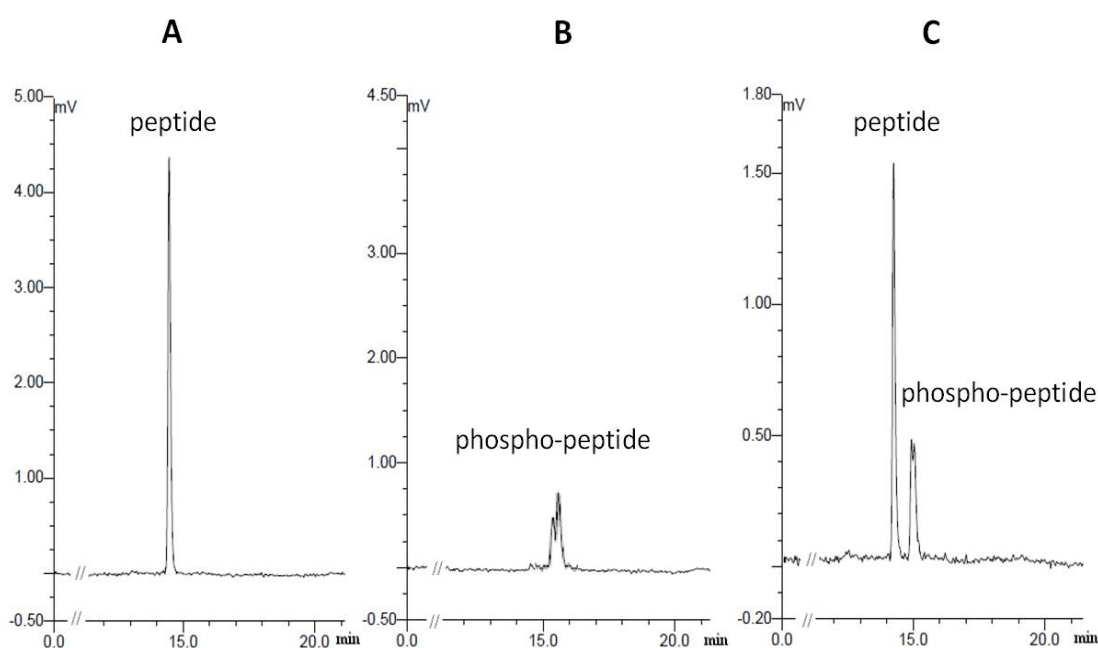
Figure 3.9: HPLC analysis of the in vitro kinase assay. Emission chromatogram registered at λ_{ex}=280nm λ_{em}=340nmfor: (**A**) Fmoc-peptide control; (**B**) kinase reaction with ATP; (**C**) kinase reaction with ATP azide analogue (**11**).

3.3.4 Study on the stability of the ATP analogues

Since the purity of the ATP analogues (**7**), (**9**), (**11**), (**18**) and therefore the absence of ATP had already been confirmed (**Figure 3.3**), we then decided to investigate whether the problems in detection derived from the low stability of such probes in the acidic conditions (0.1% TFA pH: 2) of both MALDI-TOF and HPLC analyses. Tests were carried out incubating the ATP analogue (**11**) in 0.1% TFA at 1mM final concentration and the results analysed through analytical HPLC. These tests have showed that the function most susceptible to degradation is the P-N bond which is very sensitive to acidic conditions. In fact, after 5min of incubation in 0.1%TFA only 60% of the ATP analogue (**11**) survived hydrolysis, while after 1hr in the same conditions the whole sample was completely degraded (**Figure 3.10**).
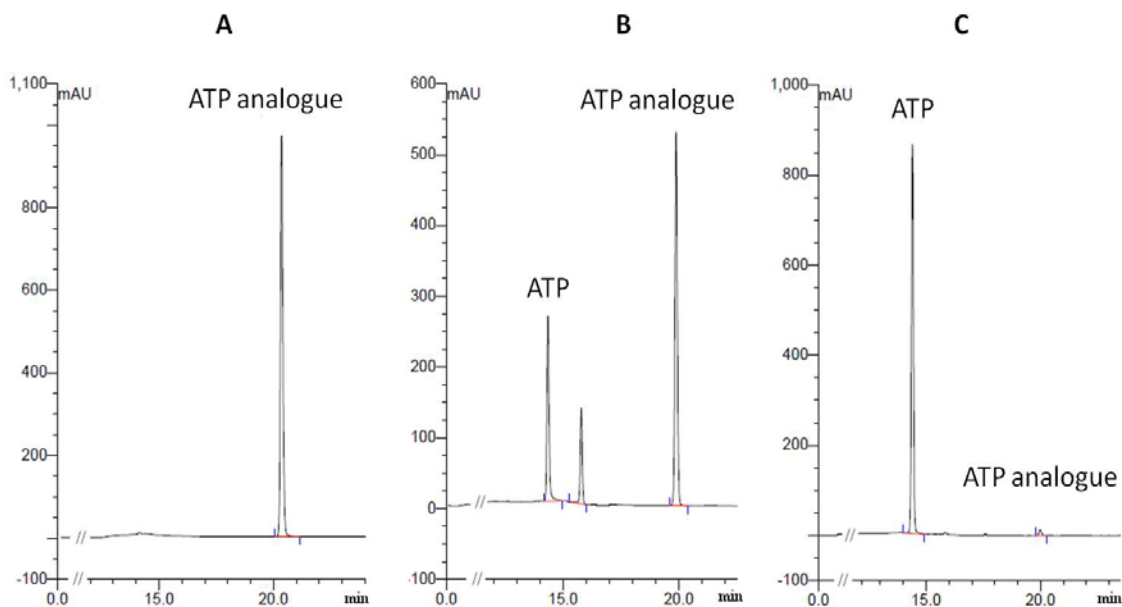
Figure 3.10: HPLC analysis for the stability of ATP analogue in acidic conditions. Chromatogram monitored at λ_{abs}=260nm for: (**A**) ATP analogue (**11**) control; (**B**) ATP analogue (**11**) after 5min in 0.1% TFA; (**C**) ATP analogue (**11**) after 1hr in 0.1% TFA.

Based on the retention times, the main degradation product was recognised to be ATP, while the peak observed at ~15.7min was most likely an intermediate of the degradation process since it disappears at long incubation times. However, it was not possible to determine the nature of such intermediate during the analysis. As expected, all the synthesised ATP analogues showed the same behaviour in this kind of tests, therefore results for just the ATP azide are presented here.

3.3.4 FRET analysis

In order to overcome the problems linked with the instability of the probes in the acidic conditions usually required by sample analysis (e.g. MALDI-TOF, HPLC), a FRET-based kinase activity assay to detect the transfer of a fluorophore tag has been developed. To this aim, a fluorescent peptide with a CK2 consensus sequence (RRREEETEEE) bearing a fluorescein function at the N-terminus has been synthesised by Fmoc SPPS and purified by HPLC as previously described for the Fmoc-peptide. In particular, the fluorescein tag has been chosen for the significant overlap between its excitation spectrum and the coumarin emission spectrum. In this way, a successful transfer of the coumarin tag to the peptide substrate catalysed by CK2 can be detected by measuring the FRET signal between the two fluorophores, due to their close proximity (**Figure 3.11**). After the peptide synthesis, the purity of the peptide has been assessed by both MALDI-TOF and HPLC analysis (**Figure 3.12**). These are therefore eluted at different times in the column given rise to the multiple-peak-shape of the chromatogram.
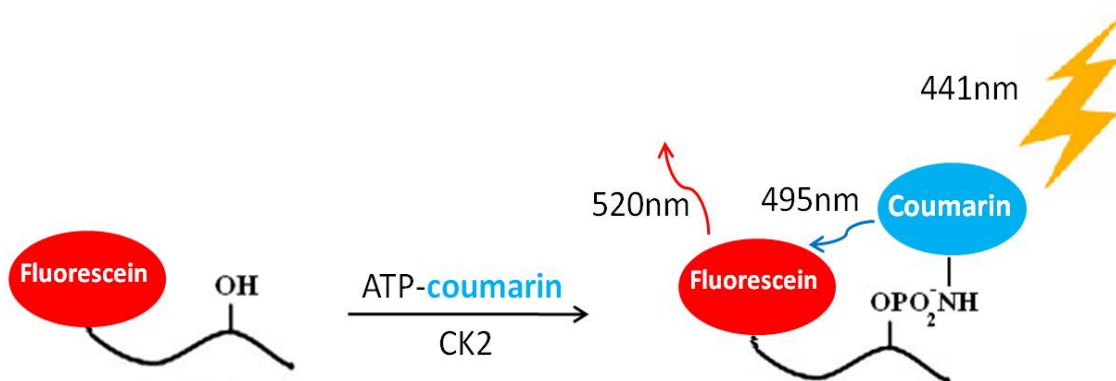
Figure 3.11: Schematic representation of the FRET-based kinase activity assay detecting the transfer of the coumarin reporting group catalysed by CK2. After the kinase reaction, the transferred coumarin is excited at 441nm acting as a FRET donor to the neighbouring fluorescein function (FRET acceptor). This generates a fluorescent signal at 520nm.

In particular, the presence of several close peaks in the HPLC chromatogram can be explained by the fact that a commercially available mixture of different carboxy-fluorescein stereoisomers has been used in the synthesis leading to the formation of different diastereoisomers of the product. There is no reason to believe that the presence of different fluorophore stereoisomers would interfere with the FRET analysis. The MALDI-TOF analysis confirmed the right molecular mass for the product without detecting any major impurities, further confirming the HPLC data.

Having demonstrated the correct nature of the fluorescent peptide, this substrate was then incubated with the ATP coumarin analogue (**18**) and CK2 for an *in vitro* kinase assay.
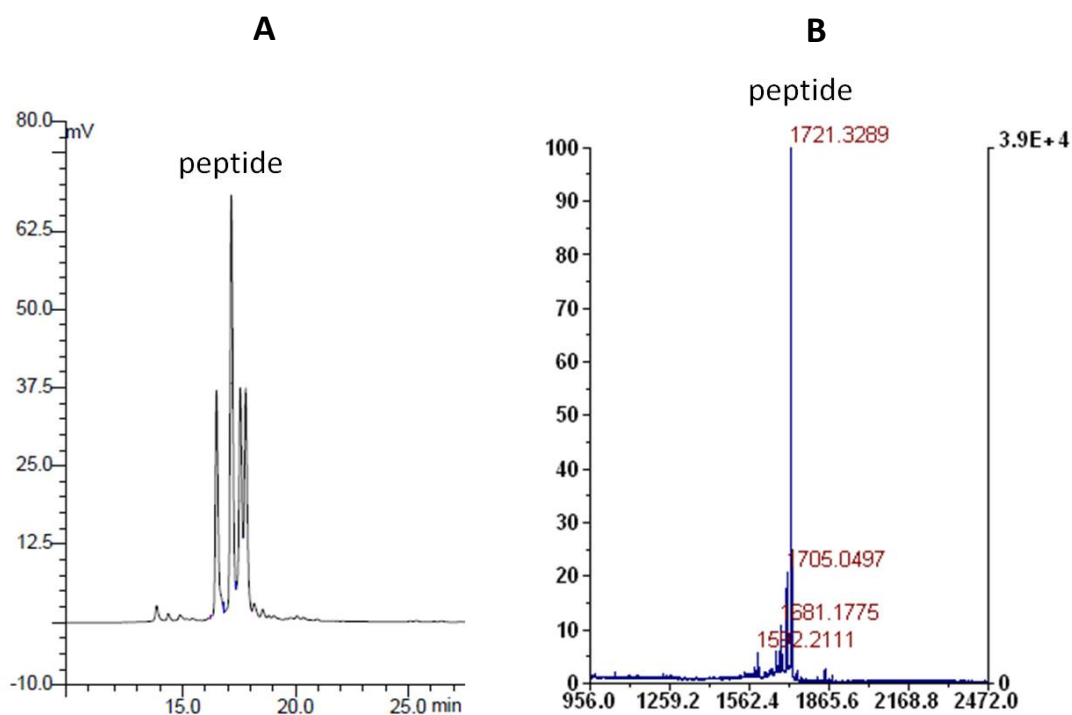
Figure 3.12: Analysis of the purity of the synthesised fluorescent peptide: 5(6)-carboxyfluorescein-RRREEETEEE. **A:** HPLC analysis (emission chromatogram registered at λ_{ex}=495nm λ_{em}=520nm); **B:** MALDI-TOF analysis.

The sample was then analysed by measuring the emission spectrum of the fluorescein chromophore (FRET acceptor) after coumarin excitation at 440nm (FRET donor). An emission spectrum for coumarin has also been recorded as a control to measure background fluorescence from the FRET donor. Results clearly showed that no emission peak at 520nm was detected in the sample, and that all the observed fluorescent is due to the tail in the emission spectrum of the FRET acceptor (**Figure 3.13**). Therefore, it can be concluded that no energy transfer occurred during the FRET analysis.
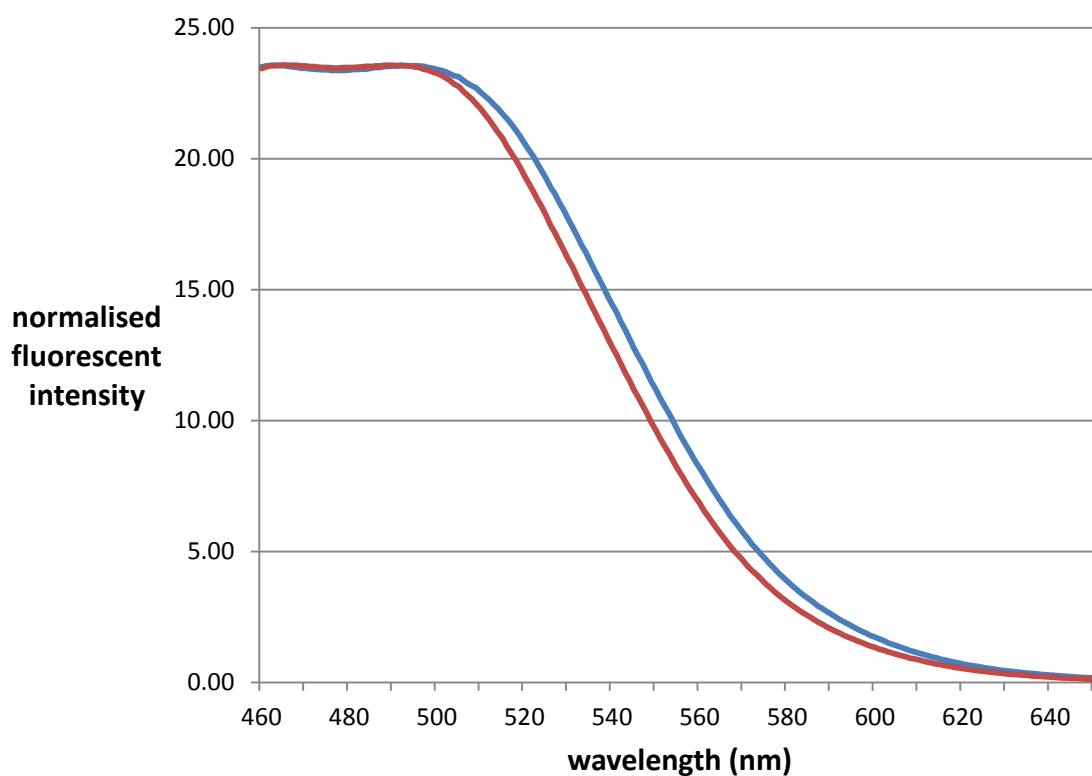
Figure 3.13: Results of the FRET-based kinase activity assay showing the emission spectrum of both the kinase reaction sample (blue line) and the FRET donor control ATP coumarin (**18**) (red line).

This evidence can be explained by three main reasons: i) the ATP coumarin analogue (**18**) is not a substrate of CK2; ii) the fluorescein peptide is not a substrate of CK2 (however, previous data reported for the Fmoc peptide suggests that N-terminal substituents do not affect peptide substrate recognition) or iii) the reaction is effectively taking place but the two fluorophores are too distant in order to produce a FRET signal.

3.3.5 Mass spectrometry analysis with *P. falciparum* CK2

Despite the fact that no tag transfer could be directly demonstrated by using the different analytical techniques, it has been decided to test one ATP analogue with *P. falciparum* CK2 in order to verify if this enzyme shows a similar behaviour to its human homologue. In this case, an *in vitro* kinase assay was carried out by incubating the enzyme with either the ATP azide analogue (**11**) or ATP as a positive control, together with a peptide that has already been shown to be recognised by *P.falciparum* CK2.[71] After the kinase reaction had occurred, the sample was then desalted using a ZIP-TIP and subsequently analysed by MALDI-TOF. In particular, the chosen peptide RRRADDSDDDDD is characterised by a mass of 1450Da, while the relative phospho-peptide has a MW of 1530Da and the resulting azide tagged phospho-peptide would present a mass of: 1729Da. As expected, in the mass spectrometry analysis a simply phosphorylated peptide (1530Da) was observed in both enzymatic reactions with either ATP or the ATP analogue (**11**) (**Figure 3.14**). These results are consistent with what has been reported before in the case of the human homologue and therefore similar conclusions can be applied also in this context (see section **3.3.2**).
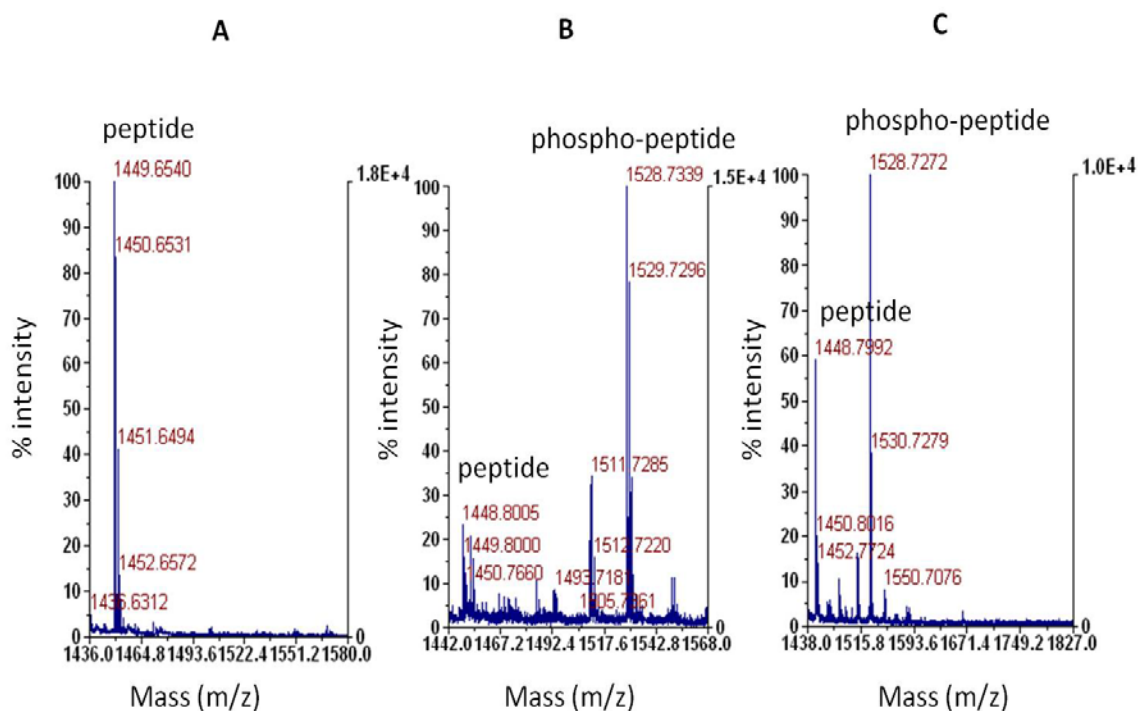
Figure 3.14: MALDI-TOF analysis of *in vitro* kinase assay with the peptide RRRADDSDDDDD with *P. falciparum* CK2 and ATP/ATP azide analogue (**11**) as phosphate donors. (A): peptide control; kinase reaction with: (B): ATP; (C) ATP azide analogue (**11**).

3.4 Discussion

CK2 is a pleiotropic Ser/Thr kinase that plays a crucial role in eukaryotic cells and it is considered to be a potential and druggable target in many diseases such as tumors, leukemia and malaria. Here we tried to develop a chemical biological approach in order to detect CK2 substrates and pathways in *P. falciparum* using γ-phosphate modified ATP analogues. In particular, syntheses of such analogues through phosphoramidate chemistry have been successful, establishing a platform of four

121

analogues bearing the following different functions at the γ-phosphate position: biotin, azide, alkyne, coumarin. These were covalently linked to the nucleotide molecule by a tetraethyl glycol linker in order to confer the probe further flexibility. At this stage, only the synthesis of a fluorophore ATP probe proved problematic. In fact, the first attempt to introduce a dansyl function by coupling ATP with dansylcadaverine using a carbodiimide was not successful. This was probably due to the low solubility properties of the fluorophore reagent in an aqueous or organic/aqueous mixed solvent. To overcome this problem the preparation of a coumarin-linked probe to ATP was attemped using the same conditions but also in this case no product was observed, probably due to the same reasons. Finally, a more soluble coumarin derivative (**17**) was successfully coupled with the ATP alkyne analogue (**9**) by a click chemistry reaction.

This set of probes was tested in *in vitro* kinase assays with a commercially available CK2. Despite the fact that results were analysed by different analytical techniques, no efficient tag transfer has been detected in the tested conditions. However, overall phosphorylation of the peptide substrate was observed in the presence of the analogues by both HPLC and MALDI-TOF analysis. In addition, stability tests for the ATP analogues in 0.1% TFA, an acidic buffer used in both HPLC and MALDI-TOF methods, showed a high liability of the P-N bond that covalently links the probe to the nucleotide γ-phosphate. The proposed mechanism for such event involves protonation of the nitrogen followed by water hydrolysis (**Figure 3.15**). These results, taken altogether, can be interpreted in two main ways, either i) the ATP analogues (**7**), (**9**), (**11**), (**18**) are not active substrates recognised by CK2 and the observed phosphorylation is due to ATP traces presents in the sample or ii) ATP analogues (**7**),
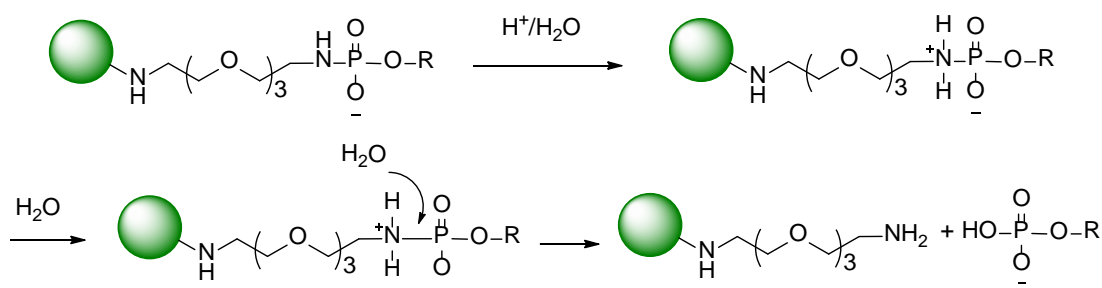
Figure 3.15: Mechanism for P-N bond hydrolysis in acidic conditions (the mechanism applies identically to both ATP analogues and the tagged phospho-peptides).

(**9**), (**11**), (**18**) are efficiently used by CK2 for the phospho-transfer reaction but the tag gets cleaved in the acidic conditions usually required during the subsequent analysis. Even if none of these two alternative scenarios can be unequivocally excluded at this stage, it is still possible to draw some reasonable conclusions on the basis of the obtained experimental data. In fact, considering the high purity of the synthesised analogues showing no detectable traces of ATP (**Figure 3.3**), it would be hard to account for the observed phosphorylation in the presence of the ATP analogues, if these were not to be tolerated by CK2. The most likely explanation is that the ATP analogues are accepted by CK2 and involved in the phospho-transfer reaction. However, the acidic conditions required by the analysis do not permit the detection of the tag leading to the hydrolysis of the P-N bond and the subsequent observation of a simple phosphate transfer (**Figure 3.15**). In this possible scenario, the negative results obtained in both the Western Blot analysis and the FRET-based kinase assay can be explained by internal problems linked with the analysis conditions. The streptavidin antibody used in the immunoblot in fact presented some cross-reactivity problems recognising several bands also in the negative control sample.

Regarding the FRET assay, the coumarin-fluorescein FRET pair was chosen due to the availability of the compounds in the laboratory and for the good overlap between the donor emission and the acceptor excitation spectra. However, no positive control for the efficiency of such FRET pair nor for the sufficient proximity of the two flourophores in the final product of the kinase reaction are available in order to unambiguously demonstrate a negative result in the assay. Finally, the same results obtained in the mass spectrometry analysis of the *P. falciparum* CK2 kinase test suggest that the two possible scenarios can be similarly applied also in that context. In conclusion, despite the efforts, it was not possible to employ the described chemical biological approach in the investigation of CK2-driven phosphorylation pathways. However, the fact that CK2 does not accept γ-modified ATP analogues has not been unambiguously proven. This leaves the field open for future work in addressing the problem of detecting the probe transfer in non-acidic conditions. One particular possibility is constituted by capillary electrophoresis and especially by the Caliper 3000HTS system developed by Caliper Technologies (Mountain View, CA USA). In fact, this highly automated detection system exploits the charge differences between the peptide, the phospho-peptide and the tagged peptide to monitor the kinase reaction and its products, without requiring acidic pH conditions during the analysis.[133]

Chapter 4: PfCK2 phosphoproteomics

4.1 Introduction

A striking feature of CK2 family enzymes is their pleiotropic and ubiquitous nature. The list of CK2 substrates includes more than 300 proteins, many of which are implicated in a number of processes such as signal transduction, DNA repair, cell division and proliferation.[55] Consistent with this wide spectrum of physiological targets is the subcellular localization of CK2, which is found in nearly all the subcellular compartments,[134] although it is especially abundant in nuclei[135] and in the soluble cytosol.[136] Despite the recognised importance of CK2 for cell functioning and survival in model eukaryotic systems, no putative PfCK2 substrates in *P. falciparum* have been reported so far in the literature. The only available information is the evidence that bacterial expressed PfCK2 is able to phosphorylate a number of proteins present in heat-inactivated parasite protein extracts.[71] Based on this observation, we decided to try and develop a new CK2 phosphoproteomic approach in order to unravel *P. falciparum* CK2 substrates, and to investigate the role played by the enzyme in the parasite cell functioning, further validating it as a potential drug target. This approach is in particular based on the identification of PfCK2 phosphorylated substrates by LC-MS/MS analysis of a heat-inactivated parasite lysate that has been previously incubated with recombinant PfCK2. This particular process starts with initial heat inactivation of the lysate aimed at disrupting any intrinsic enzymatic and kinase activity present in the sample. The next step is constituted by the incubation of this

treated cellular extract with a recombinant N-terminal GST-PfCK2 that has been immobilised on glutathione beads in *in* vitro kinase assay conditions. During the kinase assay, the recombinant enzyme phosphorylates putative PfCK2 substrates present in the sample. The enzyme is then separated from the rest of the sample by simple centrifugation and the phospho-proteins in the supernatant are finally indentified through LC-MS/MS. The immobilisation of the enzyme followed by centrifugation and removal is particularly important because otherwise, the presence of a large amount of enzyme protein would interfere with the analysis by saturating the LC-MS/MS detection system. Importantly, in order to minimise the detection of phosphorylated proteins that are naturally present in the cellular lysate, it has been proposed to previously treat the sample with calf-intestinal alkaline phosphatase. This treatment would in fact result in the de-phosphorylation of natural occurring phospho-proteins enabling the identification of only the PfCK2 phosphorylation events during the LC-MS/MS analysis (**Figure 4.1**).
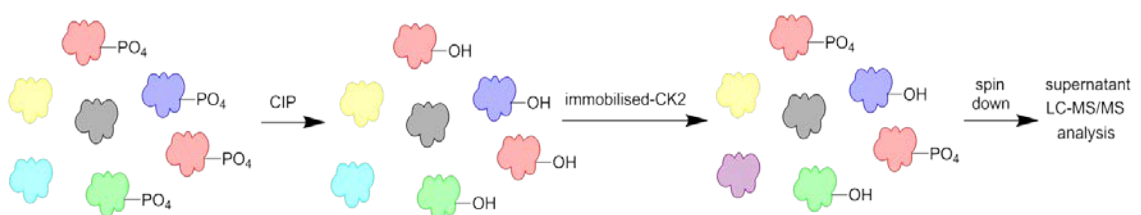
Figure 4.1: Schematic representation of the proposed CK2 phosphoproteomic approach showing dephosphorylation of phosphoproteins present in the lysate by CIP, followed by CK2 *in vitro* kinase reaction and detection of the phosphorylation sites by LC-MS/MS. (CK2 substrates are indicated in red).

If successful, this approach would lead to the identification of phosphorylation events controlled by PfCK2 in a cellular lysate providing useful information about the putative substrates of this kinase in *P. falciparum* and giving insights into the functional role played by in the parasite biology. A major drawback of this kind of approach is that it is essentially based upon an *in vitro* kinase reaction and as such it might not accurately reveal the *in vivo* substrates for PfCK2. This could give rise to the detection of phosphorylation patterns that do not truly occur *in vivo* due for example to differences in the subcellular location of the phosphorylating enzyme and the substrate. However, to overcome this problem we envisaged the possibility of matching the obtained results with the list of validated *in vivo* phosphorylation sites in *P. falciparum* recently published by our group.[83] Also, to further validate the identity of the PfCK2 phosphorylation sites it would be possible to take into consideration the peculiar consensus sequence for CK2 substrates, notably S/T-x-x-E/D.[137]

4.2 Results

In order to validate the feasibility of this new CK2 phosphoproteomic approach we first attempted to reproduce the reported evidence that PfCK2 is able to phosphorylate proteins present in a heat inactivated lysate of infected red blood cells (iRBC).[71] To this aim, an iRBC lysate was first heat inactivated in a water bath at 55°C for 3min; then, after the addition of glutathione beads containing bacterial expressed GST-PfCK2 and ^{32}P-ATP, the sample was incubated at 37°C for 20min for the kinase reaction. After that, the sample was centrifuged to remove the beads containing the CK2 enzyme. Finally, both the pellet and the supernatant were loaded on a SDS-PAGE

gel and exposed to autoradiographic film. To demonstrate that the heat-inactivation treatment was sufficient to remove any intrinsic kinase activity present in the lysate, a kinase reaction was run in parallel with ^{32}P-ATP in the presence of just glutathione beads. Also, in order to further validate the results two other tests were run in parallel with the addition of the CK2 inhibitor quinalizarin (10μM) dissolved in 1% DMSO, and with just 1% DMSO as a control. Results showed that the heat inactivation process efficiently removes any intrinsic kinase activity present in the sample, as demonstrated by the absence of detected radioactivity after the kinase assay (lane 2 **Figure 4.2**). Furthermore, results showed also that the adopted procedure successfully separate the recombinant kinase from the rest of the sample as underlined by the absence of the band relative to the PCK2 in the supernatant (lanes 5,7,9 **Figure 4.2**). Indeed, the fact that PfCK2 undergoes *in vitro* autophosphorylation[71] (see also **Chapter 6**) makes it possible to recognise the relative band in the gel autoradiograph. Finally, the presence of several radioactive bands in the supernatant after incubation with PfCK2 indicates that the enzyme actively phopshorylates proteins in the heat-inactivated iRBC lysate during the *in vitro* kinase assay (lane 5 **Figure 4.2**). This evidence is further confirmed by the lower intensity of the bands in the presence of the CK2 inhibitor quinalizarin (see also **Chapter 5**), but not in the presence of just DMSO (lane 7,9 **Figure 4.2**). In conclusion, the experiment demonstrated the feasibility of the proposed approach.

After this successful analysis, we then decided to investigate whether a CIP treatment was able to remove the presence of phospho-proteins in the iRBC lysate, prior to the heat inactivation process. To this aim, a sample of purified iRBC was first of all incubated with ^{32}P-orthophosphate before the lysis process.
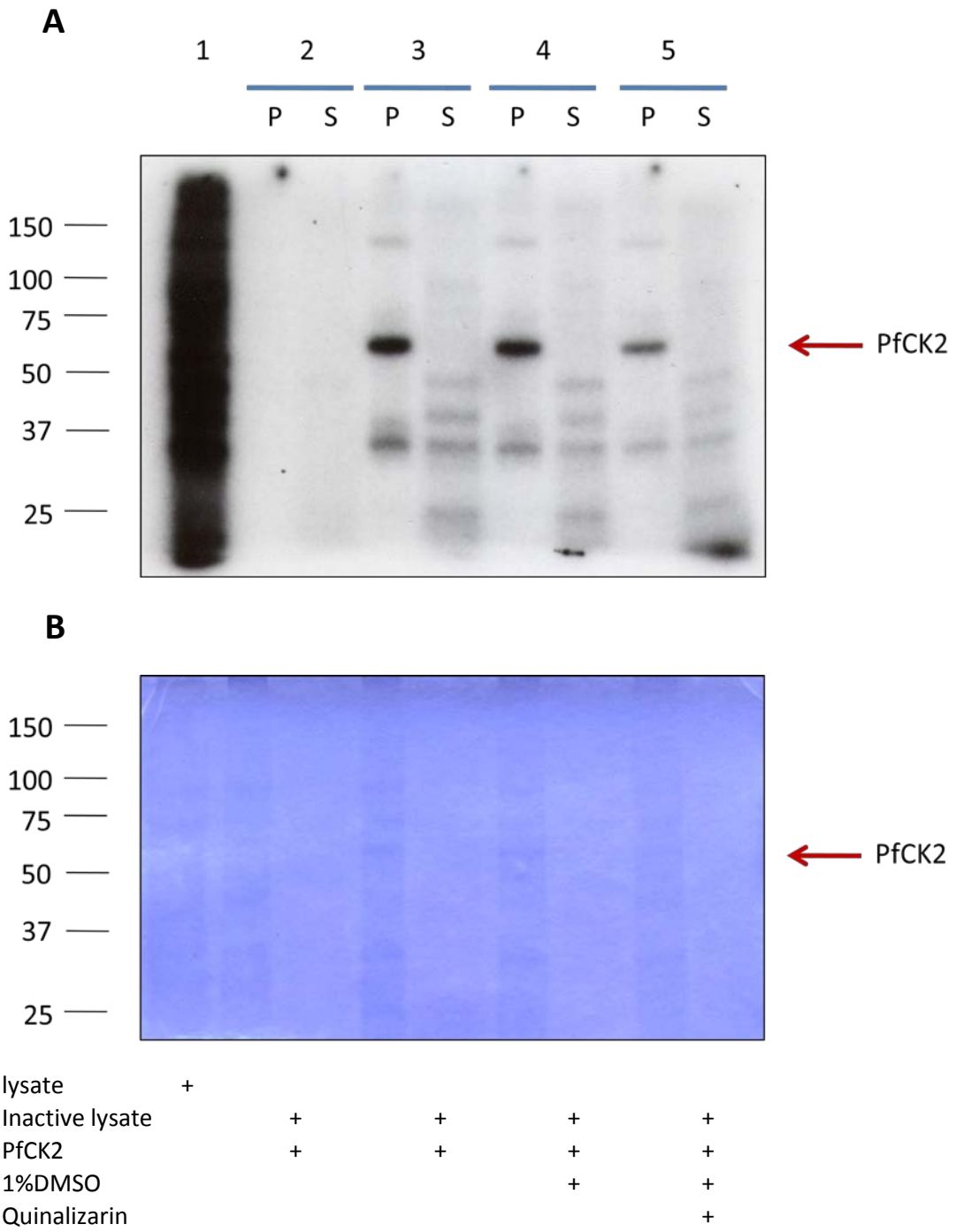
Figure 4.2: PfCK2 is able to phosphorylate proteins in a heat-inactivated iRBC lysate. A iRBC lysate was first heat inactivated for 2min at 55°C followed by incubation with glutathione beads containing PfCK2 and ^{32}P-ATP for 10min at 37°C; proteins were then resolved on SDS-PAGE and exposed to autoradiographic film. Results show that the heat inactivation process efficiently removes detectable kinase activity (lane 2) and that PfCK2 is able to phosphorylates proteins contained in the lysate (lane 3,4,5) a

process inhibited in the presence of quinalizarin (lane 5). Results are representative of three independent experiments. **A:** autoradiograph; **B:** Comassie stain; P: pellet; S: supernatant.

This step resulted in the labelling of natural occurring phospho-proteins with a radioactive phosphate group that allows an easy detection of phospho-proteins through their acquired intrinsic radioactivity. The radioactive iRBC lysate was then incubated with CIP for different lengths of time: 2hr, 4hr and overnight. Samples were finally run on a SDS-PAGE gel and exposed to autoradiographic film. In particular, a sample of radioactive iRBC was run in parallel in the absence of CIP as a negative control. Results showed that the CIP efficiently removed phosphate groups from phospho-proteins as indicated by the decreased intensity of the radioactive bands in the gel (lanes 3,5,7 **Figure 4.3**) compared to the control (lane 2,4,6 **Figure 4.3**). Moreover, from the comparison between the different incubation times (lane 3,5,7 **Figure 4.3**) it is possible to conclude that 2hrs incubation was a sufficient time to enzymatically remove most of the protein phosphorylation in the sample. The autoradiograph suggested also that no improvement in dephosphorylating the lysate was achieved at longer incubation times. Hence, for these reasons it has been decided to run the dephosphorylation reactions for only 2hrs in the following tests. In particular, the condensed shape of lanes 2,4,6 in **Figure 4.3** is caused by the presence of a large amount of CIP protein in the respectively adjacent lanes 3,5,7. Since the CIP protein present in the lysate would clearly interfere with the following CK2 kinase

reaction, we then performed a second experiment to explore the possibility of removing the CIP after the dephosphorylation reaction.
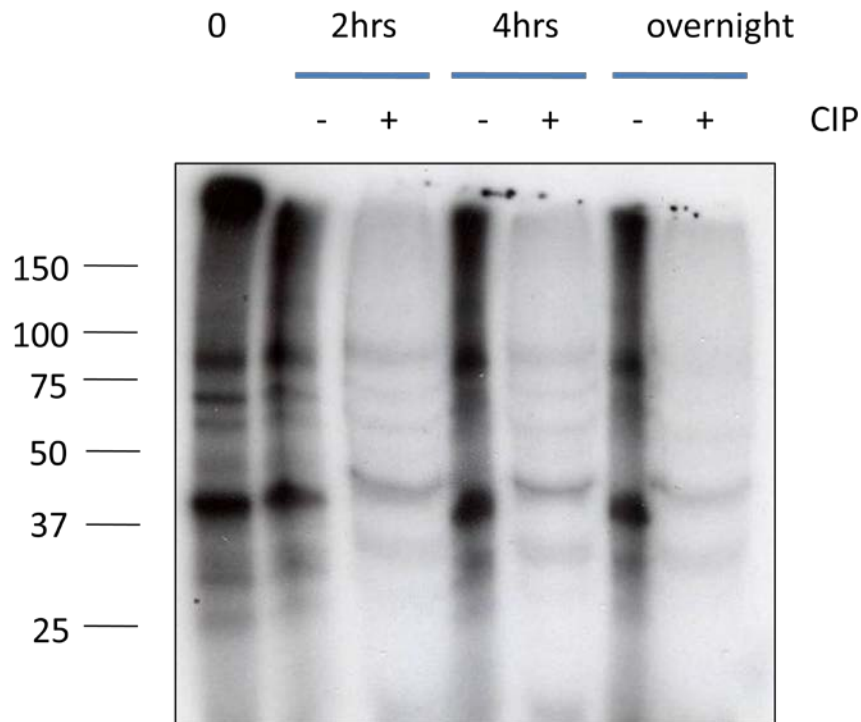
Figure 4.3: CIP efficiently dephosphorylates a parasite lysate after 2hrs. A ^{32}P-labeled iRBC lysate was incubated with CIP at 37°C for the indicated times; proteins were then resolved with SDS-PAGE and the gel exposed to autoradiographic film. Results are indicative of three independent experiments.

To this aim, this time we decided to use a commercially available biotinylated CIP, which, after the incubation with the radioactive iRBC lysate, would be pulled out from the sample by using streptavidin beads. As expected, results from this experiment showed that also the biotinylated form of CIP was able to efficiently dephosphorylate the sample (**Figure 4.4**).
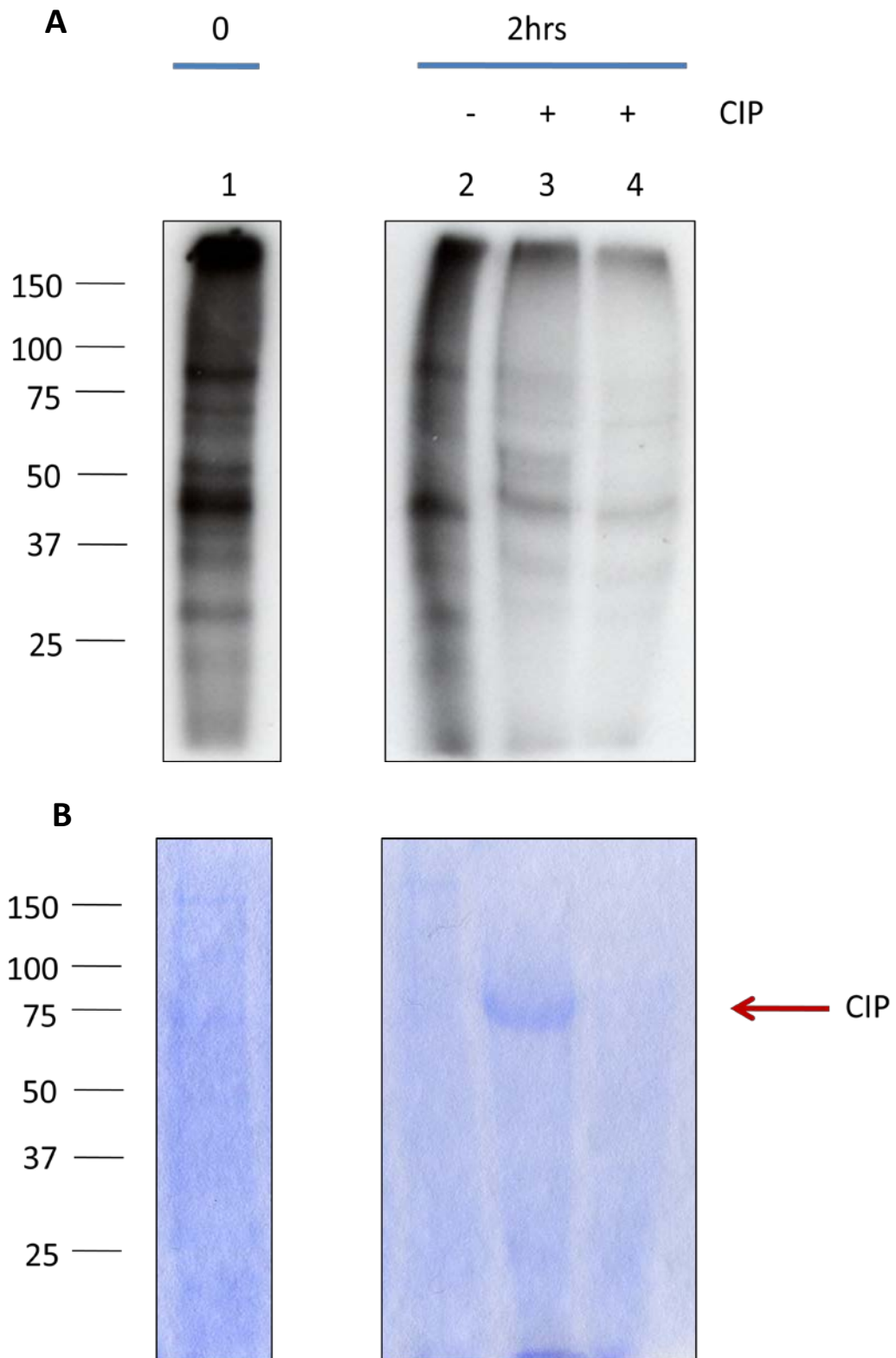
Figure 4.4: Biotinylated CIP is removed from an *in vitro* dephosphorylated reaction mixture by using streptavidin beads. A ^{32}P-labeled iRBC lysate was incubated with

biotinylated CIP for 2hrs at 37°C, biotinylated CIP was then removed by strepatadivin pull-down; proteins were resolved on SDS-PAGE and the gel exposed to autoradiographic film. **A:** autoradiograph; **B:** Comaassie stain; lane 1: ^{32}P-labeled iRBC lysate control, 2: iRBC lysate after 2hrs, 3: iRBClysate biotinylated CIP after 2hrs, 4: iRBClysate + biotinylated CIP after 2hrs followed by streptavidin pull-down. A red arrow indicates the position of biotinylated CIP in the gel.

Interestingly, the incubation with streptavidin beads removed any detectable traces of CIP from the sample as shown by the Coomassie stain of the gel (**Figure 4.4**). In conclusion, these three preliminary experiments demonstrated the feasibility of the proposed approach (**Figure 4.1**) and successfully determined experimental conditions to both dephosphorylate an iRBC lysate and perform an *in vitro* kinase assay with a PfCK2 sample immobilised on beads.

A final experiment was performed by first dephosphorylating an iRBC lysate with biotinylated CIP. This was then pulled out with streptavidin beads. The sample was subsequently heat-deactivated at 55°C for 2min and finally incubated with PfCK2 and ^{32}P-ATP in a kinase reaction assay. A kinase reaction with PfCK2 and an iRBC lysate not previously treated with CIP was also run in parallel as a control. Surprisingly, results showed that while PfCK2 actively phosphorylated proteins present in the iRBC lysate control, no phosphorylation was observed in the CIP-treated sample as indicated by the absence of detected radioactive bands in the gel (lane 7, **Figure 4.5**). Interestingly, the enzyme in this sample was still able to undergo autophosphorylation although to a lesser extent compared with the CIP untreated sample (lane 3,6 **Figure 4.5**).
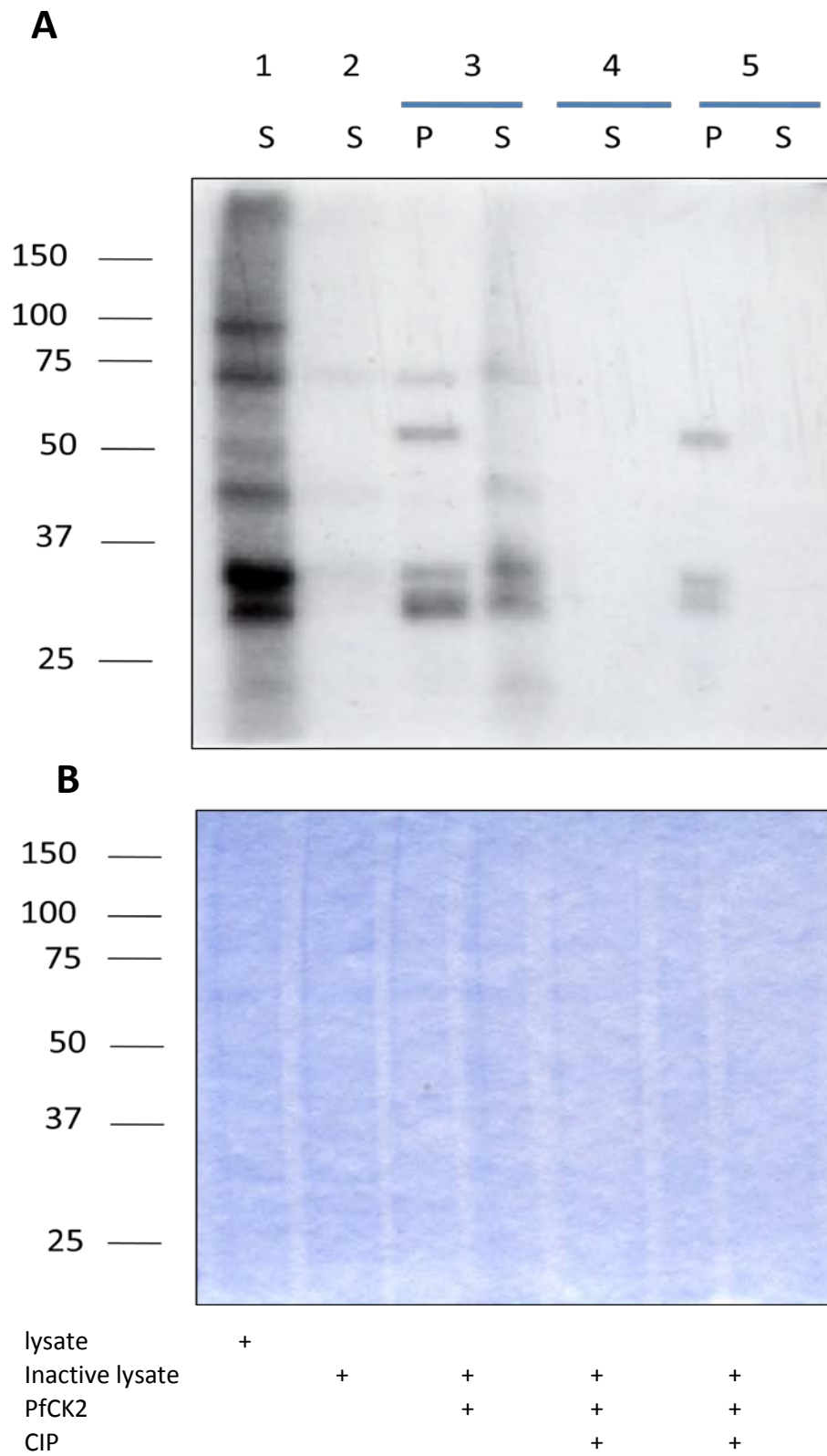
Figure 4.5: PfCK2 is not able to phosphorylate proteins in a heat-inactivated iRBC

lysate after treatment with biotinylated CIP. An iRBC lysate was first heat inactivated

for 2min at 55°C and subsequently incubated with biotinylated CIP at 37°C for 2hrs

followed by streptavidin pull-down. The treated lysate was then incubated with glutathione beads containing PfCK2 and ^{32}P-ATP for 10min at 37°C; proteins were resolved on SDS-PAGE and exposed to autoradiographic film. Results are representative of three independent experiments. **A:** autoradiograph; **B:** Comassie stain; P: pellet; S: supernatant.

4.3 Discussion

In conclusion, the attempt to develop a PfCK2 phosphoproteomic protocol in order to detect PfCK2-controlled phosphorylation events in an iRBC cellular lysate was not successful. The proposed procedure was based on an initial treatment of the lysate with CIP aimed at suppressing the natural occurring phosphorylation in the sample, followed by incubation with recombinant PfCK2 and LC-MS/MS detection (**Figure 4.1**). Despite the fact that conditions have been optimised for every step of the analysis in the reported preliminary tests, the final assay did not show any detectable PfCK2 activity with the CIP-treated lysate. Although on the basis of the obtained data it is difficult to draw a final conclusion of why this happened it is still possible to suggest some hypotheses. Based in fact on the observation that the PfCK2 autophosphorylation occurred in a less extent compared to the CIP untreated sample (lane 3,7 **Figure 4.5**) it can be proposed that the CK2 enzymatic phosphorylation activity was for some reasons inhibited or hampered in the CIP treated sample. This may be due to the presence of CIP traces that were not efficiently removed by the streptavidin pull-down step. However, previous analyses showed that no residual CIP was detected by Coomassie stain in the SDS-PAGE gel after this step (**Figure 4.4**). Such

evidence therefore suggests that if CIP traces are present, these are below the detection threshold. Another explanation of the observed PfCK2 lower activity may be linked to the incompatibility of buffers used in the dephosphorylation reaction and in the following pull-down, although no major differences between the composition of those buffers and the CK2 kinase buffer can recognised (see also **Chapter 2**).

Chapter 5: PfCK2 inhibition study

5.1 Introduction

Given the importance of protein phosphorylation in the cell biology of eukaryote organisms, ePKs have been extensively studied as attractive targets for therapeutic intervention in many different diseases.[36] It is now well known that one of the major difficulties encountered in designing small molecules inhibitors for this class of enzymes is the highly conserved nature of their catalytic site that makes absolute specificity a very challenging goal to achieve. Nevertheless, as disclosed by structural and mutational studies, compound selectivity can be obtained by targeting ancillary structural elements surrounding the ATP binding pocket which present sufficient variability.[138] A typical example for the success of this approach is represented by human CK2 for which a panel of more than 15 compounds belonging to different chemical classes and able to selectively inhibit CK2 enzymatic activity has been reported so far in literature (**Figure 5.1**). By comparing the available co-crystal structure for three of them (notably: TBB, TBI and IQA) it can be concluded that the observed selectivity towards CK2 is due to the size of the ATP binding site which is smaller than the vast majority of the other protein kinases. In particular, bulky residues such as Val66, Met163 and Ile174 are involved in hydrophobic interactions that positively contribute to the stabilisation and binding of the selective ligands.[139] Interestingly, all three bulky residues are conserved in PfCK2 suggesting that a similar set of compounds should also show efficacy against the parasite homologue.
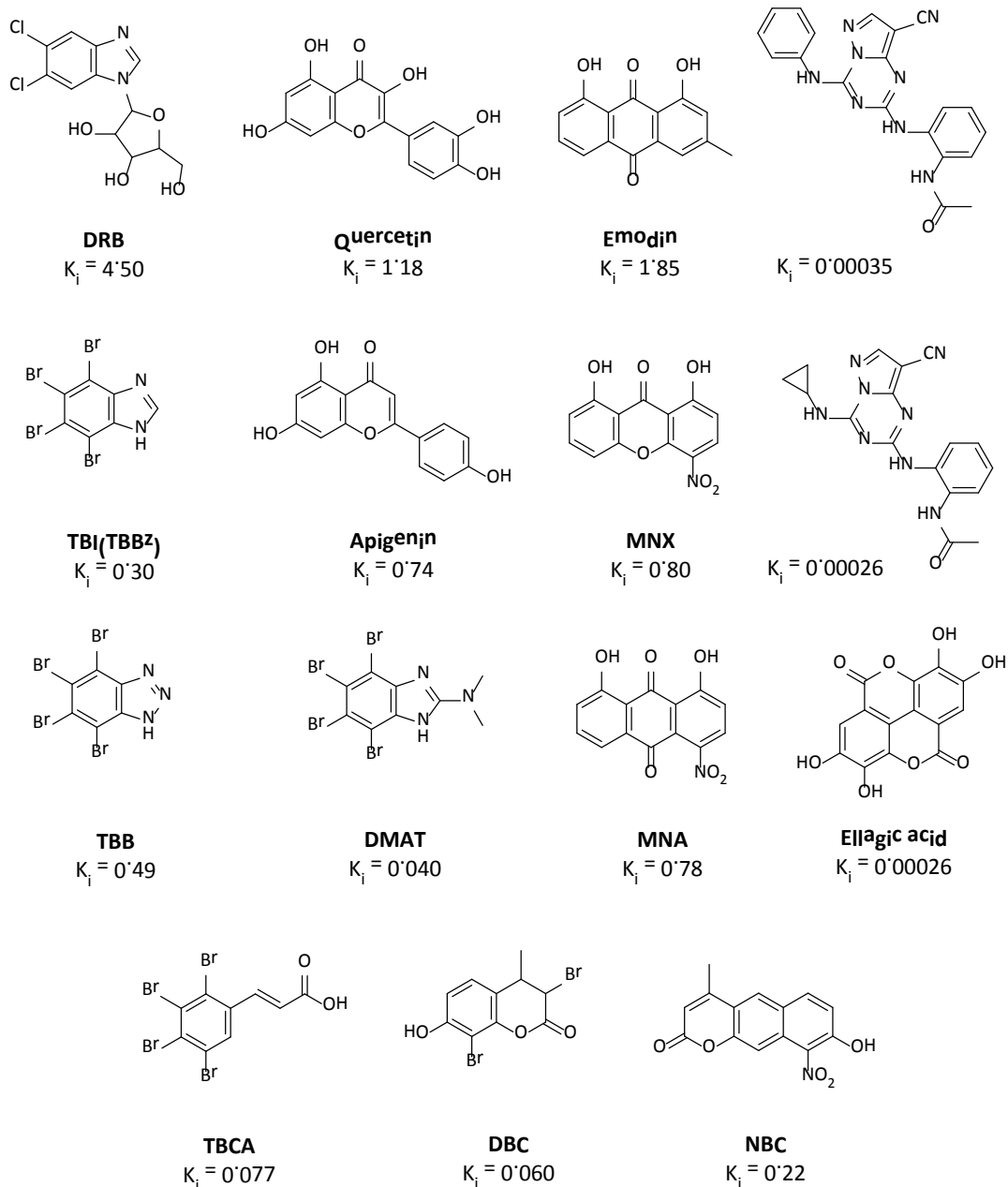
Figure 5.1: A repertoire of CK2 inhibitors representative of different chemical classes.

(K_i (µM) values obtained from assays against human CK2 from[139]).

However, it is worth noting that since active human CK2 is present in non-infected erythrocytes,[140] active compounds against this enzyme can only be regarded as a starting point for the design of more specific inhibitors against the targeted parasite

CK2. In this sense, a preliminary screening of a small set of CK2 inhibitors against PfCK2 has been reported in literature. Notably, only one compound in the set, Rottlerin exhibited slightly different IC_{50} values for the two enzymes, being $7\mu M$ and $\gg 20\mu M$ for PfCK2 and human CK2 respectively. Apart from this little divergency, the two enzymes responded essentially in the same way to the tested compounds in the *in vitro* inhibition assay. Despite demonstrating the PfCK2 is amenable to inhibition and represents therefore a feasible drug target, this evidence underlines once again the difficulties in developing selective protein kinase inhibitors due to their general highly conserved features and similarities. Moreover, particularly in the malaria field, the lack of structural information regarding the parasite kinases further hampers the rational design of selective probes and inhibitors.

To improve our understating over PfCK2 and to gain important structural information that would guide the design of new parasite kinase inhibitors it has been decided to test the most potent and selective available inhibitor of human CK2 and to perform a molecular docking experiment with the parasite enzyme. The compound chosen here was the antraquinone derivative quinalizarin, which is an ATP competitive inhibitor for human CK2, with an IC_{50} value of $0.11\mu M$, and a K_i value of $0.052\mu M$ (**Figure 5.2**).[141] Tests conducted against a panel of other 75 protein kinases at a fixed $1\mu M$ concentration have shown that, in these conditions, while CK2 residual activity was ~7%, the second most inhibited kinase (PIM1) still retained more than 50% of its activity.

$IC_{50} = 0{\cdot}11\mu M$
$k_i = 0{\cdot}11\mu M$
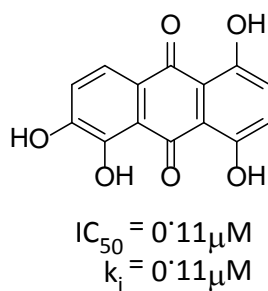
Figure 5.2: Chemical structure of the compound quinalizarin, one of the most potent and selective inhibitors for human CK2 (data from[141]).

Moreover, co-crystallization analyses have determined the main residues involved in ligand binding, showing that the compound is tightly entrapped in the ATP pocket by a set of hydrogen bonds and hydrophobic interactions involving residue side chains and main chain groups as well as a conserved water molecule (**Figure 5.3**). Interestingly, sequence alignment analyses have showed that only 21% of the protein kinases included in the screening panel have a Tyr residue at the position homologous with CK2 Tyr50, while only 10% have a Met residue homologous with CK2 Met163. It has been also reported that human CK2 was the only kinase bearing the His160 residue.[141] Such pieces of evidence could represent a possible explanation for the high specificity experimentally observed. Based on sequence alignment,[71] all the indicated residues involved in the ligand binding of quinalizarin are conserved in PfCK2 predicting that quinalizarin should also be a potent inhibitor of parasite PfCK2. Here below, results regarding PfCK2 *in vitro* kinase assays and molecular docking simulations with the quinalizarin compounds are reported.
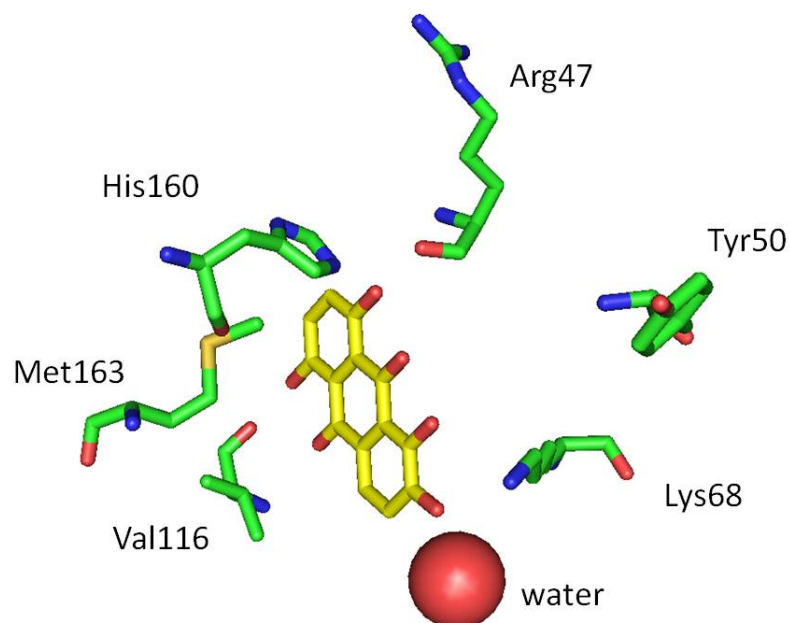
Figure 5.3: Close-up view of the inhibitor quinalizarin (yellow carbon atoms), bound to CK2, showing main residues and water molecule involved in ligand binding (PDB code: 3FL5).

5.2 Results

5.2.1 *In vitro* inhibition assay

To analyse the potency of the human CK2 inhibitor quinalizarin with the *P. falciparum* enzyme homologue an *in vitro* kinase assay was performed in the presence of either one of the two enzymes and several inhibitor concentrations in the range between 0.1 and 10μM at an ATP concentration of 100μM. Particularly, in order to compare the results between the two different enzymes, amounts performing the same phosphorylation activity with the peptide substrate in the conditions of the analysis were used in the test.

Results were obtained calculating the percentage of residual enzymatic activity, referring to the activity in the absence of inhibitor as a total (100%) (**Figure 5.4**).
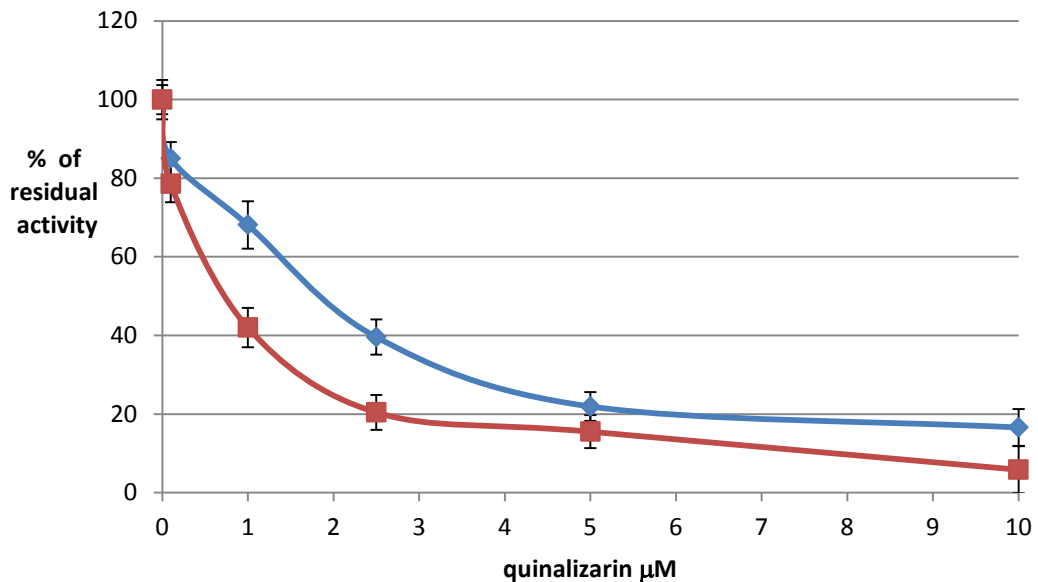
Figure 5.4: Quinalizarin inhibits PfCK2 with IC_{50} = 0.8μM and human CK2 with IC_{50} = 2μM. The graph reports the % of maximal response of human CK2 (red) and PfCK2 (blue) of an *in vitro* kinase assay in the presence of quinalizarin at different concentrations (μM). Data correspond to mean ± SD of three replicates.

As expected from the high homology between the two enzymes, the data clearly shows that the inhibitor is characterized by a strong potency also with the parasite enzyme. However, the difference between two IC_{50} values of respectively 0.8μM and 2μM for the human and the *Plasmodium* enzyme suggests that the inhibitor has a slightly lower binding affinity for the latter.

5.2.2 Molecular docking analysis

In order to investigate whether PfCK2 possesses distinct structural elements that can be exploited to design parasite specific CK2 inhibitors, a molecular docking simulation was carried out with PfCK2 and the compound quinalizarin. In particular, due to the lack of a reported crystal structure for the enzyme, a homology model has been produced to be then implemented in the docking simulation. To this aim, a sequence alignment was performed with the two enzymes using the web source ClustalW2. Results were consistent with the previously reported alignment,[71] showing a high degree of sequence homology with in particular a 62% of sequence identity (**Figure 5.5**). Such evidence supports the feasibility of the bioinformatics approach here proposed to obtain an *in silico* structure for PfCK2 based on the human crystal structure. In particular, this model was calculated using the most accurate human CK2 crystal structure available (PDB code: 1JWH, resolution 3.10Å) as a template. Furthermore, since the reported co-crystal structure with the quinalizarin inhibitor and the CK2 enzyme was obtained using *Zea mays* CK2, a second homology model was also produced on the basis of the available *Z. mays* CK2 crystal structure (PDB code 3FL5, resolution 2.30Å). As expected, both the obtained structures display a high degree of homology with the template used for the calculations (**Figure 5.6**). Also, from the comparison between the two calculated PfCK2 *in silico* models, no major differences could be observed. Therefore, on the basis of this, only the model based on the *Z. mays* CK2 was further analysed and compared with the reported *Z. mays* CK2 and quinalizarin co-crystal structure.

```
Pf  MSVSSINKKIYIPKFYADVNIHKPKEYYDYDNLELQWNKPNRYEIMKKIG   50
Hs  MSGPVPSR----ARVYTDVNTHRPREYWDYESHVVEWGNQDDYQLVRKLG   46

Pf  RGKYSEVFNGYDTECNRPCAIKVLKPVKKKKIKREIKILQNLNGGPNIIK  100
Hs  RGKYSEVFEAINITNNEKVVVKILKPVKKKKIKREIKILENLRGGPNIIT   96

Pf  LLDIVKDPVTKTPSLIFEYINNIDFKTLYPKFTDKDIRYYIYQILKALDY  150
Hs  LADIVKDPVSRTPALVFEHVNNTDFKQLYQTLTDYDIRFYMYEILKALDY  146

Pf  CHSQGIMHRDVKPHNIMIDHENRQIRLIDWGLAEFYHPGQEYNVRVASRY  200
Hs  CHSMGIMHRDVKPHNVMIDHEHRKLRLIDWGLAEFYHPGQEYNVRVASRY  196

Pf  YKGPELLIDLQLYDYSLDIWSLGCMLAGMIFKKEPFFCGHDNYDQLVKIA  250
Hs  FKGPELLVDYQMYDYSLDMWSLGCMLASMIFRKEPFFHGHDNYDQLVRIA  246

Pf  KVLGTEDLHAYLKKYNIKLKPHYLNILGEYERKPWSHFLTQSNIDIAKDE  300
Hs  KVLGTEDLYDYIDKYNIELDPRFNDILGRHSRKRWERFVHSENQHLVSPE  296

Pf  VIDLIDKMLIYDHAKRIAPKEAMEHPYFREVREE------SDLDANKYDI  344
Hs  ALDFLDKLLRYDHQSRLTAREAMEHPYFYTVVKDQARMGSSSMPGGSTPV  346

Pf  DEEDL-------------------------------------  349
Hs  SSANMMSGISSVPTPSPLGPLAGSPVIAAANPLGMPVPAAAGAQQ  391
```

Figure 5.5: Alignment of CK2 sequences from *Homo sapiens* and *Plasmodium falciparum* (conserved residues are indicated in red).

In the next step of the analysis, the obtained model was used as a template for a molecular docking experiment with the quinalizarin compound using the programme GOLD. In particular, based on the experimental evidence that quinalizarin inhibits the enzymatic activity by competing with ATP and therefore binding in the ATP binding pocket, the simulation was restricted to this specific area of the catalytic domain.[141]
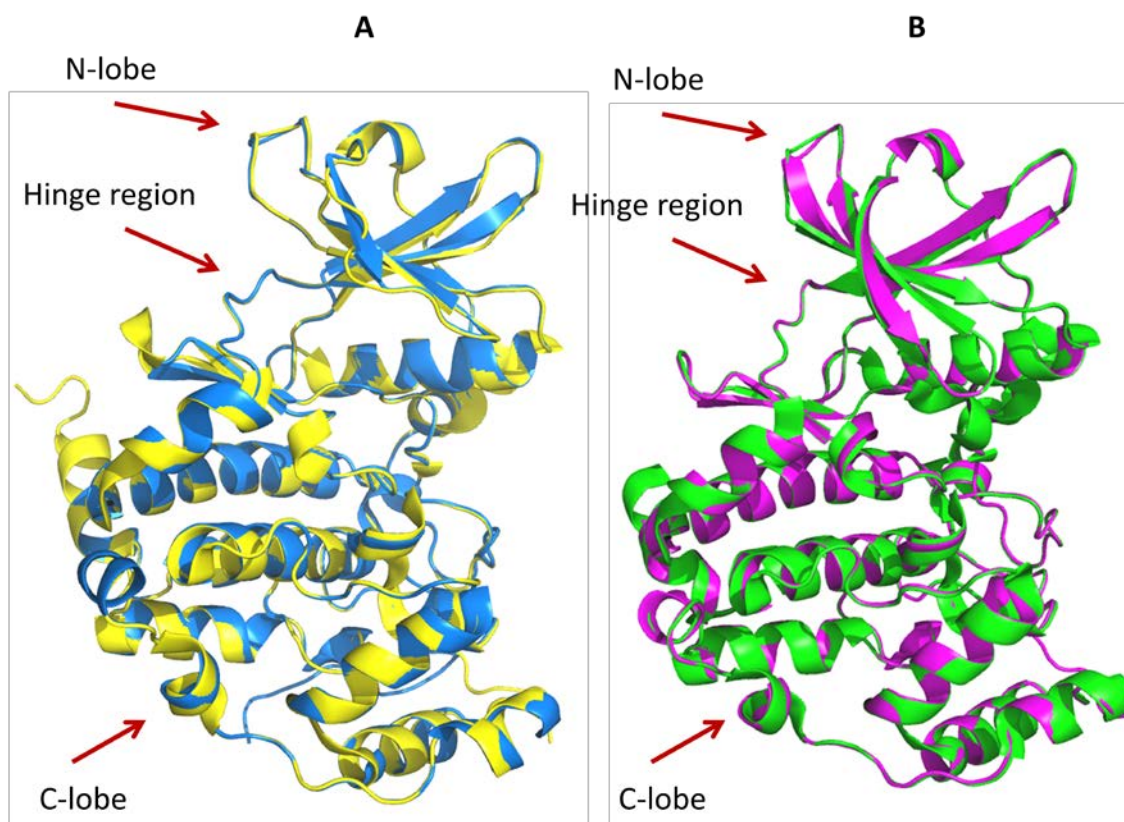
Figure 5.6: Superimposition of the calculate *in silico* model for PfCK2 with the relative CK2 crystal structures used as templates. **A:** human CK2 crystal structure (yellow, PDB code: 1JWH, resolution 3.10Å) and the calculated homology model for PfCK2 (blue); **B:** *Z. mays* CK2 crystal structure (green, PDB code: 3FL5, resolution 2.30Å) and the calculated homology model for PfCK2 (purple).

Overall, results showed that the compound presents a very similar orientation in the ATP binding pocket of PfCK2, compared with the published *Zea Mays* CK2 co-crystal structure (PDB code: 3FL5, resolution 2.30Å). However, in the calculated structure the inhibitor appears to be more deeply buried in the catalytic site (**Figure 5.7**).
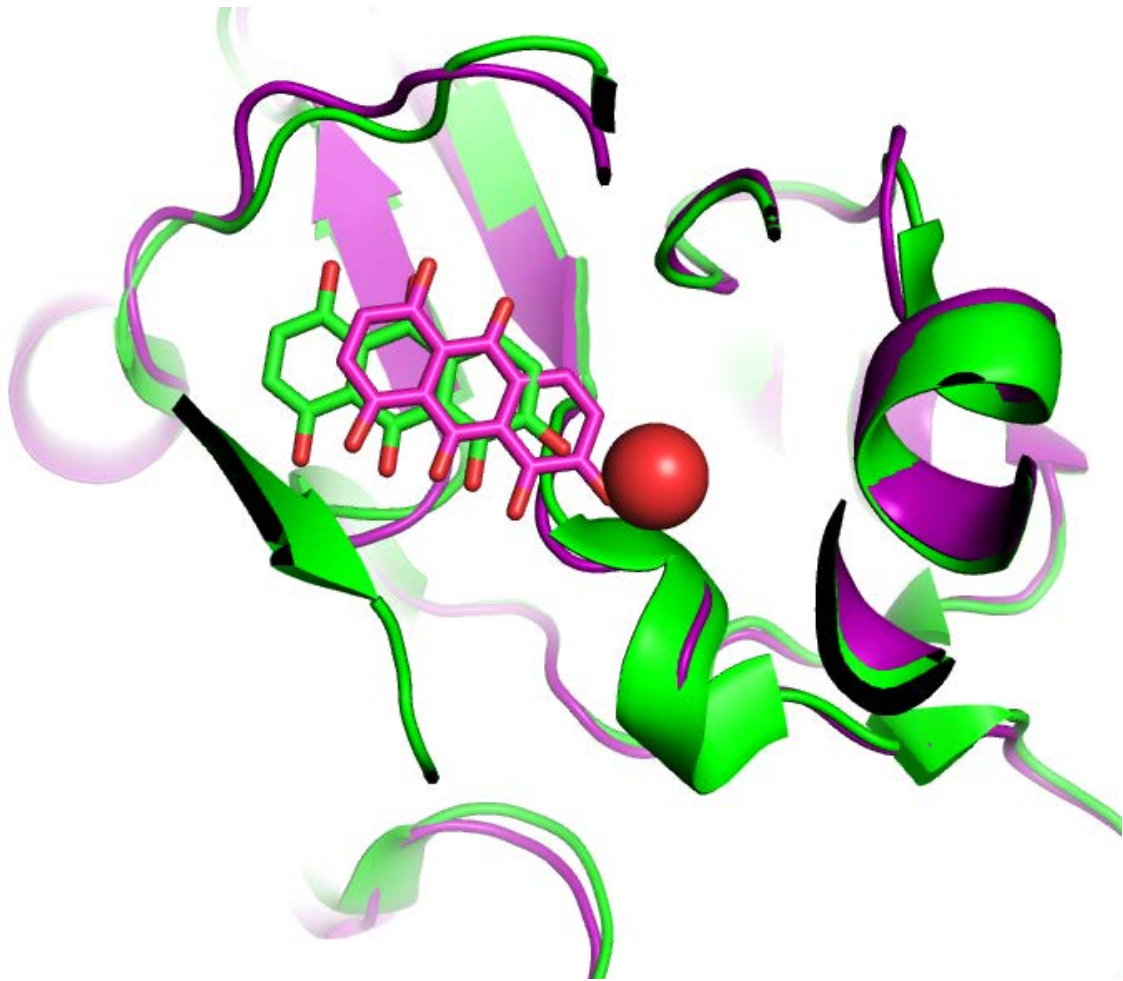
Figure 5.7: Superimposition of the result from the molecular docking of the PfCK2 homology model with quinalizarin (purple) and the co-crystal structure of *Z. mays* CK2 and quinalizarin (green).

At this level, it can be speculated that this particular difference could be due to the presence of a water molecule in the co-crystal structure that has not been considered in the modelling (see also **Figure 5.3**). Interestingly, studies in literature[142,143] showed that this specific water molecule is present in all crystal and co-crystal structures of CK2 so far reported and it is therefore considered constitutive to the active site. On the basis of such strong evidence, a new model was then produced taking into consideration this conserved water molecule, by including it in the modelling with the

Z. mays CK2 crystal structure. Also in this case, a docking simulation was then run with the obtained model. As expected, results (**Figure 5.8**) showed that the inhibitor orientation is overall conserved in the obtained docking structure and is comparable with both the orientation experimentally observed with *Z. mays* CK2 (PDB code: 3FL5) and the previously calculated one in the absence of the conserved water molecule (**Figure 5.6**).
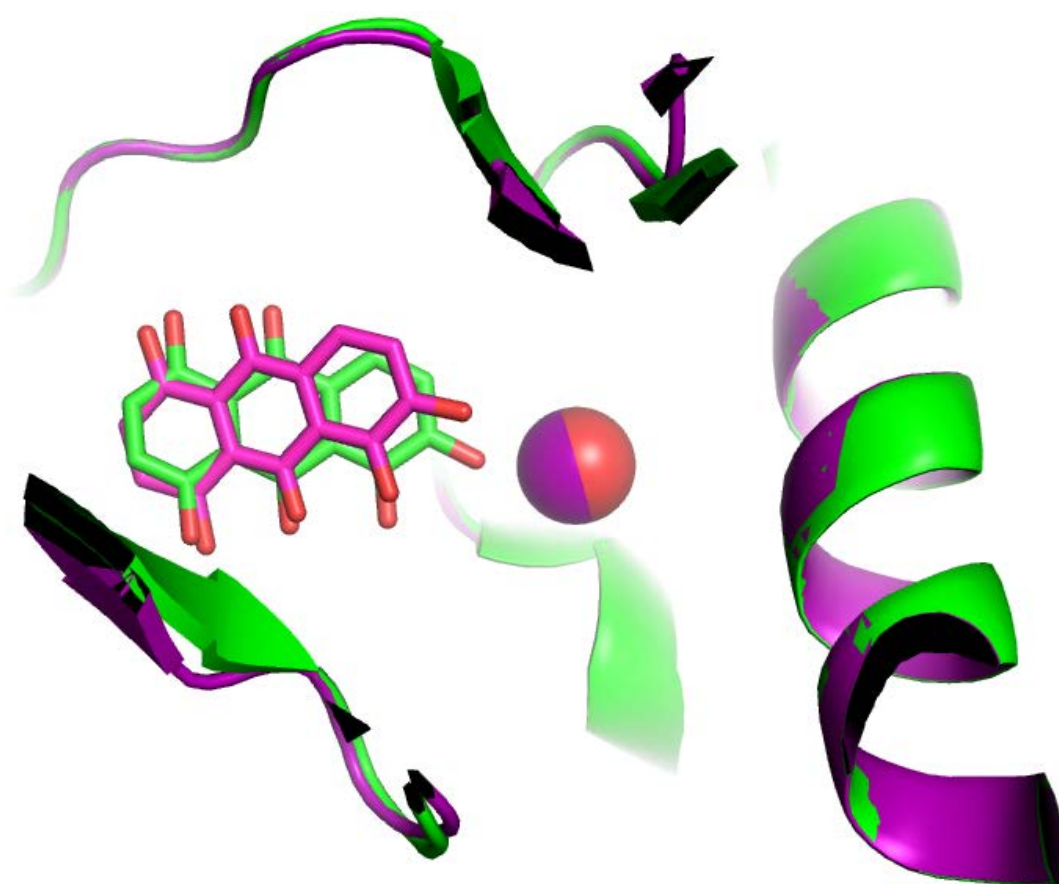
Figure 5.8: Superimposition of the result from the molecular docking of the PfCK2 homology model containing a conserved water molecule with quinalizarin (purple) and the co-crystal structure of *Z. mays* CK2 and quinalizarin (green).

However, taking into consideration the water molecule in this second analysis has substantially improved the similarity between the compound positions within the two enzyme ATP binding sites. On the basis of these observations, the study was then concluded by determining which residues in the two enzymes are located in the close proximity of the ligand and are therefore most likely to interact. This analysis was aimed in particular at defining specific elements present in PfCK2 that could both account for the slight observed difference in $IC_{50}s$ as well as guide the future design of more selective inhibitors for this enzyme. Not surprisingly, results showed that all the main residues previously recognised to be involved in ligand binding (see **Figure 5.3**) are conserved and present in an orientation comparable to the *Z. mays* CK2 co-crystal structure (**Figure 5.9**).
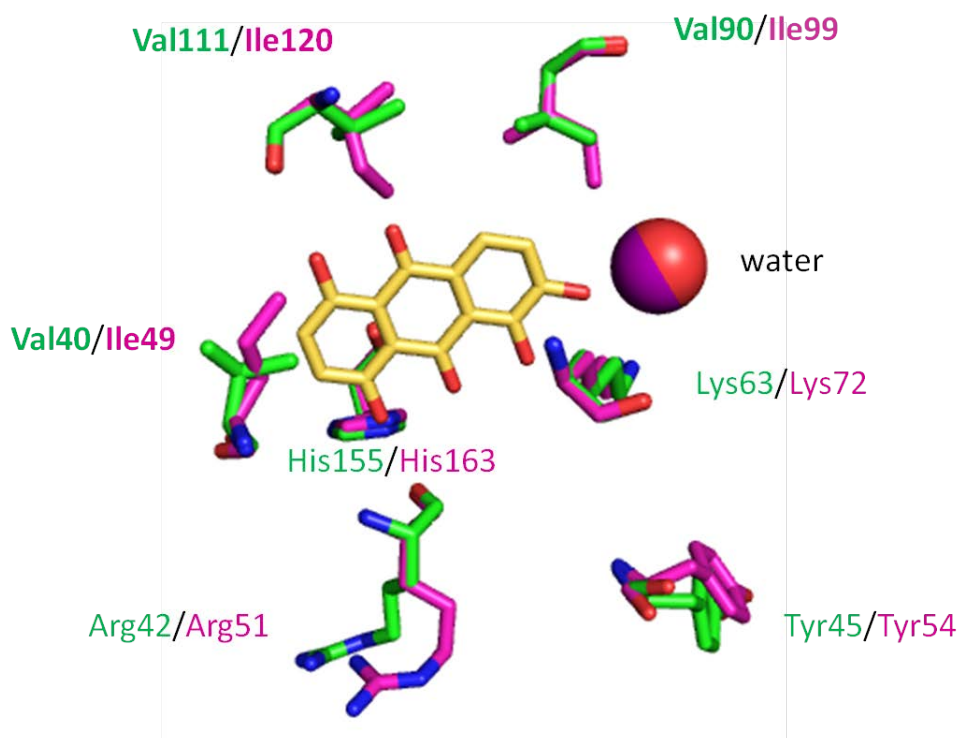
Figure 5.9: Analysis of the residues proximal to the quinalizarin ligand (yellow) in the *Z. mays* CK2 crystal structure (green) and the superimposed PfCK2 homology model (purple); non-conserved residues are indicated in bold.

However, the analysis remarkably showed that three *Z. mays* CK2 residues: Val40, Val90 and Val111 are mutated to more bulky Ile residues in PfCK2. As shown by the superimposition of the two active sites (**Figure 5.9**), the extra carbon groups in the three Ile side chains contribute to create a smaller ATP binding pocket in PfCK2 compared with the *Z. mays* homologue, at least in the calculated model. Interestingly, from the alignment between human and *Z. mays* CK2 sequences,[71] it emerges that one of the three *Z. mays* valines, Val111, is conserved in the *H. Sapiens* CK2 corresponding to Val116; while Val40 corresponds to a Leu residue (Leu45) and Val90 is mutated to an Ile (Ile95) as in PfCK2. Hence, on the basis of this analysis, it can be concluded that the size of the CK2 active site in the three enzymes are in the following order: *Plasmodium falciparum < Homo sapiens < Zea mays*.

5.3 Discussion

As previously shown, PfCK2 is a kinase essential for parasite viability[71] and constitutes therefore a potential target for malaria therapy. The study here presented showed that this enzyme is amenable to inhibition by the compound quinalizarin, a known competitor of ATP in human CK2. The compound was selected in particular being the most powerful and selective inhibitor available for CK2 enzymes. The comparative analysis with human CK2 showed that the compound is active in the same range of concentrations with a slightly higher IC_{50} value of 2μM compared with the 0.8μM value registered for the human homologue. This difference is consistent with a previously published screening of human CK2 inhibitors with PfCK2 that registered an

overall similar behaviour of the two enzymes in the inhibition assays except for Rottlerin, a compound that performed a 3x times higher IC_{50} with the human enzyme.[71] Even if this evidence demonstrates in principle that PfCK2 is amenable of inhibition, and that therefore it can be regarded as a potential drug target, it also shows that the high homology usually found among kinases strongly hampers the design of specific inhibitors. In particular, It is clear that this aspect is of crucial importance in the context of malaria treatment since host cells contain human CK2 and a potential drug candidate against PfCK2 needs therefore to be highly selective for the parasite homologue. Not surprisingly, the docking experiment performed with the quinalizarin compound and an *in silico* generated model for PfCK2 showed an overall conserved orientation of the inhibitor in the ATP binding pocket. The result is consistent with both the high sequence homology between the two enzymes (see **Figure 5.5**) and the similarity in the inhibition curves (see **Figure 5.3**), together suggesting an overall conserved interaction of the compound with the two active sites. In particular, the similarity between the two orientations improved after the introduction in the modelling process of a water molecule considered to be constitutive of CK2 enzymes[142] (see **Figure 5.8**). Finally, analyses of the residues spatially closest to the quinalizarin ligand in the two structures revealed some interesting features. In fact, while the most important amino acids in the interaction with the inhibitor are conserved, three *Z. mays* CK2 residues (Val40, Val90 and Val111) result mutated to three more bulky Ile residues in the PfCK2 primary sequence (see **Figure 5.9**). In particular, one of them, Val111, is also present in the *H. Sapiens* CK2 corresponding to Val116; while Val40 corresponds to Leu45 and Val90 is mutated to an Ile (Ile95), as in PfCK2. Such evidence underlines how the active site of PfCK2 is

notably smaller than the *Z. mays* CK2 homologue, and slightly smaller than the human one, at least on the basis of the *in silico* model structure. As no other major differences and singularities appear from this analysis, it can be speculated that this particular feature may account for the slight difference in IC_{50}s experimentally observed. In fact, the identified bulkier residues could constitute in principle a steric hindrance to the positioning of the inhibitor in the smaller PfCK2 ATP binding pocket. In conclusion, despite the fact that only subtle differences were recognised by this study, the observations made can constitute a valid starting point for future work regarding the design of more selective inhibitors of PfCK2. In particular, the evidence for the presence of a smaller ATP binding site in PfCK2 could in principle guide the synthesis of ligands able to positively exploit this specific feature of the parasite enzyme, resulting in a higher selective profile.

Chapter 6: PfCK2 autophosphorylation

6.1 Introduction

Protein kinases are extensively used to transmit signals and control complex processes in cells. Hence, given the crucial importance of this class of enzymes for the cellular homeostasis, their activity is tightly regulated in the cell. As it has been already described (see in particular section **1.6.4**), ePKs are regulated in a number of different ways: by binding of activator proteins or inhibitor proteins, small molecules, by controlling their location in the cell relative to their substrates, but most importantly by phosphorylation. In particular, kinases regulated by phosphorylation pathways are termed RD kinases due the formation of a salt bridge with a conserved Arg residue next to the catalytic Asp in subdomain VI (see section **1.6.4**). In particular, this phosphorylation event can be either due to the kinase itself (in which case it is termed autophosphorylation)[62] or by an upstream kinase, while the phosphorylation site is located in a highly conserved consensus sequence called the activation segment. CK2 enzymes are no exception to this and, despite the absence of Ser and Thr residues in their highly conserved activation segments (**Figure 6.1**), *in vitro* autophosphorylation has been showed to occur in both the *H. sapiens*[144] and the *P. falciparum*[71] homologues. In particular, in the human enzyme this phosphorylation event involves the Tyr182 residue which notably is conserved also in the parasite enzyme (**Figure 6.1**). Moreover, the autocatalytic nature of this process was further confirmed by the ability of the specific CK2 co-substrate, GTP, to replace ATP as phosphate donor; while the

specificity of the phosphorylation site was demonstrated by single point mutation

analyses.


```
PfCK2 179 DWGLAEFYHPGQEYNVRVASRYYKGPE
HsCK2 175 DWGLAEFYHPGQEYNVRVASRYFKGPE
```

Figure 6.1: Sequence alignment of the activation segment from *H. sapiens* and *P. falciparum* CK2 (conserved residues are indicated in red; see section **5.2.2** for further details).

However, despite such evidence, no structural information is currently available to suggest a role for Tyr182 phosphorylation in the human CK2 activation segment.[88] This is illustrated by the fact, determined by previous studies,[144] that the Tyr182Phe mutation in human CK2 has comparable enzymatic activity as the wild type enzyme, indicating that autophosphorylation is not absolutely required to activate CK2 in a manner analogous to common RD kinases. However, the exact modes of CK2 regulation still remain elusive nowadays and these data do not exclude the possibility that autophosphorylation might play a role to some extent in modulating CK2 activity, especially in physiological conditions.[90] Regarding the parasite CK2, there is even less published information available. In fact, the only reported evidence is for the ability of the recombinant enzyme to catalyse *in vitro* autophosphorylation.[71] However, no data regarding the specific site for this post-translational modification, nor its possible roles in the enzyme regulation have been reported so far. It is possible to speculate that the high degree of homology between the human and parasite CK2, especially in the

activation loop (**Figure 6.1**) may involve a similar pathway to that of human CK2; however no data to support this hypothesis were available prior to the study presented here. In this section, results for the investigation over the nature and the roles for PfCK2 autophosphorylation are reported.

6.2 Results

6.2.1 PfCK2 *in vitro* autophosphorylation

First of all, in order to reproduce the data reported in literature for the PfCK2 autophosphorylation, an *in vitro* kinase assay was carried out by incubating a bacterially expressed recombinant GST-PfCK2 with radioactive ^{32}P-ATP for 10min at 37°C. Samples were analysed with SDS-PAGE followed by exposure to autoradiographic film. Results showed that, while there was no activity against the GST moiety alone (lane 1**, Figure 6.2**), the full length protein incorporated radioactivity during the assay (lane 2, **Figure 6.2**). These two observations indicate therefore that the autophosphorylation was against the PfCK2 catalytic subunit itself (**Figure 6.2**). Secondly, in order to verify where this autophosphorylation event was taking place in the protein primary sequence, a sample from a PfCK2 *in vitro* kinase assay was incubated with ATP at 37°C for 10min, digested with trypsin and followed by LC-MS\MS. The analysis detected a single phosphorylation site at Thr63, with a top Mascot ion score: 81.7 for the relative phospho-peptide (**Figure 6.3**).
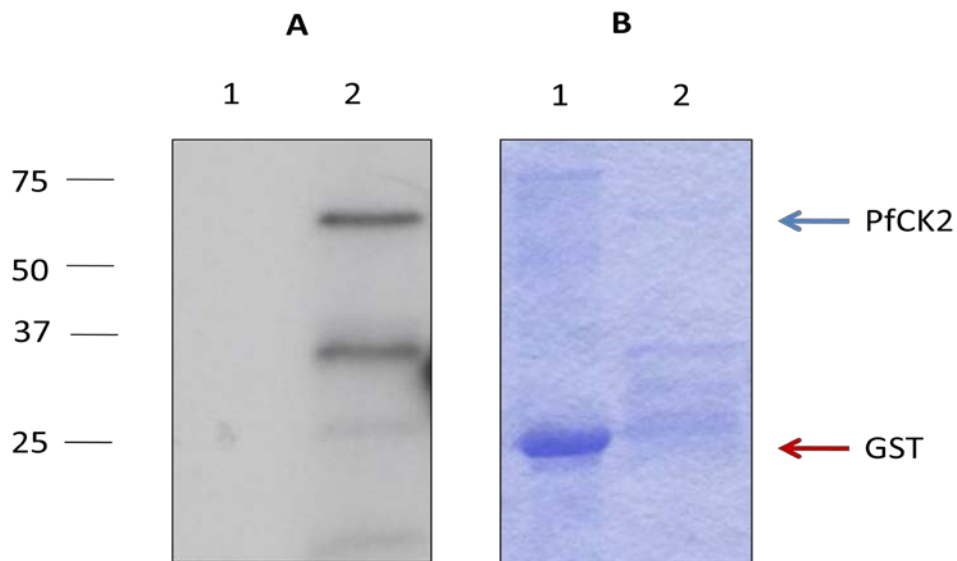
Figure 6.2: Recombinant GST-PfCK2 undergoes *in vitro* autophosphorylation. Recombinant GST-PfCK2 was incubated with ^{32}P-ATP at 37°C for 10min. The sample was then loaded on a SDS-PAGE and exposed to autoradiographic film. A sample of GST was also incubated and analysed in the absence of PfCK2. Results are representative of three independent experiments. **A**: autoradiograph, **B**: Coomassie stain. Lane 1: GST, 2: GST-PfCK2.

Surprisingly, this residue is not contained within the PfCK2 activation loop in subdomain VII which spans from Asp179 to Glu205 but belongs instead to the subdomain I (also see **Figure 5.5**).[71] Furthermore, a peptide containing the classical phosphorylation site Y186 (corresponding to HsCK2 182) was also detected: LIDWGLAEFYHPGQEYNVR with a 110.9 Mascot ion score; however no phosphorylation was reported in the LC-MS/MS.

A

PfCK2 (PF11_0096)

YSEVFNGYD**pT**ECNRPCAIK

```
  1 MSVSSINKKI YIPKFYADVN IHKPKEYYDY DNLELQWNKP NRYEIMKKIG
 51 RGKYSEVFNG YDTECNRPCA IKVLKPVKKK KIKREIKILQ NLNGGPNIIK
101 LLDIVKDPVT KTPSLIFEYI NNIDFKTLYP KFTDKDIRYY IYQILKALDY
151 CHSQGIMHRD VKPHNIMIDH ENRQIRLIDW GLAEFYHPGQ EYNVRVASRY
201 YKGPELLIDL QLYDYSLDIW SLGCMLAGMI FKKEPFFCGH DNYDQLVKIA
251 KVLGTEDLHA YLKKYNIKLK PHYLNILGEY ERKPWSHFLT QSNIDIAKDE
301 VIDLIDKMLI YDHAKRIAPK EAMEHPYFRE VREESDLDAN KYDIDEEDL
```

B
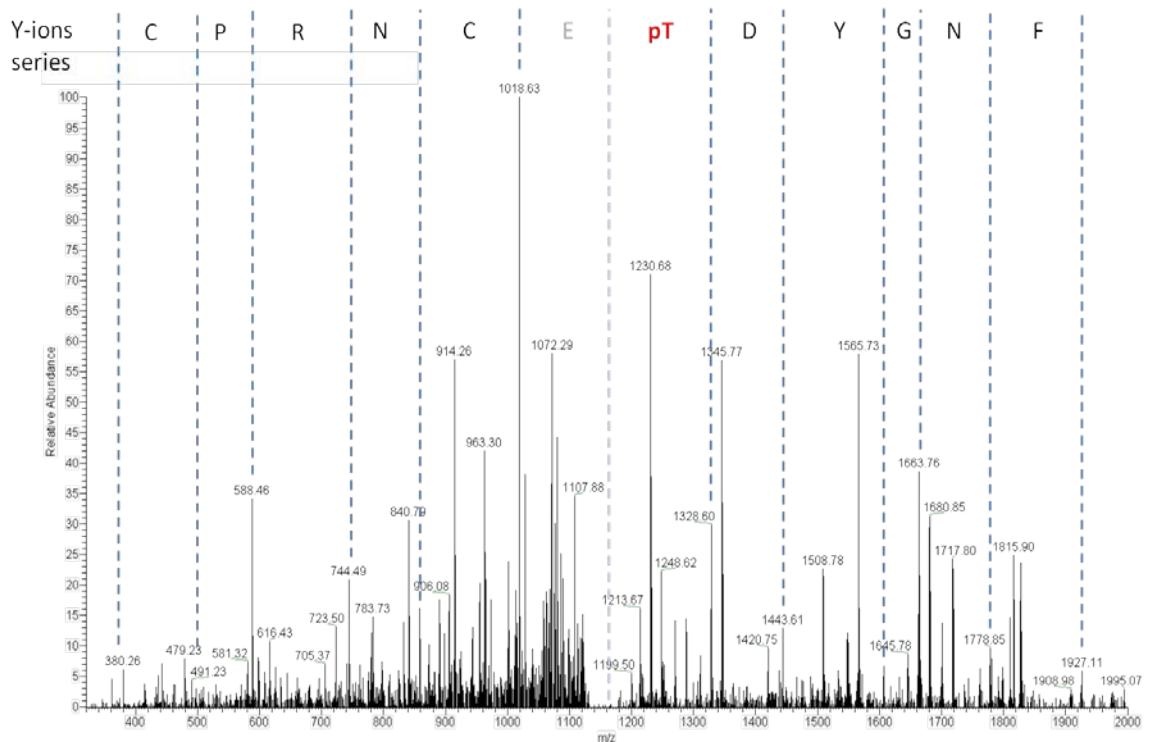
Figure 6.3: LC-MS /MS analysis of PfCK2 autophosphorylation. **A:** sequence of PfCK2 showing the phosphopeptide identified in the LC-MS/MS analysis (underlined), top Mascot ion score: 81.7. **B:** LC-MS/MS trace identifying phosphorylation of PfCK2 at T63.

b-ions	Sequence	y-ions
164.1	Y	2,403.0
251.1	S	2,239.9
380.1	E	2,152.9
479.2	V	2,023.8
626.3	F	**1,924.8**
740.3	N	**1,777.7**
797.3	G	**1,663.7**
960.4	Y	**1,606.6**
1,075.4	D	**1,443.6**
1,256.5	T+80	**1,328.5**
1,385.5	E	1,147.5
1,545.5	C+57	**1,018.5**
1,659.6	N	**858.5**
1,815.7	R	**744.4**
1,912.7	P	**588.3**
2,072.8	C+57	**491.3**
2,143.8	A	331.2
2,256.9	I	260.2
2,403.0	K	147.1

Table 6.1: Fragmentation table for the identified phosphopeptide (detected b-ions and y-ions are represented respectively in bold red and bold blue).

To further verify such an unexpected result, a Thr63Ala single point mutation was performed for the GST-PfCK2 construct through PCR (see also **Appendix**). After bacterial expression and purification, a CK2 autophosphorylation assay was then performed as previously described with the mutant protein and the wild type (wt) as a positive control. Results unambiguously demonstrated that the mutant was not able to undergo *in vitro* autophosphorylation, while the wt enzyme efficiently autophosphorylated, as previously observed (**Figure 6.4**).
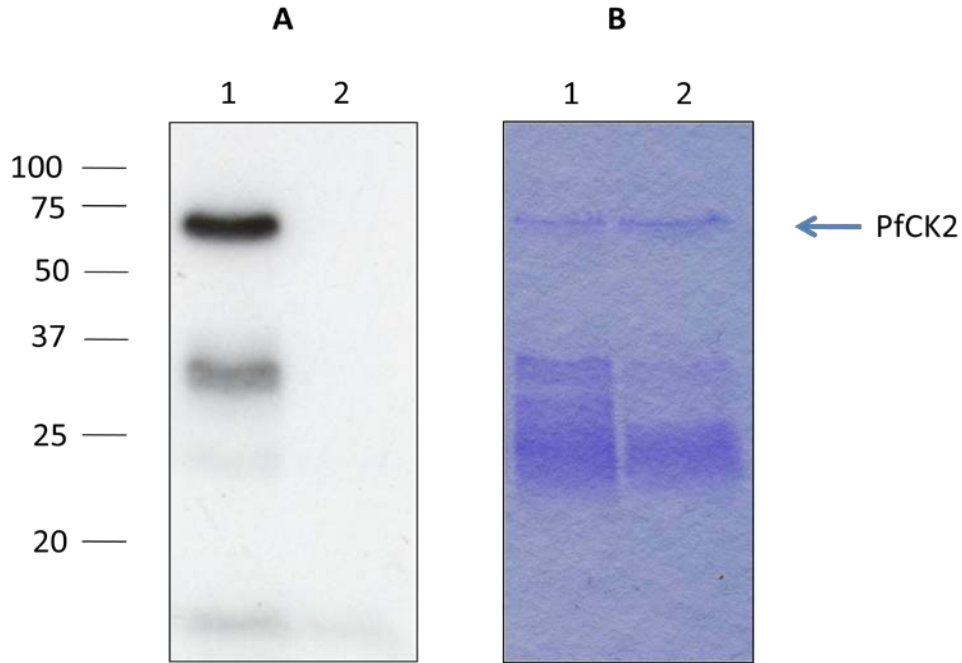
Figure 6.4: Recombinant GST-PfCK2 autophosphorylates on Thr63 *in vitro*. Recombinant GST-PfCK2 wt and Thr63Ala mutant were incubated with ^{32}P-ATP for 10min at 37°C; proteins were then resolved on SDS-PAGE and the gel exposed to autoradiographic film. Results are representative of three independent experiments. **A**: autoradiograph, **B**: Coomassie stain; lane 1: wt, 2: Thr63Ala mutant.

6.2.2 PfCK2 activity

In order to verify whether PfCK2 autophosphorylation plays a crucial role in the protein kinase activity, *in vitro* kinase assays were carried out with the wt and the Thr63Ala mutant PfCK2, using β-casein as a substrate and ^{32}P-ATP as phosphate donor. Results for the GST fusion proteins showed that, although the Thr63 phosphorylation site is not strictly required for the kinase reaction, the mutant was characterized by a ~60% decrease in kinase activity, compared to the wt (**Figure 6.5**).
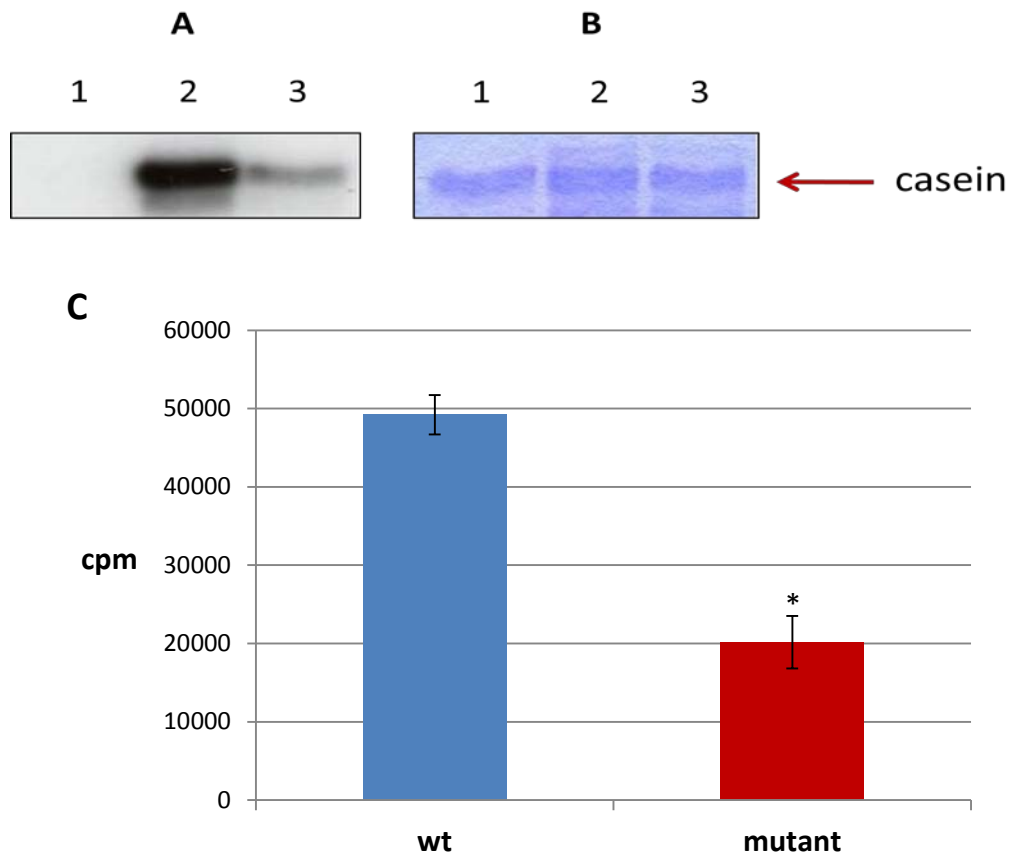
Figure 6.5: Thr63Ala mutation reduces *in vitro* GST-PfCK2 activity against casein. An *in vitro* kinase assay was run with GST-PfCK2 wt and mutant in the presence of ^{32}P-ATP and casein for 10min at 37°C; proteins were then resolved on SDS-PAGE and the gel exposed to autoradiographic film. The casein band was cut from the gel and counted. **A**: autoradiograph, **B**: Coomassie stain, **C**: The histograms represent the kinase activity (cpm) and correspond to mean ±SD of three replicates. Statistical comparison was performed with a paired T-TEST: *, P<0.05. Lane 1: no enzyme, 2: wt, 3: Thr63Ala mutant.

Preliminary studies suggested that the tag on the recombinant PfCK2 (for example the GST tag on the GST-PfCK2 used above) can influence the enzyme activity. To be sure that the tag did not influence the results of the wt or the Thr63Ala mutant a His$_6$-

tagged PfCK2 was constructed that would allow for the tag to be removed by the action of a TEV protease. Thus, purified His$_6$-wt and mutant enzymes were digested overnight with His$_6$-TEV at 4°C and subsequently loaded on a nickel column. In this way, the digested wt and mutant enzymes were recovered from the flowthrough, while the His$_6$-TEV, the cleaved His$_6$ tag, were retained on the column together with any unreacted His$_6$-PfCK2. Cleavage of the tag was confirmed by both SDS-PAGE showing a lower molecular weight for the cleaved enzyme, and more accurately by Western Blot analysis with an anti-His$_6$ antibody (**Figure 6.7**).
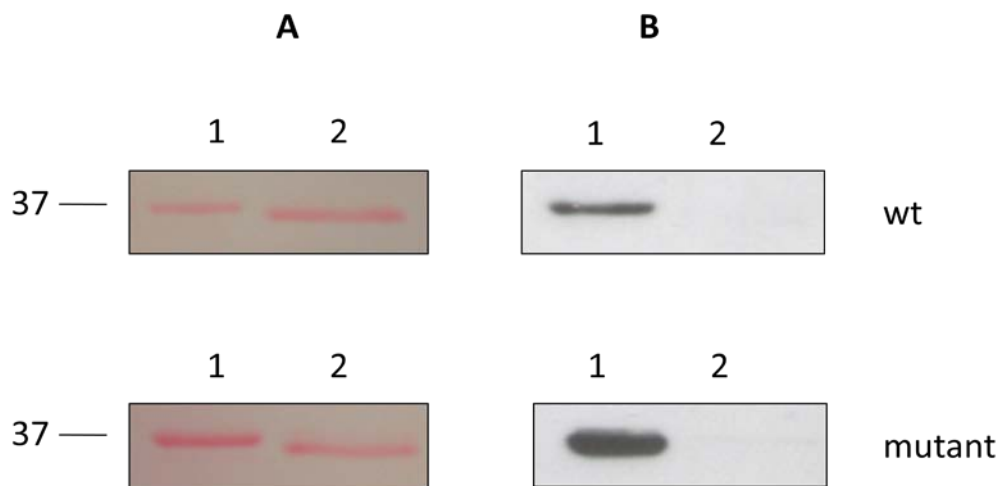
Figure 6.7: The His$_6$ tag of recombinant His$_6$-PfCK2 can be cleaved after overnight incubation with TEV enzyme. His$_6$-PfCK2 was incubated with His6-TEV at 4°C overnight and then purified with nichel charge resin. The flowthorugh containing the cleaved enzyme was loaded on SDS-PAGE and immunoblotted with anti-His$_6$ tag antibody. **A**: Ponceau stain **B**: Western Blot. Lane 1: PfCK2, 2: PfCK2 after TEV cleavage.

The untagged wild type and mutant enzymes were then incubated in *in vitro* kinase reactions in the presence of β-casein and ^{32}P-ATP, in order to detect any influence of

the Thr63Ala mutation and the subsequent lack of autophosphorylation in the kinase activity. Results overall confirmed what was previously observed in the case of GST tagged constructs, showing a 50% decrease for the mutant kinase (**Figure 6.8**).
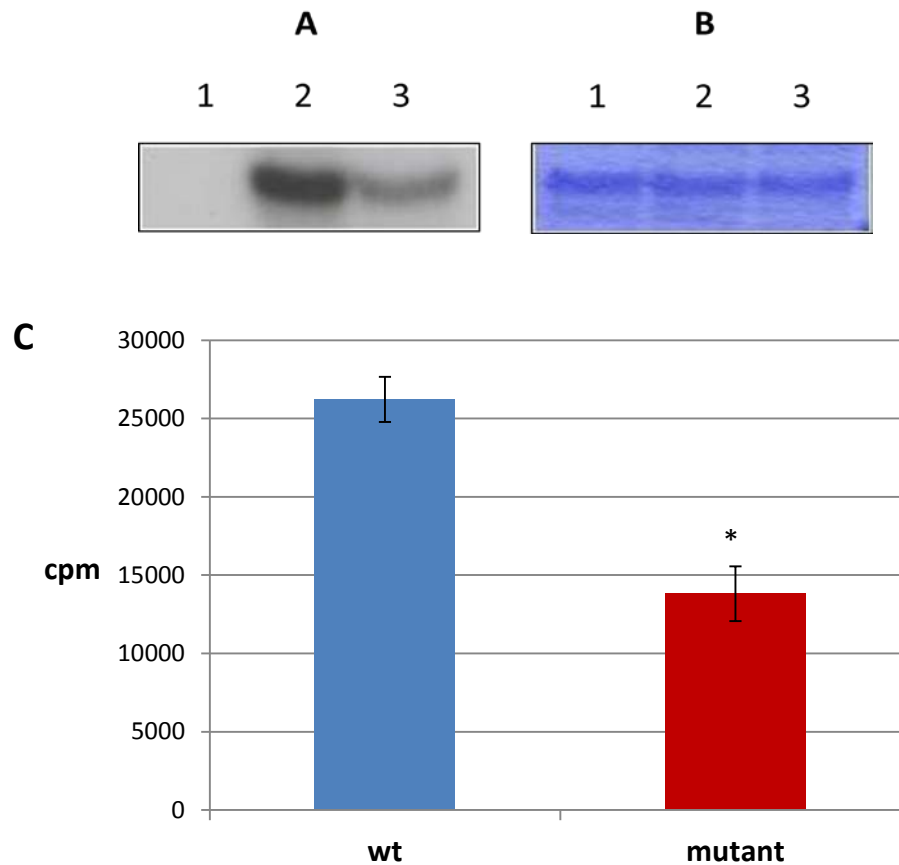
Figure 6.8: Thr63Ala mutation reduces *in vitro* PfCK2 activity against casein. After His$_6$ tag cleavage, an *in vitro* kinase assay was run with PfCK2 wt and mutant in the presence of ^{32}P-ATP and casein for 10min at 37°C; proteins were then resolved on SDS-PAGE and the gel exposed to autoradiographic film. The casein band was cut from the gel and counted. **A**: autoradiograph, **B**: Coomassie stain, **C**: The histograms represent the kinase activity (counts) and correspond to mean ±SD of three replicates. Statistical comparison was performed with a paired T-TEST: *, P<0.05. Lane 1: no enzyme, 2: wt, 3: Thr63Ala mutant.

6.2.3 Interaction with the PfCK2β₂ subunit

Despite the fact that the Thr63Ala mutation showed a remarkable influence on the overall kinase activity of the enzyme, this residue is not contained within the activation loop, and is not strictly required for kinase activity. For these reasons, it is not possible to conclude that this is a classical RD kinase activation mechanism. Hence, we decided to look at other possible roles for this PfCK2 autophosphorylation pathway. In particular, by looking at the homology model previously calculated for PfCK2 (see section **5.2.2**), it is interesting to note that the Thr residue involved is positioned on the protein surface of the N-terminal domain and that the side chain is solvent exposed (**Figure 6.9**).

Figure 6.9: Calculated homology model for PfCK2 showing the position of the Thr63 residue involved in the *in vitro* autophosphorylation process.
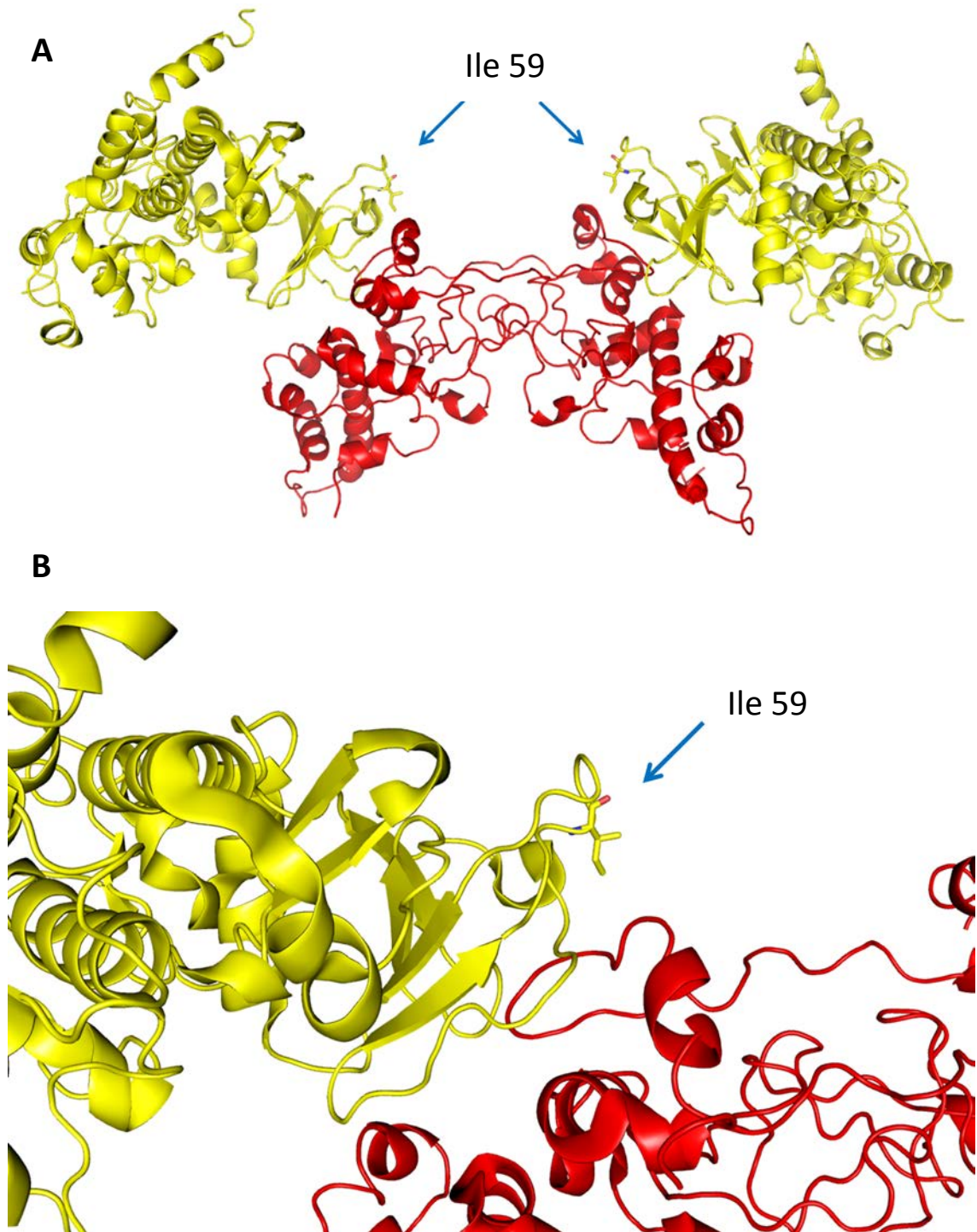
Figure 6.10: Human CK2 holoenzyme crystal structure (PDB code: 1JWH) showing the position of the Ile59 residue at the interface between the α (green) and β (yellow) subunits. **A**: holoenzyme crystal structure, **B**: zoomed portion of the interface between the α and β subunits.

Even more interestingly, the corresponding Ile59 residue on the human CK2 is found right at the interface between the α catalytic and the β regulatory subunits in the human holoenzyme crystal structure (**Figure 6.10**). Although no crystallographic data for PfCK2 is available yet to confirm it, these observations suggest that if the CK2 holoenzyme configuration is overall conserved in *P. falciparum*, the reported autophosphorylation process for the catalytic enzyme could potentially have a role in controlling or modulating its interaction with the two regulatory subunits PfCKβ_1 (PF11_0048) and PfCKβ_2 (PF13_0232). To test this hypothesis, an *in vitro* pull-down assay was designed and performed with the parasite CK2 catalytic and β_2 regulatory subunits. In particular, since the regulatory protein presents a long insert of acidic residue at the N-terminus, a common feature in the *P. falciparum* proteome whose function is still elusive (see also section **1.7**), in order to minimise problems in the protein bacterial expression, it has been decided to only express and test a "short" version of PfCK2β_2 lacking the N-terminal extension, named sh*Pf*CK2β_2 (**Figure 6.11**). Noteworthy, this "short" version has already been showed to interact *in vitro* with the full length catalytic subunit.[71]

```
  1 MEFVSNDESA DDIIQDESNE GEVELTDADF YDLTVINDK  IDEEIIEDDE
 51 EEADNDDQEN DNVQEVYNID DEDNDIHNDK LLLDQQRDN  DVNEEEEEEE
101 EEEEEEEEEE EEEEEEEEEE EEDEDDDDDD DDDDDDDDD  DDDDDYDDDD
151 EYDEDDFNEA TVSWIEWFCQ LKQNLFLVEV DEDFIRDEF  NLIGLQTKVP
201 HFKKLLKIIL DEDDDDDDDD DDDYDDEDDE INRDSEEMY  KNKDMHEQNA
251 ACLYGLIHSR FILTSKGLAL MREKYKSGIY GTCPSIYCE  NAKLLPTAIS
301 EIPKFLSPLL YCPRCCETYY PSKNSLLNQL DGCYFGTSF  ASFFALSFNI
351 ASDKKKVYYT PQICGFTINR NIRETLYMDV NKDNTESSE  ECQ
```

Figure 6.11: Primary sequence of the PfCK2β_2 full length and "short" version proteins (in blue).

His$_6$-shPfCK2β_2 was then bacterially expressed and purified on Nickel columns. However, despite the fact that the recombinant protein expressed correctly and in large amounts in the bacterial system, it was not possible to extract it and purify it from the lysate. In fact, as shown by both SDS-PAGE gel and Western blot analyses with a His$_6$-tag antibody, the expressed protein was exclusively detected in the membrane and insoluble fraction, probably present in inclusion bodies (**Figure 6.12**).
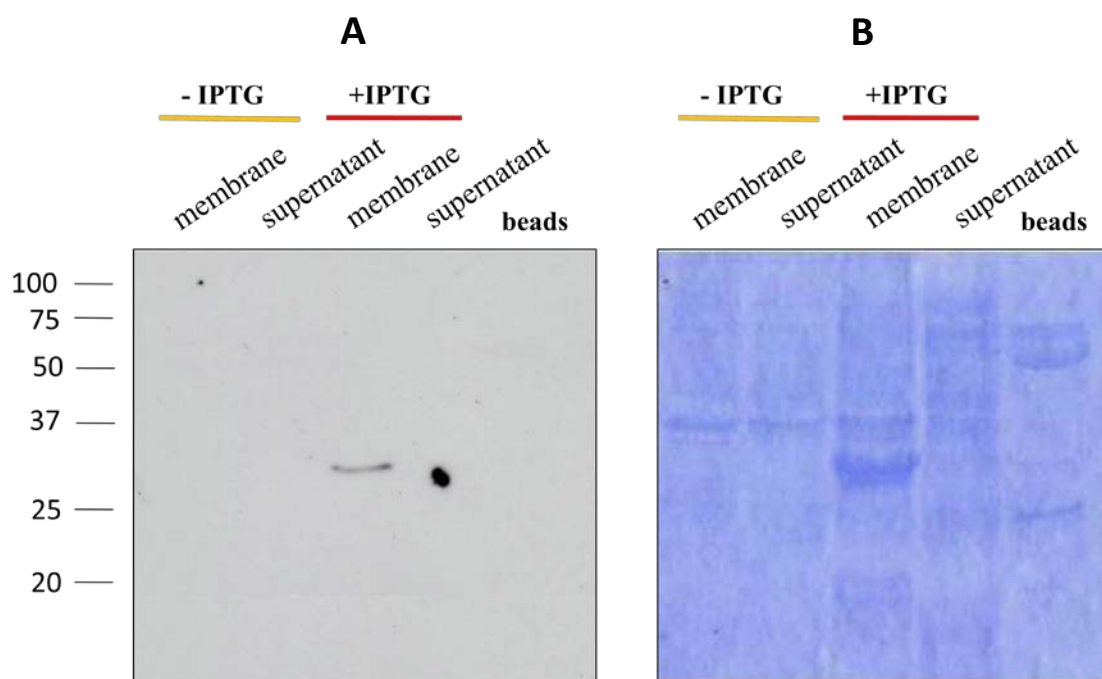
Figure 6.12: His$_6$-shPfCK2β_2 can be expressed but not efficiently purified from in *E. coli* competent cells. His$_6$-shPfCK2β_2 was expressed in transfected *E. coli* competent cells upon induction with 20mM IPTG at 22°C for 4hrs; cell cultures were spun down, lysed and purified on nickel-charged resin. The membrane and supernatant content before and after induction together with the purified sample were loaded on a SDS-PAGE and immunoblotted using anti-His$_6$ tag antibody. **A**: Western Blot, **B**: SDS-PAGE gel (Coomassie stain). Results are representative of three independent experiments.

Therefore, in order to increase the protein solubility, a GST fusion protein was then expressed and purified. In this case, as shown by SDS-PAGE gel (**Figure 6.13**) and by LC-MS/MS analysis (**Figure 6.14**), the recombinant protein was efficiently expressed, solubilised and recovered from the lysate.
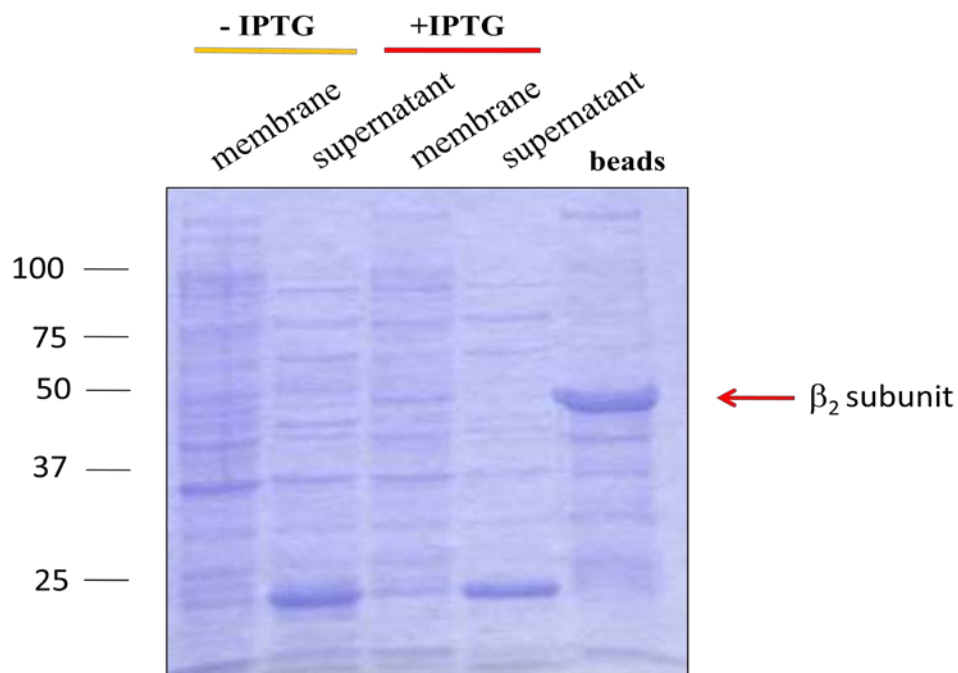
Figure 6.13: GST-shPfCK2β_2 expression and purification profile from transfected *E. coli* competent cells. GST-shPfCK2β_2 was expressed in transfected *E. coli* competent cells upon induction with 20mM IPTG at 22°C for 4hrs; cell cultures were spun down, lysed and purified on glutathione beads. The membrane and supernatant content before and after induction together with the purified sample were resolved on SDS-PAGE (Comassie stain).

Sequence	Mascot Ion score	Sequence position
MSPILGYWK	55.57	1-9
GLVQPTR	29.84	12-18
LLLEYLEEK	56.51	19-27
LLLEYLEEKYEEHLYER	95.61	19-35
YEEHLYER	35.3	28-35
YEEHLYERDEGDK	37.12	28-40
YEEHLYERDEGDKWR	41.76	28-42
KFELGLEFPNLPYYIDGDVK	90.29	45-64
FELGLEFPNLPYYIDGDVK	86.09	46-64
LTQSMAIIR	62.11	65-73
YIADKHNmLGGcPK	79.82	74-87
HNmLGGcPK	42.96	79-87
HNMLGGcPKER	50.8	79-89
ERAEISmLEGAVLDIR	104.3	88-103
AEISMLEGAVLDIR	99.68	90-103
DFETLK	30.88	114-119
LPEMLK	35.13	126-131
RIEAIPQIDK	36.96	182-191
IEAIPQIDK	37.39	183-191
sSKYIAWPLQGWQATFGGGDHPPK	43.08	195-218
YIAWPLQGWQATFGGGDHPPK	109.49	198-218
SDLVPR	48.73	219-224
QNLFLVEVDEDFIR	85.92	241-254
qNLFLVEVDEDFIRDEFNLIGLQTK	72.91	241-265
DEFNLIGLQTK	65.3	255-265
IILDEDDDDDDDDDDDYDDEDDEINR	68.04	275-300
IILDEDDDDDDDDDDDYDDEDDEINRDSEEmYK	158.2	275-307
NKDmHEQNAAcLYGLIHSR	114.51	308-326
DMHEQNAAcLYGLIHSR	108.88	310-326
FILTSK	28.65	327-332
gLALMR	28.27	333-338
yKSGIYGTcPSIYcENAK	76.15	341-358
SGIYGTcPSIYcENAK	78.92	343-358
LLPTAISEIPK	56.08	359-369
LLPTAISEIPKFLSPLLYcPR	56.77	359-379
FLSPLLYcPR	46.08	370-379
ccETYYPSK	60.69	380-388
NSLLNQLDGcYFGTSFASFFALSFNIASDK	46.63	389-418
kVYYTPQIcGFTINR	75.71	420-434
VYYTPQIcGFTINR	78.11	421-434
ETLYMDVNK	40.02	438-446
ETLYMDVNKDNTESSEEcQ	89.3	438-456

Table 6.2: list of the 42 unique peptides recovered by LC-MS/MS reported with their relative Mascot Ion score and the position in the protein sequence.

```
  1 MSPILGYWKI KGLVQPTRLL LEYLEEKYEE HLYERDEGDK WRNKKFELGL
 51 EFPNLPYYID GDVKLTQSMA IIRYIADKHN MLGGCPKERA EISMLEGAVL
101 DIRYGVSRIA YSKDFETLKV DFLSKLPEML KMFEDRLCHK TYLNGDHVTH
151 PDFMLYDALD VVLYMDPMCL DAFPKLVCFK KRIEAIPQID KYLKSSKYIA
201 WPLQGWQATF GGGDHPPKSD LVPRGSEATV SWIEWFCQLK QNLFLVEVDE
251 DFIRDEFNLI GLQTKVPHFK KLLKIILDED DDDDDDDDD YDDEDDEINR
301 DSEEMYKNKD MHEQNAACLY GLIHSRFILT SKGLALMREK YKSGIYGTCP
351 SIYCENAKLL PTAISEIPKF LSPLLYCPRC CETYYPSKNS LLNQLDGCYF
401 GTSFASFFAL SFNIASDKKK VYYTPQICGF TINRNIRETL YMDVNKDNTE
451 SSEECQ
```

Figure 6.14: LC-MS\MS analysis of recombinant shPfCK2β_2 subunit. **A:** Sequence of the shPfCK2β_2 determined by LC-MS/MS, peptides identified in the run are showed in bold (sequence coverage: 77%).

At this point, a pull-down assay was then designed and tested with GST-shPfCK2β_2 in order to verify whether the PfCK2 autophosphorylation has an active role in the interaction with the β_2 regulatory subunit. To this aim, bacterially expressed His$_6$-PfCK2 wt and Thr63Ala mutant were pre-incubated with +/- ATP at 37° for 10min. Samples were then mixed with purified GST-shPfCK2β_2 retained on glutathione beads and incubated at 37°C for 30min. The beads were then extensively washed and the protein content was loaded on SDS-PAGE and finally analysed by Western Blot using His$_6$-tag antibody (see **Scheme 6.1**).
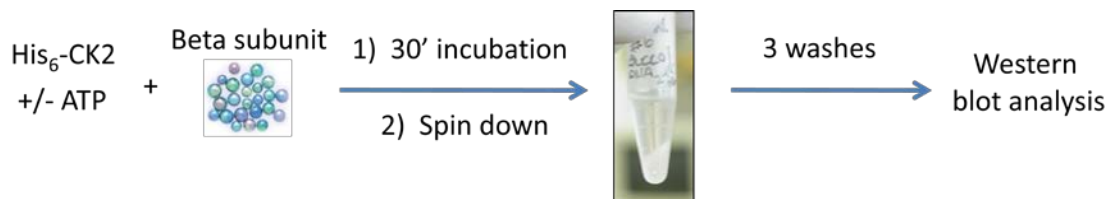
Scheme 6.1: Schematic representation of the pull-down assay with PfCK2 pre incubated with +/- ATP and the GST-shPfCK2β_2.

In this way in fact, if PfCK2-Thr63 autophosphorylation was important for the α-β subunit interaction, the wt would interact with the β_2 subunit more efficiently compared with the Thr63Ala mutant, and the wt pre-incubated with ATP would interact even more strongly, being enriched for the PfCK2 autophosphorylated form. Obviously, such differences in the interactions would increase the amount of PfCK2 protein in the pulled-down sample and would then be detected in the Western Blot by the His$_6$-tag antibody. Interestingly, results showed exactly this described behavior, with a strong signal generated in the case of the wt and a stronger one for the wt pre-incubated with ATP. On the other hand, the Thr63Ala mutant gave rise to a much less intense signal which was not affected by ATP pre-incubation (**Figure 6.15**). Moreover, loading controls demonstrated that the antibody recognised the two different protein constructs in the same extent. Altogether, these observations support the proposed notion that the Thr63 autophosphorylation process modulates the interaction of the catalytic subunit with the β_2 regulatory subunit, at least *in vitro*. In particular, the above experiment showed that incubation of the bacterial expressed wild type catalytic subunit with ATP resulted in a modest increase in the binding of the β_2 regulatory subunit. This may be due to the fact that the bacterially expressed catalytic subunit was nearly fully autophosphorylated when purified and that incubation with ATP did not substantially increase the autophosphorylation state. In order to verify whether this is the case the wt catalytic subunit was pre-treated with calf intestinal alkaline phosphatase for 2hrs at room temperature – a process designed to remove the phosphate groups from PfCK2.
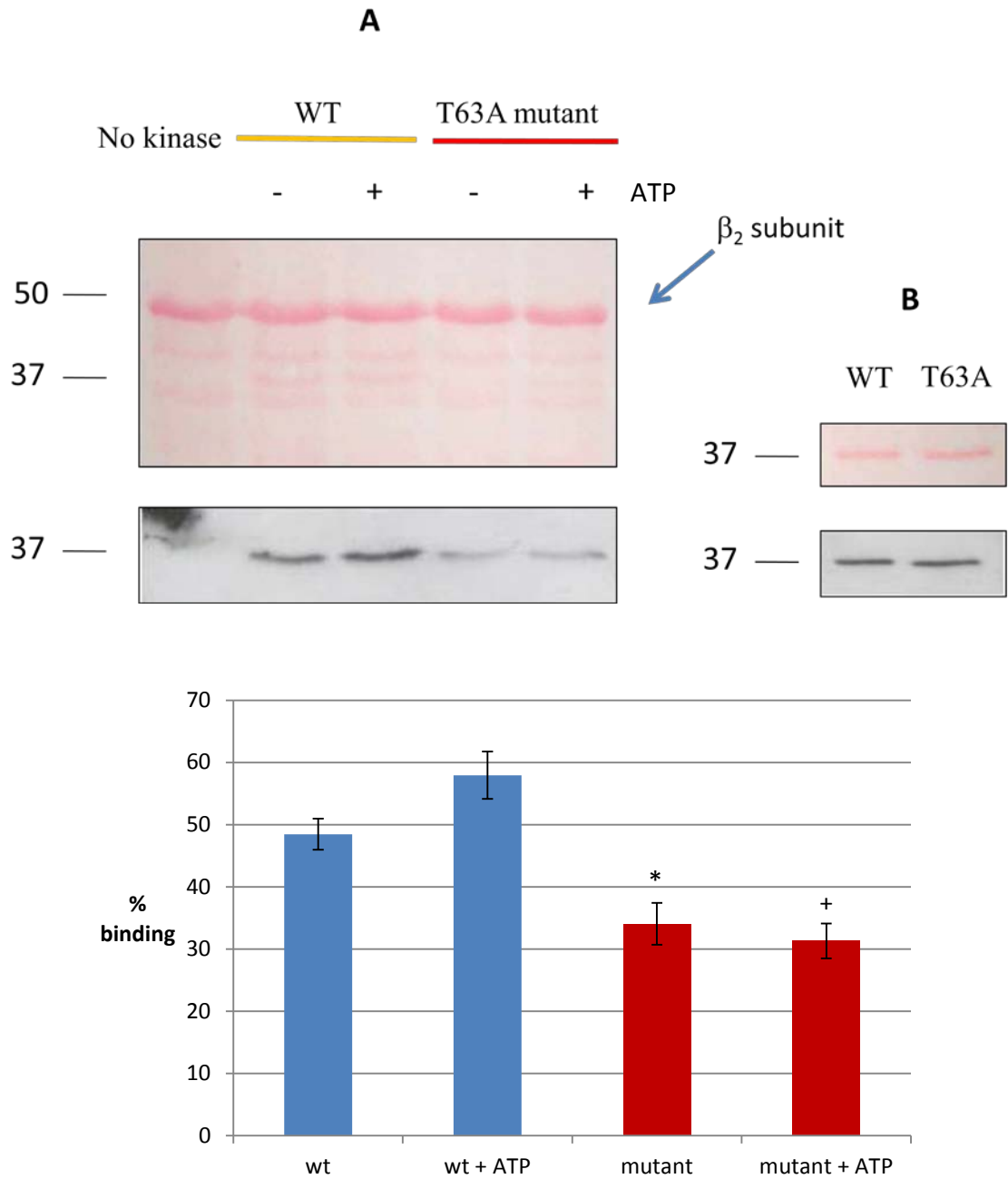
Figure 6.15: Autophosphorylation of PfCK2 on Thr63 increases the interaction with the PfCK2β_2-subunit *in vitro*. His$_6$-PfCK2 (wt and Thr63Ala mutant) was pre-incubated with +/-ATP at 37°C for 10min; the sample was then incubated with glutathione beads containing recombinant GST-shPfCK2β_2, centrifuged and washed 3x with kinase buffer; the pellet was then resolved on SDS-PAGE, immunoblotted with anti His$_6$-tag antibody and the bands quantified by densitometry. **A**: pull down assay, **B**: loading control; top

panel: ponceau staining, bottom panel: Western Blot, **C:** histograms represent the band intensity relative to and correspond to mean ±SD of three independent experiments. Statistical comparison was performed with a paired T-TEST: *, P<0.05 between wt and mutant; [+], P<0.05 between wt + ATP and mutant + ATP.
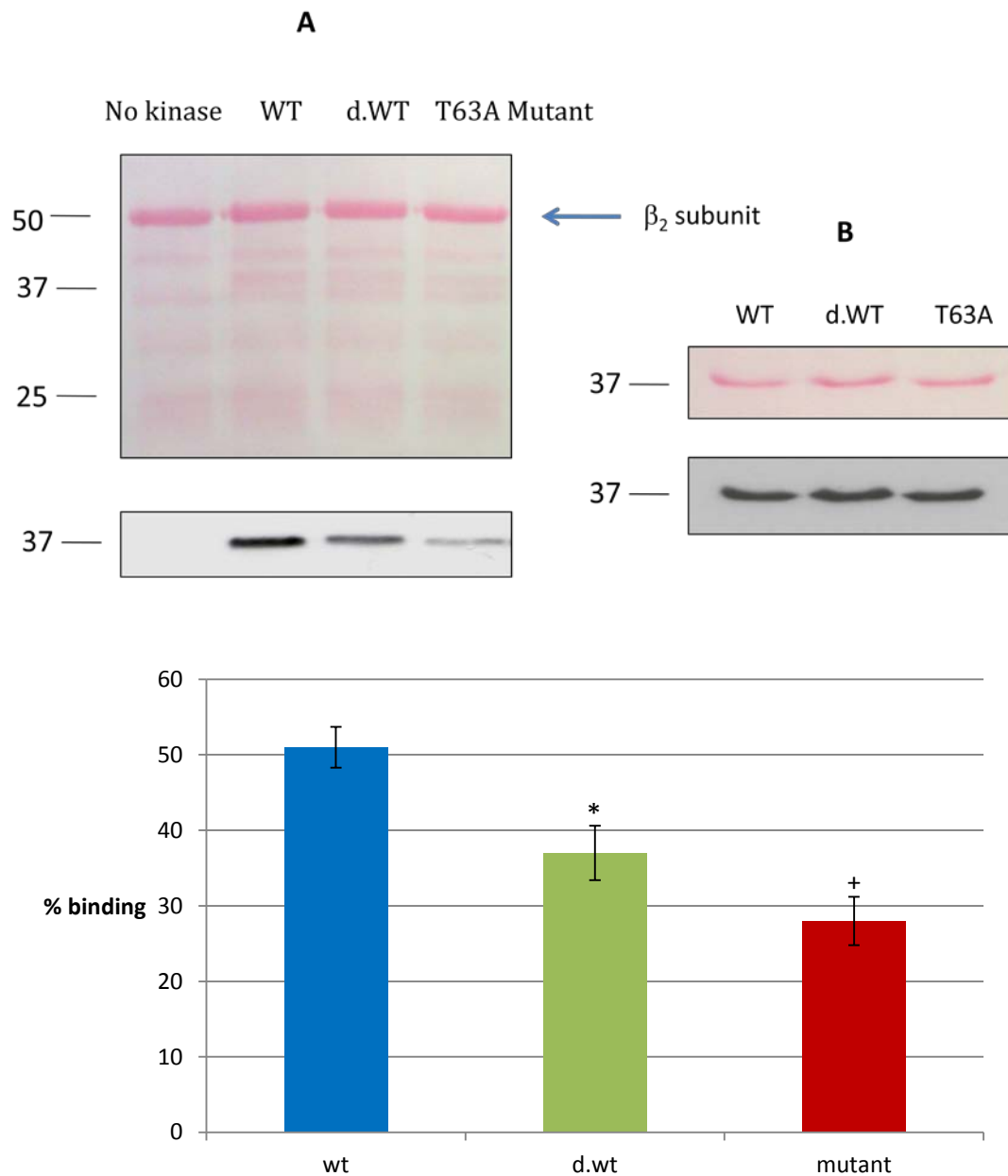
Figure 6.16: Dephosphorylation of PfCK2 on Thr63 decreases the interaction with the PfCK2β_2-subunit *in vitro*. His$_6$-PfCK2 was pre-incubated with CIP at 37°C for 10min; the

sample was purified on nickel resin and then incubated with glutathione beads containing recombinant GST-shPfCK2β_2, centrifuged and washed 3x with kinase buffer; the pellet was then resolved on SDS-PAGE, immunoblotted with anti His$_6$-tag antibody and the bands quantified by densitometry. **A**: pull down assay, **B**: loading control; top panel: ponceau staining, bottom panel: Western Blot, **C:** histograms represent the percentage binding and correspond to mean ±SD of three independent experiments. Statistical comparison was performed with a paired T-TEST: *, P<0.05 between wt and d.wt; $^{+}$, P<0.05 between wt and mutant.

The obtained de-phosphorylated wild type CK2 sample was then tested in the interation assay previously described showing a decrease in the interaction of the catalytic subunit with the β_2 regulatory subunit (**Figure 6.16**).

Thus, this result further supports a role for the Thr63 phosphorylation of the catalytic subunit in the regulation of the interaction with the β_2 regulatory subunit.

6.3 Discussion

Phosphorylation, and in particular autophosphorylation, of kinases are two of the main mechanisms controlling kinase activity both *in vitro* and *in vivo*. Data here presented showed that this is also true for PfCK2. In fact, the conducted analyses confirmed a previously published observation that PfCK2 recombinant enzyme is able to undergo *in vitro* autophosphorylation.[71] The data presented here, however, builds on this earlier observation and demonstrates that the autophosphorylation process occurs at Thr63,

while *in vitro* kinase assays showed that this autophosphorylation is able to regulate kinase activity by increasing it by ~50%. Nonetheless, it is interesting to note that the protein kinase activity was not completely abolished by the Thr63Ala mutation. This particular observation demonstrates that PfCK2 cannot be considered a true member of the RD kinase family. In fact, for this class of kinases, the mutation of the phosphorylating residue usually completely removes the basal kinase activity, since the phosphate group is crucial for the correct folding of the enzyme in an active conformation (also see section **1.6.4**). Moreover, for RD kinases the phosphorylating residue is usually contained within a highly conserved motif named activation segment which in PfCK2 spans from Asp179 to Glu206 and that therefore does not include Thr63.

Besides the role in controlling kinase intrinsic activity, PfCK2 *in silico* modeling together with the comparison with the human holoenzyme crystal structure suggested a possible additional role also in the α-β subunit interaction with the PfCK2 regulatory subunits. To prove this hypothesis two pull-down assays were performed between a short form of the PfCK2β_2 regulatory subunit lacking a highly acidic N-terminal insert, and the recombinant wt and mutant PfCK2. Overall, the experiments confirmed the tested hypothesis, showing a stronger interaction of the wt compared with the mutant lacking the phosphorylation site, with the β_2 subunit. This was particularly confirmed by pre-treating the enzyme by either ATP, in order to increase the phosphorylated form of PfCK2 in the sample, or by CIP in order to dephosphorylate it. In both cases, the results confirmed the role for the autophosphorylation process in increasing the interaction with the β_2 subunit, at least *in vitro*.

In conclusion, the results here presented describe a new interesting pathway for PfCK2 autophosphorylation modulating both *in vitro* kinase activity and *in vitro* interaction with the β_2 regulatory subunit. Such discovery is particularly surprising considering that it is still unclear what regulates CK2 activity in human cells. In fact, even though human CK2 has hundreds of reported substrates[55] underlying its crucial role in maintaining the cellular homeostasis, an unifying model for its potential cellular regulation has not been described yet.[145] This has led to consider human CK2 as a constitutively active or unregulated kinase.[90] However, despite very close sequence homology, on the basis of the data presented here the same does not seem true for the parasite CK2 homologue.

The importance of such pathway is also underlined by the fact that this is parasite specific. In fact, human CK2 autophosphorylates on a different residue, Tyr182 that is conserved in PfCK2.[144] Mutation of Tyr182 in human CK2 completely abolishes autophosphorylation activity[144] while the corresponding Tyr186 in PfCK2 is not involved in autophosphorylation based on the analyses presented here. Furthermore, Thr63 is not conserved in the human homologue and corresponds to an Ile residue (Ile59, see **Figure 5.4**) and, although there is an adjacent Thr residue to it (Thr60), there is no evidence for its phosphorylation in the literature. Interestingly, the α-β interaction has already been successfully targeted in the case of human CK2 with peptide-mimetic molecules able to disrupt the interaction and to inhibit the phosphorylation of a β-dependent substrate.[146,147] Therefore, the observation that the Thr63 autophosphorylation is a parasite-specific pathway involved in the α-β_2 subunit interaction opens up a brand-new scenario for the selective targeting of the PfCK2 holoenzyme formation and the inhibition of β_2-dependent substrates in *P. falciparum*.

In conclusion, this study has identified for the first time a major mechanism of regulation of a member of the CK2 family, regulating both the intrinsic kinase activity and the interaction with the β_2 regulatory subunit. Also, the fact that such pathway is not conserved in the human host and it is potentially druggable, on the basis of previous studies, underlies the importance of this discovery also in the context of targeting the parasite kinome in order to develop a new class of antimalarials.

Chapter 7: Tyrosine phosphorylation in *P. falciparum*

7.1 Introduction

Despite the absence of putative tyrosine kinases in the *P. falciparum* genome,[68] several studies have reported the occurrence of tyrosine phosphorylation (pTyr) both in the parasite membrane[106] and cytosol fractions.[83, 148, 149] Although, as previously described (see section **1.9**), pTyr is usually involved in pathways specific to multicellular organisms (e.g. growth factor response, innate immune system, signal transduction), similar observations have been made also in other lower eukaryotes such as the fungus *Neurospora crassa,*[150] and the protozoa: *Trypanosoma brucei,*[151] *Leishmania donovani*[152] and *Toxoplasma gondii*[153]. Regarding *P. falciparum*, the earliest accounts identified the presence of membrane-bound pTyr activity in the intra-erythrocytic stage, especially during the initial ring and throphozoite stages.[106, 148] More recently, thanks to the new technical advances in phosphopeptide enrichment followed by LC-MS\MS analysis two major studies identified specific tyrosine phosphorylated residues contained within parasite proteins and accounting respectively for ~1%[83] and ~0.5%[149] of the total detected phosphoproteome. Interestingly, in these studies pTyr was found not only in the activation loop of the Ser/Thr protein kinases such as *P. falciparum* glycogen synthase kinase 3 (PfGSK3) and *P. falciparum* CDC-like kinase 3 (PfCLK3) (where, in both cases, it has been showed to

occur through an autophosphorylation process regulating the enzyme activity),[83] but also in other kinase-unrelated proteins indicating the presence of genuine pTyr signalling pathways. Among these, a rather interesting and significant example is the *P. falciparum* protein mini-chromosome maintenance protein 2 (PfMCM2) which was found to be phosphorylated on two residues: Ser13 and Tyr16[83] (see **Figure 7.1**).

PfMCM2 (PF14_0177)

```
  1 MEDKKKLEED LESNKYDIDE EDLLEDEGRL NEEERQAELE GESLFEEDEG
 51 FIFGADDEKK EMQKLRNLGL DNDDYDDDFI DDELDYEDNL KARRAAERHM
101 QMQRKQEGKY EKNKFWKTLE DQLEGDDEEE DIFDKVAEKV AKRRENLHLT
151 AEETDIPDLS NLESAKICLS VNPKDVVFDE RYQQAADTCF RYFLHKFSLK
201 DSMGLNIDES NTELHEEEHM NSSHQYYIDK IEKMILNDKH TLIVSAKHLI
251 QFHCENLVQW IEFKPEQILE VLHECLMVEA YRISPKLYKG RICKVVLRDW
301 PYSTQLRNLR CTELNTLIKV TGVCIKRGYV LPKLRVMYLK CNSCDTTLSE
351 VPIYFADGKK PVLPRRCPHC QSATFSVDRI KTAYTDYQKI TLQESPCSVP
401 AGRAPRQREV VVTGDLVDKV KPGEEVEVLG IYKTKYDIGL NIKYGFPILQ
451 TEIEANNIER KEDIQLSELT EDDIKDILKL SKDPNIRERI ITSIAPAIWG
501 HKDIKTSIAY ALFGGVQKGG DKSFSKNNET NNFGVQNRDI LNNFKGGHTI
551 RGDINVLLLG DPGLGKSQVL QYVHKTNLRT VYTTGKGASA VGLTAGVRKD
601 HTTNEWTLEG GALVLADEGI CIIDEFDKMT DKDRVSIHEA MEQQSISISK
651 AGIVTTLRAR CAVIAAANPI YGRYNPSLTF KENVDLSDPI LSRFDLITVL
701 RDIPNVDEDF YLAEYVVTNH QLSHPKLENT QNYQKRIENL KNVIVSSSAY
751 EPIPQDLLQK YIIYARTNCK PSLSDVPYAE ISAKLSNFYS RVRQKACASG
801 GYPLTLRHIE SIIRIAEANA KMRLSHQIYS KDVDYAIATL LESYVSCQRF
851 AVAKQLSKEF ARYRALFRGG YEVLRELLRR TVQQMIQRQN LKNASAKDFQ
901 NDSESGTESE AEILNPNNVF LPLHIFMKTA MQNKFSEYQV LNWMKSKVFN
951 EHYAVIKRDG VEGIISKKFK V
```

Figure 7.1: Sequence of the *P. falciparum* protein mini-chromosome maintenance protein 2 (PfMCM2) showing the two phosphorylation sites Ser13 and Tyr16 (red) detected by LC-MS\MS.[83]

This protein is part of a heterohexameric complex composed of PfMCM2-7 that functions as a helicase, unwinding the DNA duplex during replication.[154] The basic mechanism of the pre-replication complex formation and the subsequent onset of DNA synthesis are well conserved in eukaryotes[155] and have been partly characterised in *P. falciparum* as well.[156] Regarding MCM2, in model eukaryotes it has been shown that the protein is multiple phosphorylated in a cell cycle-dependent manner (mainly by Cdc7[157] and several CDKs[158]). Interestingly, this transient phosphorylation state of MCM2 is thought to play a crucial role in the removal of the MCM complex from the chromatin and be a trigger for DNA synthesis.[159,160] Characterization of the *Plasmodium* helicase complex showed that the complex subunits are differently expressed during the intra-erythrocytyc cycle.[156] In particular, the expression profile of PfMCM2, 6 and 7 peaks in late schizont stage corresponding with DNA replication in *Plasmodium*. However, the same study did not detect any active phosphorylation of the helicase complex.

The recent observation that PfMCM2 is tyrosine phosphorylated opens up a brand-new scenario for the possible presence of a pTyr signalling pathway regulating PfMCM2 chromatin binding and DNA synthesis and which could potentially work in synergy with the together reported serine phosphorylation.

In this chapter, we investigated pTyr pathways in *P. falciparum* with the aim to identify specific protein substrates, responsible kinases and possible roles for such events. The general purpose was to further strengthen the evidence for the occurrence of this specific modification also in *P. falciparum*. In particular, we decided to focus on two of the tyrosine-phosphorylated proteins detected in the global phosphoproteomic study

being PfCLK3 and PfMCM2. With PfCLK3, our analysis was aimed to further confirm the LC-MS\MS data through Western Blot analysis. In the latter case, instead, since PfMCM2 is a non-kinase protein we also carried out *in vitro* kinase assays focused on identifying the responsible kinase.

7.2 Results

7.2.1 Analysis of tyrosine phosphorylation occurrence in *P. falciparum*

Since only preliminary data were reported in literature regarding the occurrence of Tyr phosphorylated proteins in *P. falciparum*, we decided to carry out a more systematic analysis aimed at specifically map and identify pTyr proteins during the parasite intra-erythocytic stage. To this aim, we conducted two main analyses. The first one consisted of a Western Blot analysis with an anti-pTyr antibody of the total lysate of infected red blood cells (iRBCs) and a sample of iRBCs fractionated into a RBC fraction (iRBC fraction) and a parasite fraction following saponin lysis. In particular, two controls were also loaded in the gel consisting of both a bacterial lysates and a non-infected RBC lysate. This study was focused on bringing more evidence to support the the occurrence of pTyr proteins in *P. falciparum*, especially within the parasite membrane. Results provide evidence for the fact that infected red blood cells (iRBCs) underwent a substantial increase in tyrosine phosphorylation over non-infected controls, and that the majority of this tyrosine phosphorylation was detectable within the parasite fraction (**Figure 7.1**). This evidence supports therefore the hypothesis that
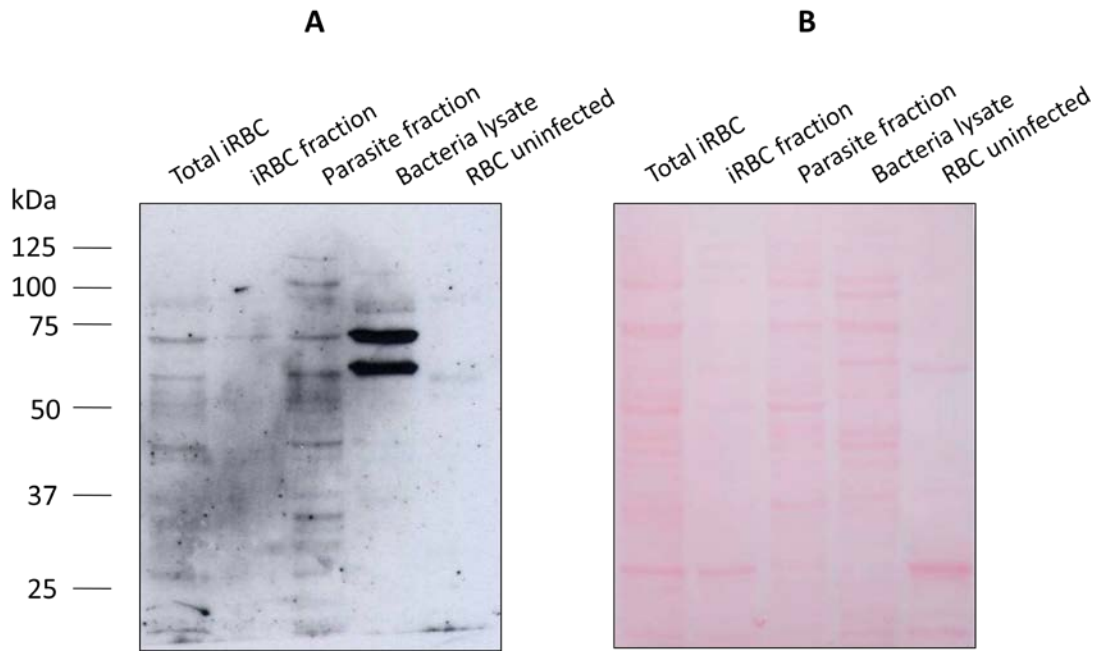
Figure 7.1: Determination of tyrosine phosphorylation in *P. falciparum* during the schizont stage with Western Blot analysis. Schizont stage-infected RBCs were either lysed in 1% NP-40 to give total iRBC sample or fractionated into a RBC fraction (iRBC fraction) and parasite fraction following saponin lysis. Controls were bacterial lysates and non-infected RBC lysates. Samples were resolved by SDS-PAGE and immunoblotted using an anti-phosphotyrosine antibody. **A:** Western Blot **B:** Ponceau staining.

tyrosine phosphorylation occurs within the parasitophorous vacuole (including within the parasite itself) rather than exclusively in the host erythrocyte. The presence of two intense bands in the bacterial lysate control could be explained by the cross-reactivity of the antibody with two proteins contained in the sample.

The second analysis involved an immunoprecipitation experiment conducted first with both a ^{32}P-radioactive labeled parasite lysate and then with a wt lysate followed by LC-MS\MS analysis. In particular, this two-step protocol was aimed at obtaining a sample enriched for pTyr-containing proteins which were then subsequently analysed by LC-MS\MS to further identify their specific nature. Results from the pull-down experiment with a ^{32}P-labeled lysate showed that radioactivity was successfully recovered after 3 washes with both a gentle affinity elution with phenyl phosphate, and a stronger elution with laemmli buffer containing 4% SDS (**Figure 7.2**, **7.3**). As expected, the one-step elution with laemmli buffer recovered more radioactivity and therefore more phosphorylated proteins from the anti-pTyr beads than the same buffer elution in the second case (**Figure 7.2**). In fact, in the second experiment, the use of a sequential elution of phenyl phosphate and then laemmli buffer caused the pull-down radioactivity to spread across the three fractions (**Figure 7.3**). Importantly, the fact that radioactivity was observed under more stringent eluting conditions in the presence of phenyl phosphate, strongly indicates that the pull-down proteins are genuinely pTyr-containing proteins. To further confirm this evidence, the same experiment was then repeated a second time with a non-radioactive labeled lysate and the pull-down fractions analysed by LC-MS\MS. However, in this case despite previous evidence, no phosphrylated proteins were observed in both the phenyl phosphate and the laemmli buffer eluted fractions. This result can be interpreted in two ways, either: i) there are no phosphorylated proteins in *P. falciparum* and the radioactivity observed is the one of the background, or ii) there are genuine tyrosine phosphorylated proteins in *P. falciparum* but their extremely low abundance prevents LC-MS\MS detection.
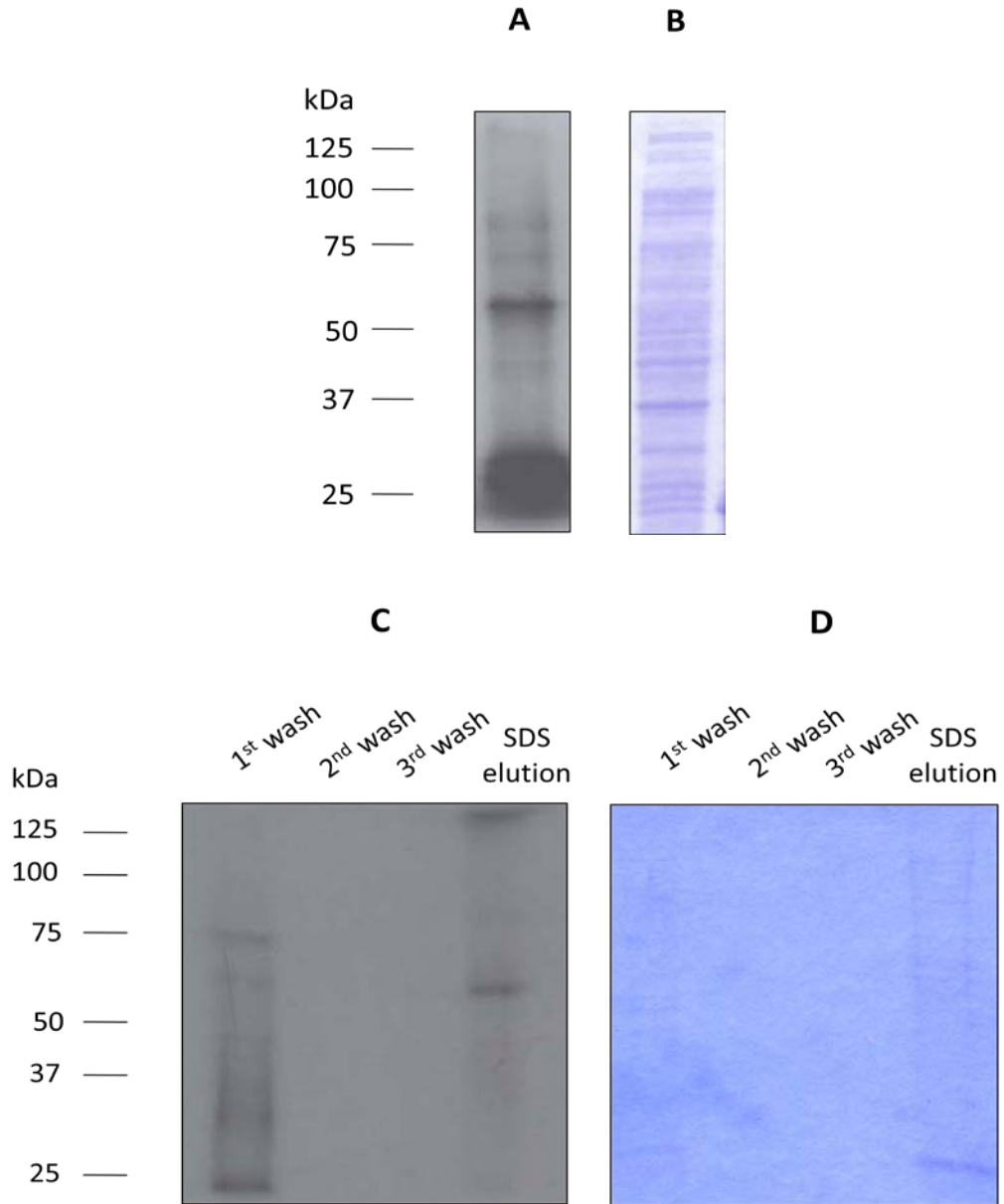
Figure 7.2: Determination of tyrosine phosphorylation in *P. falciparum* by a pull down

assay with anti-phosphotyrosine antibody coniugated agarose beads and 4% SDS

elution. A ^{32}P-labelled iRBC lysate was incubated with anti-phosphotyrosine antibody

coniugated agarose beads for 3hrs at 4°C and centrifuged, the pellet was washed three

times with TEG buffer, eluted with 4% SDS buffer resolved by SDS-PAGE and the gel

exposed to autoradiographic film. **A:** autoradiograph, **B:** Coomassie stain. Results are

representative of three independent experiments.
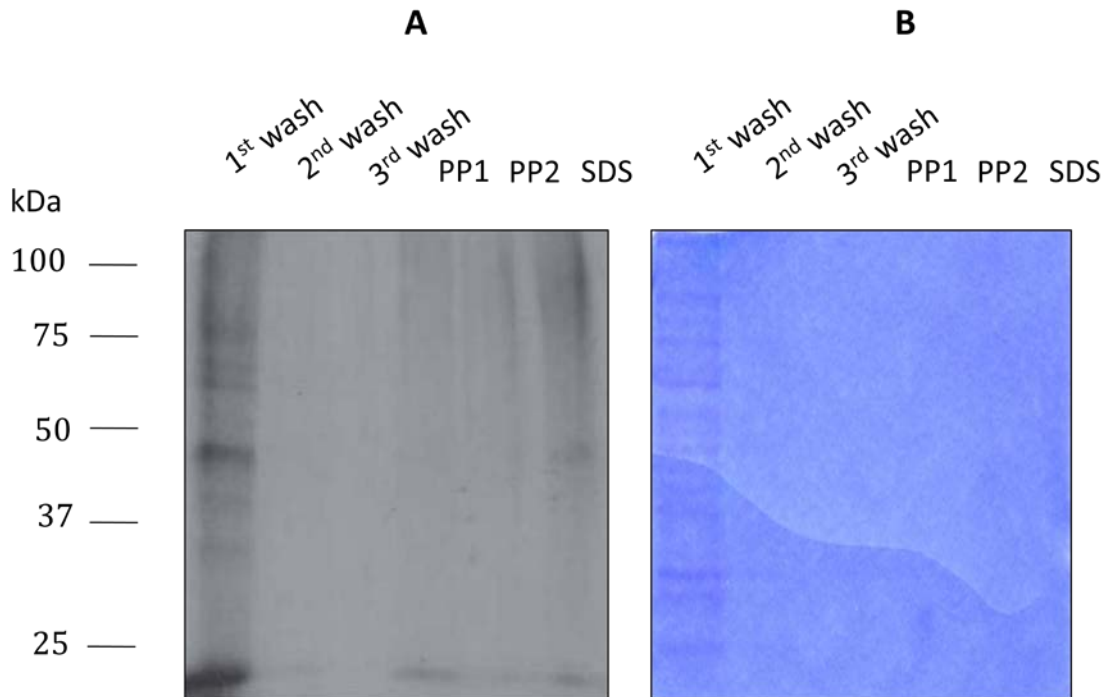
Figure 7.3: Determination of tyrosine phosphorylation in *P. falciparum* by a pull down assay with anti-phosphotyrosine antibody coniugated agarose beads and affinity elution with 20mM phenyl phosphate. A ^{32}P-labelled iRBC lysate was incubated with anti-phosphotyrosine antibody coniugated agarose beads for 3hrs at 4°C and centrifuged, the pellet was washed three times with TEG buffer, eluted twice with 20mM phenyl phosphate and then with 4% SDS buffer; proteins were resolved by SDS-PAGE and the gel exposed to autoradiographic film. **A:** autoradiograph, **B:** Coomassie stain. Results are representative of three independent experiments.

Nonetheless, the fact that no radioactivity is observed in the two washes before the final elution in the pull-down assays (see **Figure 7.2**, **7.3**), and that pTyr accounts for no more than 1% of the total phosphoproteome according to previous analyses,[161] support the second hypothesis.

7.2.2 Analysis of PfCLK3 tyrosine phosphorylation

Two of the clearest example of tyrosine phosphorylated proteins detected in the global phosphoproteome analysis were PfGSK3 and PfCLK3.[83] In particular, in both cases this modification involves a Tyr residue contained within the activation loop which normally controls the kinase activity of the protein (see also section **1.6.4**). While for PfGSK3 the role of Tyr229 phosphorylation in activating the enzymatic activity of PfGSK3 has already been described, no detailed analysis or reports about PFCLK3 Tyr526 phosphorylation were found in the literature. Therefore, in order to study in detail the role and mechanism of PfCLK3 Tyr526 phosphorylation, two anti-PfCLK3 antibodies (of which one pTyr526 specific) were characterised and used in Western Blot analyses with a parasite lysate. In particular, the structural antibody was purified from the provided serum (obtained from a custom synthesis) using a Hi-trap NHS activated HP column. The obtained purified antibody was then dialysed and run on a SDS-PAGE gel to check for the purity. As expected, results clearly showed the presence of the two light and heavy chains characteristic of antibodies (**Figure 7.4**). Also, the comparison between the sample before and after dialysis showed that the process did not alter the sample or its concentration. Both antibodies were then tested in Western Blot analyses to verify for the occurrence of the PfCLK3 protein and PfCLK3-Tyr526 phosphorylation in the parasite lysate. Results from both the two analyses demonstrated that PfCLK3 is present within the parasite membrane and that this protein is phosphorylated in Tyr526 (**Figure 7.5**, **7.6**).
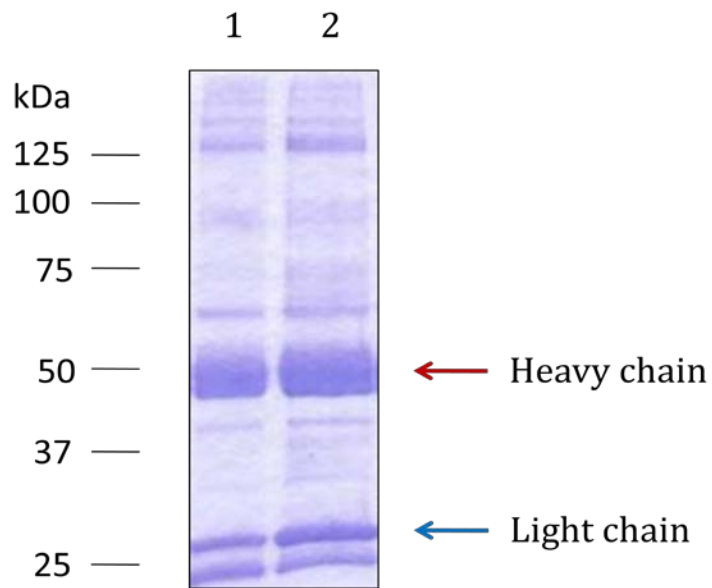
Figure 7.4: SDS-PAGE gel of the PfCLK3 antibody (Coomassie stain). Lane 1: before dialysis, 2: after dialysis, arrows indicate the heavy and light chains of the antibody.
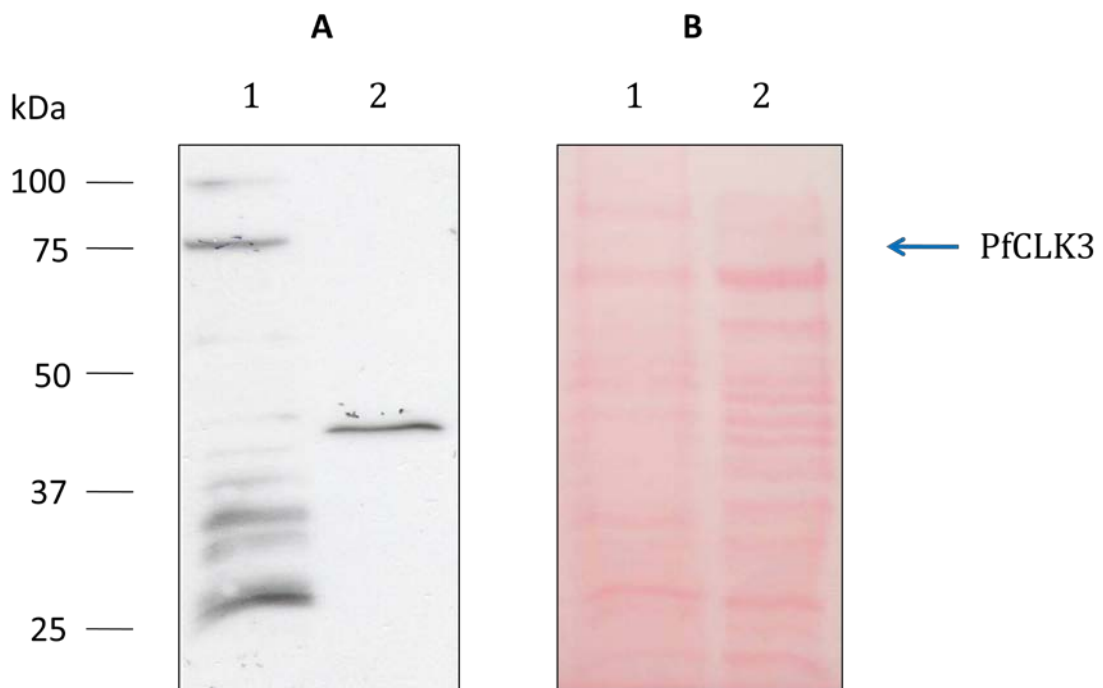
Figure 7.5: Western Blot analysis of an iRBC lysate with the PfCLK3 antibody. An iRBC lysate was resolved by SDS-PAGE and immunoblotted using the PfCLK3 antibody. **A:**

Western Blot, **B:** Ponceau staining; lane 1: iRBC lysate, 2: bacterial lysate. Results are representative of three independent experiments.

This evidence is also further validated by the fact that both antibodies recognised a protein of the same molecular weight (~75KDa) corresponding to the molecular weight of PfCLK3 and by the fact that their cross-reactivity with the rest of the parasite lysate and bacterial control was very low. Therefore, altogether these observations support the previously reported evidence for the occurrence of pTyr in *P. falciparum* and in particular for the PfCLK3-Tyr526 phosphorylation.
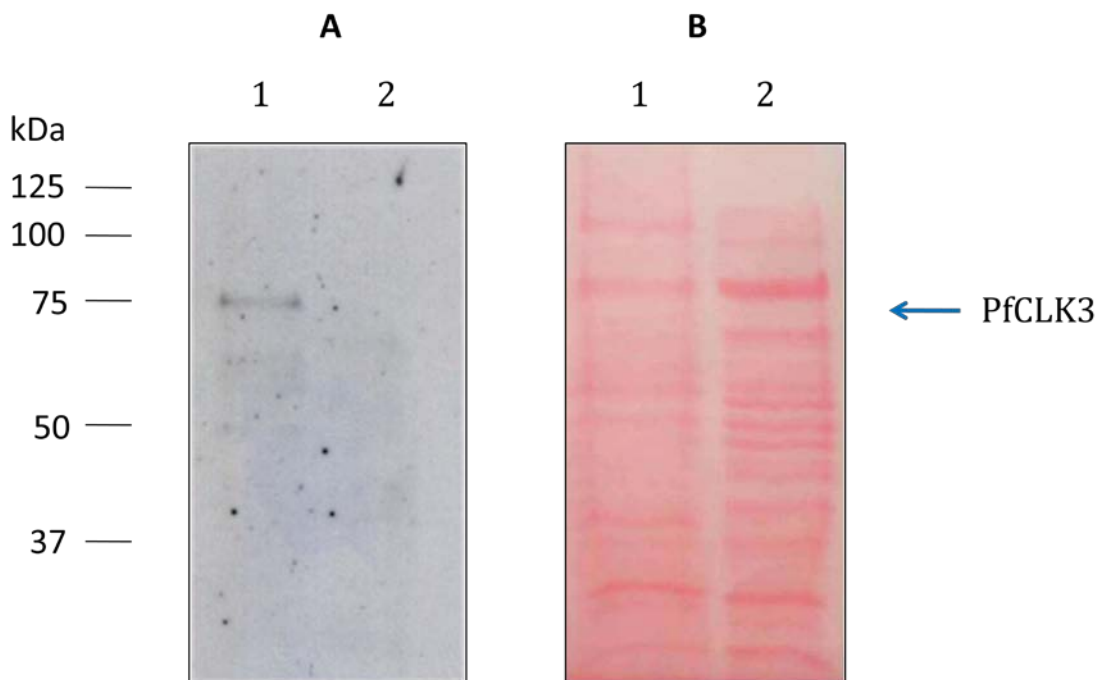
Figure 7.6: Western Blot analysis of an iRBC lysate with the PfCLK3-pTyr526 phosphospecific antibody. An iRBC lysate was resolved by SDS-PAGE and immunoblotted using the PfCLK3-pTyr526 phosphospecific antibody. **A:** Western Blot, **B:** Ponceau staining; lane 1: iRBC lysate, 2: bacterial lysate.

7.2.3 Development of an *in vitro* kinase assay for PfMCM2

In order to identify the kinase responsible for PfMCM2-Tyr 16 phosphorylation, a PfMCM2 N-terminal fragment (AA1-159) containing the two phosphorylation sites previously detected (**Figure 7.1**) was expressed as a GST-fusion protein (for simplicity this will be named GST-PfMCM2 wt for the rest of the chapter) and subsequently used as a substrate in *in vitro* kinase assays. To this aim, the chemically synthesised coding DNA was first digested with BamHI, and EcoRI DNA restriction enzymes, and subsequently ligated into a pGEX-2T plasmid. The obtained plasmid was then cloned, transfected and expressed in *E. coli* competent cells. In particular, the recombinant protein was purified and retained on gluthatione beads to allow the separation from the supernatant by centrifugation during the kinase *in vitro* assays. The correct expression and level of purity of the protein product was determined by SDS-PAGE gel (**Figure 7.7**).

At this point, in order to verify whether the GST-PfMCM2 wt was a suitable substrate for *in vitro* kinase assays, the recombinant protein was incubated with a Pf lysate and radioactive ^{32}P-ATP for 10min at 37°C. A sample of the GST moiety alone was also run in parallel as a negative control. After the kinase reaction, samples were then analysed with SDS-PAGE followed by autoradiographic film exposure. Results showed that, while there was no activity against the GST moiety alone (lane 1, **Figure 7.8**), the GST-PfMCM2 recombinant protein incorporated radioactivity during the assay (lane 2, **Figure 7.8**).
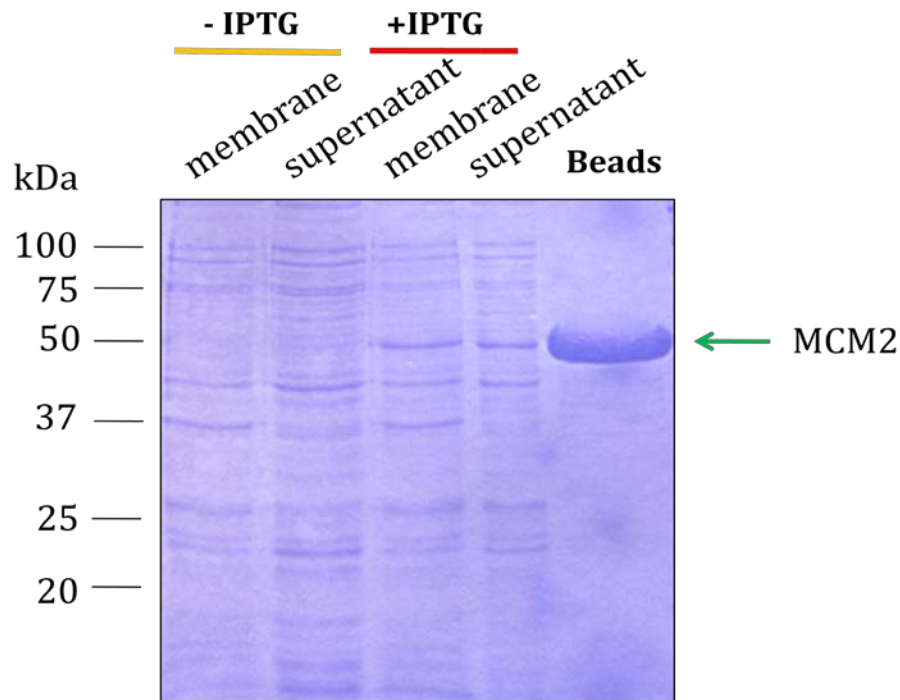
Figure 7.7: GST-PfMCM2 expression and purification profile from transfected *E. coli* competent cells. GST-PfMCM2 was expressed in transfected *E. coli* competent cells upon induction with 20mM IPTG at 22°C for 4hrs; cell cultures were spun down, lysed and purified on glutathione beads. The membrane and supernatant content before and after induction together with the purified sample were resolved on SDS-PAGE (Comassie stain).

These two observations indicated therefore that the PfMCM2 N-terminal fragment was actively phosphorylated by one or more kinases present in the parasite lysate, during the assay. In addition, single point mutagenesis reactions were carried out with the same plasmid in order to obtain a set of mutated PfMCM2 recombinant proteins lacking alternatively one or both phosphorylation sites, to use in the *in vitro* kinase assays.
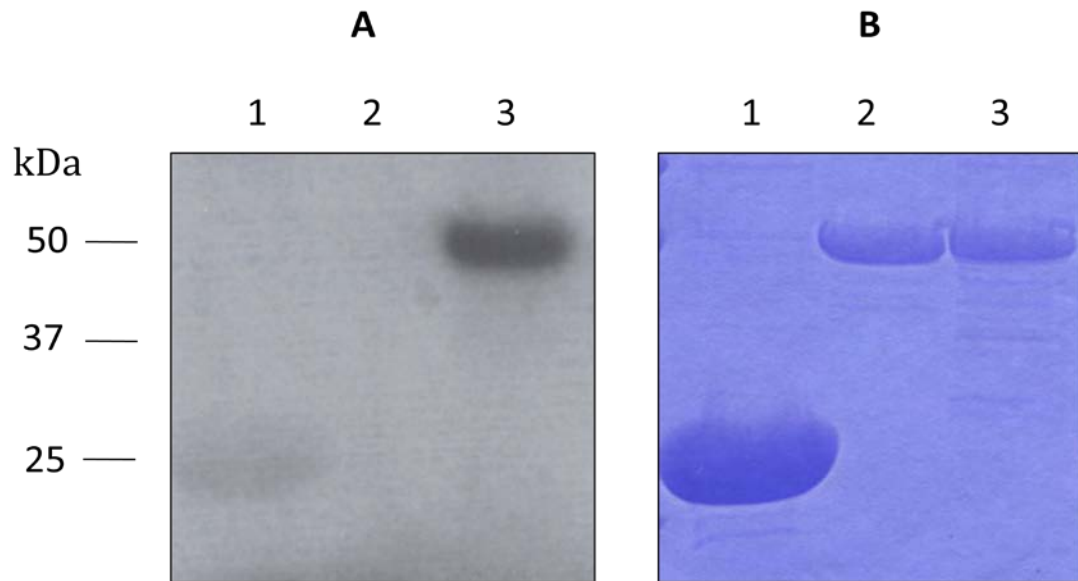
Figure 7.8: *In vitro* kinase assay with recombinant GST-PfMCM2, ^{32}P-ATP and a parasite lysate. **A**: autoradiograph, **B**: Coomassie stain. Lane 1: GST + parasite lysate, 2: GST-PfMCM2, 3: GSTPfMCM2 + parasite lysate.

To this aim, Ser13 was mutated to Ala in PfMCM2_Ala13, Tyr16 was mutated to Phe in PfMCM2Phe_16 and both residues were mutated in PfMCM2_Ala13_Phe16 (see **Table 7.1**). After PCR amplification, the reaction mixture was transfected in *E.coli* supercompetent cells and ten colonies were then selected and grown. Plasmids from each colony were extracted, digested with BamHI and EcoRI restriction enzymes and loaded on an agarose gel to check for the presence of the coding insert (see **Figure 7.9** as an example). After DNA sequencing, a plasmid coding for the desired PfMCM2 mutant was transfected in *E. coli* competent cells and the protein purified and retained on glutathione beads following the same procedure as for the wt.
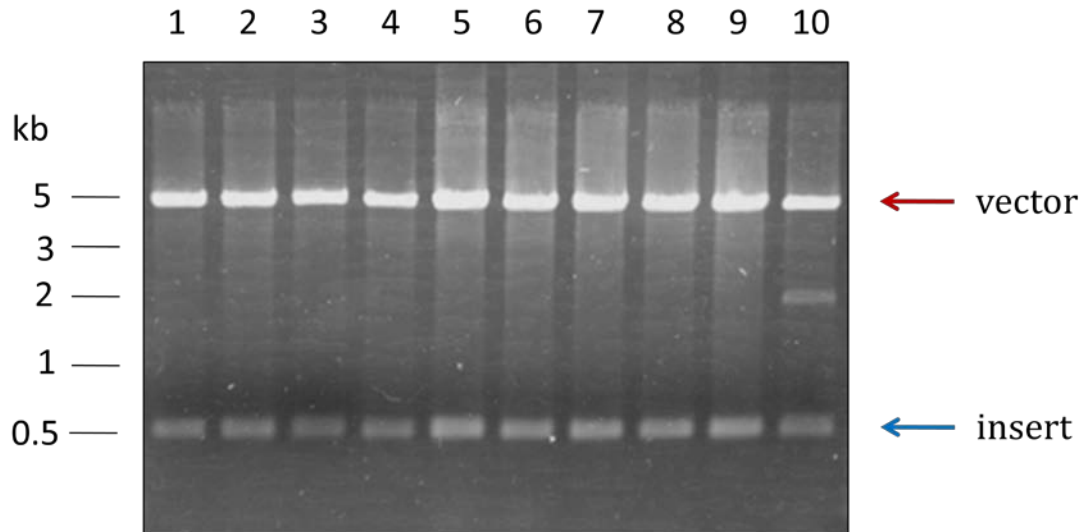
Figure 7.9: BamHI and EcoRI digestion of pGEX-2T plasmids encoding for PfMCM2_Ala13 protein expression. Plasmids were extracted from 10 selected colonies after single point mutagenesis reaction and transfection in *E. coli* supercompetent cells.

The obtained constructs and nomenclature use throughout the rest of this chapter are reported in **Table 7.1**.

Name	sequence (AA 1-20)
PfMCM2 wt	MEDKKKLEEDLESNKYDIDE-
PfMCM2_Ala13	MEDKKKLEEDLE**A**NKYDIDE-
PfMCM2_Phe16	MEDKKKLEEDLESNK**F**DIDE-
PfMCM2_Ala13_Phe16	MEDKKKLEEDLE**A**NK**F**DIDE-

Table 7.1: N-terminal sequence of recombinant GST-PfMCM2 wt and mutants used in *in vitro* kinase assays (mutated residues are shown in blue).

To further identify the specific residues involved in the *in vitro* kinase reaction, the above-mentioned assay was repeated with GST-PfMCM2 wt and the three different mutants GST-PfMCM2_Ala13, GST-PfMCM2_Phe16 and GST-PfMCM2_Ala13_Phe16. Surprisingly, results showed that only two recombinant proteins: GST-PfMCM2 wt (lane 1, **Figure 7.10**) and GST-PfMCM2_Phe16 (lane 2, **Figure 7.10**) were phosphorylated in the assay conditions, while GST-PfMCM2_Ala13 and GST-PfMCM2_Ala13_Phe16 did not incorporate any radioactivity.
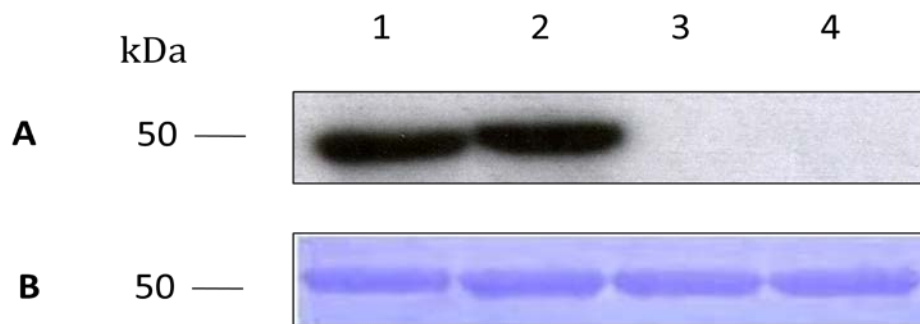
Figure 7.10: The iRBC lysate is able to phosphorylate PfMCM2 on Ser13 but not on Tyr16 in *in vitro*. Glutathione beads containing recombinant GST-PfMCM2 were incubated with an iRBC lysate and ^{32}P-ATP for 10min at 37°C; the sample was centrifuged, the pellet resolved on SDS page and the gel exposed to autoradiographic film. **A**: autoradiograph, **B**: Coomassie stain. Lane 1: GST-PfMCM2 wt, 2: GST-PfMCM2_Phe16, 3: GST-PfMCM2_Ala13, 4: GST-PfMCM2_Ala13_Phe16. Results are representative of three independent experiments.

This evidence is consistent with the phosphorylation of only one of the two residues identified in the *in vivo* global phosphoproteome analysis,[83] being in particular Ser13. The fact that Tyr16 phosphorylation was not detected can be due to two main reasons: either i) PfMCM2 is not truly phosphorylated on Tyr16 and the mass spectrometry data is therefore ambiguous, or ii) PfMCM2 is phosphorylated on Tyr16 *in vivo*, as detected by LC-MS\MS, but for physiological reasons (e.g. the responsible kinase is inhibited or not activated in the lysate) a parasite lysate is not able to phosphorylate this specific residue *in vitro*. (The investigation regarding the PfMCM2-Ser13 phosphorylation event is reported in the next chapter (see **Chapter 8**).

7.2.4 Study on the PfCK2 dual specificity

Despite the fact that *in vitro* kinase assays with a parasite lysate did not detect any PfMCM2 tyrosine phosphorylation (see section **7.2.3**) a further kinase assay was carried out with recombinant GST-PfCK2. In fact, previous studies conducted with *S. cerevisiae*[91] and *H. sapiens*[92] CK2 showed that both enzymes are able to catalyse Tyr phosphorylation as well as Ser/Thr, although with a much lower efficiency. The high degree of homology (see also section **1.8.1**) between the human and the *P. falciparum* CK2 suggest that the same might be true also for the parasite enzyme. Results from the *in vitro* assay using PfMCM2 wt, PfMCM2_Phe16, PfMCM2_Ala13 and PfMCM2_Ala13_Phe16 mutants showed that PfCK2 actively phosphorylated both Ser13 and Tyr16, *in vitro* (**Figure 7.11**). While phosphorylation of PfMCM2 wt, PfMCM2_Phe16 and PfMCM2_Ala13 efficiently occurred in the assay conditions, the
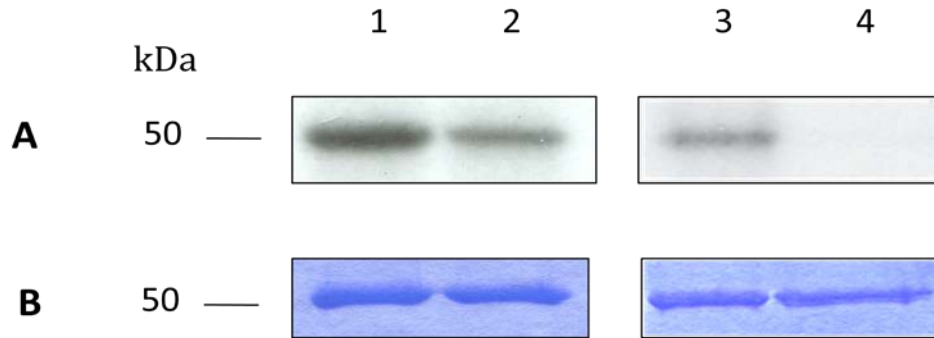
Figure 7.11: Recombinant PfCK2 is able to phosphorylate PfMCM2 on Ser13 and Tyr16 *in vitro*. Glutathione beads containing recombinant GST-PfMCM2 were incubated with recombinant PfCK2 and ^{32}P-ATP for 10min at 37°C; the sample was centrifuged, the pellet resolved on SDS page and the gel exposed to autoradiographic film. **A**: autoradiograph, **B**: Coomassie stain. Lane 1: GST-PfMCM2 wt, 2: GST-PfMCM2_Phe16, 3: GST-PfMCM2_Ala13, 4: GST-PfMCM2_Ala13_Phe16. Results are representative of three independent experiments, GST-PfMCM2 wt and mutants, and ^{32}P-ATP.

mutant lacking both the Ser13 and the Tyr16 residues did not show any detectable phosphorylation. To further support the evidence for PfCK2 driven-PfMCM2Tyr16 phosphorylation, a similar assay was repeated with the PfMCM2_Ala13 mutant and ATP, followed by LC-MS\MS analysis to unambiguously detect the residue involved in the kinase reaction. Data obtained from this analysis showed that the only phospho-peptide detected was the one containing Tyr16 (**Figure 7.12**, **Table 7.2**). Furthermore, from the peptide sequence which did not include any other Ser, Thr or Tyr residue, and from the fragmentation pattern it was also possible to conclude that the observed phosphorylation occurred on the Tyr16 residue.

A

```
  1 MEDKKKLEED LEANKYDIDE EDLLEDEGRL NEEERQAELE GESLFEEDEG
 50 FIFGADDEKK EMQKLRNLGL DNDDYDDDFI DDELDYEDNL KARRAAERHM
100 QMQRKQEGKY EKNKFWKTLE DQLEGDDEEE DIFDKVAEKV AKRRENLHLT
150 AEETDIPDL
```

B
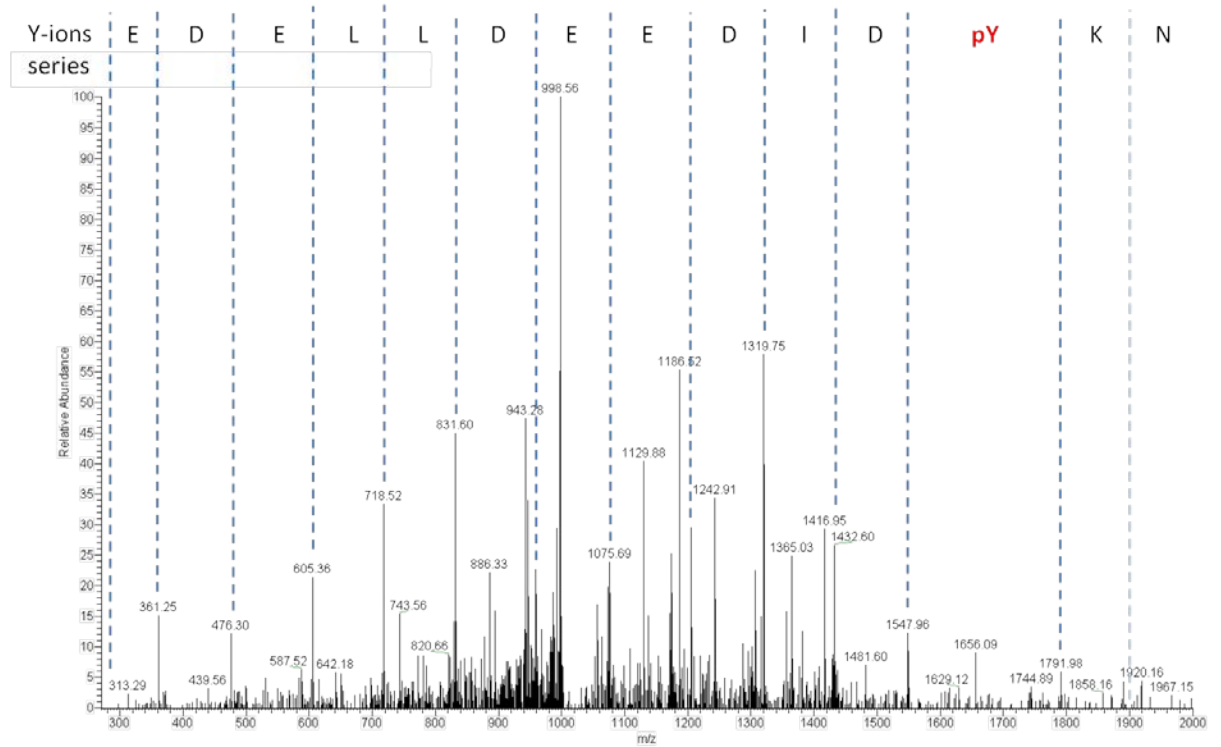
Figure 7.12: LC-MS/MS analysis of PfCK2 *in vitro* kinase assay with PfMCM2_Ala13 mutant. **A:** sequence of PfMCM2 fragment protein showing the phosphopeptide identified in the LC-MS/MS analysis (underlined), top Mascot ion score: 64.5. **B:** LC-MS/MS trace identifying phosphorylation of MCM2 fragment at Y16.

b-ions	sequence	y-ions
129.1	K	2,960.3
242.2	L	2,832.2
371.2	E	2,719.1
500.3	E	2,590.1
615.3	D	2,461.0
728.4	L	2,346.0
857.4	E	**2,232.9**
928.5	A	2,103.9
1,042.5	N	**2,032.8**
1,170.6	K	1,918.8
1,413.6	Y+80	**1,790.7**
1,528.7	D	**1,547.7**
1,641.7	I	**1,432.6**
1,756.8	D	**1,319.6**
1,885.8	E	**1,204.5**
2,014.9	E	**1,075.5**
2,129.9	D	**946.5**
2,243.0	L	**831.4**
2,356.1	L	**718.3**
2,485.1	E	**605.3**
2,600.1	D	**476.2**
2,729.2	E	**361.2**
2,786.2	G	232.1
2,960.3	R	175.1

Table 7.2: Fragmentation table for the identified phosphopeptide (detected b-ions and y-ions are represented respectively in bold red and bold blue).

To further support the evidence for CK2 tyrosine phosphorylation activity, an *in vitro* kinase assay was carried out with recombinant PfCK2, using a heat-inactivated parasite lysate as a substrate in the presence of ATP. The sample, was subsequently analysed by Western Blot with an anti-pTyr antibody, together with a control incubated in the absence of recombinant PfCK2. Interestingly, results showed that the intensity of at least two bands recognised by the antibody increased upon incubation with PfCK2 compared with the control (**Figure 7.13**). Since the intrinsic kinase activity of the

parasite sample was disrupted by the heat inactivation treatment, this result supports

the previous evidence that PfCK2 is able to catalyse tyrosine phosphorylation, at least

in vitro. Hence, these two studies demonstrated that PfCK2, as its two other yeast and

human homologues, can therefore be classified as a true dual specificity kinase.
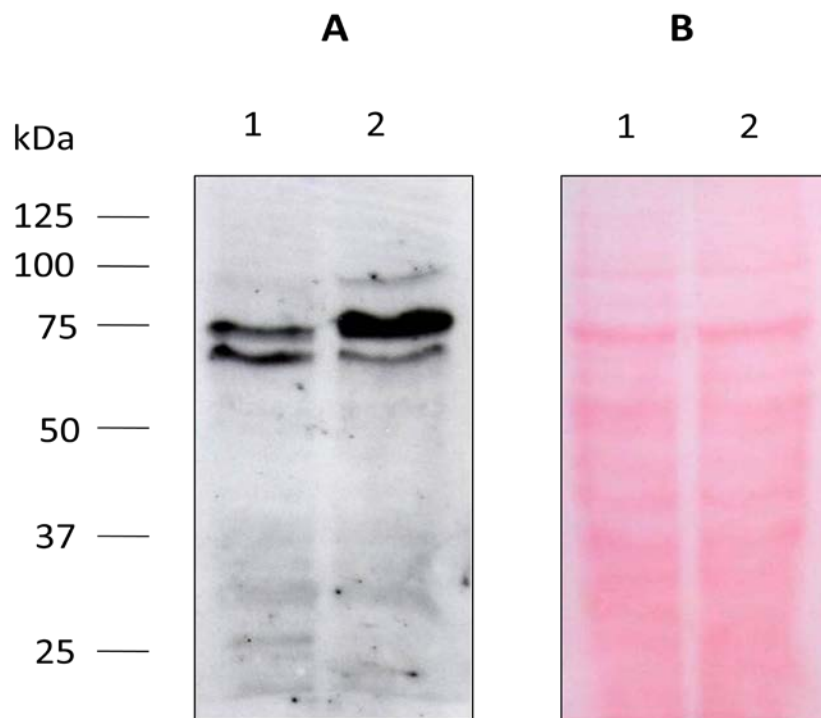
Figure 7.13: PfCK2 catalise tyrosine phosphorylation in a heat inactivated *P. falciparum*

lysate upon *in vitro* incubation with ATP. A *P. falciparum* lysate was heat inactivated at

55°C for 2min and then incubated with glutathione beads containing recombinant

GST-PfCK2 and ATP; the sample was then centrifuged and the supernantant resolved

on a SDS-PAGE followed by immunoblotting with anti phospho-tyrosine antibody. **A**:

Western Blot analysis, **B**: ponceau staining. Lane 1: heat inactivated control + ATP, 2:

heat inactivated control + ATP + GST-PfCK2. Results are representative of three

independent experiments.

7.3 Discussion

Despite the fact that tyrosine phosphorylation is usually a peculiar feature of multicellular organisms, regulating processes that are not found in lower eukaryotes, previous studies have reported the occurrence of this post-traslational modification also in *P. falciparum*.[83, 106, 149] However, although specific tyrosine-phosphorylated proteins have been previously identified, no pTyr pathways have been so far described or characterised. This is partly due to the absence of conserved putative tyrosine kinases in the *P. falciparum* genome.[68] Here we carried out a detailed analysis of pTyr pathways in *P. falciparum* aimed at identifying specific substrates, responsible kinases, cellular localisations and potential roles for pTyr events in the parasite schizont stage. Results overall confirmed previous evidence for the general pTyr occurrence in *P. falciparum*; however, no specific substrate was identified other than the previously detected PfCLK3-Tyr526 phosphorylation. In particular, global analyses were conducted to map tyrosine phosphorylated proteins in *P. falciparum*, by both Western Blot analyses with anti-pTyr antibody, and by using beads coniugated to an anti-pTyr antibody in pull-down assays. The Western Blot analysis confirmed the presence of pTyr proteins in *P. falciparum*, especially within the parasite membrane, supporting the hypothesis that the pTyr activity detected is associated with the parasite and not with the host cell. In the case of the pull down assay, despite the fact that radioactive bands were observed by SDS-PAGE gel in the pulled-down fraction after ^{32}P labeling, no tyrosine phosphorylated proteins were detected by LC-MS\MS in the pulled-down fraction. This lack of observed phosphorylation is most probably due to the low abundance of pTyr-containing proteins in *P. falciparum*, together with the limitations

of the LC-MS\MS technique which requires a certain amount of protein in order to be unambiguously detected. Finally, data supporting the specific PfCLK3-Tyr526 phosphorylation event were also here presented. In fact, with the use of both a structural and a Tyr526-phosphospecific antibody it was possible to confirm the occurrence of this specific tyrosine phosphorylated residue in the schizont stage, further validating the previously reported LC-MS\MS data.[83] Moreover, subsequent analyses conducted in our laboratory using the same antibodies here characterised have demonstrated that this particular event occurs through an autophosphorylation process that is required for full kinase activity. This particular observation is consistent with the fact that PfCLK3 belongs to the DYRK kinase subgroup. In fact, members of this family are serine/threonine kinases of the CMGC kinase group characterized by the formation of an active transient intermediate during translation that is able to catalyse cis-auto-phosphorylation on tyrosine.[162] Therefore, this specific analysis on PfCLK3 provided a mechanism by which tyrosine phosphorylation can occur in *Plasmodium*, even in the absence of a tyrosine kinase family, and have an impact on the biology of the parasite.

The study on the PfMCM2 parasite protein did not confirm the previous LC-MS\MS reports for its Tyr16 phosphorylation.[83] This result can be due to the conditions of the kinase assay, which was carried out *in vitro* with a parasite lysate and only a recombinant fragment of the PfMCM2 substrate. In fact, in these conditions it can be hypothesised that the kinase reaction did not occur because either the chosen fragment was not sufficient for enzyme recognition or because of physiological reasons (e.g. the responsible kinase was inhibited or not activated in the lysate). The second possible explanation is that PfMCM2-Tyr16 phosphorylation does not truly

occur in *P. falciparum* and that the observed LC-MS\MS trace is of ambiguous interpretation. In particular, the consideration that PfMCM2-Tyr16 phosphorylation was only observed once and in a single biological replicate in the global phospho-proteomic study would seem to support this second conclusion. However, the general low abundance of pTyr proteins accounting for no more that 1% of the total phosphoproteome,[161] and the common transient state of protein phosphorylation suggest that detection of pTyr is very difficult to achieve. Furthermore, *in vitro* kinase assays and LC-MS\MS data here presented showed that the parasite kinase PfCK2 is able to phosphorylate PfMCM2 on both Ser13 and Tyr16. This important result demonstrates both that PfMCM2 can be phosphorylated *in vitro* on the same tyrosine residue previously observed *in vivo*, and that PfCK2, despite being a Ser/Thr kinase is also able catalyse tyrosine phosphorylation. Interestingly, this latter feature is conserved also in the *Z. mays* and the *H. sapiens* CK2 homologues. In particular, in human cells it has been also demonstrated that CK2-driven tyrosine phosphorylation occurs *in vivo*, despite the presence of specialised putative tyrosine kinases in the human genome.[92] Moreover, the fact that PfCK2 can act as a dual specificity kinase was further demonstrated here by the *in vitro* kinase assay with a heat inactivated parasite lysate. The Western Blot analysis with an anti-pTyr antibody showed in fact an increase of the pTyr containing proteins upon incubation with PfCK2. In conclusion, the data here presented constitute the first report of a dual specificity kinase in *P. falciparum* which can also constitute an explaination of the reported evidence for tyrosine phosphorylated proteins occurrence in the parasite.

In conclusion, the studies here reported have contributed to describe new important processes in *P. falciparum* such as: Tyr phosphorylation pathways, dual specificity

activity of parasite kinases and the specific PfMCM2 phosphorylation pathway never reported before in the parasite. Therefore, these studies have further advanced our knowledge over the *P. falciparum* biology. Further to this, the fact that some of these pathways are divergent (e.g. the absence of putative members of the tyrosine kinase family), or not conserved (e.g. the PfMCM2-Ser13 phosphorylation) in other eukaryotes and, more specifically in the human host, suggest that such studies could potentially lead to a future development of chemical compounds able to selectively interfere with these biological events.

Chapter 8: Analysis of the Serine 13 phosphorylation pathway in PfMCM2

8.1 Introduction

In the previous chapter it was showed how, during the investigation of the Tyr16 phosphorylation of PfMCM2, Ser13 phosphorylation was efficiently detected in *in vitro* kinase assays using a *P. falciparum* lysate (see section **7.2.3**) and was efficiently phosphorylated *in vitro* by recombinant PfCK2. Such result is in accordance with previous data obtained in the global phosphoproteomic study which reported both sites (Ser13 and Tyr16) to be phosphorylated in the schizont stage of the parasite.[83] As also previously discussed (see section **7.1**), this protein is part of a heterohexameric complex composed of PfMCM2-7 that functions as a helicase, unwinding the DNA duplex during replication.[154] Interestingly, in model eukaryotes it has been showed that MCM2 phosphorylation regulates the removal of the MCM complex from the chromatin triggering for DNA synthesis.[159, 160] In this chapter, we decided to undertake a different approach based on biochemical fractionation followed by LC-MS\MS analysis in order to verify whether PfCK2 is the kinase responsible for PfMCM2 phosphoryaltion in the lysate. In addition to this we also further investigated the PfMCM2-Ser13 phosphorylation pathway by attempting to identify the cellular localisation of the phosphorylated form and possible roles for this post-translational modification (e.g. interaction with chromatin).

8.2 Results

8.2.1 Identification of the kinase responsible for PfMCM2-Ser phosphorylation

In order to identify the kinase responsible for the PfMCM2-Ser13 phosphorylation a parasite lysate was fractionated with ion exchange chromatography and the eluted fractions were tested in *in vitro* kinase assays using ^{32}P-ATP and GST-PfMCM2 wt as a substrate. The active fraction was then selected each time and further fractionated with a different column. The so-purified kinase was finally identified by LC-MS\MS (see **Scheme 8.1**).
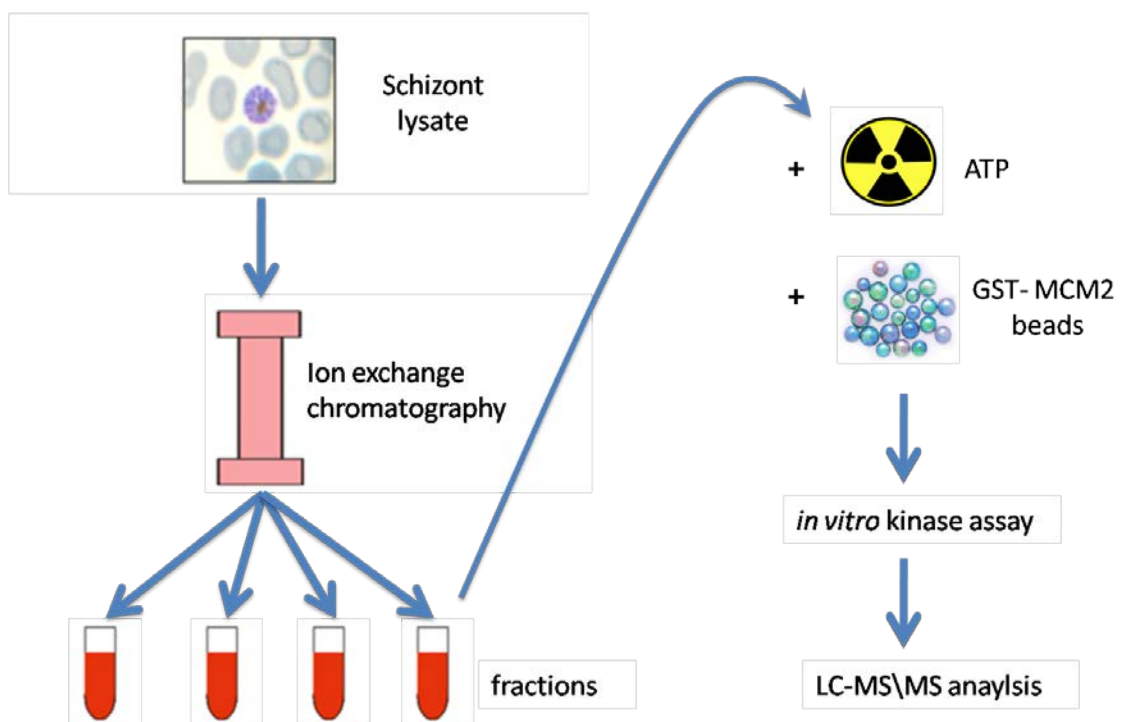
Scheme 8.1: Schematic representation of the proposed approach to identify the kinase responsible for PfMCM2-Ser13 phosphorylation.

As a first attempt, a sample from a batch elution of a parasite lysate using an anion exchange RQ column was tested, together with the corresponding flowthrough. In particular, due to the high salt concentration, the sample from the batch elution was tested before and after dialysis. Results showed that kinase activity against the GST-PfMCM2 wt substrate is both present in the eluted fraction and in the flowhtrough of the column (**Figure 8.1**).
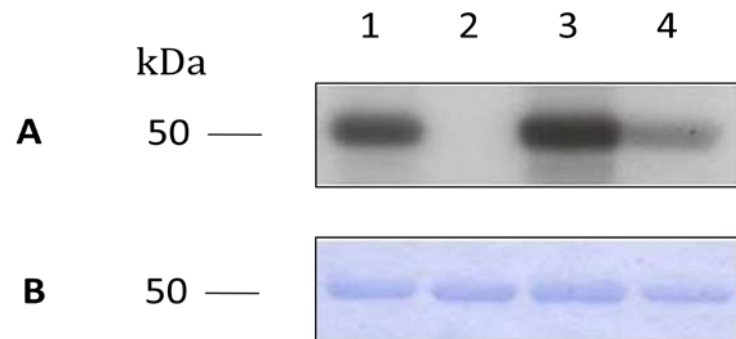
Figure 8.1: *In vitro* kinase assay for PfMCM2-Ser13 phosphorylation with fractions from anion exchange RQ protein chromatography. A *P. falciparum* lysate was purified using an anion exchange RQ column; the obtained fractions were dialysed with a desalting column and incubated with ^{32}P-ATP and glutathione beads containing GST-PfMCM2 wt at 37°C for 10min; samples were centrifuged, pellets resolved on SDS-PAGE and the gel exposed to autoradiographic film. **A**: autoradiograph, **B**: Coomassie stain. Lane 1: *P. falciparum* lysate, 2: batch elution sample before dialysis, 3: batch elution sample after dialysis, 4: flowthrough. Results are representative of three independent experiments.

Moreover, the absence of active phosphorylation with the batch elution sample prior to dialysis indicated that the high salt concentration interfered with the analysis, suppressing the kinase activity. For this reason, during all the following experiments samples eluted from ion exchange columns were always dialysed before the kinase assays. Since kinase activity was recovered in both the eluted and the flowthorugh fractions, both samples were further fractionated using other ion exchange columns and tested in *in vitro* kinase assays with GST-PfMCM2 wt. However, the best results were obtained with the flowthrough fraction. In fact, regarding the RQ eluted sample, after an RQ followed by heparin fractionation it was not possible to further purify the active fraction. None of the attempts carried out with a cation exchange RS column and two columns based on hydrophobic interactions (hydroxyapatite and Blue columns) were successful in detecting any kinase activity neither in the eluted fractions nor in the flowthrough (**Figure 8.2**).
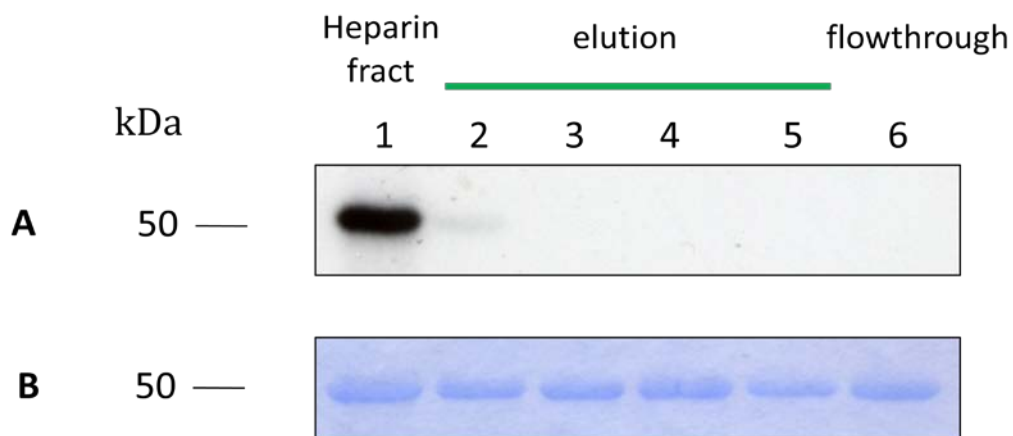
Figure 8.2: *In vitro* kinase assay for PfMCM2-Ser13 phosphorylation with fractions from hydroxyapatite column chromatography. The active fraction against PfMCM2-Ser13 phosphorylation obtained with a heparin column was further purified using a

hydroxyapatite column; the obtained fractions were dialysed with a desalting column and incubated with ^{32}P-ATP and glutathione beads containing GST-PfMCM2 wt at 37°C for 10min; samples were centrifuged, pellets resolved on SDS-PAGE and the gel exposed to autoradiographic film. **A**: autoradiograph, **B**: Coomassie stain. Lane 1: heparin column eluted fraction, 2-5: eluted samples from the hydroxyapatite column, 6: flowthrough.

These observations can be explained by the fact that the kinase activity did not probably bind to the column and was too diluted in the flowhtrough to efficiently phosphorylate the GST-PfMCM2 wt substrate in the subsequent *in vitro* kinase assay. Despite of this, the main active fraction eluted from the heparin column was analysed anyway by LC-MS\MS in order to detect any putative kinase present in the sample and potentially responsible for the observed *in vitro* PfMCM2 wt phosphorylation. In particular, such analysis showed the presence of only two putative parasite protein kinases: PfCK1 (**Figure 8.3**) and PfPKA (**Figure 8.4**) together with the human protein kinase CK1 (**Figure 8.5**).

On the basis of these results, it was not possible to unambiguously determine which of the three different kinases was responsible for the observed phosphorylation reaction. However, the fact that many more peptides for PfCK1 were recognized in the LC-MS\MS (16 compared to 8 and 5 respectively for PfPKA and human CK1) could potentially represent the fact that PfCK1 was the kinase present in the largest amount in the sample.

A

```
  1 MEIRVANKYA LGKKLGSGSF GDIYVAKDIV TMEEFAVKLE STRSKHPQLL
 51 YESKLYKILG GGIGVPKVYW YGIEGDFTIM VLDLLGPSLE DLFTLCNRKF
101 SLKTVLMTAD QMLNRIEYVH SKNFIHRDIK PDNFLIGRGK KVTLIHIIDF
151 GLAKKYRDSR SHTHIPYKEG KNLTGTARYA SINTHLGIEQ SRRDDIEALG
201 YVLMYFLRGS LPWQGLKAIS KKDKYDKIME KKISTSVEVL CRNASFEFVT
251 YLNYCRSLRF EDRPDYTYLR RLLKDLFIRE GFTYDFLFDW TCVYASEKDK
301 KKMLENKNRF DQTADQEGRD QRNN
```

B

Sequence	Mascot Ion score	Sequence position
KLGSGSFGDIYVAK	65.77	14-17
LGSGSFGDIYVAK	83.79	15-27
DIVTMEEFAVK	45.63	28-38
HPQLLYESK	43.06	46-54
ILGGGIGVPK	49.68	58-67
TVLmTADQMLNR	65.03	104-115
DIKPDNFLIGR	41.39	128-138
KVTLIHIIDFGLAK	42.15	141-154
VTLIHIIDFGLAK	63.06	142-154
SHTHIPYK	39.04	161-168
YASINTHLGIEQSR	74.45	179-192
GSLPWQGLK	36.11	209-217
KISTSVEVLcR	62.92	232-242
ISTSVEVLcR	48.95	233-242
FEDRPDYTYLR	29.57	260-270
FDQTADQEGR	64.3	310-319

Figure 8.3: Identification by LC-MS\MS of *P. falciparum* CK1 in the purified fraction from heparin column (after RQ fractionation) active against PfMCM2 in *in vitro* kinase assay. **A:** protein sequence showing the identified peptide in the LC-MS\MS run in blue bold (sequence coverage: 44%). **B:** list of the 16 unique peptides recovered by LC-MS/MS reported with their relative Mascot Ion score and the position in the protein sequence.

A

```
  1 MQFIKNLQLN KKKDSDSSEQ VLTNKKNKMK YEDFNFIRTL GTGSFGRVIL
 51 ATYKNGNYPP VAIKRFEKCK IIRQKQVDHV FSERKILNYI NHPFCVNLHG
101 SFKDDSYLYL VLEFVIGGEF FTFLRRNKRF PNDVGCFYAA QIVLIFEYLQ
151 SLNIVYRDLK PENLLLDKDG FIKMTDFGFA KIVETRTYTL CGTPEYIAPE
201 ILLNVGHGKA ADWWTLGIFI YEILVGCPPF YANEPLLIYQ KILEGIIYFP
251 KFLDNNCKHL MKKLLSHDLT KRYGNLKKGA QNVKEHPWFS NIDWVNLLNK
301 NVEVPYKPKY KNIFDSSNFE RVQEDLTIAD KITNENDPFY DW
```

B

Sequence	Mascot Ion score	Sequence position
DSDSSEQVLTNK	74.74	14-25
VILATYK	21.63	48-54
qVDHVFSER	24	76-84
DLKPENLLLDKDGFIK	17.72	158-173
TYtLcGTPEYIAPEILLNVGHGK	36.48	187-209
ILEGIIYFPK	53.53	242-251
EHPWFSNIDWVNLLNK	29.45	285-300
NIFDSSNFER	33.02	312-321

Figure 8.4: Identification by LC-MS\MS of *P. falciparum* PKA in the purified fraction from heparin column (after RQ fractionation) active against PfMCM2 in *in vitro* kinase assay. **A:** protein sequence showing the identified peptide in the LC-MS\MS run in blue bold (sequence coverage: 30%). **B:** list of the 8 unique peptides recovered by LC-MS/MS reported with their relative Mascot Ion score and the position in the protein sequence.

This, together with the observation that PfMCM2 Ser13 is contained within a consensus sequence for CK1 enzymes with notably an acidic residue at the position n-3[163] strongly suggest that PfCK1 is the kinase responsible for PfMCM2 Ser 13 phosphorylation.

A

```
  1 MASSSGSKAE FIVGGKYKLV RKIGSGSFGD IYLAINITNG EEVAVKLESQ
 51 KARHPQLLYE SKLYKILQGG VGIPHIRWYG QEKDYNVLVM DLLGPSLEDL
101 FNFCSRRFTM KTVLMLADQM ISRIEYVHTK NFIHRDIKPD NFLMGIGRHC
151 NKLFLIDFGL AKKYRDNRTR QHIPYREDKN LTGTARYASI NAHLGIEQSR
201 RDDMESLGYV LMYFNRTSLP WQGLKAATKK QKYEKISEKK MSTPVEVLCK
251 GFPAEFAMYL NYCRGLRFEE APDYMYLRQL FRILFRTLNH QYDYTFDWTM
301 LKQKAAQQAA SSSGQGQQAQ TPTGKQTDKT KSNMKGF
```

B

Sequence	Mascot Ion score	Sequence position
TVLMLADQMISR	59.3	112-123
LFLIDFGLAK	46.96	153-162
RDDMESLGYVLMYFNR	30.23	201-216
GFPAEFAMYLNYcR	32.1	251-264
AAQQAASSSGQGQQAQTPTGK	81.68	305-325

Figure 8.5: Identification by LC-MS\MS of the *H. sapiens* CK1 α isoform protein in the purified fraction from heparin column (after RQ fractionation) active against PfMCM2 in *in vitro* kinase assay. **A:** protein sequence showing the identified peptide in the LC-MS\MS run in blue bold (sequence coverage: 22%). **B:** list of the 5 unique peptides recovered by LC-MS/MS reported with their relative Mascot Ion score and the position in the protein sequence.

Regarding the flowthrough from the RQ column, the sample was further fractionated using first a cation exchange RS column and fractions tested again in *in vitro* kinase assays for GST-PfMCM2 wt phosphorylation. Results using a gradient of 0M to 0.5M NaCl over 10min showed that the kinase activity was concentrated mainly in one fraction (**Figure 8.6**).
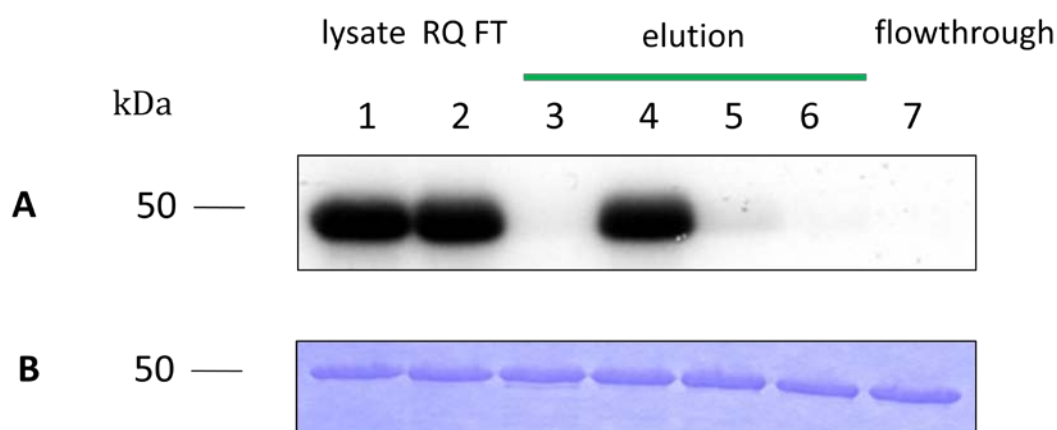
Figure 8.6: *In vitro* kinase assay for PfMCM2-Ser13 phosphorylation with fractions from RS column chromatography. The flowthorugh from RQ column of a *P. falciparum* lysate was further purified using a cation exchange RS column; the obtained fractions were dialysed with a desalting column and incubated with ^{32}P-ATP and glutathione beads containing GST-PfMCM2 wt at 37°C for 10min; samples were centrifuged, pellets resolved on SDS-PAGE and the gel exposed to autoradiographic film. **A**: autoradiograph, **B**: Coomassie stain. Lane 1: *P. falciparum* lysate, 2-8: eluted samples from the RS column, 9: flowthrough.

This fraction was then further purified using a heparin column with the same gradient previously used. Results for the *in vitro* kinase assay showed that also in this case the kinase activity was mainly detected in a single fraction (**Figure 8.7**). At this point, the purified fraction was analysed by LC-MS\MS in order to identify putative kinases present in the sample. In particular, such analysis showed the presence of only a single parasite protein kinase: PfCK1 (**Figure 8.8**) confirming the previous data obtained with the RQ-bound fraction further purified with heparin column (**Figure 8.3**).
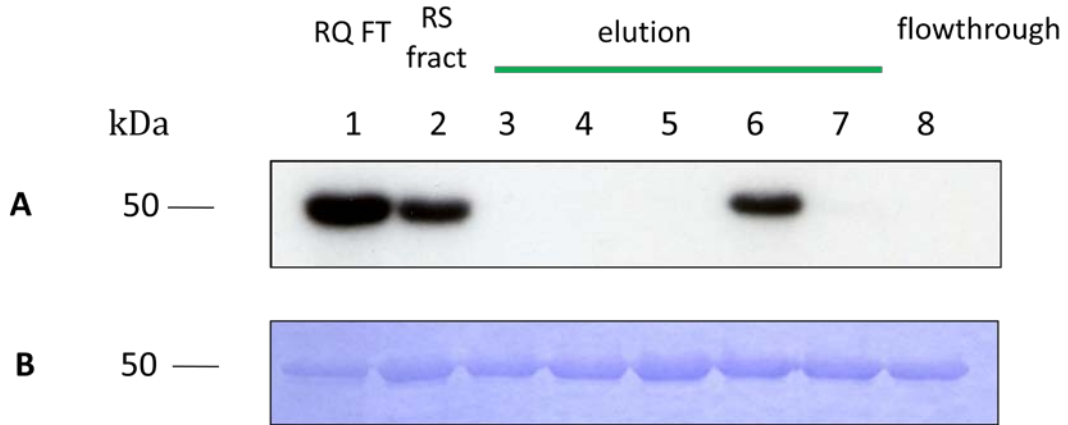
Figure 8.7: *In vitro* kinase assay for PfMCM2-Ser13 phosphorylation with fractions from heparin column chromatography. The active fraction eluted from the cation RS column of a *P. falciparum* lysate was further purified using a heparin column; the obtained fractions were dialysed with a desalting column and incubated with ^{32}P-ATP and glutathione beads containing GST-PfMCM2 wt at 37°C for 10min; samples were centrifuged, pellets resolved on SDS-PAGE and the gel exposed to autoradiographic film. **A**: autoradiograph, **B**: Coomassie stain. Lane 1: *P. falciparum* lysate, 2-8: eluted samples from the heparin column, 9: flowthrough.

Moreover, no human protein kinase was detected nor PfPKA. Such result, consistent with the previous observations, strongly support the hypothesis that PfCK1 is the kinase responsible for the PFMCM2 Ser13 phosphorylation, at least *in vitro*. To further demonstrate such hypothesis, *in vitro* kinase assays were attempted also with bacterial expressed PfCK1 (see section **8.2.2**) together with inhibition studies with the CK1 specific inhibitor D4476 (see section **8.2.3**).

A

```
  1 MEIRVANKYA LGKKLGSGSF GDIYVAKDIV TMEEFAVKLE STRSKHPQLL
 51 YESKLYKILG GGIGVPKVYW YGIEGDFTIM VLDLLGPSLE DLFTLCNRKF
101 SLKTVLMTAD QMLNRIEYVH SKNFIHRDIK PDNFLIGRGK KVTLIHIIDF
151 GLAKKYRDSR SHTHIPYKEG KNLTGTARYA SINTHLGIEQ SRRDDIEALG
201 YVLMYFLRGS LPWQGLKAIS KKDKYDKIME KKISTSVEVL CRNASFEFVT
251 YLNYCRSLRF EDRPDYTYLR RLLKDLFIRE GFTYDFLFDW TCVYASEKDK
301 KKMLENKNRF DQTADQEGRD QRNN
```

B

Sequence	Mascot Ion score	Sequence position
KLGSGSFGDIYVAK	32.66	14-27
LGSGSFGDIYVAK	72.24	15-27
SKHPQLLYESK	52.57	44-54
TVLmTADQMLNR	66.14	104-115
KVTLIHIIDFGLAK	27.14	141-154
VTLIHIIDFGLAK	32.99	142-154
SHTHIPYK	27.87	161-168
YASINTHLGIEQSR	25.53	179-192
RDDIEALGYVLmYFLR	28.37	193-208
FEDRPDYTYLR	45.66	260-270
NRFDQTADQEGR	40.85	308-319
FDQTADQEGR	39.64	310-319

Figure 8.8: Identification by LC-MS\MS of *P. falciparum* CK1 in the purified fraction from heparin column (after RQ flowthrough and RS fractionation) active against PfMCM2 in *in vitro* kinase assay. **A:** protein sequence showing the identified peptide in the Lc-MS\MS run in blue bold (sequence coverage: 35%). **B:** list of the 12 unique peptides recovered by LC-MS/MS reported with their relative Mascot Ion score and the position in the protein sequence.

8.2.2 GST-PfCK1 bacterial expression

In order to insert the coding region for PfCK1 into a pGEX plasmid vector for GST tag bacterial protein expression, the PfCK1 gene was first amplified from a *P. falciparum*

cDNA library. In particular, due to the natural presence of an EcoRI site into the PfCK1 coding region, primers were designed to present BamHI recognition sites at both ends of the PCR product. The amplified product were also run on a 1% agarose gel in order to verify their correct size of ~1kb (**Figure 8.9**).
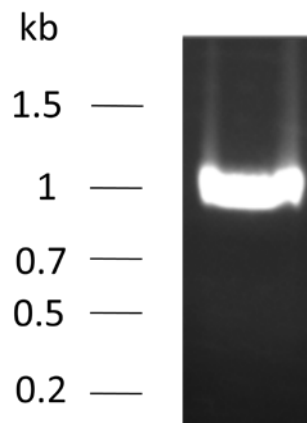
Figure 8.9: 1% agarose gel showing the product of the amplification reaction of the PfCK1 gene from a *P. falciparum* cDNA library.

After that, the amplified gene for the GST-fusion protein expression was inserted into a pGEX vector and the plasmid transfected into supercompetent cells. Ten colonies were then selected from this experiment and the plasmid extracted, digested with BamHI restriction enzyme and analysed by agarose gel to check for the correct insertion. Results showed that out of ten colonies, only five contained an insertion into the coding region of the plasmid (**Figure 8.10**). DNA sequencing analysis confirmed that out of these seven colonies only one contained the PfCK1 insertion gene in the correct orientation. The so-obtained pGEX plasmid vector was transfected into *E. coli* competent cells and the protein product purified.
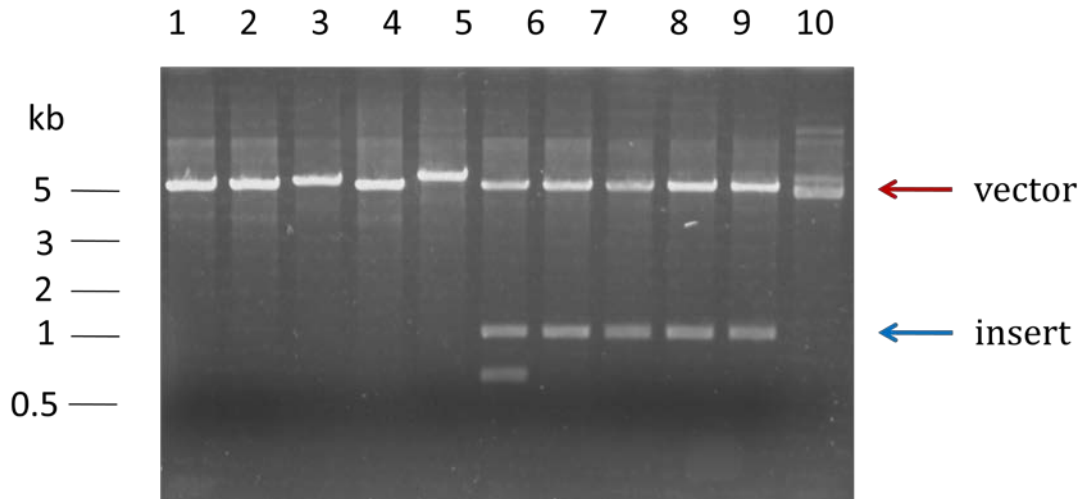
Figure 8.10: : BamHI digestion of pGEX-2T plasmids encoding for GST-PfCK1 protein expression. Plasmids were extracted from 10 selected colonies after transfection in *E. coli* supercompetent cells.

Unfortunately, in this case the recombinant protein was mainly observed in the membrane insoluble fraction and only a very small portion was purified and recovered from the affinity column purification (**Figure 8.11**). Despite the low expression and purification efficiency, the purified GST-PfCK1 was tested in *in vitro* kinase assays with ^{32}P-ATP and β-casein or PFMCM2 wt as a substrate. Results showed that the recombinant protein was not active in the conditions of the analysis with both substrates (**Figure 8.12**). The most likely explanation for this result lies in the fact that the recombinant protein was not recovered in the active conformation and therefore did not exhibit any detectable kinase activity. Such conclusion is also consistent with the fact that the recombinant protein was mostly observed in the insoluble fraction after protein expression, probably entrapped in inclusion bodies.
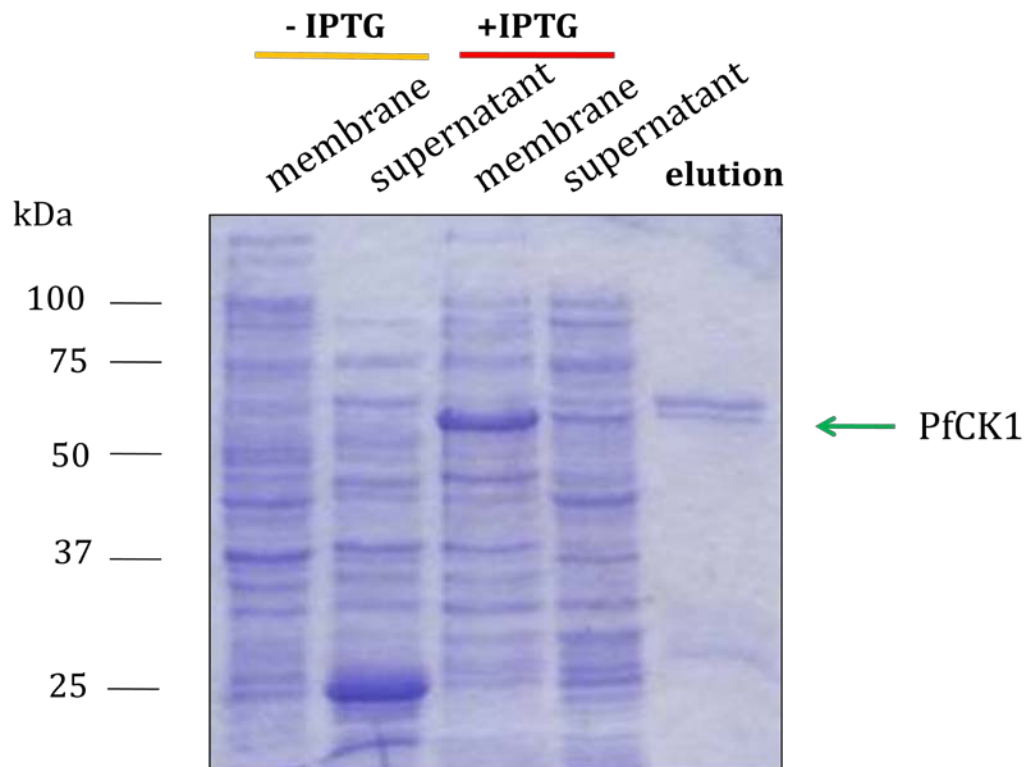
Figure 8.11: GST-PfCK1 expression and purification profile from transfected *E. coli* competent cells. GST-PfCK1 was expressed in transfected *E. coli* competent cells upon induction with 20mM IPTG at 22°C for 4hrs; cell cultures were spun down, lysed and purified on glutathione beads. The membrane and supernatant content before and after induction together with the purified sample were resolved on SDS-PAGE (Comassie stain).

Hence, in this scenario, the negative result for the PfMCM2 wt phosphorylation by recombinant PfCK1 cannot overrule previous evidence for the occurrence of this pathway, at least *in vitro*.
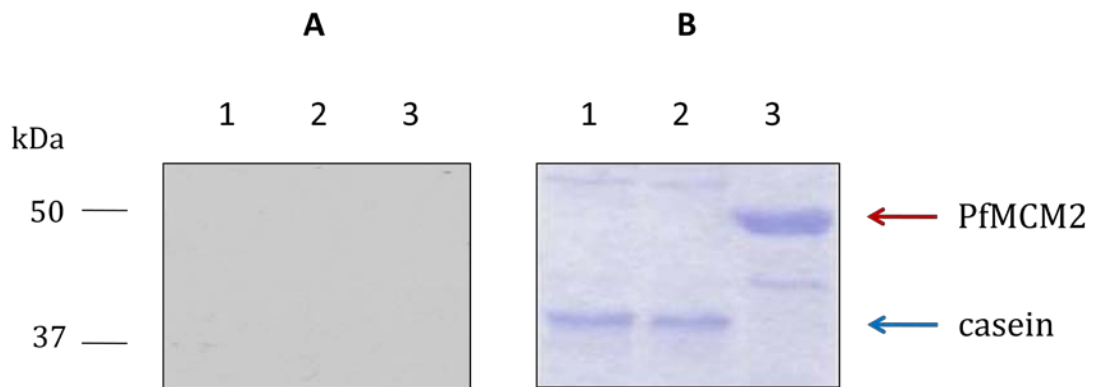
Figure 8.12: Investigation of recombinant GST-PfCK1 *in vitro* kinase activity against PfMCM2 and casein. Recombinant PfCK1 was incubtated with casein or PfMCM2 and ^{32}P-ATP for 10min at 37°C; proteins were resolved on SDS-PAGE and the gel exposed to autoradiographic film. **A**: autoradiograph, **B**: Coomassie stain. Lane 1: casein control, 2: GST-PfCK1+ β-casein, 3: GST-PfCK1+GST-PfMCM2 wt. Results are representative of three independent experiments.

8.2.3 PfCK1 *in vitro* and *in vivo* inhibition study

Since *in vitro* kinase assays with recombinant PfCK1 were not successful, a different route to further validate the detected PfCK1-PfMCM2 phosphorylation pathway, based on PfCK1 inhibition was undertaken. A previous characterization study of PfCK1 showed that the enzyme was inhibited by compound CK1-7 in an essentially similar fashion to the rat homologous enzyme.[78] On the basis of such evidence, it was then decided to test D4476, the commercially available most potent and selective CK1 inhibitor, in both *in vitro* and *in vivo* kinase tests. First of all, the compound was tested in *in vitro* assays with a parasite lysate and also with the purified CK1 fraction from the tandem RQ, RS and heparin fractionation (see section **7.2.1**), together with GST-

PfMCM2 wt and ^{32}P-ATP. In particular, since no data regarding the sensitivity of PfCK1 against D4476 was available, it was decided to test the compound in the same concentration range as previously reported for *H. sapiens* and *S. pombe* CK1.[164] Interestingly, results showed that the compound was active against the lysate and the purified CK1 fraction in the same range of concentrations used for selective *H. sapiens* and *S. pombe* CK1 inhibition (**Figure 8.13**).
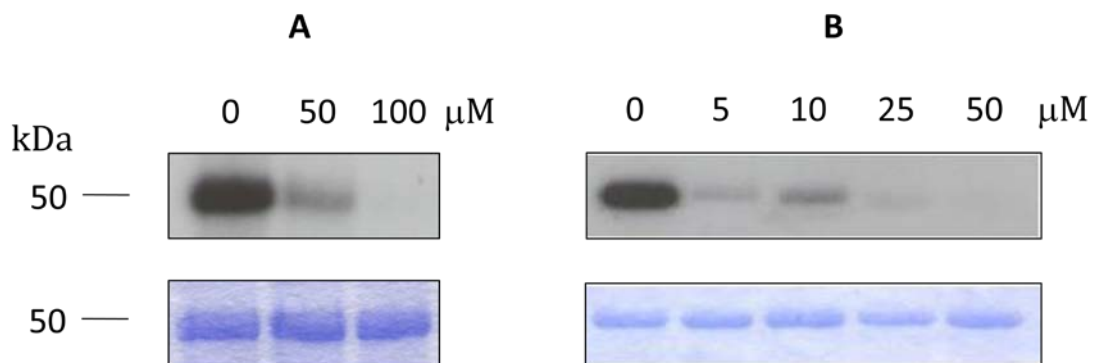
Figure 8.13: Inhibition of PfMCM2-Ser13 phosphorylation by the CK1 specific inhibitor D4476. Glutathione beads containing recombinant GST-PfMCM2were incubated with either a *P. falciparum* lysate or a PfCK1 purified fraction ^{32}P-ATP and D4476 at the indicated concetrations for 10min at 37°C; samples were centrifuged, pellets resolved on SDS-PAGE and the gel was exposed to autoradiographic film. **A**: Pf lysate, **B**: PfCK1 purified fraction. Top panel: autoradiograph, bottom panel: Coomassie stain; inhibitor concentrations are indicated above. Results are representative of three independent experiments.

In particular, in the case of the parasite lysate, kinase activity was completely suppressed at the lowest tested concentration of 50μM D4476, while for the purified CK1 fraction the IC_{50} was in the range between 0.1 and 1μM. Afterwards, a similar *in vitro* inhibition assay was repeated for both a parasite lysate and the purified CK1 fraction in the presence of ATP. However, this time the samples were analysed with a phospho-specific antibody against PfMCM2-Ser13 phosphorylation and PfMCM2. Results overall confirmed previous observations and showed a very similar pattern of inhibition (**Figure 8.14**). In particular, the observation that the IC_{50} for the purified CK1 fraction fell in the range between 0.5 and 5μM D4476 is consistent with the reported IC_{50} value of 0.63μM for human CK1[164] and further confirms the tested hypothesis that PfCK1 is the kinase responsible for PfMCM2-Ser13 phosphorylation in the purified fraction.
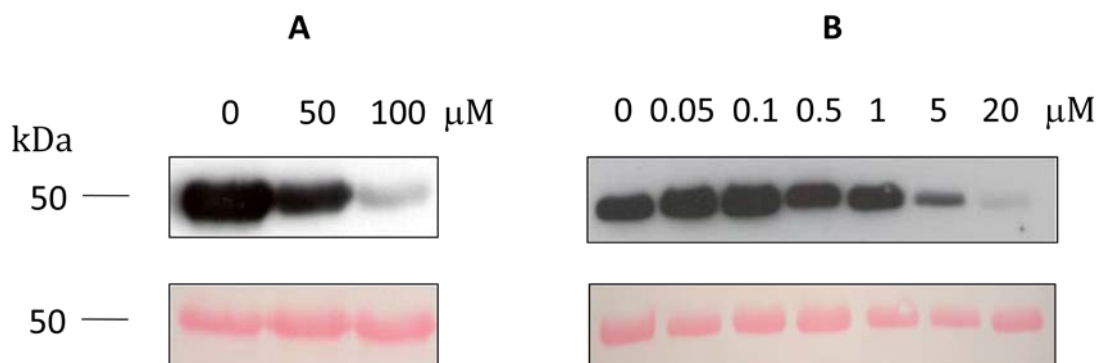
Figure 8.14: Inhibition of PfMCM2-Ser13 phosphorylation by the CK1 specific inhibitor D4476, Western Blot analysis. Glutathione beads containing recombinant GST-PfMCM2were incubated with either a *P. falciparum* lysate or a PfCK1 purified fraction, ^{32}P-ATP and D4476 at the indicated concetrations for 10min at 37°C; samples were centrifuged, pellets resolved on SDS-PAGE and immunoblotted using a PfMCM2-Ser13

phospho-specific antibody. **A**: Pf lysate, **B**: PfCK1 purified fraction. Top panel: Western Blot, bottom panel: Ponceau staining; inhibitor concentrations are indicated above.

The same compound was also tested *in vivo* by incubation with *P. falciparum* culture for 30min in physiological conditions, followed by cell lysis and Western Blot analysis with both the PfMCM2-Ser13 phospho-specific and PfMCM2 structural antibody. Results showed that the compound was not active *in vivo* and that the phosphorylation state of PfMCM2 did not change in the presence of 50 or 100µM D4476 (**Figure 8.15**). Due to the previously demonstrated activity of the compound in the *in vitro* assays in the same range of concentrations, such evidence can be explained by the likely low permeability of the compound in either the RBC or the parasite membrane.
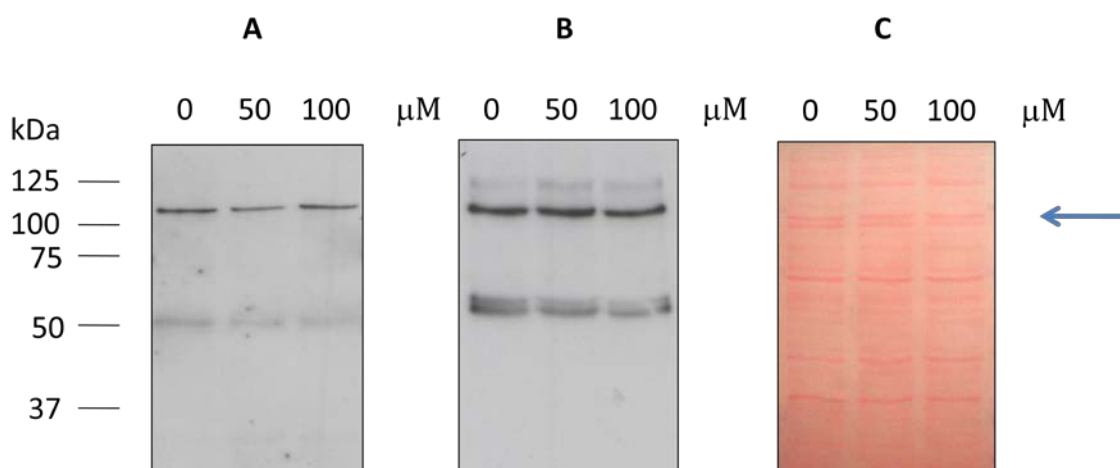
Figure 8.15: *In vivo* inhibition of PfMCM2-Ser13 phosphorylation by the CK1 specific inhibitor D4476. iRBCs were incubated with D4476 at the indicated concentrations for 30min and then lysed; proteins were resolved on SDS-PAGE and immunoblotted using

bot a PfMCM2 antibody and a PfMCM2-Ser13 phosphospecific antibody. **A:** PfMCM2 antibody, **B:** PfMCM2-pSer13 phosphospecific antibody, **C:** Ponceau staining; inhibitor concentrations are indicated above the panel, the arrow indicates the position of PfMCM2 in the gel. Results are representative of three independent experiments.

8.2.4 Analysis of the localisation and expression of PfMCM2 during the intra-erythrocytic cell cycle

In order to further characterise the PfMCM2 protein and to identify the pattern of PfMCM2-Ser13 phosphorylation during the parasite intra-erythrocytic cycle, parasite lysates from different stages were run on a SDS-PAGE gel and analysed by Western Blot using both the PfMCM2-Ser13 phospho-specific and PfMCM2 structural antibody. Results showed that the PfMCM2 protein expression levels peak at the schizont and trophozoite stages but drop quickly at the ring stage (**Figure 8.16**).
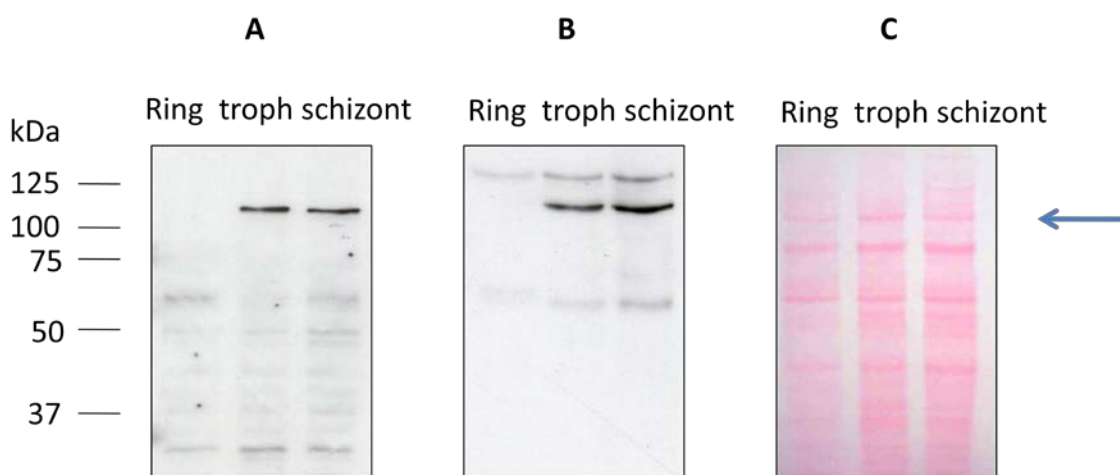
Figure 8.16: Western Blot analysis of a *P. falciparum* lysate from three different intra-erythorcitic stages: ring, trophozoite (troph) and schizont with two PfMCM2

antibodies. Protein content from iRBCs at three different stages were resolved on SDS-PAGE and immunoblotted with two PfMCM2 antibodies. **A:** PfMCM2 antibody, **B:** PfMCM2-pSer13 phosphospecific antibody, **C:** Ponceau staining; the arrow indicates the position of PfMCM2 in the gel. Results are representative of three independent experiments.

Such observations are consistent with previously reported data showing overall a similar expression profile for PFMCM2 and two other components of the parasite helicase complex: PfMCM6 and 7.[156] Interestingly, results with the phospho-specific antibody demonstrated that PfMCM2-Ser13 phosphorylation followed the same pattern as the protein expression, peaking at the schizont and trophozoite stages but drastically disappearing at the ring stage (**Figure 8.16**). Altogether these data support the conclusion that Ser13 phosphorylation is PfMCM2-constitutive and does not fluctuate during the parasite intra-erythrocytic life cycle modulating the protein function. However, to further investigate the role of PfMCM2-Ser phosphorylation and in particular its intracellular localization, the two phospho-specific and structural antibodies were also tested in immunocytochemistry analyses with parasite samples from the three main different stages: ring, trophozoite and schizont. As expected, results from the ring stage analysis (**Figure 8.17**) did not detect the occurrence of any PfMCM2 protein or phosphorylated forms, as previously showed also in the Western Blot analysis (**Figure 8.16**).
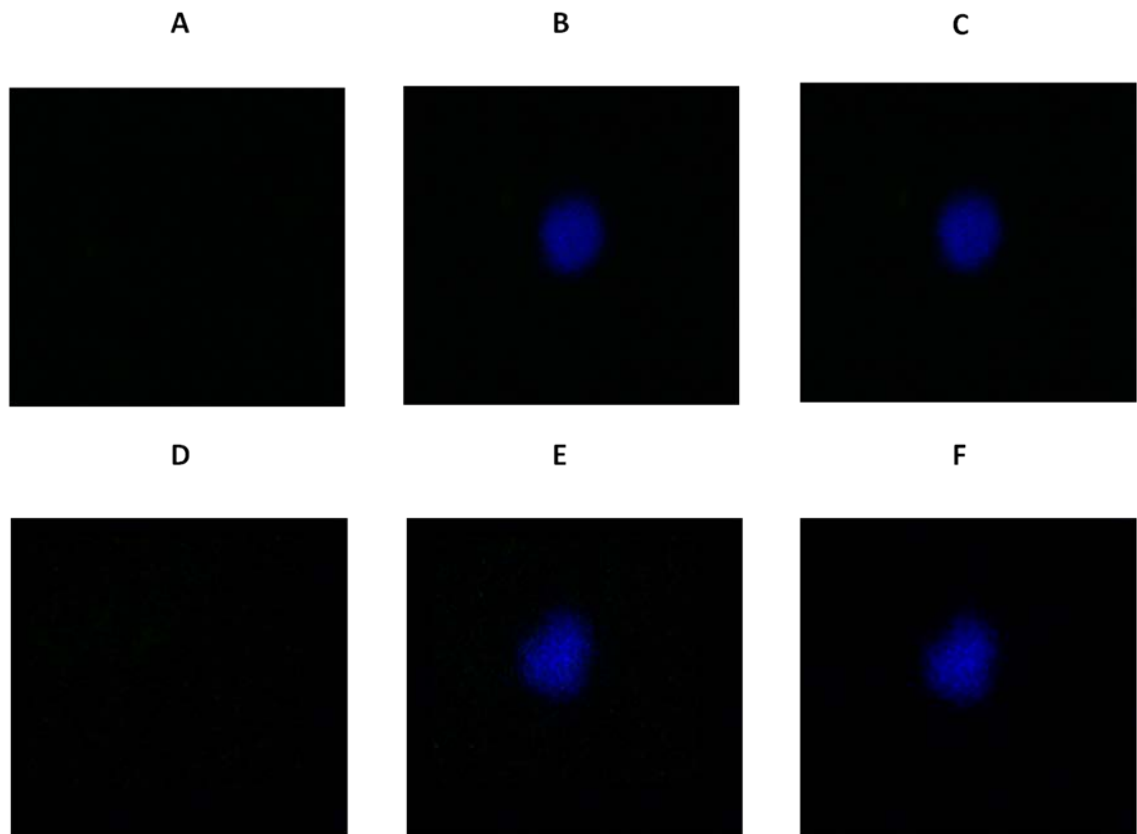
Figure 8.17: Immunolabeling of ring stage parasites with the PfMCM2 structural and PfMCM2-pSer13 phospho-specific antibody. **A:** PfMCM2 structural antibody, **B:** DAPI, **C:** merging of **A** and **B**, **D:** PfMCM2-pSer13 phospho-specific antibody, **E:** DAPI, **F:** merging of **D** and **E**.

Regarding the two other stages were PfMCM2 was previously showed to occur, results overall detected a general co-localization of the phosphorylated form with the PfMCM2 protein detected by the structural antibody (**Figure 8.18**, **8.19**).
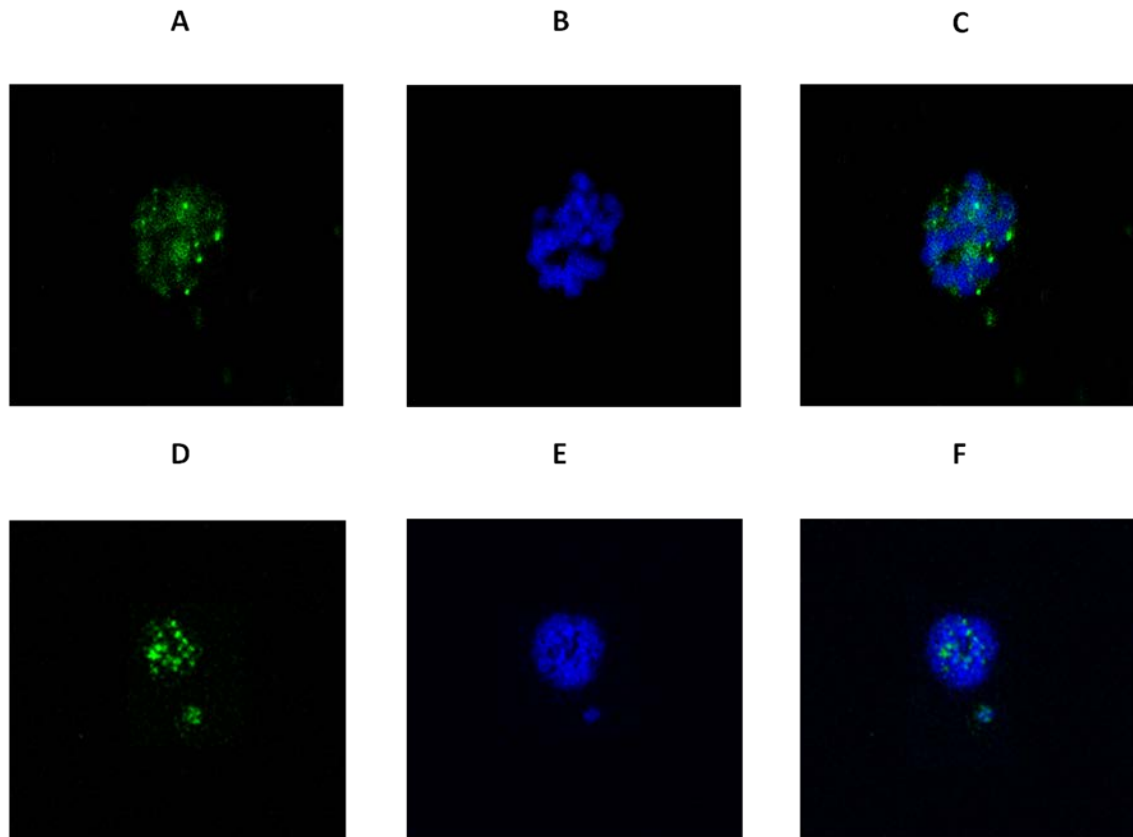
Figure 8.18: Immunolabeling of trophozoite stage parasites with the PfMCM2 structural and PfMCM2-pSer13 phospho-specific antibody. **A:** PfMCM2 structural antibody, **B:** DAPI, **C:** merging of **A** and **B**, **D:** PfMCM2-pSer13 phospho-specific antibody, **E:** DAPI, **F:** merging of **D** and **E**.

In particular, both proteins were characterized by a cytosolic rather than a nuclear localization. Surprisingly, no selective localization or sub-pools were detected for the phosphorylated form in the any of the analysed samples. Such evidence, in contrast with the functional role of the protein in the helicase complex which would require a nuclear localization, can be explained by the fact that this localization is likely to be only transient and that it was probably not successfully isolated in this specific analysis.
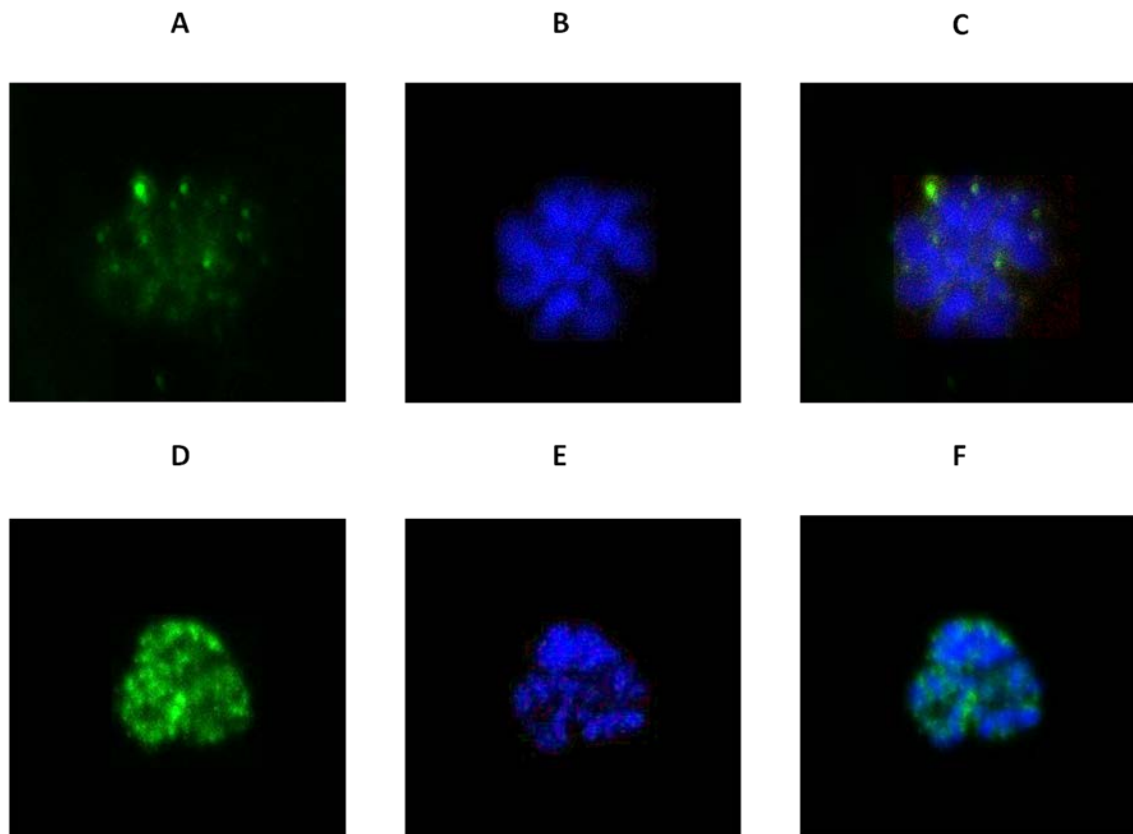
Figure 8.19: Immunolabeling of schizont stage parasites with the PfMCM2 structural and PfMCM2-pSer13 phospho-specific antibody. **A:** PfMCM2 structural antibody, **B:** DAPI, **C:** merging of **A** and **B**, **D:** PfMCM2-pSer13 phospho-specific antibody, **E:** DAPI, **F:** merging of **D** and **E**.

8.3 Discussion

During the study on PfMCM2 tyrosine phosphorylation, PfMCM2-Ser13 phosphorylation was also detected, confirming previous LC-MS\MS data.[83] In the same study PfCK2 was identified as a kinase able to phosphorylate both the Ser and the Tyr residues in vitro (see section **7.2.4**). In order to verify whether PfCK2 is also able to phosphorylate PfMCM2 on Ser13 in the parasite lysate we a different approach was

undertook based on a biochemical fractionation of a parasite lysate followed by *in vitro* kinase tests and LC-MS\MS analysis. With this particular approach PfCK1 was determined as the only kinase present in the purified active fraction. Therefore, this result did not confirm previous *in vitro* kinase assays showing that recombinant PfCK2 can efficiently phosphorylate PfMCM2 on Ser13 *in vitro* (see section **7.2.4**). Such discrepancy could be partly explained by the more complex nature of the lysate sample which may inhibit or alter the activity of PfCK2 against the PfMCM2 substrate. In addition to this, the observation that PfCK1 is the kinase responsible for PfMCM2 Ser13 phosphorylation using a lysate was further supported with the use of a CK1 specific inhibitor in *in vitro* tests. In particular, despite the fact that the compound was also a human CK1 kinase inhibitor lacking therefore absolute specificity, this evidence demonstrates once again that parasite phosphorylation pathways can be targeted with small molecular probes and constitute therefore an opportunity for the development of new antimalarial compounds. Further analyses showed also that this specific phosphorylation event occurs in both the trophozoite and schizont stage but not in rings. Interestingly, this phosphorylation pattern matches the expression levels of PfMCM2 suggesting that the Ser13 phosphorylation is protein-constitutive rather than dynamic. However, the intrinsic transient nature of protein phosphorylation does not exclude that un-phosphorylated PfMCM2 is present in trophozoites and schizonts but its quick turnover hampers experimental isolation and detection. The same is also true for the experiments regarding the protein localisation. Immunocytochemistry analyses showed in fact a co-localization of both PfMCM2 and PfMCM2-pSer13 in the cytosolic compartment. Such result is surprising since the PFMCM2 protein is thought to be part of the helicase complex which would therefore involve a nuclear

localisation. However, as stated above, given the dynamic nature of protein phosphorylation it can be argued that it was not possible to isolate experimentally the un-phosphorylated form of PfMCM2 in the immunocytochemistry analysis. Nevertheless, this study on PfMCM2-Ser13 phosphorylation successfully described a parasite-specific phosphorylation pathway previously identified in the global phospho-proteomic analysis; identifying in particular the responsible kinase, the protein localisation and a compound that selectively inhibits this event. Such study therefore constitute an example of how biological techniques can be applied to the identified list of phosphorylation sites in *P. falciparum* in order to both improve our understanding over the complex nature of phosphorylation pathways in the parasite and guide the development of molecular probes able to selectively target such events.

Chapter 9: General discussion and future perspectives

9.1 General summary of results and conclusions

The main aim of this thesis was to study phosphorylation pathways in *Plasmodium falciparum*, the protozoa organism responsible for the most virulent form of malaria in humans. In particular, the studies conducted were focused to progress our understanding of the basic biology of the organism, as well as to further strengthen the role that targeting protein phosphorylation could potentially play in the design of the next generation of antimalarials. To this aim, two major studies were conducted analysing different aspects of protein phosphorylation in *P. falciparum*. Interestingly, both areas of research have registered important and un-expected discoveries that have advanced our knowledge of the *P. falciparum* biology and that can also lead future drug-development based projects.

In the first study, the role and functioning of the specific PfCK2 protein kinase was investigated. This is in fact an essential *P. falciparum* kinase that is both crucial for the parasite survival and thought to be a promising drug target.[71] In spite of this, no putative substrates or mechanisms of action *in vivo* and *in vitro* have been reported so far in the literature. Therefore, in the first two chapters we described the attempts undertaken to develop two novel techniques able to detect and identify PfCK2 substrates in a *P. falciparum* lysate. In particular, the first technique was based on the

acceptance by CK2 enzymes of γ-phosphate modified ATP analogues bearing substituent groups that enable labelling and identification of the CK2-driven phosphorylated proteins. Unfortunately, despite the fact that both the ATP analogues and the recombinant PfCK2 were efficiently obtained in the laboratory, the designed approach was not overall successful due to the lack of stability of such analogues in the acidic conditions required by the analysis (e.g. HPLC buffers, MALDI matrixes etc.). The second approach was based instead on an *in vitro* kinase assay carried out with recombinant PfCK2 and a parasite lysate which was previously heat-inactivated and treated with calf intestinal phosphatase. These two treatments were aimed at respectively suppressing the intrinsic kinase activity of the lysate and removing the natural occurrence of phospho-proteins. In this way, the phospho-proteins detected after the incubation with PfCK2 could be linked with the kinase activity of this recombinant enzyme and considered therefore putative CK2 substrates. However, also this second global PfCK2 phospho-proteomics approach was not successful due to the loos of activity of PfCK2 in the *in vitro* kinase assay after the CIP treatment. Overall, these two first analyses underline once more the complex and intricate nature of phosphorylation pathways in eukaryotes which hampers the experimental detection, but they also constitute the basis for novel and further efforts in the development of an efficient global phospho-proteomic protocol for PfCK2, which will be discussed in the next section (see section **9.2**). In particular, these efforts in the identification of protein phosphorylation pathways are also of crucial importance in target-based drug development studies since they underline the role played by the enzyme of interest in the biology of the parasite. Since our study was also aimed at exploring the possibility to target the parasite kinome, we carried in parallel an analysis regarding the

inhibition of PfCK2. In this case, the most potent and selective inhibitor of human CK2 was tested with PfCK2 in *in vitro* kinase tests and in docking simulations in order to study the interaction of the compound with the enzyme ATP binding pocket, in the absence of a reported PfCK2 crystal structure. These analyses have essentially showed an analogous behaviour between the human and the parasite CK2, with very close IC_{50} values and very similar contacts between the compound and the two active sites, as expected by the highly conserved nature of CK2 enzymes. However, the study has also underlined a subtle difference in size between the two ATP binding pockets, being in particular smaller in the parasite CK2 due to the presence of three valine residues not conserved in the *Z. mays* and *H. sapiens* CK2s. Such evidence, which is reported here for the first time, is particular important in a drug target perspective and it could in principle guide the synthesis of novel ligands able to positively exploit this feature to build in selectivity.

Another crucial aspect of protein kinase enzymes is the complex nature of their regulation in the eukaryotic cell which often involves intricate autophosphorylation pathways controlled by the kinase itself or by up-stream kinases, leading to a cascade of phosphorylation events. Based on the previous evidence that also PfCK2 is able to autophosphorylate,[71] we therefore decided to study mechanisms and roles of this process. Surprisingly, the experiments showed that PfCK2 autophosphorylation plays a central role in both the protein kinase activity, and in the interaction with the β_2 regulatory subunit. In particular, it was possible to demonstrate that the PfCK2-T63A mutant lacking the site of autophosphorylation showed a ~50% of decrease in protein phosphorylation and a substantial decrease in the interaction with the β_2 subunit as well. Importantly, this residue is not part of the enzyme activation segment, which

usually contains the phosphorylating residue in the vast majority of the other kinases, and is not conserved in the human homologue. On the other hand, human CK2 autophosphorylates on Tyr182, a residue that is conserved in PfCK2 (but not phosphorylated) and it was previously showed that this event does not influence protein kinase activity or the interaction with the β-subunit. Interestingly, these two discoveries constitute the first reported evidence of a central regulation mechanism for a member of the CK2 kinase family. In fact, the protein kinase activity of CK2 enzymes is not usually influenced by mechanisms common to other kinases (e.g. autophosphorylation, growth factors, phosphorylation cascades etc.) and they are therefore considered constitutively active. Furthermore, the fact that this process is parasite-specific, since it is not observed in the human CK2, opens up a brand-new scenario for targeting the PfCK2 α-β subunit interaction.

In conclusion, these studies regarding the PfCK2 characterization have importantly contributed to identify structural elements, mechanisms of regulation and parasite specific features that altogether strengthens the notion that targeting the parasite kinome has a high potential for the development of the next new generation of antimalarials. In particular, the data obtained suggest that in principle, selective inhibition, although challenging, is an achievable goal.

The second area of research focused on the analysis of tyrosine phosphorylation pathways in *P. falciparum*. Tyrosine phosphorylation is usually a prerogative of multicellular organisms where it controls specific processes such as growth factor response and immune system regulation that are not found in lower eukaryotes. Despite this and the fact that no putative tyrosine kinases are found in the *Plasmodium* genome by functional annotation,[68] previous reports showed occurrence

of tyrosine phosphorylated proteins also in this unicellular organism.[161] On the basis of these evidence we therefore carried out an analysis aimed at mapping tyrosine phosphorylation pathways identifying in particular substrates, kinases and potential roles for these events. In fact, such investigation, constituted an interesting opportunity to learn new and important aspects of phosphorylation pathways in *P. falciparum*, and to identify fundamental divergences between the parasite and the host biology. Results overall confirmed previous evidence for the presence of tyrosine phosphorylated proteins in *P. falciparum*. Attempts were undertaken to define these proteins by enrichment protocols followed by LC-MS\MS analysis. This approach did not reveal any tyrosine phosphorylated proteins probably due to the very low occurrence of such modifications and to the limitations in the detection threshold of the technique. However, our Western Blot data confirmed the presence of tyrosine phosphorylated proteins within the parasitophorous vacuole membrane and in particular of a tyrosine phosphorylated form of PfCLK3 (on Tyr526) that was previously identified in a global phosphoproteomic study by LC-MS\MS.[83] Furthermore, in the latter case, the antibodies here purified and characterised were also subsequently used in a following study to show that this event is an autophosphorylation process regulating the kinase activity.[83] To further strengthen this picture, it was also demonstrated here that PfCK2, despite being a Thr\Ser kinase, is also able to catalyse Tyr phosphorylation. In particular, it was showed that this enzyme phosphorylates the parasite protein PfMCM2 on Tyr16, a residue that is contained in the *in vivo* phosphosite list obtained from a global phosphoproteomic analysis.[83] In addition to this, our Western Blot analysis showed that recombinant PfCK2 increased the level of tyrosine phosphorylated proteins contained in a heat-inactivated parasite lysate upon

incubation. This is the first evidence of a dual specificity kinase in the *P. falciparum* kinome and together with the PfCLK3 tyrosine autophosphorylation constitute two important examples of how tyrosine phosphorylation can occur in *Plasmodium*, even in the absence of a tyrosine kinase family, having an impact on the biology of the parasite. Finally, the study regarding PfMCM2 tyrosine phosphorylation was not overall successful due to the lack of detection of tyrosine kinase activity in the lysate after the *in vitro* kinase assay with a recombinant PfMCM2 fragment. This could be due to the specific conditions of the analysis that involved only a protein fragment that could not have been recognised by the kinase, or by the presence for example of the kinase in an inactive conformation in the lysate. However, the fact that PfCK2 efficiently phosphorylated the same residue *in vitro* suggests that the previous LC-MS\MS data reporting the *in vivo* occurrence of this modification could be potentially valid. In conclusion this second study contributed to further strengthen the hypothesis for the presence of tyrosine phosphorylation pathways in *P. falciparum*, identifying examples of specific substrates, kinases and roles for this post-traslational modification.

Finally, alongside the study of PfMCM2 tyrosine phosphorylation, a detailed analysis regarding the PfMCM2 Serine 13 phosphorylation also detected in the same global phosphoproteomic study was conducted. This study successfully determined PfCK1 to be the kinase responsible for this modification contained in the lysate, at least *in vitro*. With the use of specific antibodies, it was also possible to demonstrate that the levels of Ser13 phosphorylation matched the levels of protein expression during the parasite intra-erythrocytic cycle, peaking in particular at the trophozoite and schizont stage. At this point, it was hypothesised that, since PfMCM2 is part of the helicase complex, its

reversible phosphorylation might have a role in modulating the helicase activity by controlling its affinity towards chromatin, as previously showed in other model organisms.[158, 160] However, the use of the same antibodies in immunocytochemistry analyses did not establish a role for this modification in controlling the protein localisation. Despite this, we successfully targeted this process *in vitro*, with the use of a commercially available CK1 inhibitor. This particular result, other than further supporting the evidence that PfCK1 is the kinase responsible for PfMCM2-Ser13 phosphorylation, also demonstrated that it is feasible to target such pathways with small molecules that could potentially constitute a starting point in a drug-discovery effort focused on PfCK1. In this way, our study constitutes therefore an example of how the knowledge of the validated list of *in vivo* phosphorylation sites of *Plasmodium falciparum* schizonts can be used as a starting point for following studies aimed at determining specific phosphorylation pathways and their role in the parasite biology. Remarkably, the fact that it was also possible to efficiently interfere and inhibit this particular biological mechanism, at least *in vitro*, further supports the feasibility of a drug-development approach based on targeting protein kinases.

9.2 Future perspective

The results obtained from this investigation constitute potentially a starting point for further studies regarding phosphorylation pathways in *P. falciparum* and the development of selective protein kinases inhibitors with the purpose of generating novel antimalarials. First of all, the discovery that the ATP analogues containing a P-N bond are too acidic-sensitive in order to be detected opens up a brand-new scenario

for the synthesis of different classes of analogues based on alternative types of linkage such as P-S or P-C bonds, that would confer higher stability to the probes. These analogues would then have to be tested for their ability of acting as phosphate donors in PfCK2 *in vitro* kinase reactions and, if successful, they would represent a platform for the identification of PfCK2 substrates in a parasite lysate. An alternative solution to the described stability problems could also be represented by the Caliper 3000HTS system recently developed by Caliper Technologies. In fact, this is a highly automated capillary electrophoresis used to track enzymatic reactions that do not involve the use of acidic buffers during any stage of the analysis. Regarding the second PfCK2 phosphoproteomic approach, future work would involve optimisation of the conditions in which to carry out the initial de-phosphorylating reaction and the subsequent *in vitro* kinase assay with PfCK2. In fact, if compatible conditions (e.g. choice of buffers) between the two steps will be found this will then lead to the identification of phosphorylation event controlled by recombinant PfCK2 in a parasite lysate using the protocol here developed.

The next area that would benefit from further investigation is the PCK2 inhibition study. In fact, the observations made (particularly regarding the smaller ATP binding site of PfCK2 compared to the host homologue and the non-conserved residues recognised) could be potentially exploited in the design of novel inhibitors that would perform a higher selective profile towards PfCK2. Furthermore, due to the lack of a crystal structure, the obtained *in silico* model for PfCK2 can in principle be used in computer-aided virtual screenings of compound libraries in order to find molecules that would interact with the enzyme active site. In particular, this latter approach has

already successful in the design of enzyme inhibitors for several protein kinases (e.g. human CK1δ and CK2).[141, 165]

Future work regarding the PfCK2 autophosphorylation process would involve the study of the physiological consequences of such event. The first analysis would then be the verification of the fact that this autophosphorylation process occurs also *in vivo* and the eventual implications of that. This can be achieved by using for example tagged episomal PfCK2 to pull-down from the culture and analyse by LC-MS\MS and by checking as well the phenotype of parasite cultures transfected with PfCK2 mutants lacking the site of autophosphorylation. Furthermore, efforts in obtaining a holoenzyme crystal structure would clarify the role of the phosphorylated Thr63 in the protein-protein interaction. Notably, this would eventually constitute also the basis for designing inhibitors of the α-β_2, a route already turned successful in the case of the human CK2 holoenzyme.[147]

The investigation over tyrosine phosphorylation pathways in *P. falciparum* could be continued by searching for the presence of other dual-specificity kinases that could further account for the occurrence of tyrosine-phosphorylated proteins in the parasite. Efforts in this area should also concentrate in trying to identify novel pTyr substrates and further validating the ones already reported.[161]

Finally, the study carried out on the phosphorylation state of PfMCM2 can be progressed by looking at the *in vivo* occurrence and roles of such pathways. This can be done for example by transfecting episomally mutated versions of the protein lacking alternative one or both the phosphorylating residues identified (Ser13 and Tyr16) and then observing the phenotype. In fact, such analysis would strengthen and

complete the picture here described showing what is the *in vivo* significance of these

modifications, and it would clarify whether PfMCM2 is tyrosine phosphorylated or not

in vivo.

Appendix

Primers for PfCK2_T63A mutation:

Forward: 5'-TACAGTGAGGTGTTTAATGGATATGAT<u>GCG</u>GAATGTAATAGACC-3'

Reverse: 5'-GGTCTATTACATTC<u>CGC</u>ATCATATCCATTAAACACCTCACTGTA-3'

Primers for PfMCM2_Y16F mutation:

Forward: 5'-CTGGAAAAGCAACAAA<u>TTC</u>GATATTGATGAAGAAGATCTGCTGG-3'

Reverse: 5'-CCAGCAGATCTTCTTCATCAATATC<u>GAA</u>TTTGTTGCTTTCCAG-3'

Primers for PfMCM2_S13A mutation:

Forward: 5'-GAAGATCTGGAA<u>GCC</u>AACAAATATGATATTG-3'

Reverse: 5'-CAATATCATATTTGTT<u>GGC</u>TTCCAGATCTTC-3'

Primers for PfMCM2_S13A_Y16F mutation:

Forward: 5'-GAAGATCTGGAA<u>GCC</u>AACAAATTCGATATTG-3'

Reverse: 5'-CAATATCGAATTTGTT<u>GGC</u>TTCCAGATCTTC-3'

Primers for PfCK1 amplification to insert in pGEX-2T vector:

Forward: 5'- ATGCGGATCCATGGAAATTAGAGTGGCAAATAAATATGC-3'

Reverse: 5'- ATGCGGATCCTCAATTATTTCGTTGATCTCTTCCTTCTT-3'

References

1. Kennedy EP. Sailing to byzantium. Annu Rev Biochem 1992;61:1-28.

2. Murray CJ, Rosenfeld LC, Lim SS, Andrews KG, Foreman KJ, Haring D, Fullman N, Naghavi M, Lozano R, Lopez AD. Global malaria mortality between 1980 and 2010: A systematic analysis. Lancet 2012 Feb 4;379(9814):413-31.

3. Gallup JL, Sachs JD. The economic burden of malaria. Am J Trop Med Hyg 2001 Jan-Feb;64(1-2 Suppl):85-96.

4. Ralph SA, van Dooren GG, Waller RF, Crawford MJ, Fraunholz MJ, Foth BJ, Tonkin CJ, Roos DS, McFadden GI. Tropical infectious diseases: Metabolic maps and functions of the plasmodium falciparum apicoplast. Nat Rev Microbiol 2004 Mar;2(3):203-16.

5. Roberts L, Enserink M. Malaria. did they really say ... eradication? Science 2007 Dec 7;318(5856):1544-5.

6. Poinar G,Jr. Plasmodium dominicana n. sp. (plasmodiidae: Haemospororida) from tertiary dominican amber. Syst Parasitol 2005 May;61(1):47-52.

7. Liu W, Li Y, Learn GH, Rudicell RS, Robertson JD, Keele BF, Ndjango JB, Sanz CM, Morgan DB, Locatelli S, et al. Origin of the human malaria parasite plasmodium falciparum in gorillas. Nature 2010 Sep 23;467(7314):420-5.

8. Cox FE. History of human parasitology. Clin Microbiol Rev 2002 Oct;15(4):595-612.

9. Reiter P. From shakespeare to defoe: Malaria in england in the little ice age. Emerg Infect Dis 2000 Jan-Feb;6(1):1-11.

10. World malaria report. WHO, geneva switzerland. Geneva, Switzerland: ; 2008. .

11. Cowman AF, Crabb BS. Invasion of red blood cells by malaria parasites. Cell 2006 Feb 24;124(4):755-66.

12. Sato S. The apicomplexan plastid and its evolution. Cell Mol Life Sci 2011 Apr;68(8):1285-96.

13. Baumeister S, Winterberg M, Przyborski JM, Lingelbach K. The malaria parasite plasmodium falciparum: Cell biological peculiarities and nutritional consequences. Protoplasma 2010 Apr;240(1-4):3-12.

14. Rosenthal PJ, Meshnick SR. Hemoglobin catabolism and iron utilization by malaria parasites. Mol Biochem Parasitol 1996 Dec 20;83(2):131-9.

15. Kikuchi G, Yoshida T, Noguchi M. Heme oxygenase and heme degradation. Biochem Biophys Res Commun 2005 Dec 9;338(1):558-67.

16. Wells TN, Alonso PL, Gutteridge WE. New medicines to improve control and contribute to the eradication of malaria. Nat Rev Drug Discov 2009 Nov;8(11):879-91.

17. Cox-Singh J, Davis TM, Lee KS, Shamsul SS, Matusop A, Ratnam S, Rahman HA, Conway DJ, Singh B. Plasmodium knowlesi malaria in humans is widely distributed and potentially life threatening. Clin Infect Dis 2008 Jan 15;46(2):165-71.

18. Bray RS, Garnham PC. The life-cycle of primate malaria parasites. Br Med Bull 1982 May;38(2):117-22.

19. Miller LH, Baruch DI, Marsh K, Doumbo OK. The pathogenic basis of malaria. Nature 2002 Feb 7;415(6872):673-9.

20. Trampuz A, Jereb M, Muzlovic I, Prabhu RM. Clinical review: Severe malaria. Crit Care 2003 Aug;7(4):315-23.

21. Price RN, Tjitra E, Guerra CA, Yeung S, White NJ, Anstey NM. Vivax malaria: Neglected and not benign. Am J Trop Med Hyg 2007 Dec;77(6 Suppl):79-87.

22. Woolley IJ, Hotmire KA, Sramkoski RM, Zimmerman PA, Kazura JW. Differential expression of the duffy antigen receptor for chemokines according to RBC age and FY genotype. Transfusion 2000 Aug;40(8):949-53.

23. Collins WE, Jeffery GM. Plasmodium malariae: Parasite and disease. Clin Microbiol Rev 2007 Oct;20(4):579-92.

24. Hempelmann E. Hemozoin biocrystallization in plasmodium falciparum and the antimalarial activity of crystallization inhibitors. Parasitol Res 2007 Mar;100(4):671-6.

25. Gatton ML, Martin LB, Cheng Q. Evolution of resistance to sulfadoxine-pyrimethamine in plasmodium falciparum. Antimicrob Agents Chemother 2004 Jun;48(6):2116-23.

26. Luo XD, Shen CC. The chemistry, pharmacology, and clinical applications of qinghaosu (artemisinin) and its derivatives. Med Res Rev 1987 Jan-Mar;7(1):29-52.

27. White N. Antimalarial drug resistance and combination chemotherapy. Philos Trans R Soc Lond B Biol Sci 1999 Apr 29;354(1384):739-49.

28. Lim P, Alker AP, Khim N, Shah NK, Incardona S, Doung S, Yi P, Bouth DM, Bouchier C, Puijalon OM, et al. Pfmdr1 copy number and arteminisin derivatives combination therapy failure in falciparum malaria in cambodia. Malar J 2009 Jan 12;8:11.

29. Wells TN. Microbiology. is the tide turning for new malaria medicines? Science 2010 Sep 3;329(5996):1153-4.

30. Rottmann M, McNamara C, Yeung BK, Lee MC, Zou B, Russell B, Seitz P, Plouffe DM, Dharia NV, Tan J, et al. Spiroindolones, a potent compound class for the treatment of malaria. Science 2010 Sep 3;329(5996):1175-80.

31. Gardner MJ, Hall N, Fung E, White O, Berriman M, Hyman RW, Carlton JM, Pain A, Nelson KE, Bowman S, et al. Genome sequence of the human malaria parasite plasmodium falciparum. Nature 2002 Oct 3;419(6906):498-511.

32. Sadanand S. Malaria: An evaluation of the current state of research on pathogenesis and antimalarial drugs. Yale J Biol Med 2010 Dec;83(4):185-91.

33. Hunter T. Protein kinases and phosphatases: The yin and yang of protein phosphorylation and signaling. Cell 1995 Jan 27;80(2):225-36.

34. Manning G, Whyte DB, Martinez R, Hunter T, Sudarsanam S. The protein kinase complement of the human genome. Science 2002 Dec 6;298(5600):1912-34.

35. Gray N, Detivaud L, Doerig C, Meijer L. ATP-site directed inhibitors of cyclin-dependent kinases. Curr Med Chem 1999 Sep;6(9):859-75.

36. Cohen P. Protein kinases--the major drug targets of the twenty-first century? Nat Rev Drug Discov 2002 Apr;1(4):309-15.

37. Deininger MW, Druker BJ. Specific targeted therapy of chronic myelogenous leukemia with imatinib. Pharmacol Rev 2003 Sep;55(3):401-23.

38. Canduri F, Perez PC, Caceres RA, de Azevedo WF,Jr. Protein kinases as targets for antiparasitic chemotherapy drugs. Curr Drug Targets 2007 Mar;8(3):389-98.

39. Leroy D, Doerig C. Drugging the plasmodium kinome: The benefits of academia-industry synergy. Trends Pharmacol Sci 2008 May;29(5):241-9.

40. Gamo FJ, Sanz LM, Vidal J, de Cozar C, Alvarez E, Lavandera JL, Vanderwall DE, Green DV, Kumar V, Hasan S, et al. Thousands of chemical starting points for antimalarial lead identification. Nature 2010 May 20;465(7296):305-10.

41. Baldauf SL. The deep roots of eukaryotes. Science 2003 Jun 13;300(5626):1703-6.

42. BURNETT G, KENNEDY EP. The enzymatic phosphorylation of proteins. J Biol Chem 1954 Dec;211(2):969-80.

43. Cohen P. The origins of protein phosphorylation. Nat Cell Biol 2002 May;4(5):E127-30.

44. FISCHER EH, KREBS EG. Conversion of phosphorylase b to phosphorylase a in muscle extracts. J Biol Chem 1955 Sep;216(1):121-32.

45. KREBS EG, FISCHER EH. The phosphorylase b to a converting enzyme of rabbit skeletal muscle. Biochim Biophys Acta 1956 Apr;20(1):150-7.

46. Hanks SK, Quinn AM, Hunter T. The protein kinase family: Conserved features and deduced phylogeny of the catalytic domains. Science 1988 Jul 1;241(4861):42-52.

47. Knighton DR, Zheng J, Ten Eyck LF, Ashford VA, Xuong N, Taylor SS, Sowadski JM. Crystal structure of the catalytic subunit of cyclic adenosine monophosphate-dependent protein kinase. Science 1991;253(5018):407-14.

48. Hanks SK. Genomic analysis of the eukaryotic protein kinase superfamily: A perspective. Genome Biol 2003;4(5):111.

49. Hanks SK, Quinn AM. Protein kinase catalytic domain sequence database: Identification of conserved features of primary structure and classification of family members. Methods Enzymol 1991;200:38-62.

50. Pearce LR, Komander D, Alessi DR. The nuts and bolts of AGC protein kinases. Nat Rev Mol Cell Biol 2010 Jan;11(1):9-22.

51. Yamauchi T. Neuronal Ca2+/calmodulin-dependent protein kinase II--discovery, progress in a quarter of a century, and perspective: Implication for learning and memory. Biol Pharm Bull 2005 Aug;28(8):1342-54.

52. Hanks SK, Hunter T. Protein kinases 6. the eukaryotic protein kinase superfamily: Kinase (catalytic) domain structure and classification. FASEB J 1995 May;9(8):576-96.

53. Flotow H, Graves PR, Wang AQ, Fiol CJ, Roeske RW, Roach PJ. Phosphate groups as substrate determinants for casein kinase I action. J Biol Chem 1990 Aug 25;265(24):14264-9.

54. Eide EJ, Virshup DM. Casein kinase I: Another cog in the circadian clockworks. Chronobiol Int 2001 May;18(3):389-98.

55. Meggio F, Pinna LA. One-thousand-and-one substrates of protein kinase CK2? FASEB J 2003 Mar;17(3):349-68.

56. Abdi A, Eschenlauer S, Reininger L, Doerig C. SAM domain-dependent activity of PfTKL3, an essential tyrosine kinase-like kinase of the human malaria parasite plasmodium falciparum. Cell Mol Life Sci 2010 Oct;67(19):3355-69.

57. Duda T. Atrial natriuretic factor-receptor guanylate cyclase signal transduction mechanism. Mol Cell Biochem 2010 Jan;334(1-2):37-51.

58. Aparicio JG, Applebury ML. The photoreceptor guanylate cyclase is an autophosphorylating protein kinase. J Biol Chem 1996 Oct 25;271(43):27083-9.

59. Taylor SS, Kornev AP. Protein kinases: Evolution of dynamic regulatory proteins. Trends Biochem Sci 2011 Feb;36(2):65-77.

60. Manning G, Plowman GD, Hunter T, Sudarsanam S. Evolution of protein kinase signaling from yeast to man. Trends Biochem Sci 2002 Oct;27(10):514-20.

61. Johnson LN, Noble ME, Owen DJ. Active and inactive protein kinases: Structural basis for regulation. Cell 1996 Apr 19;85(2):149-58.

62. Johnson LN, Lewis RJ. Structural basis for control by phosphorylation. Chem Rev 2001 Aug;101(8):2209-42.

63. Kornev AP, Haste NM, Taylor SS, Eyck LF. Surface comparison of active and inactive protein kinases identifies a conserved activation mechanism. Proc Natl Acad Sci U S A 2006 Nov 21;103(47):17783-8.

64. Dardick C, Ronald P. Plant and animal pathogen recognition receptors signal through non-RD kinases. PLoS Pathog 2006 Jan;2(1):e2.

65. Anamika, Srinivasan N, Krupa A. A genomic perspective of protein kinases in plasmodium falciparum. Proteins 2005 Jan 1;58(1):180-9.

66. Talevich E, Mirza A, Kannan N. Structural and evolutionary divergence of eukaryotic protein kinases in apicomplexa. BMC Evol Biol 2011 Nov 2;11:321.

67. Kappes B, Doerig CD, Graeser R. An overview of plasmodium protein kinases. Parasitol Today 1999 Nov;15(11):449-54.

68. Ward P, Equinet L, Packer J, Doerig C. Protein kinases of the human malaria parasite plasmodium falciparum: The kinome of a divergent eukaryote. BMC Genomics 2004 Oct 12;5(1):79.

69. Doerig C, Endicott J, Chakrabarti D. Cyclin-dependent kinase homologues of plasmodium falciparum. Int J Parasitol 2002 Dec 4;32(13):1575-85.

70. Droucheau E, Primot A, Thomas V, Mattei D, Knockaert M, Richardson C, Sallicandro P, Alano P, Jafarshad A, Baratte B, et al. Plasmodium falciparum glycogen synthase kinase-3: Molecular model, expression, intracellular localisation and selective inhibitors. Biochim Biophys Acta 2004 Mar 11;1697(1-2):181-96.

71. Holland Z, Prudent R, Reiser JB, Cochet C, Doerig C. Functional analysis of protein kinase CK2 of the human malaria parasite plasmodium falciparum. Eukaryot Cell 2009 Mar;8(3):388-97.

72. Beraldo FH, Almeida FM, da Silva AM, Garcia CR. Cyclic AMP and calcium interplay as second messengers in melatonin-dependent regulation of plasmodium falciparum cell cycle. J Cell Biol 2005 Aug 15;170(4):551-7.

73. Gurnett AM, Liberator PA, Dulski PM, Salowe SP, Donald RG, Anderson JW, Wiltsie J, Diaz CA, Harris G, Chang B, et al. Purification and molecular characterization of cGMP-dependent protein kinase from apicomplexan parasites. A novel chemotherapeutic target. J Biol Chem 2002 May 3;277(18):15913-22.

74. McRobert L, Taylor CJ, Deng W, Fivelman QL, Cummings RM, Polley SD, Billker O, Baker DA. Gametogenesis in malaria parasites is mediated by the cGMP-dependent protein kinase. PLoS Biol 2008 Jun 3;6(6):e139.

75. Marte BM, Downward J. PKB/Akt: Connecting phosphoinositide 3-kinase to cell survival and beyond. Trends Biochem Sci 1997 Sep;22(9):355-8.

76. Doerig C, Billker O, Haystead T, Sharma P, Tobin AB, Waters NC. Protein kinases of malaria parasites: An update. Trends Parasitol 2008 Dec;24(12):570-7.

77. Billker O, Lourido S, Sibley LD. Calcium-dependent signaling and kinases in apicomplexan parasites. Cell Host Microbe 2009 Jun 18;5(6):612-22.

78. Barik S, Taylor RE, Chakrabarti D. Identification, cloning, and mutational analysis of the casein kinase 1 cDNA of the malaria parasite, plasmodium falciparum. stage-specific expression of the gene. J Biol Chem 1997 Oct 17;272(42):26132-8.

79. Dorin D, Le Roch K, Sallicandro P, Alano P, Parzy D, Poullet P, Meijer L, Doerig C. Pfnek-1, a NIMA-related kinase from the human malaria parasite plasmodium falciparum biochemical properties and possible involvement in MAPK regulation. Eur J Biochem 2001 May;268(9):2600-8.

80. Shiu SH, Li WH. Origins, lineage-specific expansions, and multiple losses of tyrosine kinases in eukaryotes. Mol Biol Evol 2004 May;21(5):828-40.

81. Schneider AG, Mercereau-Puijalon O. A new apicomplexa-specific protein kinase family: Multiple members in plasmodium falciparum, all with an export signature. BMC Genomics 2005 Mar 7;6:30.

82. Nunes MC, Goldring JP, Doerig C, Scherf A. A novel protein kinase family in plasmodium falciparum is differentially transcribed and secreted to various cellular compartments of the host cell. Mol Microbiol 2007 Jan;63(2):391-403.

83. Solyakov L, Halbert J, Alam MM, Semblat JP, Dorin-Semblat D, Reininger L, Bottrill AR, Mistry S, Abdi A, Fennell C, et al. Global kinomic and phospho-proteomic

analyses of the human malaria parasite plasmodium falciparum. Nat Commun 2011 Nov 29;2:565.

84. Doerig C, Abdi A, Bland N, Eschenlauer S, Dorin-Semblat D, Fennell C, Halbert J, Holland Z, Nivez MP, Semblat JP, et al. Malaria: Targeting parasite and host cell kinomes. Biochim Biophys Acta 2010 Mar;1804(3):604-12.

85. Lasa M, Marin O, Pinna LA. Rat liver golgi apparatus contains a protein kinase similar to the casein kinase of lactating mammary gland. Eur J Biochem 1997 Feb 1;243(3):719-25.

86. Lozeman FJ, Litchfield DW, Piening C, Takio K, Walsh KA, Krebs EG. Isolation and characterization of human cDNA clones encoding the alpha and the alpha' subunits of casein kinase II. Biochemistry 1990 Sep 11;29(36):8436-47.

87. Wirkner U, Voss H, Lichter P, Pyerin W. Human protein kinase CK2 genes. Cell Mol Biol Res 1994;40(5-6):489-99.

88. Niefind K, Guerra B, Ermakowa I, Issinger OG. Crystal structure of human protein kinase CK2: Insights into basic properties of the CK2 holoenzyme. EMBO J 2001 Oct 1;20(19):5320-31.

89. Sarno S, Moro S, Meggio F, Zagotto G, Dal Ben D, Ghisellini P, Battistutta R, Zanotti G, Pinna LA. Toward the rational design of protein kinase casein kinase-2 inhibitors. Pharmacol Ther 2002 Feb-Mar;93(2-3):159-68.

90. Litchfield DW. Protein kinase CK2: Structure, regulation and role in cellular decisions of life and death. Biochem J 2003 Jan 1;369(Pt 1):1-15.

91. Wilson LK, Dhillon N, Thorner J, Martin GS. Casein kinase II catalyzes tyrosine phosphorylation of the yeast nucleolar immunophilin Fpr3. J Biol Chem 1997 May 16;272(20):12961-7.

92. Vilk G, Weber JE, Turowec JP, Duncan JS, Wu C, Derksen DR, Zien P, Sarno S, Donella-Deana A, Lajoie G, et al. Protein kinase CK2 catalyzes tyrosine phosphorylation in mammalian cells. Cell Signal 2008 Nov;20(11):1942-51.

93. Dastidar EG, Dayer G, Holland ZM, Dorin-Semblat D, Claes A, Chene A, Sharma A, Hamelin R, Moniatte M, Lopez-Rubio JJ, et al. Involvement of plasmodium falciparum protein kinase CK2 in the chromatin assembly pathway. BMC Biol 2012 Jan 31;10:5.

94. Eckhart W, Hutchinson MA, Hunter T. An activity phosphorylating tyrosine in polyoma T antigen immunoprecipitates. Cell 1979 Dec;18(4):925-33.

95. Hunter T, Eckhart W. The discovery of tyrosine phosphorylation: It's all in the buffer! Cell 2004 Jan 23;116(2 Suppl):S35,9, 1 p following S48.

96. Hunter T. Tyrosine phosphorylation: Thirty years and counting. Curr Opin Cell Biol 2009 Apr;21(2):140-6.

97. Pawson T. Protein modules and signalling networks. Nature 1995 Feb 16;373(6515):573-80.

98. van der Geer P, Pawson T. The PTB domain: A new protein module implicated in signal transduction. Trends Biochem Sci 1995 Jul;20(7):277-80.

99. Lim WA, Pawson T. Phosphotyrosine signaling: Evolving a new cellular communication system. Cell 2010 Sep 3;142(5):661-7.

100. Yaffe MB. Phosphotyrosine-binding domains in signal transduction. Nat Rev Mol Cell Biol 2002 Mar;3(3):177-86.

101. Schemarova IV. The role of tyrosine phosphorylation in regulation of signal transduction pathways in unicellular eukaryotes. Curr Issues Mol Biol 2006 Jan;8(1):27-49.

102. Pincus D, Letunic I, Bork P, Lim WA. Evolution of the phospho-tyrosine signaling machinery in premetazoan lineages. Proc Natl Acad Sci U S A 2008 Jul 15;105(28):9680-4.

103. Schieven G, Thorner J, Martin GS. Protein-tyrosine kinase activity in saccharomyces cerevisiae. Science 1986 Jan 24;231(4736):390-3.

104. Wilkes JM, Doerig C. The protein-phosphatome of the human malaria parasite plasmodium falciparum. BMC Genomics 2008 Sep 15;9:412.

105. Pendyala PR, Ayong L, Eatrides J, Schreiber M, Pham C, Chakrabarti R, Fidock DA, Allen CM, Chakrabarti D. Characterization of a PRL protein tyrosine phosphatase from plasmodium falciparum. Mol Biochem Parasitol 2008 Mar;158(1):1-10.

106. Sharma A. Protein tyrosine kinase activity in human malaria parasite plasmodium falciparum. Indian J Exp Biol 2000 Dec;38(12):1222-6.

107. Noller CR, Luchetti CA, Acton EM, Bernhard RA. The reaction of methanesulfonyl chloride with alcohols in the presence of pyridine. J Am Chem Soc 1953 08/01; 2012/06;75(15):3851-2.

108. Brase S, Gil C, Knepper K, Zimmermann V. Organic azides: An exploding diversity of a unique class of compounds. Angew Chem Int Ed Engl 2005 Aug 19;44(33):5188-240.

109. Englund EA, Gopi HN, Appella DH. An efficient synthesis of a probe for protein function: 2,3-diaminopropionic acid with orthogonal protecting groups. Org Lett 2004 Jan 22;6(2):213-5.

110. Sigal GB, Mammen M, Dahmann G, Whitesides GM. Polyacrylamides bearing pendant α-sialoside groups strongly inhibit agglutination of erythrocytes by influenza virus:‰ the strong inhibition reflects enhanced binding through cooperative polyvalent interactions. J Am Chem Soc 1996 01/01; 2012/06;118(16):3789-800.

111. Huang F, Wang G, Coleman T, Li N. Synthesis of adenosine derivatives as transcription initiators and preparation of 5' fluorescein- and biotin-labeled RNA through one-step in vitro transcription. RNA 2003 Dec;9(12):1562-70.

112. Glynn IM, Chappell JB. A simple method for the preparation of 32-P-labelled adenosine triphosphate of high specific activity. Biochem J 1964 Jan;90(1):147-9.

113. Neises B, Steglich W. Simple method for the esterification of carboxylic acids. Angewandte Chemie International Edition in English 1978;17(7):522-4.

114. Gololobov YG, Zhmurova IN, Kasukhin LF. Sixty years of staudinger reaction. Tetrahedron 1981;37(3):437-72.

115. Sivakumar K, Xie F, Cash BM, Long S, Barnhill HN, Wang Q. A fluorogenic 1,3-dipolar cycloaddition reaction of 3-azidocoumarins and acetylenes. Org Lett 2004 Nov 25;6(24):4603-6.

116. Fields GB, Noble RL. Solid phase peptide synthesis utilizing 9-fluorenylmethoxycarbonyl amino acids. Int J Pept Protein Res 1990 Mar;35(3):161-214.

117. Eswar N, Webb B, Marti-Renom MA, Madhusudhan MS, Eramian D, Shen MY, Pieper U, Sali A. Comparative protein structure modeling using MODELLER. Curr Protoc Protein Sci 2007 Nov;Chapter 2:Unit 2.9.

118. Jones G, Willett P, Glen RC, Leach AR, Taylor R. Development and validation of a genetic algorithm for flexible docking. J Mol Biol 1997 Apr 4;267(3):727-48.

119. Lambros C, Vanderberg JP. Synchronization of plasmodium falciparum erythrocytic stages in culture. J Parasitol 1979 Jun;65(3):418-20.

120. Cohen P. Signal integration at the level of protein kinases, protein phosphatases and their substrates. Trends Biochem Sci 1992 Oct;17(10):408-13.

121. Elphick LM, Lee SE, Gouverneur V, Mann DJ. Using chemical genetics and ATP analogues to dissect protein kinase function. ACS Chem Biol 2007 May 22;2(5):299-314.

122. Gronborg M, Kristiansen TZ, Stensballe A, Andersen JS, Ohara O, Mann M, Jensen ON, Pandey A. A mass spectrometry-based proteomic approach for identification of serine/threonine-phosphorylated proteins by enrichment with phospho-

specific antibodies: Identification of a novel protein, frigg, as a protein kinase A substrate. Mol Cell Proteomics 2002 Jul;1(7):517-27.

123. Wang JY. Antibodies for phosphotyrosine: Analytical and preparative tool for tyrosyl-phosphorylated proteins. Anal Biochem 1988 Jul;172(1):1-7.

124. Corthals GL, Aebersold R, Goodlett DR. Identification of phosphorylation sites using microimmobilized metal affinity chromatography. Methods Enzymol 2005;405:66-81.

125. Reinders J, Sickmann A. State-of-the-art in phosphoproteomics. Proteomics 2005 Nov;5(16):4052-61.

126. Allen JJ, Lazerwith SE, Shokat KM. Bio-orthogonal affinity purification of direct kinase substrates. J Am Chem Soc 2005 Apr 20;127(15):5288-9.

127. Green KD, Pflum MK. Kinase-catalyzed biotinylation for phosphoprotein detection. J Am Chem Soc 2007 Jan 10;129(1):10-1.

128. Green KD, Pflum MK. Exploring kinase cosubstrate promiscuity: Monitoring kinase activity through dansylation. Chembiochem 2009 Jan 26;10(2):234-7.

129. Suwal S, Pflum MK. Phosphorylation-dependent kinase-substrate cross-linking. Angew Chem Int Ed Engl 2010 Feb 22;49(9):1627-30.

130. Diamandis EP, Christopoulos TK. The biotin-(strept)avidin system: Principles and applications in biotechnology. Clin Chem 1991 May;37(5):625-36.

131. Kolb HC, Finn MG, Sharpless KB. Click chemistry: Diverse chemical function from a few good reactions. Angew Chem Int Ed Engl 2001 Jun 1;40(11):2004-21.

132. Staudinger H, Meyer J. Über neue organische phosphorverbindungen III. phosphinmethylenderivate und phosphinimine. Helv Chim Acta 1919;2(1):635-46.

133. Pang HM, Kenseth J, Coldiron S. High-throughput multiplexed capillary electrophoresis in drug discovery. Drug Discov Today 2004 Dec 15;9(24):1072-80.

134. Faust M, Montenarh M. Subcellular localization of protein kinase CK2. A key to its function? Cell Tissue Res 2000 Sep;301(3):329-40.

135. Krek W, Maridor G, Nigg EA. Casein kinase II is a predominantly nuclear enzyme. J Cell Biol 1992 Jan;116(1):43-55.

136. Issinger OG. Casein kinases: Pleiotropic mediators of cellular regulation. Pharmacol Ther 1993;59(1):1-30.

137. Meggio F, Marin O, Pinna LA. Substrate specificity of protein kinase CK2. Cell Mol Biol Res 1994;40(5-6):401-9.

138. Cohen P. The development and therapeutic potential of protein kinase inhibitors. Curr Opin Chem Biol 1999 Aug;3(4):459-65.

139. Sarno S, Pinna LA. Protein kinase CK2 as a druggable target. Mol Biosyst 2008 Sep;4(9):889-94.

140. Uhle S, Medalia O, Waldron R, Dumdey R, Henklein P, Bech-Otschir D, Huang X, Berse M, Sperling J, Schade R, et al. Protein kinase CK2 and protein kinase D are associated with the COP9 signalosome. EMBO J 2003 Mar 17;22(6):1302-12.

141. Cozza G, Mazzorana M, Papinutto E, Bain J, Elliott M, di Maira G, Gianoncelli A, Pagano MA, Sarno S, Ruzzene M, et al. Quinalizarin as a potent, selective and cell-permeable inhibitor of protein kinase CK2. Biochem J 2009 Jul 15;421(3):387-95.

142. Battistutta R, Mazzorana M, Cendron L, Bortolato A, Sarno S, Kazimierczuk Z, Zanotti G, Moro S, Pinna LA. The ATP-binding site of protein kinase CK2 holds a positive electrostatic area and conserved water molecules. Chembiochem 2007 Oct 15;8(15):1804-9.

143. Mazzorana M, Pinna LA, Battistutta R. A structural insight into CK2 inhibition. Mol Cell Biochem 2008 Sep;316(1-2):57-62.

144. Donella-Deana A, Cesaro L, Sarno S, Brunati AM, Ruzzene M, Pinna LA. Autocatalytic tyrosine-phosphorylation of protein kinase CK2 alpha and alpha' subunits: Implication of Tyr182. Biochem J 2001 Jul 15;357(Pt 2):563-7.

145. Filhol O, Cochet C. Protein kinase CK2 in health and disease: Cellular functions of protein kinase CK2: A dynamic affair. Cell Mol Life Sci 2009 Jun;66(11-12):1830-9.

146. Laudet B, Barette C, Dulery V, Renaudet O, Dumy P, Metz A, Prudent R, Deshiere A, Dideberg O, Filhol O, et al. Structure-based design of small peptide inhibitors of protein kinase CK2 subunit interaction. Biochem J 2007 Dec 15;408(3):363-73.

147. Laudet B, Moucadel V, Prudent R, Filhol O, Wong YS, Royer D, Cochet C. Identification of chemical inhibitors of protein-kinase CK2 subunit interaction. Mol Cell Biochem 2008 Sep;316(1-2):63-9.

148. Mishra NC, Sharma M, Sharma A. Inhibitory effect of piceatannol, a protein tyrosine kinase inhibitor, on asexual maturation of plasmodium falciparum. Indian J Exp Biol 1999 Apr;37(4):418-20.

149. Treeck M, Sanders JL, Elias JE, Boothroyd JC. The phosphoproteomes of plasmodium falciparum and toxoplasma gondii reveal unusual adaptations

within and beyond the parasites' boundaries. Cell Host Microbe 2011 Oct 20;10(4):410-9.

150. Fawell SE, Lenard J. A specific insulin receptor and tyrosine kinase activity in the membranes of neurospora crassa. Biochem Biophys Res Commun 1988 Aug 30;155(1):59-65.

151. Parsons M, Valentine M, Deans J, Schieven GL, Ledbetter JA. Distinct patterns of tyrosine phosphorylation during the life cycle of trypanosoma brucei. Mol Biochem Parasitol 1991 Apr;45(2):241-8.

152. Salotra P, Ralhan R, Sreenivas G. Heat-stress induced modulation of protein phosphorylation in virulent promastigotes of leishmania donovani. Int J Biochem Cell Biol 2000 Mar;32(3):309-16.

153. Roisin MP, Robert-Gangneux F, Creuzet C, Dupouy-Camet J. Biochemical characterization of mitogen-activated protein (MAP) kinase activity in toxoplasma gondii. Parasitol Res 2000 Jul;86(7):588-98.

154. Tye BK, Sawyer S. The hexameric eukaryotic MCM helicase: Building symmetry from nonidentical parts. J Biol Chem 2000 Nov 10;275(45):34833-6.

155. Bell SP, Dutta A. DNA replication in eukaryotic cells. Annu Rev Biochem 2002;71:333-74.

156. Patterson S, Robert C, Whittle C, Chakrabarti R, Doerig C, Chakrabarti D. Pre-replication complex organization in the atypical DNA replication cycle of plasmodium falciparum: Characterization of the mini-chromosome maintenance (MCM) complex formation. Mol Biochem Parasitol 2006 Jan;145(1):50-9.

157. Forsburg SL. Eukaryotic MCM proteins: Beyond replication initiation. Microbiol Mol Biol Rev 2004 Mar;68(1):109-31.

158. Montagnoli A, Valsasina B, Brotherton D, Troiani S, Rainoldi S, Tenca P, Molinari A, Santocanale C. Identification of Mcm2 phosphorylation sites by S-phase-regulating kinases. J Biol Chem 2006 Apr 14;281(15):10281-90.

159. Lei M, Kawasaki Y, Young MR, Kihara M, Sugino A, Tye BK. Mcm2 is a target of regulation by Cdc7-Dbf4 during the initiation of DNA synthesis. Genes Dev 1997 Dec 15;11(24):3365-74.

160. Stead BE, Brandl CJ, Davey MJ. Phosphorylation of Mcm2 modulates Mcm2-7 activity and affects the cell's response to DNA damage. Nucleic Acids Res 2011 Sep 1;39(16):6998-7008.

161. Lasonder E, Treeck M, Alam M, Tobin AB. Insights into the plasmodium falciparum schizont phospho-proteome. Microbes Infect 2012 May 5.

162. Aranda S, Laguna A, de la Luna S. DYRK family of protein kinases: Evolutionary relationships, biochemical properties, and functional roles. FASEB J 2011 Feb;25(2):449-62.

163. Pulgar V, Marin O, Meggio F, Allende CC, Allende JE, Pinna LA. Optimal sequences for non-phosphate-directed phosphorylation by protein kinase CK1 (casein kinase-1)--a re-evaluation. Eur J Biochem 1999 Mar;260(2):520-6.

164. Rena G, Bain J, Elliott M, Cohen P. D4476, a cell-permeant inhibitor of CK1, suppresses the site-specific phosphorylation and nuclear exclusion of FOXO1a. EMBO Rep 2004 Jan;5(1):60-5.

165. Cozza G, Gianoncelli A, Montopoli M, Caparrotta L, Venerando A, Meggio F, Pinna LA, Zagotto G, Moro S. Identification of novel protein kinase CK1 delta (CK1delta) inhibitors through structure-based virtual screening. Bioorg Med Chem Lett 2008 Oct 15;18(20):5672-5.